ADDIS ABABA UNIVERSITY
ETHIOPIAN INSTITUTE OF WATER RESOURCES

Hydrological processes under changing climate and land use scenarios in the Baro–Akobo River Basin, Ethiopia

Abiy Getachew Mengistu (ID: GSR/7281/10)

Ph.D. DISSERTATION SUBMITTED
TO
ETHIOPIAN INSTITUTE OF WATER RESOURCES
WATER RESOURCES ENGINEERING AND MANAGEMENT PROGRAM

04/11/2023

ADDIS ABABA, ETHIOPIA

Declaration

I, the undersigned, declare that this dissertation is based on my original work and that it has not been submitted and presented for a degree at any other university. All sources of materials have been duly acknowledged.

Name: Abiy Getachew Mengistu

Signature: _____

Date:

This dissertation has been submitted for examination with my approval as supervisor of the dissertation.

Main Advisor: Tekalegn Ayele (Ph.D.)

Signature: _____

Date:

Co-Advisor: Yihun Taddele (Ph.D.)

Signature: 

Date:

DATE OF THE DAY

ADDIS ABABA

Hydrological processes under changing climate and land use scenarios in the Baro–Akobo River Basin, Ethiopia

Abiy Getachew Mengistu ID: GSR/7281/10

Ph.D. Dissertation Submitted

To

Ethiopian Institute of Water Resources (EIWR)

Water Resources Engineering and Management (Surface Water Management Specialization)

Addis Ababa University

Approved by the Board of Examiners:

Tekalegn Ayele (Ph.D.) Main Advisor	Signature	Date
Yihun Taddele (Ph.D.) Co-Advisor	Signature	Date
Adane Abebe (Assoc. Prof.) External Examiner	Signature	Date
Alemseged Tamiru (Ph.D.) Internal Examiner	Signature	Date
Sirak Tekleab (Ph.D.) Internal Examiner	Signature	Date
Tilahun Derib (Ph.D.) Chair Person	Signature	Date
Tekalegn Ayele (Ph.D.) EIWR Education Coordinator	Signature	Date
Zeleke Agide (Ph.D.) EIWR Director	Signature	Date

Acknowledgments

First, I would like to thank God for his never-ending love and for giving me the strength to complete this study and all the other things in my life.

I would like to express my deepest heartfelt gratitude to my advisors, Dr. Tekalegn Ayele and Dr. Yihun Taddele, for their valuable guidance, encouragement, critical feedback, and support from the beginning up until the end of this research work. Your assistance enabled me to develop original concepts and publish them. Without your help, I would not have been able to complete this Ph.D. study. Thank you so much. I am also deeply thankful to Dr. Haimanote Kebede and Dr. Gebrekidan Worku for their valuable comments and feedback that helped me progress in my study.

I would like to thank my entire class for all of the challenges and knowledge sharing since the development of the Ph.D. proposal until now and for the enjoyable time, we spent together at the Ethiopian Institute of Water Resources (Akaky campus) and Addis Ababa University (main campus). My special thanks go to my friends, Dr. Gebrekidan Worku, Dr. Kirubel Mekonen, and Mr. Yonas Ademe. Thanks also to all of my colleagues at the Department of Natural Resource Management, especially Feyera Deressa, Mehari Hadush, and Tesfay Talossa, for their help and the challenging discussions during this study. The fieldwork activities, particularly the GPS point collection work, would not have been possible without the support from Benchi-Sheko and Sheka Zone water supply practitioners, namely Atrse and Fekadu, and my college staff, Feyera, and Zewde. My sincere thanks also go to the Ethiopian National Meteorological Service Agency and the Ministry of Water and Energy for providing the weather and streamflow data sets, respectively. I am very respectful to thank the Ethiopian Institute of Water Resources, Addis Ababa University for all the services I have got. I would like to express my thanks to Mizan-Tepi University for allowing me to pursue my Ph.D.

I would like to express my gratitude to my brothers, sisters, and families, who have supported and encouraged me throughout all the stages of my life. I would like to offer my great gratitude to my brothers, Dr. Tesfaye and his wife Meseret; Dr. Anteneh and his wife Selam; Thegaye and his wife Mestawet; and to my sister Hiwot and her husband Endalegeta, for their unreserved support. Last but not least, I want to thank my wife, Merkeb Getachew. Her patience while I was away and caring for our cute little daughter, Hana, was incredible.

List of original papers

This dissertation is based on the following original papers

1. **Mengistu, A. G**., Woldesenbet, T. A., & Dile, Y. T. (2021). Evaluation of the performance of bias corrected CORDEX regional climate models in reproducing the Baro–Akobo basin climate. *Theoretical and Applied Climatology*. *144*(1–2), 751–767. https://doi.org/10.1007/s00704-021 03552-w.
2. **Mengistu, A. G**., Woldesenbet, T. A., & Dile, Y. T. (2021). Evaluation of observed and satellite-based climate products for hydrological simulation in data-scarce Baro–Akobo River basin, Ethiopia. *Ecohydrology & Hydrobiology*. https://doi.org/10.1016/j.ecohyd.2021.11.006.
3. **Mengistu, A. G**., Woldesenbet, T. A, Dile, Y. T, Bayabil, H. K. (2022). Modeling the impacts of climate change on hydrological processes in the Baro–Akobo River basin, Ethiopia. *Acta Geophysica: hydrology*. https://doi **:** 10.1007/s11600-022-00956-8.
4. **Mengistu, A. G**., Woldesenbet, T.A, Dile, Y. T, Bayabil, H. K, Tefera, G.W (2023). Modeling the impacts of projected climate and land use changes on the water balance in the Baro basin, Ethiopia. Helyion https://doi **:**10.1016/j.heliyon.2023.e13965.

The published papers could be reprinted with the kind agreement of the publishers

Summary

Water is an essential component of agricultural productivity and is crucial for food security. It is also a vital component of the environment. Water security is becoming a global issue, but the issue is chronic in most developing countries, including sub-Saharan Africa. Therefore, sustainable water resource management is essential to achieve food and water security in Ethiopia. The Baro–Akobo River basin, which is found in the southwest part of Ethiopia, has witnessed a substantial change in population, climate, and land use during the last four decades. The climate of the region is warming at an alarming rate, and it is expected that this tendency will persist in the coming century. On the other hand, the impacts of climate and land use change on the hydrology of this basin are not well understood. Understanding the impacts of climate and land use change on basin hydrology is critical for developing effective water management practices. Therefore, this study examined the individual and combined impacts of climate and land use changes on the basin hydrology.

This study combines a statistical, geospatial, and hydrological model to investigate the hydrologic impacts of climate and land use change. First, seven raw and bias-corrected RCMs (RCA4 (CNRM), RCA4 (ICHEC), RCA4 (MPI), CCLM4 (CNRM), CCLM4 (MPI), REMO (MPI)) and the ensemble mean were evaluated for model skill in reproducing the observed baseline climate for the period 1975–2005 at several weather stations in the basin. A pixel-to-point approach was used to compare RCMs against weather stations. Monthly distribution patterns and several statistical metrics were used for evaluating the performance of RCMs in capturing the historical observed climate of the basin. The Mann-Kendall test and Sen's slope estimate were used to examine the decreasing and increasing trend of the climatic variables, as well as to estimate the magnitudes of the significant decreasing and increasing trends. Furthermore, the ensemble mean and five bias corrected RCMs were used to examine climate and hydrological changes in the baseline and future 2021–2050 (2030s) and 2071-2100 (2080s) periods under the representative concentration pathway (RCP4.5 and RCP8.5) scenarios. On the other hand, the geospatial and synergistic techniques of cellular automata (CA) and artificial neural networks (ANN) were used to develop historical and future land use change scenarios. The maximum likelihood classifier (MLC) in the Earth Resource Data Analysis System (ERDAS) was used to conduct land use change classification for Landsat imagery from 1985, 2002, and 2019. Three land use maps with seven classes were identified, and then a change detection process was conducted. The classified

(1985–2002) and (2002–2019) land use maps, along with a transition matrix and spatial drivers, were put into the Module for Land-use Change Evaluation (MOLUSCE) model to predict land use maps for 2019 (current) and 2040 (a business-as-usual scenario) land use scenarios, respectively, using the CA-ANN multilayer perceptron methods (MLP). Besides, this study considered a further increase in altitudinal forest expansion and watershed management practices (conservation) in a land use scenario. Then the best-performing climate model (ensemble mean) under RCP4.5 and RCP8.5 for the 2023–2040 time frame and plausible land use scenarios considering the current, business as usual, and conservation was used as inputs to the calibrated models to examine the individual and combined impacts of climate and land use changes on the hydrology.

Three independent climate datasets, including observed, Climate Hazards Group InfraRed Precipitation with Stations (CHIRPS), and Climate Forecast System Reanalysis (CFSR), were used to calibrate and validate the Soil and Water Assessment Tool (SWAT) model for the periods 1990–1998 and 1999–2002, respectively. The Sequential Uncertainty Fitting 2 (SUfI2) method in the SWAT-CUP program was used for model calibration and sensitivity. The Nash–Sutcliffe Efficiency (NSE), Coefficient of Determination (R^2), and Percent Bias (PBIAS) as well as two uncertainty measurements (r-factor and p-factor), were used to assess the model's performance. Then the calibrated model using the water balance equation was used to examine the individual and combined impacts of climate and land use change scenarios on the basin hydrology. The climate and land use change impacts on hydrology were analyzed on monthly, seasonal, and annual scales with respect to the baseline period. Statistical tests such as the t-test and Levene test were also used to determine the change in mean and standard deviation between the baseline and different climate and land use scenarios. Besides, the Indicators of Hydrologic Alterations (IHA) method was used to assess the hydrologic changes between the baseline conditions and future climate change scenarios.

Results from the global climate models (GCMs) downscaled through the CCLM4, RCA4, and REMO modeling schemes are characterized by several biases, such as shifting the rainy season and under- and overestimation of the observed climate. However, the skill of the models was substantially enhanced after bias correction. All models best capture the annual cycle with less bias. Therefore, it was beneficial to account for such biases using a robust statistical bias correction method before utilizing RCM simulations to generate climatic scenarios and climate impact scenarios. Results from future bias-corrected RCMs show a consistent increase in monthly Tmax

and Tmin under RCP4.5 and RCP8.5 in the 2030s and 2080s relative to the baseline climate, while rainfall does not show consistency. The future climate change projections from the ensemble mean show an increase in the R20mm, CDD, R95p, RX1, and RX5 indices, but the R10 indices show a decreasing value under both RCPs.

Observed climate and CHIRPS rainfall combined with the CFSR dataset yielded reasonable and comparable streamflow simulation performance in terms of statistical metrics at both Baro and Sore hydrological stations. All climate impact scenarios from the ensemble mean demonstrated a decline in surface runoff and water yield and an increase in evapotranspiration. Except for the extreme flow segment (i.e., 0–3% exceedance probability), the projection for simulation under climate change scenarios shows a decrease in flow. The increase in temperature and the decrease in rainfall is attributed to a relatively higher impact than the combined and land-use change-alone scenarios. This will have an impact on future agricultural production and water availability. Moreover, the projected increase in rainfall extremes, the expansion of agricultural land, and urbanization all lead to increased surface runoff and flooding. Therefore, to implement adaptation and mitigation strategies, the inclusion of predicted climate and land use change in hydrological impact studies is useful.

.

Table of contents

List of Figures

List of tables

List of Abbreviations

AfSIS	African Soil Information Service
ANN	Artificial Neural Network
BAU	Business-As-Usual
BP	Back Propagation
CA	Cellular Automata
CCLM	Consortium for Small-scale Modeling (COSMO) Climate Limited-Area Model
CDD	Consecutive dry days
CDF	Cumulative Distribution Function
CFSR	Climate Forecast System Reanalysis
CHIRPS	Climate Hazards Group InfraRed Precipitation with Stations
CMhyd	Climate Model data for Hydrologic Modeling
CMIP	Climate Model Intercomparison Project
CMORPH	Climate Prediction Center Morphing method
CNRM-CM5	ESM developed at Météo- France and CERFACS
CON	Conservation
CORDEX	Coordinated Regional Downscaling Experiment
DEM	Digital Elevation Model
DM	Distribution Mapping
EC-EARTH	European Community Earth-System Model
ECMWF	European Centre for Medium-Range Weather Forecasts
EFC	Environmental Flow Components
EMA	Ethiopian Mapping Agency
ENMA	Ethiopian National Meteorological Agency
EPFCC	Ethiopian Panel for Climate Change
ERDAS	Earth Resource Data Analysis System
ET	Evapotranspiration
ETCCDI	Expert Team on Climate Change Detection and Indices
ETM+	Enhanced Thematic Mapper Plus
FAO	Food and Agricultural Organization of the United Nations
FDRE	Federal Democratic Republic of Ethiopia
GCMs	General Circulation Models
GHG	Greenhouse Gas
GIS	Geographic Information System
GPCC	Global Precipitation Climatology Center
GPS	Global Position System
GSFLOW	Coupled Ground-Water and Surface-Water Flow Model
GWQ	Groundwater flow
HadGEM2-ES	Hadley Global Environment Model 2-Earth System
HEC-HMS	Hydrologic Engineering Centers Hydrologic Modeling System

HRUs	Hydrologic Response Units
HSPF	Hydrological Simulation Program Fortran
IGBP	International Geosphere-Biosphere Programme
IHA	Indicators of Hydrologic Alteration
IHDP	International Human Dimensions Programme
IMERG	Integrated Multi-satellitE Retrievals for Global Precipitation Measurement
IPCC	Intergovernmental Panel for Climate Change
LS	Linear Scaling
MICE	Multivariate Imputation by Chained Equations
MLC	Maximum Likelihood Classifier
MOLUSCE	Module for Land-Use Change Evaluation
MPI-ESM-LR	ESM of the Max-Planck-Institut für Meteorologie ESM
MPL	Multi-Layer Perception
MOWE	Ministry of Water and Energy
NOAA	Ethiopian National Meteorology Agency
NSE	Nash-Sutcliffe Efficiency
OLI	Operational Land Inventory
PBIAS	Percent Bias
PERSIANN	Precipitation Estimation from Remotely Sensed Information using Artificial Neural Networks
PET	Potential Evapotranspiration
PRMS	Precipitation-Runoff Modeling System
R^2	Coefficient of determination
R	Correlation Coefficient
RCA4	Rossby Center Regional Atmospheric Model
RCMs	Regional Climate Models
RCPs	Representative Concentration Pathways
REMO	Max Planck Institute Regional Model
RMSE	Root Mean Square Error
RS	Remote Sensing
RVA	Range of Variability Approach
RX1day	Monthly maximum one-day rainfall
RX5day	Monthly maximum consecutive five-day precipitation
R10	Number of heavy rainfall days
R20	Number of very heavy rainfall days
SLURP	Semi-distributed land-use-based runoff processes
SRES	Special Report on Emission Scenarios
SREs	Satellite Rainfall Estimates
SRTM	Shuttle Radar Topographic Mission
SUFI	Sequential Uncertainty Fitting

SURQ	Surface Runoff
SWAT	Soil and Water Assessment Tool
SWAT-CUP	Soil and Water Assessment Tool Calibration and Uncertainty Procedures
TAMSAT	Tropical Applications of Meteorology using Satellite Data and Ground-Based Observations
TFPW	Trend Free Pre-Whitening
TM	Thematic Mapper
TMPA	Tropical Rainfall Measuring Mission Multi-satellite Precipitation Analysis
Tmax	Maximum Temperature
Tmin	Minimum Temperature
TRMM	Tropical Rainfall Measuring Mission
UNESCO	United Nations Educational, Scientific and Cultural Organization
USGS	United States Geological Survey
UTM	Universal Transverse Mercator
VIC	Variable Infiltration Capacity
WCRP	World Climate Research Program
WMO	World Meteorological Organization
WWAP	World Water Assessment Programme
WYLD	Water Yield

1. Introduction

1.1. Background and justification

Climate and land use changes are the two well-understood key driving forces impacting hydrological processes (IPCC, 2019; UNEP, 2012). Such changes have an impact on evapotranspiration, surface runoff, groundwater flow, and streamflow, among other hydrological processes (Kim et al., 2013; Yang et al., 2017). Because of the acceleration of global warming and the rising conversion of virgin forest lands to agricultural use, the impact of climate and land use change is expected to worsen in the future (Jung et al., 2011; UNEP, 2012). Therefore, understanding the impacts of future climate and land use changes on the hydrology of the basins requires more attention.

One of the three well-documented worldwide changes is the amount of carbon dioxide (CO2) in the atmosphere (IGBP, 2001; UNEP, 2012). The principal cause of these global changes is the expansion of human activity. The amount of CO2 in the atmosphere is increasing. It was 280 ppm (parts per million) in 1750, 365 ppm in 1998, 391 ppm in 2011, and 419 ppm in 2022, and it is anticipated to be considerably above 500 ppm by the year 2100 (IPCC, 2013; NOAA, 2022). Global emissions of greenhouse gases increased as a result of these changes, which also affected the entire human population and the planet's ecosystem.

There is unequivocal evidence to support the claim that the globe is warming at an unprecedented rate. Findings from the IPCC (2021) show that the mean temperature of the Earth's surface between 2011 and 2020 was 1.1ºC warmer than the pre-industrial period (1880–1900). Global temperatures are projected to rise by 2–4°C by 2100 if greenhouse gas emissions can't be mitigated in the future. Additionally, changes in the spatial and temporal pattern of rainfall, an increase in rainfall and temperature extremes, and a rise of 19 to 21 cm in the global sea level were noted (IPCC, 2019). The fact that climate change differs in different parts of the world is another issue. For instance, over the 20th century, rainfall in the majority of mid-high latitudes of the Northern Hemisphere and the tropical regions of the planet, respectively, increased by 0.5–1% and decreased by 0.2-0.3% every decade (IPCC, 2013). From 1983 to 2010, there was a similar increase in yearly rainfall in the Sahel and Southern Africa regions but a drop in rainfall in East Africa (Maidment et al., 2015). The impacts of climate change are huge, including altering global

energy patterns, ecosystems, and the global economy. This highlights the need to employ climate model simulations to examine change at different regional and local scales.

Climate models are essential tools for researching how the climate system responds to changes in the atmosphere's composition brought on by the concentration of greenhouse gases (IPCC, 2013). In water resource impact assessment, there are numerous global climate model (GCM) outputs available, each with a different spatial and temporal resolution. But GCM outputs don't offer a complete picture of the variables at the scale that hydrological models need (Kay et al., 2009). As a result, it has become common practice to downscale large-scale variables to watershed scale variables, as required by hydrological models (Abdo et al., 2009; Fowler et al., 2007; Sharma et al., 2007). The two approaches that are currently known for downscaling the climate variables from GCMs are statistical and dynamic (Fowler & Kilsby, 2007; Salathé, 2003). The statistical downscaling process entails establishing quantitative relationships between large-scale regional atmospheric variables and local-scale atmospheric variables. While, RCMs, which were produced using the same representations of atmospheric dynamical and physical processes as GCMs, are used in the dynamical downscaling technique. RCMs offer a better representation of orographic effects, land-sea surface contrast, and land-surface characteristics due to their larger spatial domain (10–50km) (Christensen et al., 2007; Zhang et al., 2019). However, due to inaccurate conceptualization, discretization, and spatial averaging within grid cells, the RCMs are computationally costly and prone to systemic model errors (Teutschbein & Seibert, 2012). As a result, it is advised that bias correction should be applied to the RCM outputs before carrying out climate change and hydrologic impact assessments (Teutschbein & Seibert, 2010; Wood et al., 2004; Worku et al., 2021).

Changes in evaporation, soil water, and runoff are caused by climate change, which also has an impact on the hydrological cycle, which further influences the availability of freshwater resources (Bates et al., 2008). Many geographical regions around the world saw an upsurge in surface runoff and flood events, particularly since the 1950s (IPCC, 2019). For many more years to come, climate change will have a substantial impact on both the natural ecosystem and humanity. For instance, according to various emission scenarios, it is expected that between 12 and 81 million people will experience water stress in the 2020s and between 79 and 178 million in the 2050s (Arnell, 2004). By the end of the 21st century, regional and worldwide projections indicate that a decrease in soil moisture could lead to an increase in agricultural drought (IPCC, 2014). These hydrologic changes

brought on by climate change have an impact on every area of human well-being, including water availability and agricultural output.

Land use change is another of the most documented global changes, causing numerous impacts on the environment (IGBP, 2001; UNEP, 2012; Zheng et al., 2016). Environmentalists have shown considerable interest in information about land use change due to its effects on the environment at large (Meiyappan & Jain, 2012; Subedi et al., 2013). The unprecedented increase of cultivated land and urban areas at the expense of natural ecosystems such as forests and grasslands is the dominant land use change. (Bal et al., 2021; Lambin & Meyfroidt, 2011). Land use changes are vastly prevalent in developing countries that are characterized by agriculture-based economies and rapidly increasing human populations. For instance, Sub-Saharan Africa has lost 5% of its grasslands and 16% of its forests over the past 25 years (Midekisa et al., 2017). In Ethiopia, land use changes from natural vegetation to farmland and urban areas are common (Desalegn et al., 2014; Woldesenbet et al., 2017; Wubie et al., 2016; Zeleke & Hurni, 2001).

These land-use changes have significant effects on how the Earth's climate will change in the future, which in turn has significant effects on future land-use changes. Thus, the International Geosphere-Biosphere Programme (IGBP) and the International Human Dimensions Programme on Global Environmental Change (IHDP) jointly proposed the land use change research program in 1995, making it the forefront and hot spot of global change research to reveal the interaction between the global environment for human survival as well as the evolving production systems (agriculture, and urbanization) (Vitousek, 1994). Remote sensing (RS) and geographic information systems (GIS) are used in the larger context of land use science due to the rapid advancement of satellite-based technologies (Anh et al., 2021; Mannan et al., 2019). Up until 2005, researchers in land use science were confined to figuring out historical and current trends in land use changes (Aspinall, 2004). However, in recent times, scientists have attempted to forecast future land use change because of improvements in data sources and sophisticated technologies (Ahmed & Ahmed, 2012; Guo et al., 2019). Daye & Healey (2015) show that modeling land use change in this aspect is becoming more vital as there will be time to address expected changes at various spatial and temporal scales. Researchers mostly use numerous models that have been proposed by researchers to analyze and project the land use change mechanism, along with GIS and RS methods. The most widespread methods are models based on equations (Shamsi, 2010), statistics (Hyandye, 2015), Markov chains (Han et al., 2015), and cellular models (Cao et al., 2019; Li &

Li, 2015). Among these models, cellular automata (CA) combined with an artificial neural network (ANN) were used in this study. Changes in land use can affect processes occurring on the earth's surface, including hydrology, soil erosion, and the exchange of water and energy with the atmosphere (Ban et al., 2015).

There is rising concern that the sustainability of freshwater resources is challenged in many regions of the world since climate and land-use changes are predicted to continue throughout the twenty-first century (Jung et al., 2011; McMartney & Girma, 2012). As a result, several studies understand the individual effect of either climate or land use change on hydrology (e.g., Koch et al., 2012; Taye et al., 2018; Teferi et al., 2103; Woldesenbet et al., 2017; Worku et al., 2021; Zhang et al., 2019). However, it is important to appreciate the combined impact of these factors. There are limited studies that understand the combined impact of climate and land change (Kim et al., 2013; Yin et al., 2017). An increasing number of basin-scale hydrological modeling studies incorporate how climate and land use change impact basin hydrology. Because climate and land use changes may either mitigate or aggravate each other at various spatial and temporal scales, this area of research is crucial for managing water resources (Praskievicz & Chang, 2009).

In hydrological impact studies of climate and land use change, the common approaches used are the paired catchment approach, statistical analysis, and hydrological modeling (Li et al., 2012). Among these approaches, hydrological modeling is an appealing alternative because it is most suitable to be used as a part of scenario studies. To this end, hydrological modeling, such as SWAT, is a valuable scientific tool for investigating hydrological responses to various climate and land use change scenarios (Kiprotich et al., 2021; Seibert & Vis, 2012). In addition, the IHA method, which is based on the Range of Variability Approach (RVA), was used to evaluate the streamflow parameters under different climate change scenarios (Pradhanang et al., 2013).

1.2 Statement of the problem

The Nile River's water resources have been under immense pressure due to different competitive uses such as socio-economics, geopolitics, and legislative conditions. Moreover, previous research shows that several parts of the Nile basin are sensitive to climatic variations (Conway, 2005; Beyene et al., 2010), indicating that climate change will have a substantial effect on water resources. The Baro–Akobo River basin, one of the sub-basins of the Eastern Nile, has been highly impacted by different environmental changes. For example, climate and land use changes have

been observed in this basin over the last four decades (Alemayehu et al., 2016; Mengistu et al., 2021a). Further, climate extremes trigger frequent and severe floods, landslides, soil erosion, soil fertility decline, and ultimately a decline in crop productivity in large areas of the study basin (World Bank, 2006; Yang et al., 2013). These climate, hydrology, and natural resources-related repercussions trigger multifarious effects on the rain-fed agriculture-based economy of the inhabitants, which is strongly dependent on rainfall. Unfortunately, the effect of climate change on water could be further worsened due to a lack of a strong water resource database, a lack of adequate meteorological stations, insufficient water resource planning, and a lack of hydraulic structures to retain water (World Bank, 2006). Consequently, an alternative climate data source for hydrological applications, a projection of the climatic scenarios, and an assessment of how the hydrology changes relative to the baseline condition could help identify suitable mitigation and adaptation strategies for the future in the basin.

At the same time, the rapid urbanization of the basin's population over the past four decades has caused land use changes in the basin. The conversion of forest and rangeland into cultivated land, the excessive use of wood and plants as fuel sources, resettlement, and investment in commercial agriculture was evident in the study basin. Commercial agricultural developments, introducing new varieties of seeds, have expanded rapidly in forested areas of the basin, particularly in the last four decades. Large areas of forestland have been set aside for investment in tea, coffee, soapberry, rubber tree, black pepper, mango, and cereal crop production in large areas of the basin (Alemayehu et al., 2016; Engida et al., 2021; Mekuria et al., 2011; Wakjira & Gole, 2016). The presence of numerous irrigation and hydropower development projects, which are under planning and implementation (e.g., Tams, Birbir A and Birbir R, Baro-1 and Baro-2, Geba-A, and Geba-R) (Alemayehu et al., 2016; Sileet et al., 2013), may lead to further deforestation and pose a threat to the environment. On the other hand, the effectiveness of watershed management practices such as filter strips, terracing, and contouring was not investigated in the basin. Thus, studies that examine the changes in hydrological components as a response to various land use change scenarios are important for sustainable land use planning and water resource management.

Therefore, assessing the availability of water resources in the basin in a changing climate and land use is a prerequisite to implementing evidence-based water and land management options. Previous studies have separately examined the impact of climate change (Abdo et al., 2009; Beyene et al., 2010; Elshamy et al., 2009; Gebremedhin et al., 2017; Muleta, 2021) or land use

change (Alemayehu et al., 2016; Engida et al., 2021) on the hydrology of the basin. However, the combined impact of climate and land-use change scenarios on the hydrology of the basin is not well understood. The aforementioned climate change studies in the basin most often used the coarse spatial resolution of GCMs or not used the bias correction approach (e.g., Mengistu & Sorteberg, 2012) to examine the impacts of climate change on the hydrology of the basin. However, the GCM model may not well represent the climate variables of the study basin, and it has implications for hydrology because of its coarse resolution (Fowler & Kilsby, 2007; Sharma et al., 2007).

Most of the studies undertaken in Ethiopia in general and the study basin in particular that investigated the impact of climate change on basin hydrology have considered that land use remains static (e.g., Beyene et al., 2010; Mengistu & Sorteberg, 2012). In contrast, studies that investigated the impact of land-use change considered climate as static (e.g., Alemayehu et al., 2016; Engida et al., 2021). Nevertheless, it is important to note that there is a feedback between climate and land use change, which subsequently affects rainfall, climatology, and hydrology. Therefore as climate and land use in the future will change continuously due to accelerated population growth, economic development, and global warming (McCartney & Girma, 2012), it is important to assess the future impacts of these environmental changes on the hydrology of the basin using the SWAT model and IHA tools that are not well understood by the previous studies.

This study is distinguished from previous ones by using high-resolution RCMs and plausible land use scenarios to examine the impacts on hydrology. The climate scenarios were obtained from multiple bias-corrected RCMs and the ensemble mean to develop robust climate change scenarios. The land use scenarios were generated from a model that takes into account the historical trend and spatial factors as well as the effort of watershed management scenarios. This study evaluated the individual and combined climate and land use modeling results to evaluate their impacts on the hydrology of the basin.

1.3 Research question

- How well does the regional climate model perform in reproducing the basin climate?
- How well are the different statistical bias correction approaches in adjusting the daily rainfall and temperature simulations of RCM?
- Is there any significant trend observed in rainfall and temperatures in the study basin?

- How good are the gridded climate products at calibrating the hydrological models?
- How may the streamflow be impacted in future periods under different climate scenarios?
- What are the individual and combined impacts of climate and land use change on the Baro basin water balance? Which of these impacts has the greatest impact on water availability in the basin?

1.4 Objectives of the study

The general objective of this study was to investigate the individual and combined impacts of climate and land use change on the hydrological processes of the Baro–Akobo River basin

The specific objectives were to:

- ✓ Examining the raw and bias adjusted RCMs, as well as the ensemble mean in reproducing the Baro–Akobo basin historical climate
- ✓ Comparing the observed and gridded climate products in simulating the hydrology of the Baro and Sore River stations using the SWAT model
- ✓ Assessment of future climate change projections based on various RCMs and the ensemble mean for the representative concentration pathways (RCP4.5 and RCP8.5)
- ✓ Examining the impacts of climate change on the streamflow under the representative concentration pathways (RCP4.5 and RCP8.5).
- ✓ Examining the impact of land use change on the water balance of the Baro basin under different land use change scenarios
- ✓ Evaluations of the combined impacts of climate and land use changes on the water balance of the Baro basin

1.5 Significance of the study

This study integrates different climate and land use change scenarios. A comprehensive quantification and assessment of future hydrology due to the impacts of both climate and land change in the basin are required for several important reasons: First, this study develops a robust baseline and future climate, land use, and impact scenarios for the basin. Such scenarios encourage the development of sustainable water and land resource management strategies that can provide optimal benefits for climate mitigation and adaptation. This study is also crucial to resisting the effects of both drought and flooding under current and future climatic conditions. Looking at alternative climate products like gridded satellite climate estimates in such remotely located and

poorly gauged regions is also very important, and it provides an alternative climate data set for hydrological modeling and applications. In general, this study provides useful information for water and land resource management decisions that can maximize water storage as well as water yield under different climate and land use conditions. This research can also serve as a foundation for reviewing current land and water management policies and programs in light of climate and land use change.

1.6 Study scope and limitations

Several socio-economic and environmental problems in the basin can be active areas of research. However, the scope of this study is limited to the hydrologic impact of climate and land use change as an environmental problem.

The impact of climate and land use change studies on hydrology tends to contain a range of limitations. It is important to acknowledge that the performance evaluation results may be limited by the spatial scale mismatch among the RCMs/gridded climate products and weather stations, the number and distribution of weather stations, and the position of weather stations within the pixel of the RCMs/gridded climate products. The lack of good quality data causes a lower level of performance by a hydrological model during the calibration and validation processes, as well as the comparison of the baseline conditions with the simulation of climate impact scenarios. The impact of future climate change was assessed in meteorological terms of rainfall and temperature, while other climate variables, such as relative humidity, solar radiation, and wind speed, were assumed to remain the same in the future. The climate variables used in this study are the results of the Coordinated Regional Climate Downscaling Experiment Program (CORDEX) Africa RCM simulations under different RCPs with a spatial resolution of 50 x 50 km, which is a little bit coarse.

The spatial data used, such as soil, are assumed to remain the same in the future. However, in the real world, soil properties will change when land use is changed. The land use change scenarios could be influenced by the factors influencing land use changes (e.g., land use policy, economic development, and the natural environment). For example, the business-as-usual land use scenario is generated based on the assumption of future development in line with historical trends. It will most likely be the trend of land use change in the study basin. Nevertheless, the change would not always be linear because future trends are uncertain due to uncertainties in future population growth, economic policy, and government policy.

A hydrologic model SWAT is a semi-distributed parameter. To obtain the ‘‘best fit" for observed and simulated data, the model parameters considered in this study are adjusted using literature and default values without being confirmed by field measurements during calibration. Furthermore, the model parameters after calibration are kept for modeling future conditions without adjustment under future scenarios. Nevertheless, future climate and land use changes might change the parameters.

Despite the limitations, this study makes every effort (e.g., looking for the best available data, bias correction, accuracy assessment, model calibration, and validation, using the most plausible climate and land use scenarios, etc.) to reduce the uncertainty in the model estimate and attempt to understand the possible impact of climate and land use change on the water resource availability in the study area. Considering the limitations of this study, the results are only valid under the presently used climate and land use scenarios. Nevertheless, the results and methodology used in this study still have implications for water management and land use planning in the future for the study area and other areas facing similar problems from climate and land use change.

1.7 Dissertation organization

This dissertation is organized into eight chapters.

Chapter 1 presents a general overview, a statement of the problem, objectives, significance, and scope and limitations of the dissertation.

Chapter 2 is a comprehensive literature review covering the science of climate and land use change and the role of hydrological modeling for climate and land use change impact studies.

Chapter 3 presents the general procedure of the study, and a description of the study area in terms of location, climatology, land use and soil, natural resources, data collection, and methods. Data quality control and missing data estimation were also carried out.

Chapter 4 presents the long-term baseline climate comparison with the historical climate models. This chapter includes an evaluation of the performance of statistical bias correction methods in adjusting the rainfall and temperature simulation climate models and a comparison of the RCMs' skills using several statistical metrics.

Chapter 5 presents the evaluation of different gridded satellite products’ skills in capturing the historical rainfall and temperature and their applicability for hydrological modeling at the Baro and Sore watersheds in the Baro–Akobo River basin.

Chapter 6 deals with the evaluation of near-term and long-term future climate change scenarios using RCMs and their ensemble simulations adjusted through a robust statistical bias correction method. A hydrological model combined with indicators of hydrological alteration was performed using the multi-model ensemble mean of climate models to examine the future hydrological condition.

Chapter 7 presents the historical climate model performance and land use change and then develops future climate and land use scenarios to investigate the individual and their combined impacts on the hydrology of the basin

Chapter 8 presents the synthesis, summary, and conclusions of all the results. Additionally, some recommendations for future research are given.

2. Literature review

2.1 Climate change

Climate change is defined as a change in the state of the climate that can be detected by variations in the mean and/or variability of its attributes and that lasts for a considerable amount of time, usually decades or longer. Most African countries have also seen a strong warming trend in global climate change during the past few decades, and the trend is anticipated to continue in the future (IPCC, 2013). The IPCC report states that developing countries will be more susceptible to climate change (IPCC, 2007). Ethiopia is especially vulnerable to the effects of climate change due to its less adaptable economic structure and heavy reliance on agriculture. Between 1948 and 2006, upward trends in annual air temperature and downward trends in annual rainfall were observed over Ethiopia (Jury & Funk, 2013); however, findings show that Ethiopia will continue to warm by 0.7°C to 2.3°C by the 2020s and between 1.4°C and 2.9°C by the 2050s (World Bank, 2006). The variations in both the temperature and the amount of precipitation show striking geographic variety (Laprise et al., 2013). Significant hydrological effects could result from the combination of rising temperatures and changing rainfall patterns and intensities, which could speed up the hydrological cycle and increase the frequency of hydrological extremes (Taye et al., 2011).

2.2 Climate modeling and downscaling

The atmosphere-land-ocean system is closely tied to the warming of the climate system and changes in its state variables. The study of climate modeling combines these intricate systems with GCMs to simulate and predict future climate change over decades and centuries. GCMs are the primary source of data for projecting likely future climate change. These GCM-derived climate change scenarios are the first step in this process. The majority of GCMs depict the global climate using a 3-dimensional grid over the globe, often with a horizontal resolution of between 250 and 600 km, 10 to 20 vertical layers in the atmosphere, and up to 30 layers in the ocean. GCMs' spatial resolution is too low to resolve effects at the regional scale. Downscaling is therefore necessary (Bates et al., 2008; Gautam & Arora, 2015).

The primary downscaling methods used to create regional and local-scale climate data from GCMs are statistical and dynamic downscaling (Murphy, 1999; Wilby et al., 2000). There is evidence showing the superiority of dynamical downscaling over statistical downscaling methods for simulating rainfall in places with varying topography (Schmidli et al., 2007). The dynamical

downscaling approach is reliant on GCM boundary forcing, which is the same as statistical downscaling. Dynamic downscaling, however, does not rely on a stable link between predictor and predictand and is more effective at modeling physically consistent atmospheric processes on a smaller scale (Fowler & Kilsby, 2007). Dynamic downscaling is similar to GCMs in that it uses mathematical representations of the physical processes that form the climate system, but it has a better geographical resolution and can account for the influence of mountains, coastlines, and local climate drivers (Schmidli et al., 2007).

There are important regional and global climate modeling centers that use the dynamical downscaling strategy to construct large ensembles of RCM simulations by layering RCMs onto the third and fifth phases of Climate Model Intercomparison Project GCMs (CMIP3 and CMIP5) (Christensen et al., 2007; Kim et al., 2014). For instance, the CORDEX, run under the auspices of the World Climate Research Program (WCRP), is an international program to make downscaled climate datasets available, combine model evaluation frameworks, and use climate model data for climate change impact studies (Giorgi et al., 2009). The results of CORDEX were assessed and used to research the effects of climate change in various parts of Africa, and they demonstrated reasonable performance (Endris et al., 2013; Haile & Rientjes, 2015; Nikulin et al., 2012; Worku et al., 2020b). However, it was found that the skill of the RCM differs depending on the skill measures used for assessment. These are because of the variation in initial boundary conditions, local forcing, the parameters considered, and parameterization of key variables, RCMs have different skills in predicting the climate of a specific region. Thus, it is crucial to identify RCMs that can simulate the historical climate of the study region. In addition, the output of downscaled RCMs shows consistent biases (Elshamy et al., 2009; Gudmundsson et al., 2012; Worku et al., 2020b). As a result, climate information from climate model simulations without bias corrections is less accurate, especially when it comes to the production of extreme climate events. For example, runoff simulation using RCMs is less trustworthy than runoff simulation using bias-corrected climatic data (Fang et al., 2015; Fiseha et al., 2014; Worku et al., 2021). Therefore, bias-adjusted RCM simulations must be used before assessing the impact of climate change.

2.3 Climate change scenarios

The climate scenario is a plausible indication of what the future could be like over the coming decades or centuries, providing a specific assumption. These assumptions include future trends in

energy demand, emissions of greenhouse gases, and land use change, as well as assumptions about the behavior of the climate system over long time scales. It is largely the uncertainty surrounding this assumption that determines the range of possible scenarios (Kay et al., 2009). In addition to the no-climate-policy scenarios like the Special Report on Emission Scenarios (SRES), there has recently been an increase in interest among the scientific community in scenarios that specifically study the impact of various climate policies (Moss et al., 2010). These SRES developed future evolutions of atmospheric greenhouse gas emission scenarios based on the future evolution of socioeconomic changes and assumed that no climate policies would be implemented to mitigate climate change, so these emission scenarios do not account for interventions or the impact of policy changes on interventions (van Ruijven et al., 2014).

The need for new scenarios prompted the IPCC to request the scientific community to develop a new set of scenarios for the assessment of future climate change. The fifth IPCC report presents a new approach to emission scenarios called RCPs. Therefore, a set of new scenarios is constructed containing emission, concentration, and land-use trajectories referred to as RCPs. In its name, the word "representative" signifies that each of the RCPs represents a larger set of scenarios in the literature. This implies that this set of RCPs should be compatible with the full range of emission scenarios (with and without climate policy) available in the current scientific literature. The word "concentration pathway" emphasizes that these RCPs are not the final new, fully integrated scenarios (i.e., they are not a complete package of socio-economic, emission, and climate projections), but instead are internally consistent sets of projections of the components of radiative forcing that are used as input to climate models. The word "concentration" also emphasizes that instead of emissions, concentrations are used as the primary product of the RCPs, designed as input to climate models (IPCC, 2013; van Ruijven et al., 2014). Four RCPs scenarios (Moss et al., 2010) named according to the radiative forcing target level for 2100 are used (Table 2.1).

The RCPs were developed through an innovative collaboration between integrated assessment modelers, climate modelers, terrestrial ecosystem modelers, and emission inventory experts (van Ruijven et al., 2014). The dynamically downscaled regional climate multi-model outputs of CORDEX-Africa emphasize the RCP4.5 and RCP8.5 scenarios. The RCP8.5 scenario gives projections that correspond to the business-as-usual development pathways, and the RCP4.5 scenario represents the middle situation. The fifth assessment report of the ICCP provided global

and regional climate projections for the new RCP scenarios under CMPI5. Few validation studies indicated good agreement with observations (e.g., Chaturvedi et al., 2012).

Table 2. 1 Overview of the representative concentration pathways (RCPs).

S.No	Scenarios	Description
1	RCP8.5	Rising radiative forcing pathways leading to 8.5 W/m^2 (~ 1,370 parts per million [ppm] carbon dioxide [CO2]) by 2100. It is one very high reference emission scenario
2	RCP6	RCP6 Stabilization without overshoot pathway to 6 W/m^2 (~850 ppm CO2) at stabilization after 2100
3	RCP4.5	RCP4.5 Stabilization without overshoot pathway to 4.5 W/m^2 (~650 ppm CO2) at stabilization after 2100. It is a medium stabilizing scenario
4	RCP2.6	The peak in radiative forcing at ~3 W/m^2 (~490 ppm CO2) before 2100 and then declines to 2.6 W/m2 by 2100

2.4 Bias correction of climate model simulations

The process of bias correction involves modifying model variables to more accurately match the observed distribution and statistics (Teutschbein & Seibert, 2012). Additionally, bias correction involves rescaling and post-processing the results of climate models to lessen the impact of systematic errors in the models (Piani et al., 2010). Even though they are based on physical principles, the information generated by global climate models also comprises numerical approximations, which may lead in some cases to biases resulting in deviations of the simulated climate from the observed one (Fang et al., 2015; IPCC, 2015; Teutschbein & Seibert, 2012). It is nowadays widely recognized that climate model results cannot be used directly as inputs to other more specialized impact models and that an adjustment (bias correction) towards the observed climatology is necessary. A bias correction is therefore applied to compensate for any tendency to overestimate or underestimate the mean of downscaled variables. Several bias correction methods, such as local intensity scaling, power transformation, variance scaling, linear scaling, and distribution mapping of precipitation and temperature, exist for RCM projections, and detailed information on different bias correction methods is provided (Teutschbein & Seibert, 2012).

There are typically biases in the RCM statistics of key hydro-meteorological variables, such as precipitation and temperature. Many of these biases originate from either the driving GCM model or the RCM used for downscaling. Since hydrological models are very sensitive to anomalies in rainfall amounts, direct use of RCM outputs in impact studies is therefore usually not appropriate, and the hydrological important variables of precipitation and temperature need to be adjusted before use in impact studies (Fang et al., 2015). In addition to reducing uncertainty in climate scenarios, bias correction in RCM simulations improves the reliability of findings in scenarios involving the effects of climate change. For instance, runoff simulations using bias-corrected RCMs are more accurate than those using non-biased RCM simulations (Fang et al., 2015; Teutschbein & Seibert, 2012).

2.5 Land use change and modeling

According to FAO, land use refers to the intended use or management of the land cover type by human beings, such as agriculture, forestry, and building construction. A regionally pervasive and internationally relevant ecological trend is land-use change. According to Vitousek (1994), three of the well-documented worldwide changes are rising carbon dioxide concentrations in the atmosphere; changes in the global nitrogen cycle's biochemistry; and ongoing land-use and land-cover changes. Between 1990 and 2010, 75 million hectares of forest in Africa were converted to agriculture and grazing, the second-highest rate behind South America (FAO, 2010). Over the same 20-year period, over 13 million hectares of the original East African forest were gone, and the surviving forest is fragmented and always in danger. More than other influences, population increase has been the primary driver of change in land use and land cover in the majority of emerging countries. In the majority of African, Asian, and Latin American nations, there is a statistically significant association between population growth and changes in land cover (FAO, 2010).

Land use change is mainly caused by high population growth, and it is most common in developing countries like Ethiopia (Andualem et al., 2018; Maitima et al., 2009; Tegene, 2002; Zeleke & Hurni, 2001). In various parts of Ethiopia, land use changes were studied from a small scale to a large scale (Mekuria et al., 2011; Teferi et al., 2013; Toma et al., 2022; Zeleke & Hurni, 2001). All of these studies demonstrate that natural vegetation, such as forests, grazing lands, and shrublands, has suffered as agricultural land has increased. Agriculture has increasingly moved

from gently sloping terrain into the steeper slopes of the nearby mountains in several areas of Ethiopia's highlands (Toma et al., 2022). In contrast, Bewket & Sterk (2005) note that recent years have seen an increase in woodland areas as a result of afforestation initiatives in the Blue Nile basin. In addition, Teferi et al. (2013), showed that the change in natural vegetation to grassland was dominant, followed by grassland to agricultural land in the Jedeb watershed, Ethiopia.

These land-use changes have significant effects on how the Earth's climate will change in the future, which in turn has significant effects on future land-use changes. One of the most active areas of research internationally in recent years has been global change research. An unprecedented rate and scale of environmental change are being caused by human activity. Land use change is one of the many aspects of global environmental change that is claimed to be intimately correlated with both natural and human processes. Thus, the IGBP and IHDP on global environmental change jointly proposed the land use change research program in 1995, making it the forefront and hot spot of global change research to reveal the interaction between the global environment for human survival as well as the evolving production systems (agriculture, industrialization) (Turner et al, 1995; Vitousek, 1994).

Land-use change models are used by several researchers and experts to investigate the dynamics and causes of land use change and to provide information for policies affecting such change. The RS and GIS technologies are utilized for detecting the change, giving basic data for the model, and then predicting the future land use map (Bal et al., 2021; Kumar et al., 2014; Siddiqui et al., 2017; Sinha et al., 2015). Some of the commonly used models for the projection and simulation of future land use change include Markov Chain Analysis (MCA) (Jafarpour et al., 2022), CA-Markov (Subedi et al., 2013), ANN (Pereira et al., 2019; Rahman et al., 2020), CA-ANN (Islam et al., 2018), and Binary Logistic Regression (Siddiqui et al., 2017). Among these models, CA combined with ANN was used in this study. CA is a common approach to simulating land use maps and can efficiently represent nonlinear, spatially stochastic land-use change processes (Abbas et al., 2021; Almeida et al., 2008).

The fundamental characteristics of CA include: a regular discrete lattice of cells, the evolution of each cell takes place in discrete time points, each cell being in one of a finite set of exhaustive states (no other states are possible), and exclusive (a cell cannot be in more than one state at any one time), the future state of the cells is determined by the current states of the cell itself and the

cells in the neighborhood following transition rules (these rules are identical for all cells in the lattice), the neighborhood relation influences the studied cell. Because of these characteristics, CA can simulate complicated systems (Couclelis, 1985). For example, it simulates several land use types and takes into account spatial interaction, this paradigm has been widely applied in land use change modeling (Abbas et al., 2021; Khawaldah et al., 2020; Ramdani et al., 2021; Siddiqui et al., 2017). It is an effective method for comprehending land-use dynamics and systems (Wu, 2002), especially when combined with additional tools like ANNs (Li & Yeh, 2002). The CA-ANN analyzes hypothetical situations, making it valuable for planning and the assessment of land-use change simulations (Pahlavani et al., 2017).

One of the most crucial elements of a CA model that must be well defined to give appropriate simulation in the context of a CA-based land use model is the transition rule (Couclelis, 1985). To project land usage, a range of techniques were used in the literature, including standard logistic regression (Siddiqui et al., 2017), a combination of linear and geometric formulations (Lau and Kam, 2005), and rule-based models (Betel and Flocchini, 2011). New artificial intelligence techniques have recently been used to simulate changes in land use (Szuster et al., 2011). Artificial neural networks (ANN) (Rahman et al., 2020) and support vector machine (SVM) are the two techniques that have recently been used (Yang et al., 2008). They both showed competitive performance (Szuster et al. 2011). In the present study, the ANN methods were used. ANNs are self-learning computer models that are employed in a variety of fields for pattern recognition. The ANN algorithm can be linked to suitability maps and assumes a relationship between historical and future land-use change. The model "trains" itself on a dataset and the corresponding land-use maps of different years, enabling it to identify and reproduce the pattern of land-use classes (Li & Yeh, 2002). In general, in the ANN-CA model, the CA provides the spatiotemporal framework for land use change simulations, and ANN is applied to discover the local transition rules of the CA in the input layer of ANN. Neurons are a set of cellular attributes, which are social, economic, and physical factors. It was assumed that these attributes determined the land use change probabilities. A neuron in the output layer of ANN corresponds to a land use class. The value of a neuron in the output layer represented the transition probability from the existing class to the corresponding land use class. In general, because of improvements in processing performance and the greater accessibility of powerful and flexible software over the past few years, the usage of ANNs in land-use modeling has significantly grown (Abbas et al., 2021; Liping et al., 2018).

In general, when ANNs were integrated into CA models, their predictive skills can be improved (De Almeida and Gleriani 2005; Li and Yeh 2001; Pijanowski et al. 2002). The widely applied CA-ANN model is modified in three aspects, namely, the multiple land use maps can be input and predicted, a threshold parameter is introduced to make the model controllable and the Monte Carlo method is introduced to determine the final state of the cell. One of the most widely used neural network models is the backpropagation (BP) neural network method, which is a multi-layer feedforward network trained using the error BP technique (Bishop, 1995). It is used to generate the model's transition rule (Li & Yeh, 2002). Figure 2.1 depicts the framework of the proposed model for business-as-usual scenario development.

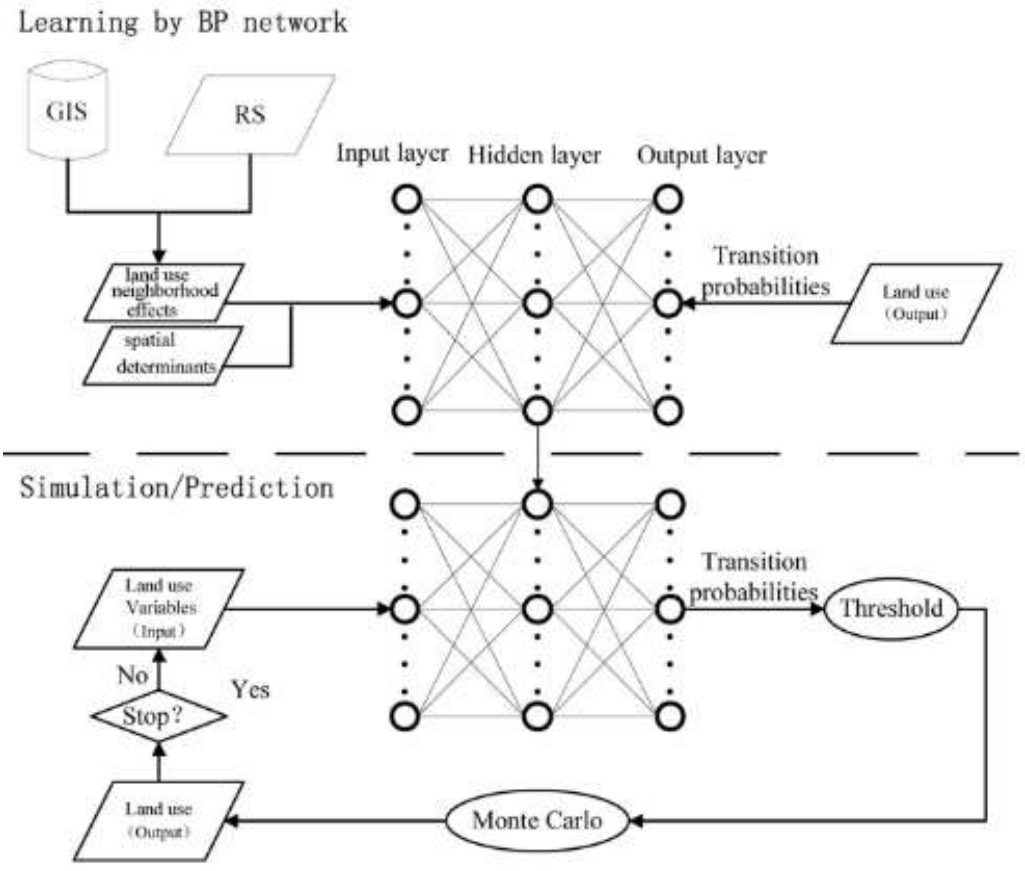

Figure 2. 1 Framework of a dynamic cellular automaton model based on neural networks (Li & Yeh, 2002).

2.7 Climate change impacts on hydrology

Numerous hydrological modeling techniques have been extensively employed in assessing climate change. For instance, the HSAMI lumped rainfall-runoff model demonstrated greater winter

discharge under climate change, resulting in an adjustment of the hydrology and the geomorphological process to the riparian environment (Arsenault & Brissette, 2016; Boyer et al., 2010). The Siruana watershed in Spain was subjected to the Hydrological Modeling System (HEC-HMS), which demonstrated that the local soil moisture conditions had a significant impact on the impact of climate change on water resources (Candela et al., 2012). Seasonal fluctuations in temperature and precipitation were found to be crucial in predicting how watersheds will respond in the future by the hydrological simulation program Fortran (HSPF) carried out in Western Turkey (Göncü & Albek, 2010). Three hydrological models were evaluated for use in assessing climate change by Surfleet et al. (2012) in various basins in the USA. They employed the Variable infiltration capacity (VIC) model as a large-scale method, the PRMS model as a basin-scale strategy, and the Coupled Groundwater and Surface Water Flow Model (GSFLOW) model as a site-specific approach. The findings demonstrate how proper parameterization of a model, estimations of uncertainty, and understating a model's limitations can alter how climate change projections are interpreted.

Bae et al. (2011) compared variations in PET response to climate change in the Chungju Dam basin, Korea, using three distinct hydrological models (PRMS, SLURP, and SWAT). The outcome has shown that while all hydrological models performed similarly during historical calibration for runoff simulation, different outcomes were achieved when future GCM outputs were incorporated into the models. Recent studies (Abbaspour et al., 2007; Basheer et al., 2016) on the effects of climate change on water resources, stream flow, and water quality have made extensive use of the SWAT model. SWAT was chosen as the basic model in this study to simulate the effects of climate change on hydrology. Water resource managers must take into account the possible effects of climate change and global warming, which could further strain the supply of water for human use, the environment, or even extensive animal use (Tu, 2009).

2. 8 Land use change impacts on hydrology

Land use change alters hydrologic processes by influencing ecosystem evapotranspiration, surface and subsurface flow regimes, soil infiltration capacity, transpiration, interception, and conservation (Tu, 2009). Deforestation, for example, can increase streamflow, which may lead to short-term positive feedback. Moreover, the clearing of forests raises the risk of damaging floods and causes increased soil erosion. In the past time, the impact of deforestation and reforestation on

watershed hydrology has been well-understood around the world (Brown et al., 2005; Crouzeilles et al., 2017; Hu et al., 2017; Sun et al., 2004; Swank et al., 2001). Such studies used a "paired watershed" approach or examined long-term hydrologic data for a watershed that experienced land use change. These studies have revealed that changes in land use can impact hydrological processes. For example, Hu et al. (2017) concluded that ecological restoration accounted for 72.18% of the streamflow reduction using a meta-analysis based on field experimental data in the Loess Plateau.

Several studies are also carried out on the hydrology of the watershed by utilizing land use data in different parts of Ethiopia using hydrological and statistical methods (e.g., Chaemiso et al., 2016; Engida et al., 2021; Geremew, 2013; Haile and Assefa, 2012; Setegn et al., 2008; Tekleab et al., 2014; Teferi et al., 2013; Woldesenbet et al., 2017). Most of the hydrological-based study's comparisons of land use change for the different periods showed that the mean wet monthly stream flow increased and the dry average monthly flow decreased. However, conclusions varied significantly. For example, Haile and Assefa (2012) reported that the mean wet monthly streamflow increased by 39% and the dry average monthly flow decreased by 46% for the 2011 land use relative to the 1985 land use due to land use change in the Angereb watershed in Ethiopia. Bekele et al. (2021) found that land use change affected the water balance of the Keleta watershed, Ethiopia. An increase in the volume of surface runoff and base flow by 10.4% and 0.6%, respectively, and a decrease in groundwater flow (3.5%) were estimated during the period 1985–2010 because of land use changes.

Most of these evaluations focused on a base land use change (earlier year) and changed land use (later year). The base and changed land uses are used individually as inputs for a hydrological model, and the model responses for different land use changes are used to represent the land use impacts on hydrology. The disadvantage of these approaches is that the land use is assumed to be unchanged over a period, whereas, in reality, it is dynamically changing. In contrast, the land use transition models can provide land use change dynamics over a period, which provides the potential for hydrological models to represent the dynamic land use change processes. Furthermore, land use transition models can project possible future land use scenarios, which could integrate projected climate data to assess the combined impacts of climate change on hydrology (Fan & Shibata, 2015). Because climate and land use change are likely to occur jointly in the future, assessing combined climate and land use change impacts on hydrology is important for

future land use planning and sustainable water resource management (Fan & Shibata, 2015; Tong et al., 2012).

On the other hand, the effectiveness of watershed management practices such as terracing, filter strips, and contour in improving the moisture holding capacity and reducing surface runoff has been studied in various hydrological modeling studies (Arnold et al., 2012; Berihun et al., 2020; Worku et al., 2020b). However, there is limited information about their effectiveness in reducing the impact of climate and land use change on the Baro basin.

2.9 Climate and land use change impacts on hydrology

As climate and land use change and their impacts become pressing issues, it is useful to understand the effect they will have on water resources (IPCC, 2019; Praskievicz & Chang, 2009). The quantity of river water could be dramatically impacted by climate and land use changes, and their negative consequences could lead to a decline in the services it provides. Most of the previous studies have quantitatively evaluated the hydrologic impact of climate or land use changes individually (e.g., Koch et al., 2012; Mengistu et al., 2022a; Taye et al., 2018; Teferi et al., 2103; Woldesenbet et al., 2017; Worku et al., 2021; Worqlul et al., 2018; Zhang et al., 2019). However, only a few studies have analyzed and compared the combined impact of climate and land use changes on hydrology (e.g., Getachew et al., 2021; Fan & Shibata, 2015). These studies have revealed that changes in climate and land use can impact hydrological processes. Because of this, analyzing the effects of climate change and land use change has received a lot of attention in the past 20 years (Guo et al., 2008; Legesse et al., 2003; Mango et al., 2011; Yang et al., 2017). As a result, it is very helpful and valuable to estimate and understand how hydrology will respond to future changes in climate and land use to optimize water management, land-use planning, management, and policy in a basin. Analyzing the effects of land use and climate change on hydrological responses is also difficult due to changes in hydro-meteorological variables and basin features at various spatiotemporal scales.

Methods used to assess the impacts of climate and land use change on hydrology can be classified as (i) experimental paired catchment approach, (ii) statistical techniques; and (iii) hydrological model. Among these techniques, the paired catchment approach is the most difficult but often considered the best approach for smaller catchments. However, the applicability of the paired catchment approach over large catchments may not be possible (Lørup et al., 1998) since it requires

years of continuous monitoring to gather sufficient data for the analysis. Statistical trend detection tests have been proven to be very useful in qualitatively determining the presence of a significant trend in the time series along with direction and rate of change (Li et al., 2009; Zhang et al., 2008). But these techniques cannot be used for quantifying the change and attributing it to a particular cause due to a lack of a physical mechanism (Li et al., 2009). Hydrological models are also useful research tools in the study of climate and land use change. Mathematical equations are the foundation of empirical models. Based on the process description, there are three types of hydrological models (Cunderlik, 2003).

Lumped models: these hydrologic models do not vary geographically within the basin or watershed, and thus, the parameters are spatially averaged to a single value for the whole modeled area without explicitly considering the response of each sub-basin. This method is known as conceptual models, which are simple hydrologic models that require only a few parameters to simulate a catchment. The parameters often do not characterize the physical features of hydrologic processes and usually involve a certain degree of empiricism, and thus may lack the ability to correctly represent a catchment. These models are not commonly applicable to event-scale processes. If the goal is to estimate the discharge, these models can provide comparable simulations to complex physically based models (Seiller et al., 2012).

Distributed models: by far the most appealing tools for conducting impact assessment studies are distributed, physically based hydrologic models (Mango et al., 2011; Wang et al., 2012). These models operate within a distributed framework to take the meteorological and physical conditions of the basin or watershed into account. These hydrological models are fully allowed to vary in space at a resolution usually chosen by the user. The distributed modeling approach attempts to incorporate data concerning the spatial distribution of parameter variations together with computational algorithms to evaluate the influence of this distribution on simulated precipitation-runoff behavior. Distributed models generally require a large amount of (often unavailable) data. However, the governing physical processes are modeled in detail, and if properly applied, they can provide the highest degree of accuracy (Abbott, 1996).

Semi-distributed models: the parameters of semi-distributed models are partially allowed to vary spatially by dividing the basin into several smaller sub-basins. The main advantages of these models are that their structures are more physically based than lumped models' structures, and they

require fewer input data points than fully distributed models. Due to their extensive parameterization, fully distributed hydrological models are difficult to apply at a large basin scale, which makes comparatively less demanding semi-distributed hydrological models a practical option. Many recent studies (Kiprotich et al., 2021; Teklay et al., 2021; Tong et al., 2012; Woldesenbet et al., 2018; Yin et al., 2017) demonstrate that hydrological models such as SWAT can estimate the components of the water balance and assess the effects of climate or land use change. This study presents a semi-distributed hydrologic modeling-based approach to evaluate the individual and combined impacts of climate and land use change on hydrology.

2.6.1 Soil and water assessment tool model

The United States Department of Agriculture's Agricultural Research Service created the SWAT over about 30 years of modeling. It was created to predict the effects of land management techniques on water, sediment, and agricultural chemical yields over many years in large, complex watersheds with a range of soil, land use, and management circumstances. SWAT has several advantages, including the ability to be used at various temporal scales, a spatially distributed model, open access with in depth documentation, and the ability to use multiple-input constraints and a process-based hydrological model. The model has recently gained recognition on a global scale as a reliable interdisciplinary watershed modeling tool. SWAT is used globally and is regarded as a flexible model that can be used to combine many environmental processes, allowing for more effective watershed management and the formulation of more informed policy decisions (Arnold et al., 1998; Gassman et al., 2007).

In SWAT, a watershed is split up into sub-basins, and these sub-basins are then split up into hydrological response units (HRUs) with uniform land use, soil, and management characteristics. The soil water balance is taken into account in each HRU. Snow, the soil profile, the shallow aquifer, and the deep aquifer are its four storage volumes. There may be multiple strata in the soil profile. Infiltration, percolation, evaporation, plant absorption, and lateral flow are all components of the soil water cycle (Neitsch et al., 2011). The hydrological process estimates surface runoff using the SCS curve number or Green-Ampt infiltration equation. Using layered storage routing and a crack flow model, percolation can be estimated. Potential evapotranspiration can be simulated by using the Priestley-Taylor, Hargreaves, or Penman-Monteith methods. Using the

Modified Universal Soil Loss Equation (MUSLE), the SWAT model can also simulate erosion from the watershed (Arnold et al., 1998; Neitsch et al., 2011).

2.6.2 Indicators of hydrological alteration software

The IHA is a software program that offers important information for those trying to recognize the hydrologic effects of human activities or generate environmental flow recommendations for water resource managers (The Nature Conservancy, 2009). This tool has been used by nearly 2,000 water resource managers, hydrologists, ecologists, researchers, and policymakers from around the world to analyze potential water management strategies or to study how human activities have altered rivers, lakes, and groundwater basins through time. The IHA methodology, which is conceptually based on the Range of Variability Approach (RVA), is used to evaluate the degree of alteration to the natural flow regime due to dam construction and projected climate change (Richter et al., 1996). It is useful to compare flow parameters under different scenarios and particularly for assessing key flow regimes characteristics, such as magnitude, timing, frequency, and duration (Pradhanang et al., 2013). Magnitude is a measurement of the volume of flow associated with a specific hydrologic event; frequency describes how frequently events occur within a given period; duration is the length of an event (above a certain flow rate threshold); timing is when the event takes place within a specific period; and rate of change is how rapidly the hydrograph falls and rises; the pulse is defined as an event that takes place above or below a certain threshold. Hydrologic pulses can be defined as the daily mean water condition that either rises above the 75th percentile (a high pulse) or drops below the 25th percentile (low pulse) of the mean daily values. The IHA program, for instance, may determine the date and maximum flow of the largest floods or lowest flows each year. It can then determine the mean and variation of these values for a certain period. To describe statistically how these patterns have evolved for a specific river or lake as a result of sudden effects like dam construction or more gradual trends brought on by changes in land- and water use, comparative analysis can be used. In general, to investigate the degree of hydrologic change in ecologically important statistics, the IHA estimates 67 hydrologic parameters resulting from daily streamflow statistics. These are divided into two categories: 34 environmental flow components (EFC) and 33 IHA parameters (Annex 6.1). Further information on the IHA methods is available in the Indicators of Hydrologic Alteration Version 7.1 User's Manual.

2.10 Hydrological evaluation of satellite rainfall estimates

In recent times, hydrological analysis and simulations have used satellite precipitation products with high temporal and spatial resolution over a wide range of locations to provide new information to support water resources management globally. Satellite-based precipitation products are particularly useful for hydrological simulation in large watersheds in developing countries or remote locations because they can effectively extend precipitation estimates to regions where conventional measuring stations are scarce, unevenly distributed, or erratic. Furthermore, the selection of the optimal precipitation data for hydrological models depends on the basin, and it is becoming more accepted that the choice of the precipitation input is more crucial than the hydrological model itself (Dhanesh et al., 2020; Tuo et al., 2016).

Satellite-based precipitation products vary in terms of their domain sizes, sources, and methods of acquisition, as well as their geographical and temporal resolutions. These products need to be assessed in terms of how well they capture the spatiotemporal variability in rainfall when compared to observed rain gauge data because they are an indirect estimate of rainfall (Gao et al., 2013; Luo et al., 2019). A statistical assessment of the skill of different rainfall datasets to simulate streamflow within a hydrological modeling framework provides a good approach for comparing rainfall data (Getirana et al., 2011; Wilk et al., 2006). Several studies have been conducted to assess the suitability of several gridded satellite climate products, particularly the CFSR, TRMM, and CHIRPS precipitation datasets for streamflow simulation using various hydrological models (Bitew et al., 2012; Dhanesh et al., 2020; Luo et al., 2019; Tuo et al., 2016). However, investigations revealed different results in terms of how well the datasets drive hydrological models. The findings of these studies demonstrated that the structure of the model, climate, and topography have a significant impact on the performance of SREs.

The majority of the hydrological assessment research results show that the satellite climate products can be used for hydrological modeling when the model is calibrated to each climate product independently (Camici et al., 2018; Tuo et al., 2016). Although gridded rainfall datasets have been extensively employed in hydrological modeling research, biases and uncertainties related to the data have been found to affect the model calibration and, subsequently, hydrological simulations (Uhlenbrook et al., 2010). The degree of inaccuracy introduced in the hydrological simulations varies with the geographic region as a result of the uncertainty in rainfall among the

datasets, which is then translated into error in the estimations of streamflow (Gebrehiwot et al., 2013). Thus, climate variability must be taken into consideration in hydrological modeling since it influences the performance of gridded datasets. A dataset that could depict the geographical variety of rainfall in each geographic location may perform differently in another area. Furthermore, it is important to note that the errors of satellite products are compensated by model parameters when the model is recalibrated. Therefore, satellite product evaluation at specific watersheds and quantifying the effect of model recalibration on hydrological performance are very important.

3. Materials and Methods

3.1. Conceptual framework

A conceptual framework is intended to aid in gaining a comprehensive understanding of the individual and combined effects of climate and land use change on the hydrology of the basin. The basin can be expected to continue to change in the future due to climate and land use changes. The SWAT is a comprehensive hydrological model that is based on physical mechanisms and provides a framework for analysis. The methodology includes four phases: performance evaluation of RCMs using several statistical approaches; hydrological model calibration and validation using three independent climate datasets and spatial data including DEM, land use, and soil; projection of future climate and its impact; and evaluation of the individual and combined impacts of climate and land use change on the hydrology. Figure 3.1 provides the general conceptual framework of the study procedures.

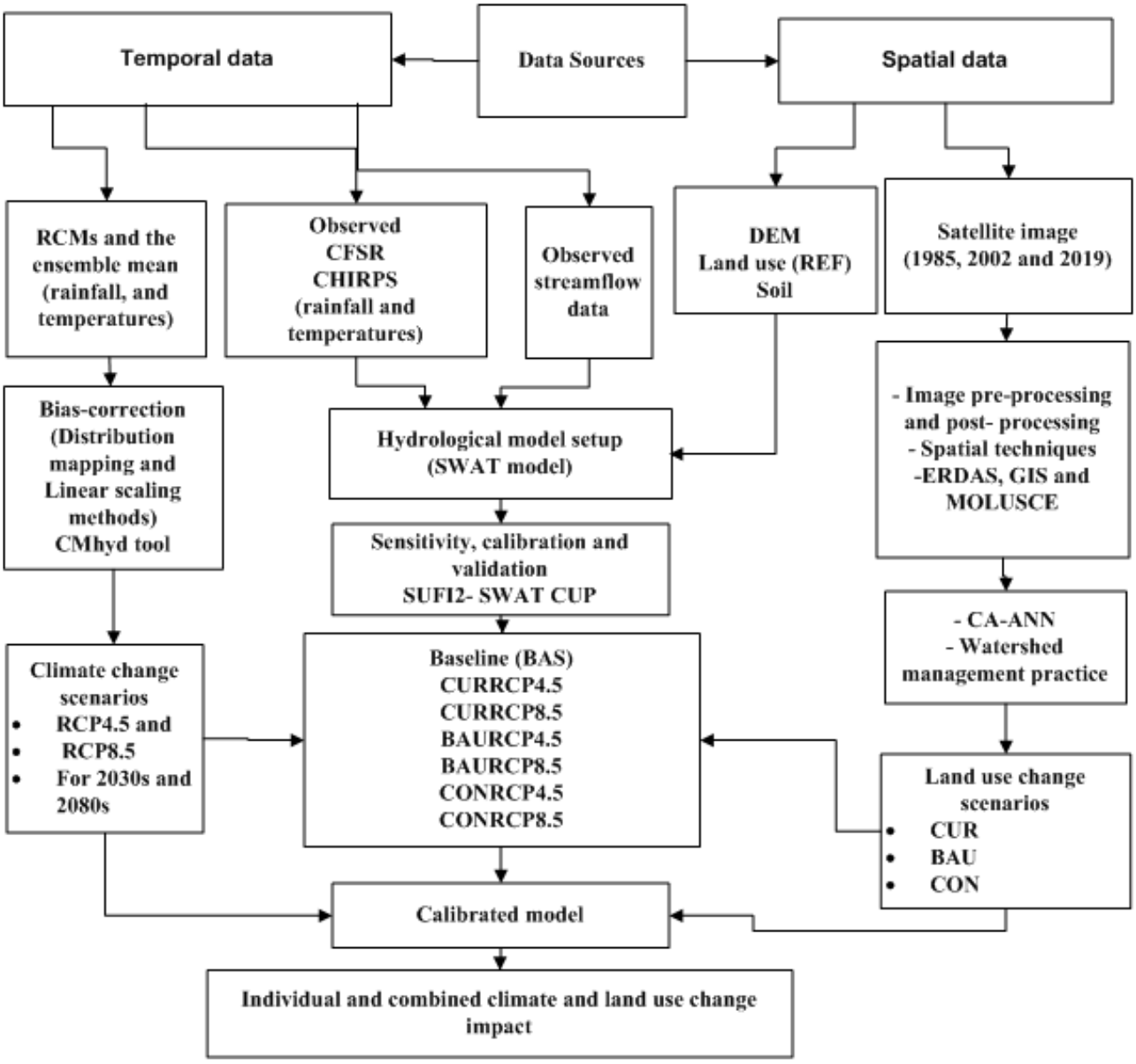

Figure 3.1 The conceptual framework of the study procedures used to study the climate and land use change impacts on the hydrology.

3.2 Description of the study area

3.2.1 Location

The Baro–Akobo River basin is one of the 12 major river basins of Ethiopia. The basin has high strategic significance for Ethiopian development, at both the regional and national levels. It is situated between 5° 31` and 10° 54` North latitudes and 33° and 36° 17´ East longitudes (Figure 3.2). It drains from the western highlands of Ethiopia to the Sudanese border to join the White

Nile. It is bordered by South Sudan in the west and southwest, Sudan in the northwest, and the Abbay and Omo–Gibe basins in the east. Parts of the Benshangul-Gumuz, Gambella, Oromia, and SNNP administrative areas are included in the basin. In the Eastern Nile basin, it is the second-largest sub-basin, next to the Abbay (Blue Nile) sub-basin. The Baro-Akobo-Sobat (White Nile) sub-basin, the Abbay (Blue Nile) sub-basin, the Tekeze-Atbara sub-basin, and the main Nile basin from Khartoum to the Nile delta are the four sub-basins that make up the Eastern Nile Basin. It drains from the western highlands of Ethiopia to the Sudanese border to join the White Nile. The basin area is approximately 75,912 km^2 and its major river is 380 km long. It has a complex topography with an elevation range of 293 to 3266 meters above sea level (masl), which results in different rainfall regimes. The complex terrain and land surface heterogeneity and their interactions with large-scale climate forcings contribute to the diverse spatial rainfall patterns over the basin. The geographic distribution of the hydro-meteorological stations in the basin is presented in Figure 3.2.

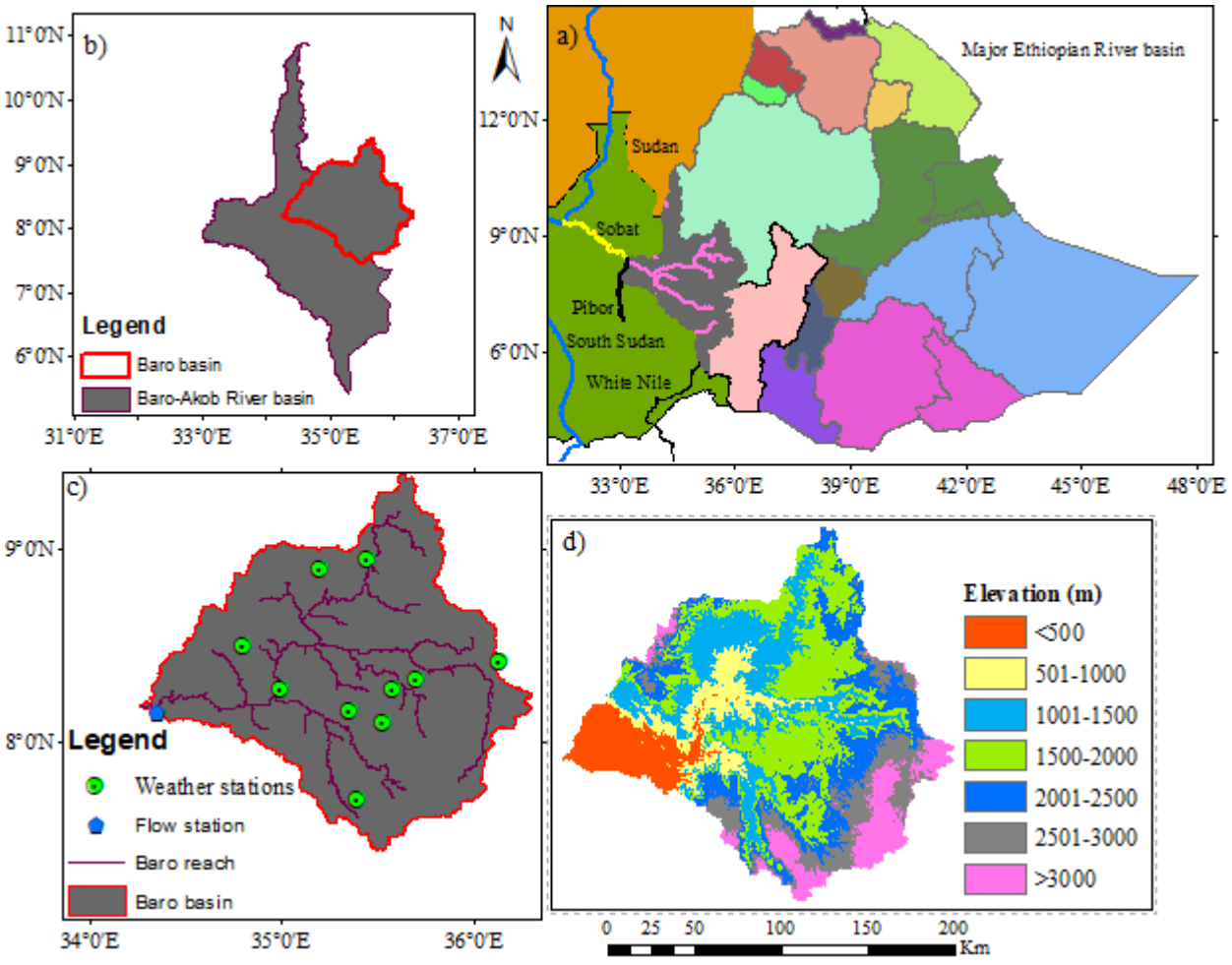

Figure 3.2 Location map of the study area, a) Major Ethiopian river basin, the downstream countries, White Nile and tributaries b) Baro-Akobo River basin c) weather and flow stations, and d) elevation of the basin.

3.2.2 Climate and hydrology

In this study, 12 weather stations were used because of their reliability and better data quality for rainfall estimates. However, only six of the 12 stations have good records of the daily maximum and minimum temperatures. Rainfall and temperature in the basin show substantial spatial and seasonal variability. The basin predominantly has a tropical monsoon climate with distinct wet and dry seasons. Months from March to October represent the wet season, while months from November to February represent the dry season (Figure 3.3). The mean annual rainfall in the basin from 1975–2005 varied from 1251 mm to 2400.6 mm (Table 3.1). The mean rainfall in the basin is estimated to be 1749.8 mm/year, with mean daily maximum and minimum temperatures of 26.8 and 13.4°C, respectively.

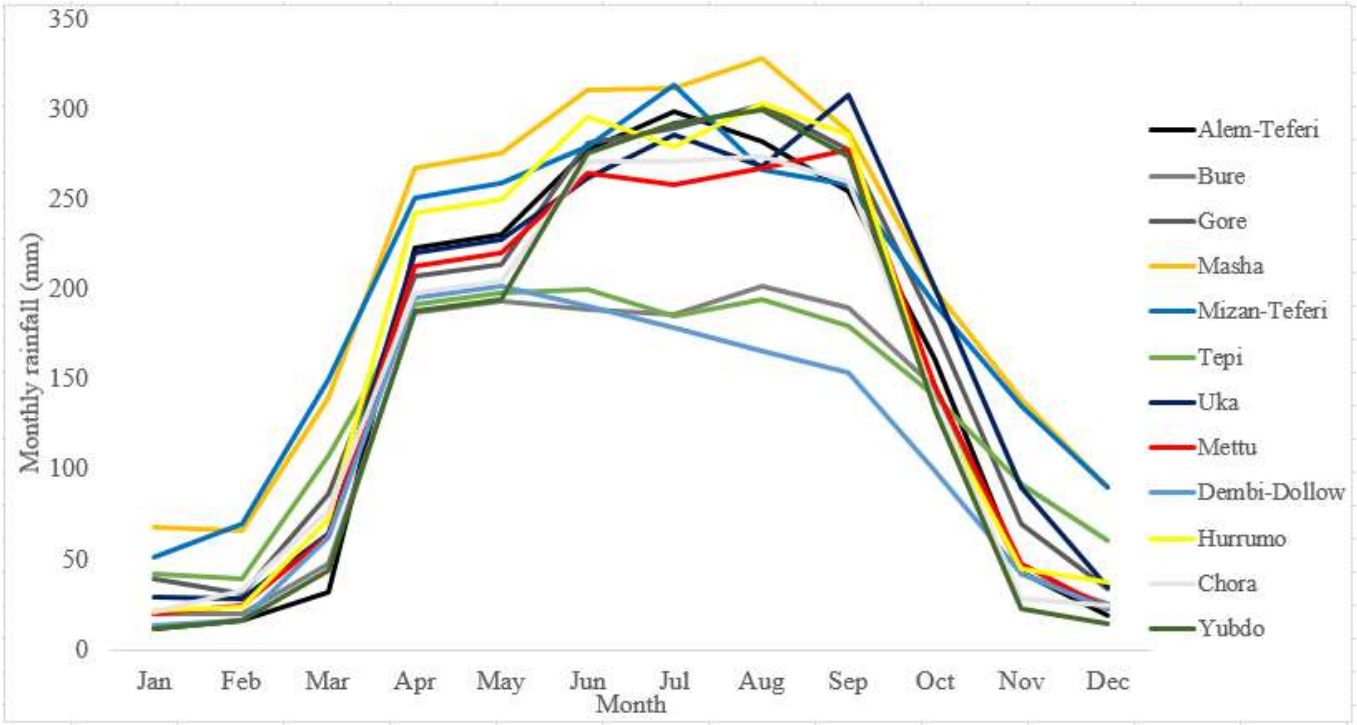

Figure 3.3 Mean monthly rainfall (mm) of selected weather stations in the Baro–Akobo basin for the period (1975–2005).

Table 3.1 The weather stations considered in this study with their annual summer statistics of the Baro-Akobo basin for the period 1975–2005.

Station	Lon	Lat	Min.	1st Qu	Mean	3rd Qu	Max.	sd	cv	Skewness	Missing data(%)
Alem-Teferi	35.2	8.9	1172	1491	1695.8	1815	2799	344	0.20	1.16	8.6
Bure	35	8.3	993	1206	1343.6	1480	1673	194	0.14	0.18	10.2
Gore	35.5	8.1	1446	1751	1911.4	2040	2684	261	0.14	0.90	1.13
Masha	35.4	7.7	1879	2123	2400.6	2529	3328	374	0.16	1.00	8.1
Mizan-Teferi	35.6	7	1545	1898	2289.8	2236	3001	364	0.17	0.85	19.7
Tepi	35.4	7.2	1216	1431	1591.3	1740	2098	225	0.14	0.15	14.2
Uka	35.4	8.2	1508	1713	1909.4	2048	2794	297	0.16	1.28	20.2
Mettu	35.6	8.3	828	1622	1704.4	1913	2180	325	0.19	-1.00	4.2
Dembi-Dollo	34.8	8.5	871	1142	1251	1368	1499	165	0.13	-0.43	11.3
Hurumu	35.7	8.3	1257	1578	1851.8	1867	3010	464	0.25	1.19	8.6
Chora	36.1	8.4	1012	1494	1706.9	1913	2159	315	0.18	-0.47	7.7
Yubdu	35.5	9	1332	1508	1659.6	1769	2002	194	0.12	0.17	14.4

3.2.3 Land use and soil

The main forms of land cover in the basin include forest, agriculture, grassland, and scrubland. Perennial and cash crops like coffee, mango, and avocado are examples of major crops in the basin. Since the soils in the river basin are typically deep and rich in organic matter, they have a great potential for infiltration. Chromic Cambisols, and Eutric Gleyisols are among the dominant soil type in the basin. Wide variations in soil types are seen in the basin. This is one of the basin's distinctive features that helps determine its hydrologic characteristics. Figure 3.4 shows the spatial distribution of different land uses and soil types in the basin.

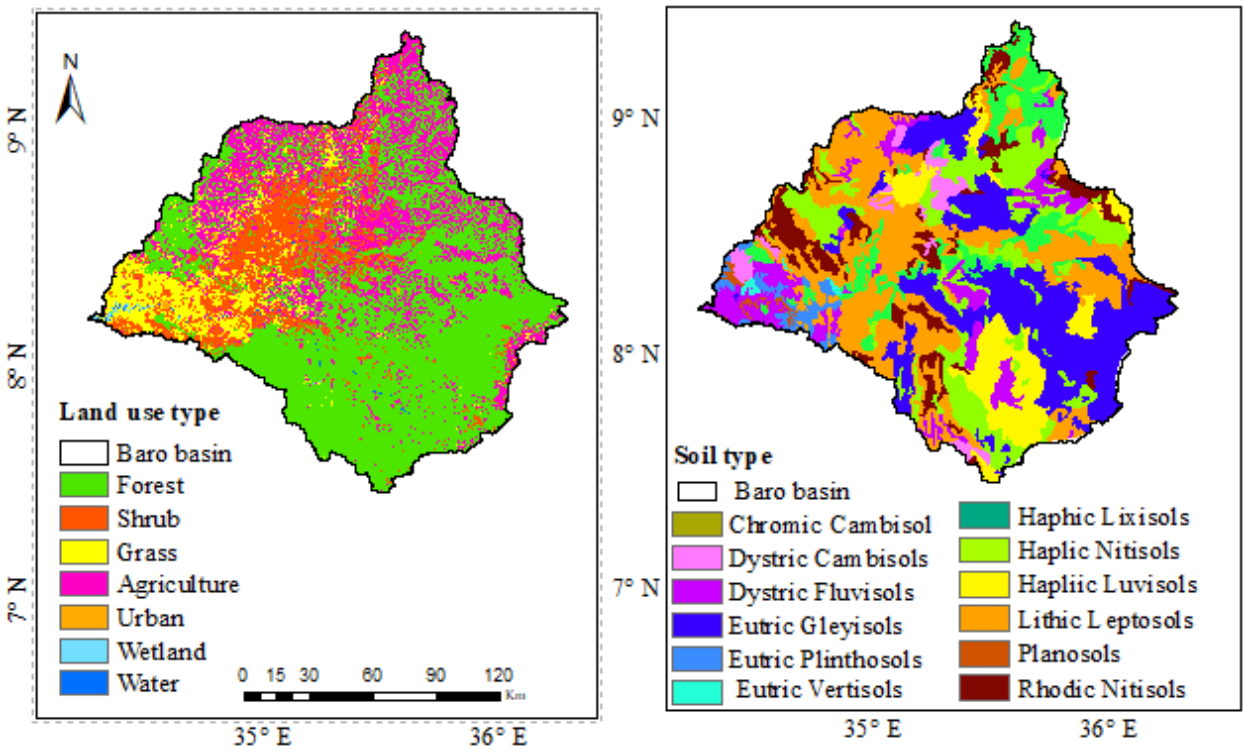

Figure 3.4 Land use (a) and soil map (b) of the Baro basin

3.2.4 Development of natural resources/water resources

One of Ethiopia's most widely used river basins is the Baro–Akobo. With an area of 75,912 km^2, or 6.9% of the country, the basin is the second-smallest river basin among the Ethiopian major river basins. However, it has the second-highest runoff potential (23.6 Bm^3), 27 percent of the country's potential irrigable land, and 8.9 percent of the hydropower potential (Awulachew et al. 2007). In the basin, a variety of hydropower and irrigation schemes, ranging from small-scale to large-scale, have been widely used. The Birbir A, Birbir R, Baro-1, Baro-2, Geba-A, Geba-R, Itang, and Gilo-2 are among the numerous water resources development projects currently being planned and implemented in the basin. These projects will impact the local area and downstream Nile countries such as Sudan and Egypt (Sileet et al., 2013).

One of Ethiopia's wettest and best-watered regions is the Baro–Akobo River basin wetland. For instance, the Machar Marshe, which is part of the basin, is one of the peculiar features of the basin's extensive wetland area. Local rainfall, torrents flowing from the western Ethiopian plateau, and runoff from the Baro, Akobo, Gilo, and Alwero rivers all contribute to the feeding of the wetlands (Sileet et al., 2013). The Baro–Akobo River basin is home to three of Ethiopia's four

UNESCO-designated biodiversity sites. The Yayu Coffee Forest Biosphere Reserve, the Sheka Forest Biosphere Reserve, and the Kafa afromontane cloud forests are known to contribute to the unique biological diversity of the basin (UNESCO, 2012). Both plant and animal species are abundant in the forest. In all ecosystems, there are more than 300 higher plants, 50 animals, 200 bird species, and 20 amphibian species. Of them, Ethiopia is home to at least 55 plants and 10 bird species alone. Additionally, the area is home to around 38 endangered species, including 30 plant species, 3 animal species, and 5 bird species. In general, the richness of the river basin's plants and animals is noteworthy. Major rivers like the Baro and Akobo rivers, which are the principal tributaries of the White Nile, are also derived from it. The forest is also highly recognized for preserving biodiversity, preventing floods and erosion, and sequestering carbon to lessen the consequences of climate change.

3.3 Data collection

3.3.1 Historical and future climate change scenarios

The National Meteorology Agency of Ethiopia provided the baseline observed daily rainfall maximum and minimum temperature data used in this study for the period 1975–2010. In addition, to analyze the historical and future climate data for the basin, seven RCMs (RCA4 (CNRM), RCA4 (ICHEC), RCA4 (MPI), CCLM4 (CNRM), CCLM4 (ICHEC), CCLM4 (MPI), and REMO (MPI)) and the ensemble mean under RCP4.5 (medium) and RCP8.5 (extreme) emission scenarios were obtained from the CORDEX Africa data portal (http://www.cordex.org). Climate data (rainfall and temperature) is initially obtained from each RCM. The distribution mapping (DM) and linear scaling (LS) techniques are employed to correct biases in the historical and future climate data for the basin. Because the RCM output of the given grid is the spatial mean of this grid, for each weather station point, the RCM dataset of the grid containing this point is extracted using a point-to-pixel approach. Annual rainfall statistics for the observed and the raw and bias corrected RCMs for annual rainfall are presented in Figure 3.5. Further information is available in chapters 4, 6, and 7.

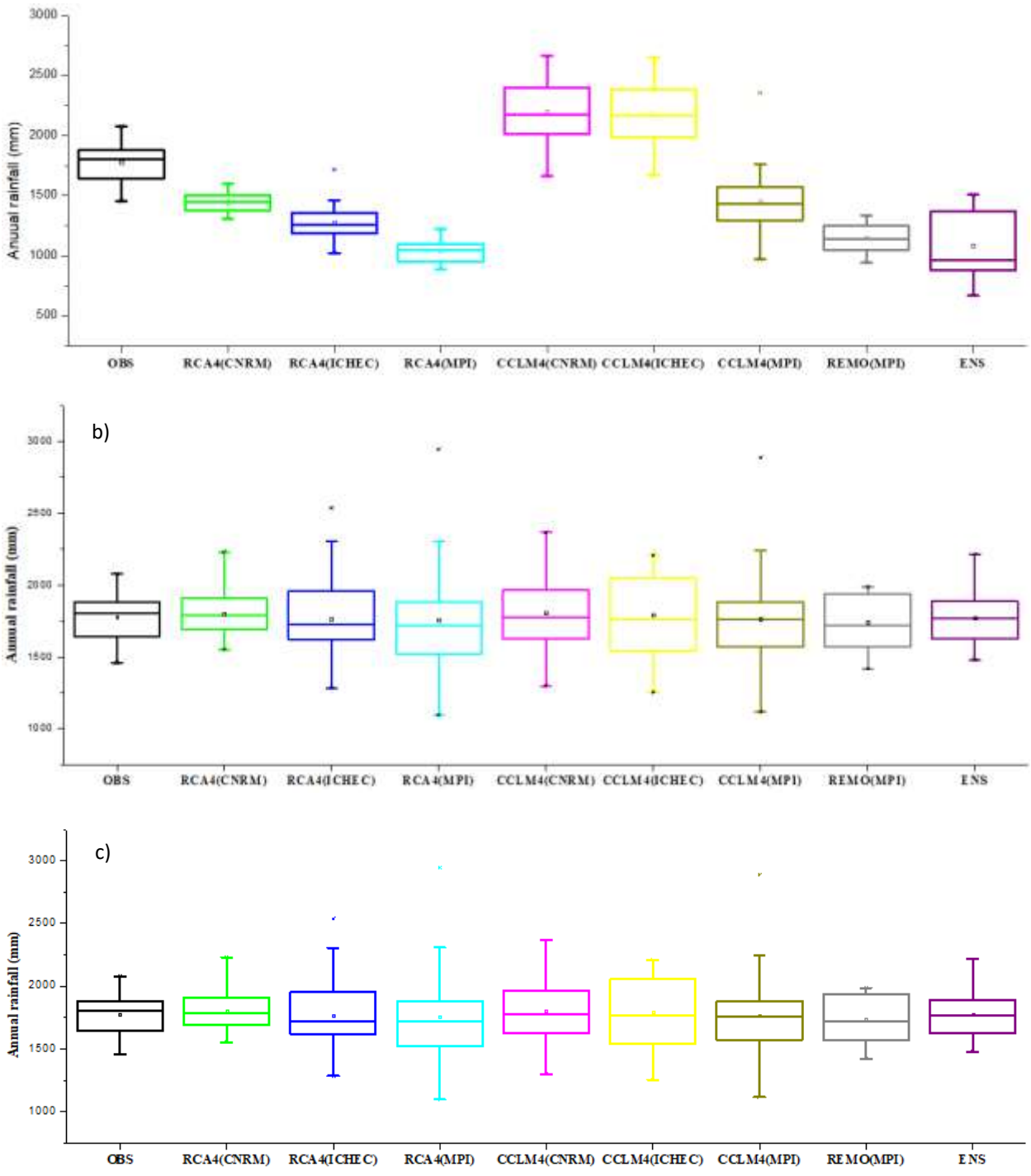

Figure 3.5 Annual rainfall statistics for the observed with a) raw, b) DM, and c) LS bias corrected RCMs for the Baro–Akobo basin for the period 1975–2005.

3.3.2 Data quality check

A total of 12 stations were chosen and used as a benchmark to assess the effectiveness of RCMs and SREs. The double mass plot (Figure 3.6) is used to evaluate the consistency and continuous data of these stations (Searcy & Hardison, 1960). The double mass curve analysis revealed that there had not been a substantial break in the time series of the chosen rain gauge stations. Following a gauge consistency check, Multiple Imputation by Chained Equation (MICE), available in R programming, was used to impute missing data from the chosen gauge stations (van Buuren & Groothuis-Oudshoorn, 2011).

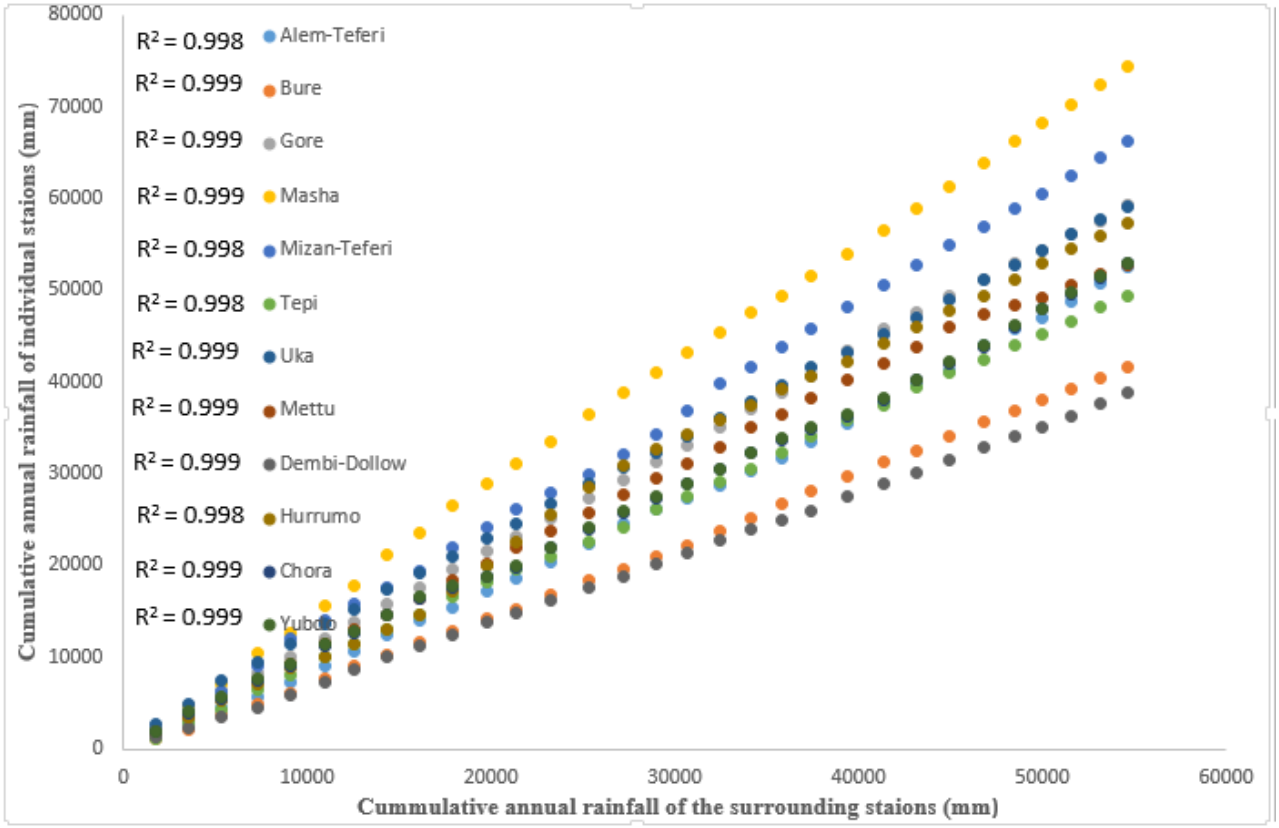

Figure 3.6 Double mass curve used to show the consistency of the weather stations.

3.3.3 Historical and future land use

Land use classification

In this study, land-use maps of 1985 (Landsat 4–5 Thematic Mapping (TM)), 2002 (Landsat 7 Enhanced Thematic Mapping (ETM+)), and 2019 (Landsat 8 Operational Land Inventory (OLI)) were obtained from the USGS at http://earthexplorer.usgs.gov/. Each image has a spatial resolution

of 30 m. The maximum likelihood classifier (MLC) algorithm was used for image classification undertaken in ERDAS Imagine 2014. To determine the accuracy of land use classification, the users, producers, the overall classification, and the kappa coefficient were also estimated using ERDAS. The accuracy assessment is measured by applying Kappa statistical analysis (K). After analyzing the land-use patterns from 1985–2019, seven major land-use classes were identified: forest, agricultural land, shrubland, grassland, built-up areas, wetlands, and water bodies. Further information is available in chapter 7 and Annex 7.6 and 7.7.

Transition Potential Modeling and Model Validation

The MOLUSCE plugin integrates some well-known algorithms for transition potential modeling, such as the ANN (multilayer perceptron), weights of evidence, multi-criteria evaluation, logistic regression, and CA algorithm, for future simulation. In this study, the CA-ANN approach for transition potential modeling and projection was used. The spatial variables for model calibration were chosen based on their relatively good association with the land use map, as measured by Cramer's coefficient. Land use data from 1985–2002 and 2002–2019, along with spatial variables, were employed to project land use maps for 2019 and 2040 (business as usual), respectively. After obtaining the projected land use map, the current land use map of 2019 was compared with the projected land use map and obtained an acceptable % of correctness, Kappa (overall), Kappa (historical), and Kappa (location) value of 83.48%, 0.71, 0.89 and 0.79, respectively. Further information is available in chapter 7 and Annex 7.8.

Projection of land use map

After obtaining acceptable results from model validation, the land use map for 2040 (the BAU land use scenario) was predicted. For this purpose, the temporal land use data from 2002 and 2019, the spatial variables such as slope and DEM, and the transition probability matrix were employed to predict the land use map for 2040 using the CA-ANN multilayer perceptron approach (MLP) within the MOLUSCE (Abbas et al., 2021). On the other hand, this study considered a further increase in altitudinal forest expansion and watershed management practice (conservation). Detailed information is available in chapter 7.

3.3.4 Hydrological model setup

Hydrological models are generally employed as a standard tool for studying hydrological processes, many of which have varying applications, ranging from small watersheds to worldwide models. Each model has unique applications, characteristics, advantages, and disadvantages. In this study, the SWAT model is used to estimate the water balance of the baseline and future climate and land use changes. The model has shown good performance in estimating the separate and combined climate and land use change impacts (Kiprotich et al., 2021; Teklay et al., 2021; Zhang et al., 2018).

ArcSWAT 2012.10.24 compatible with ArcGIS 10.4 was used to set up the model. Using the automatic watershed delineation tool in ArcSWAT, basin properties such as slope gradient, slope length, and stream network were extracted from the DEM. A threshold area of 210 km^2 was used during the SWAT model setup. The HRUs are the smallest modeling units with a similar area of aggregated land use, soil, and slope. Multiple HRU creation approaches were used with a 2, 20, and 10% threshold for land use, soil, and slop units, respectively. The land use, the soil, and the slope class derived from the DEM were overlaid together to produce 71 sub-basins and 773 HRUs in the basin. Following this spatial data setup, the weather data from each station were used to run the model. The centroid method was used to link the weather station data to the subbasin (Neitsch et al., 2011; Dile and Srinivasan, 2014). The SWAT model estimates the important hydrologic components for each HRU unit based on the following water balance equation and their outputs are aggregated at the basin level to compare the baseline with the future period and scenarios (Neitsch., 2011).

$$S_{wt} = S_{wo} + \sum_{i=1}^{t}(R_{day} - Q_{surf} - E_a - E_{seep} - Q_{gw}) \quad \text{.....3.1}$$

Where, S_{wt} is the soil water content (mm), S_{wo} is the initial soil water content (mm), R_{day} is the amount of precipitation (mm), Q_{surf} is the surface runoff (mm), E_a is the amount of evapotranspiration (mm), E_{seep} is the soil infiltration I (mm), and Q_{gw} is the return flow (mm). In this study, surface runoff was estimated using the curve number (CN) method, potential evapotranspiration was estimated using the Penman-Monteith equation and the channel routing processes were simulated using the Variable Storage Routing method (Neitsch et al., 2011).

3.3.5 Parameter sensitivity, calibration, and validation

Successful application of a hydrologic model depends on parameter sensitivity analysis and model calibration and validation processes. This study used the SUFI2 algorithm in the SWAT-CUP to conduct sensitivity analysis, calibration, and validation (Abbaspour et al., 2015). Model calibration and validation processes are determined using the most sensitive parameters for a given watershed. In this study, eighteen model parameters were selected for sensitivity analysis based on SWAT default values and literature recommendations (Dile et al., 2013; Mengistu & Sorteberg, 2012; Setegn et al., 2008).

The streamflow data for the period 1988–1989 was used for model warm-up. Model warm-up is used to initialize different biophysical processes in the model to get the full hydrological cycle operational. The model was calibrated using observed streamflow data at the Baro and Sore River gauging stations for the period 1990–1998. Model calibration involves the adjustment of sensitive model parameter values until a reasonable model simulation performance is achieved. The model was validated using observed streamflow at both stations for the period 1999–2002. Model validation is the process of evaluating the performance of the calibrated model on an independent dataset without making further parameter adjustments.

3.3.6 Model performance evaluation

The model performance was evaluated using NSE, R^2, and PBIAS as presented in the following equation. The NSE is a normalized statistic that estimates the relative magnitude of the residual variance compared to the observed and determines how well the plot of observed versus simulated data fits the 1:1 line (Nash & Sutcliffe, 1970). The R^2 describes the proportion of variance in observed and simulated data, and its value ranges between 0 and 1, with higher values indicating less error variance (Krause et al., 2005). PBIAS measures the average tendency of the simulated data to be larger or smaller than the observed data. Low values of PBIAS designate an accurate model simulation in which positive values indicate model underestimation and negative values indicate model overestimation bias (Gupta et al., 2009).

$$NSE = 1 - \frac{\sum_{i=1}^{n}(O_i - s_i)^2}{\sum_{i=1}^{n}(O_i - \bar{O})^2} \quad \ldots\ldots (5.2)$$

$$R^2 = \frac{[\sum_{i=1}^{n}(o_i - \bar{O})\,(s_i - \bar{s})]^2}{\sum_{i=1}^{n}(O_i - \bar{O})^2 * \sum_{i=1}^{n}(s_i - \bar{s})^2} \quad \ldots\ldots (5.3)$$

$$PBIAS = \frac{\sum_{i=1}^{n}(o_i - s_i)*100}{\sum_{i=1}^{n}(o_i)} \quad \text{..... (5.4)}$$

Where O_i is the observed streamflow (m^3/sec), S_i is the simulated streamflow (m^3/sec), $\bar{0}$ is the average measured streamflow (m^3/sec); $\bar{s}$ is the average simulated streamflow (m^3/sec) and n is the number of observations. Based on the values of the performance parameters above, the model simulation may be considered satisfactory when the NSE > 0.5, R^2 > 0.5, and PBIAS = ±25% for streamflow simulation (Moriasi et al., 2007).

3.3.7 Model prediction uncertainty

The calibrated model uncertainty analysis was estimated using the SUFI-2 algorithm in the SWAT-CUP. Generally, model uncertainty may arise due to several sources, such as driving variables (e.g., climate data), model conceptualization, model parameters, and observed data (e.g., streamflow). SUFI-2 handles all sources of uncertainty as parameter certainty and measures uncertainty in terms of p-factor and r-factor. The p-factor has a range of values from 0 to 1, with 1 representing the ideal value or 100% of observed data being bracketed in the 95PPU band. For streamflow simulation, the value of the p-factor is suggested to be greater than a threshold of 0.7 to indicate a highly acceptable simulation result. The ratio between the 95PPU band's average width and the standard deviation of the observed variable is used to calculate the r-factor, which displays the 95PPU band's thickness. Ideally, the r-factor should be near zero. For streamflow simulation, the value of the r-factor is suggested to be less than a threshold of 1.5 to indicate an acceptable simulation result.

4. **Evaluation of the performance of bias-corrected CORDEX–RCMs in reproducing the Baro–Akobo basin climate**[1]

Abstract

The applicability of the regional climate models (RCMs) for catchment hydroclimate is obscured due to their systematic bias. As a result, bias correction has become an essential precondition for the study of climate change. This study aimed to evaluate the skill of seven rainfall, five maximum and minimum temperature RCMs outputs against observed data in simulating the characteristics of climate at several locations over the Baro–Akobo River basin in Ethiopia. The evaluation was performed based on raw and bias-corrected individuals as well as the ensemble mean RCM simulation. The RCMs data has been compared to long-term observations. Several statistical metrics were used to compare RCMs against the observed using a pixel-to-point approach. The findings of this study show that pronounced biases, such as a lower correlation coefficient and higher PBIAS and RMSE, were observed in the rainfall and minimum temperature estimates than in the maximum temperature. However, all RCMs after bias correction shows better performance in reproducing the mean monthly rainfall and temperature and improve all the statistical metrics. The Mann–Kendall trend test for observed and RCMs indicates a decreasing annual rainfall trend, while the maximum and minimum temperatures show an increasing trend in most stations. In most metrics, the ensemble indicates better agreement with observations than individual models at most stations. In general, after bias correction, the ensemble simulates the Baro–Akobo basin climate adequately and can be used for the evaluation of future climate projections in the region.

4.1 Introduction

Human activities over the last century increased greenhouse emissions in the atmosphere, which caused global warming. Several types of research conducted during recent decades indicate that the increase in the atmospheric greenhouse gas concentration due to anthropogenic emissions has begun altering the global climate (IPCC, 2007). Such impacts are expected to be more intense in

[1] This chapter is based on Mengistu, A.G., Woldesenbet, T.A, Dile, Y.T., 2021a. Evaluation of the performance of bias-corrected CORDEX regional climate models in reproducing Baro–Akobo basin climate. Theor. Appl. Climatol. 144:751–767 https://doi.org/10.1007/s00704-021-03552-w

sub-Saharan Africa, where the social-ecological system is not resilient to shocks (IPCC, 2007; Davies et al., 2010). As ongoing climate change has been confirmed, assessing its impact on regionally important sectors has become a major concern, especially for policymakers who develop action plans to mitigate and adapt to the impacts of future climate change (IPCC, 2001).

Climate change studies are conducted using data from general circulation models (GCMs). However, since the GCMs have a coarse resolution, they are not suitable for regional climate change impact studies. Rather, Regional climate models (RCMs) have been used to dynamically downscale GCM output to scales more suitable to end regional applications. Therefore, GCM-driven RCM output may provide valuable information for climate adaptation practices, risk assessment studies, and policy planning. Such efforts enabled the application of RCM outputs to understand the impacts of climate change in local climates that are influenced by complex topographies and landscapes (Alley et al., 2007; Giorgi et al., 2009). Currently, the Coordinated Regional Climate Downscaling Experiment (CORDEX) program, initiated by the World Climate Research Program, provides an opportunity for generating high-resolution regional climate projections, which can be used for assessment of the future impacts of climate change at regional scales (Haile & Rientjes, 2015; Giorgi et al., 2009).Furthermore, because of the RCM model outputs have biases, which makes it difficult to use them directly for climate and hydrological impact studies. Several researchers suggested applying bias correction and the use of an ensemble mean to reduce errors in RCM outputs (Christensen et al., 2008; Kim et al., 2014; Teutschbein & Seibert, 2010; Worku et al., 2021).

This study aims to assess the performance of the CORDEX RCMs in simulating the climate characteristics over the Baro-Akobo basin. The basin is one of Ethiopia's transboundary rivers that join the Nile. The Nile River is the main water resource for riparian countries, which are already under immense pressure due to various competitive uses as well as social, geopolitical, and legislative conditions. Moreover, the Nile basin region, including the study basin, is vulnerable to climatic variability (Beyene et al., 2010; Kim et al., 2008; Mengistu & Sortbereg, 2012). To cope with the climatic variability and improve food security and energy provision in the Baro–Akobo basin and Nile basin regions, large irrigation and hydropower schemes are planned and under implementation (McCartney et al., 2009). Since climate change may have a considerable impact on water resources (IPCC, 2014), planning water resources in the basin requires a robust study that explores the long-term climate trend and variability to optimize outcomes from such investments.

There are limited studies that evaluate the performance of the raw and bias corrcetd RCMs to replicate the observed climate in Ethiopia in general and in the Baro–Akobo basin in particular. This study, therefore, evaluated the performance of the raw and bias-corrected CORDEX–Africa RCMs simulation in reproducing observed rainfall and temperatures at several locations in the basin for the period 1975–2005. Such studies help to select reliable RCM outputs that can be used for future climate change impact studies in highly vulnerable areas, like the study basin.

4.2 Materials and Methods

4.2.1 Observed data

Observed daily rainfall, maximum (Tmax), and minimum (Tmin) temperatures for the period 1975–2005 were obtained from the National Meteorology Agency (NMA). The rainfall pattern over the Baro–Akobo basin is predominantly unimodal with two distinct seasons, the main (rainy) season, which is locally called "Kiremt," and the dry season, which is locally called "Bega,".There is spatial rainfall variability in the basin. Stations located in the southern parts of the basin, including Masha, Mizan–Teferi, Chena, and Tepi, have the Bega season from December to February and the Kiremt season from March to November. The Bega season runs from November to February in the northern parts of the basin, including Alem-Teferi, Begi, Bure, Gore, Uka, Mettu, Dembi-Dollo, Hurumu, Chora, and Yubdu, and the Kiremt season runs from March to October (NMA, 1996).

Despite some missing records, most of the data obtained from the NMA captures the climatologies of the regions (Diro et al. 2011). Fourteen rainfall and six temperature stations were obtained from the NMA and then applied to correct the bias and evaluate the performance of the RCMs output. Quality control for the observed climate data (e.g., checking the presence of daily rainfall values less than zero and a daily maximum temperature less than the daily minimum temperature values) was conducted using RClimDex 1.1 software (Zhang and Yang, 2004). Getting complete datasets with no missing records was difficult in remote areas like the Bar-Akobo basin of Ethiopia. However, to balance data quality and availability, this study used stations that had missing data of less than 20% for the period 1975–2005. The missing data were filled in using the Multivariate Imputation by Chained Equations (MICE) algorithm of the R statistical software (van Buuren & Groothuis-Oudshoorn, 2011), demonstrating that the MICE algorithm outperforms other methods such as multiple linear regression (MLR) and inverse distance weighting (IDW) in estimating

missing climate data using solar radiation data under different atmospheric conditions in Galicia, Spain.

4.2.2 Regional climate models dataset

The CORDEX project (http://cordexesg.dmi.dk/esgf-web-fe/) provided RCMs with simulated daily rainfall and maximum and minimum temperature data. The spatial resolution of the RCM data is 0.44, which corresponds to a 50 × 50 km bounding box. The RCMs and their driving GCMs used in this study are written in short forms as (CNRM) for the CNRM-CERFACS-CNRM-CM5, (ICHEC) for the ICHEC-EC-EARTH, and (MPI) for the MPI-M-MPI-ESM-LR (Table 4.1). It's noted that RCA4 and CCLM4 are each driven by three GCMs (CNRM, ICHEC, and MPI), and REMO is driven by MPI. These RCMs were selected for evaluation because the outputs of CCLM4, RCA4, and REMO were evaluated and showed reasonable performance over East Africa (Endris et al., 2013; Nikulin et al., 2012; Worku et al., 2020b).

Table 4.1 List of RCMs with their institutes and driving GCMs considered in this study

RCM	Institute	Driving GCM	Reference
CCLM4	Climate Limited-area Modelling Community (CLMcom)	CNRM-CERFACS-CNRM-CM5	(Rockel et al., 2008)
CCLM4	Climate Limited-area Modelling Community (CLMcom)	ICHEC-EC-EARTH	(Baldauf et al., 2011)
CCLM4	Climate Limited-area Modelling Community (CLMcom)	MPI-M-MPI-ESM-LR	(Rockel et al., 2008)
RCA4	Sveriges Meteorologiska och Hydrologiska Institute (SMHI)	CNRM-CERFACS-CNRM-CM5	(Samuelsson et al., 2015)
RCA4	Sveriges Meteorologiska och Hydrologiska Institute (SMHI)	ICHEC-EC-EARTH	(Samuelsson et al., 2015)
RCA4	Sveriges Meteorologiska och Hydrologiska Institute (SMHI)	MPI-M-MPI-ESM-LR	(Samuelsson et al. 2015)
REMO	Climate Service Centre Germany (CSC) and Max Planck Institute (MPI)	MPI-M-MPI-ESM-LR	(Jacob et al., 2012)

In areas with sparse station networks and complex terrain, the accuracy and precision of interpolation are questioned when evaluating grid measurements of the climate model (Bhowmik & Costa, 2015; Osborn & Hulme, 1997). Therefore, due to the sparse distribution of rain gauge networks in the basin, a pixel-to-point approach was used to compare gridded RCMs data against point rainfall data from the rain gauge observations. Bhattacharya et al. (2020) show that a point-

to-pixel approach to the comparison of observed data with gridded climate data has resulted in good agreement in the Beas river basin of the North-Western Himalaya.

4.3 Bias correction methods

From the gridded RCMs model data, a representative value for each station was extracted and bias-corrected using the CMhyd tool. The tool has been tested using the CORDEX archive for different regions and has provided satisfactory performance (Rathjens et al., 2016). It is used to correct bias in rainfall data from seven RCM outputs and temperature data from five RCM outputs. This study used distribution mapping (DM) and linear scaling (LT) methods to correct the rainfall data, and the DM method was used to correct temperature data because they have been effective in removing RCM bias in several studies (Christensen et al., 2008; Fang et al., 2015; Teutschbein & Seibert, 2012).

The performance of the RCMs was evaluated in terms of their skill at reproducing the mean monthly characteristics of observed rainfall and temperature data. Moreover, the agreement between the observed and RCM (raw and bias-corrected) data was evaluated using the most widely used statistical methods, such as the correlation coefficient (R), percent of bias (PBIAS), and root mean square error (RMSE). Monthly values of stations' rainfall and minimum and maximum temperature data for the period 1975–2005 were used to evaluate the performance of RCM's simulated counterparts.

A correlation coefficient is used to evaluate the linear relationship between the observed and RCM outputs in equation (4.1). A correlation coefficient value close to 1 shows a very good fit between observed and modeled data.

$$\text{Correlation coefficient (R)} = \frac{\sum_{t=1}^{N}(S_{i-}\overline{S_i})\,(O_{i-}\overline{O_i})}{\sqrt{\sum_{t=1}^{N}(S_{i-}\overline{S_l})\sum_{t=1}^{N}(O_{i-}\overline{O_i})}} \quad \ldots\ldots\ldots\ldots\ldots\ldots\ldots\ldots\ldots\ldots\ldots\ldots\ldots \quad (4.1)$$

Percent of bias measured systematic bias between two observed and RCM outputs variables in terms of percent equation (4.2). A PBIAS value of zero indicates no systematic difference between simulated and observed amounts, whereas a large PBIAS indicates that the RCM rainfall amount largely diverges from the observed one. A positive PBIAS indicates overestimation whereas a negative PBIAS indicates an underestimation of observed variables.

Percent of bias (PBIAS) = $\frac{\sum_{i=1}^{n}(S_i - O_i)}{\sum_{i=1}^{n} O_i} \times 100$ ..... (4.2)

RMSE equation (4.3) is used to show the differences between observed and model outputs. A *RMSE* value close to zero indicates a very good agreement between studied variables.

RMSE = $\sqrt{\frac{\sum_{i=1}^{n}(S_i - O_i)^2}{n}}$ ..... (4.3)

The coefficient of variation (CV) equation (4.4) and third quantile for both the observed and RCM rainfall data were estimated to evaluate the agreement between the monthly observed and RCM rainfall data variability in each station.

CV= 100 $\times \frac{\sigma}{\mu}$..... (4.4)

Where Si and Oi are the ith simulated and observed variables, the bar over the symbols denotes the variables representing mean values for the analysis period of (1975–2005); and n represents the analysis period, which was 30 years; σ *and* μ represents to standard deviation and mean of either the RCM or observed.

This study examines trends in annual rainfall as well as maximum and minimum temperature from 1975-2005 in the Baro-Akobo basin because lack of information on climate trends at the station level. Therefore, the ability of RCMs to simulate trends in rainfall and temperatures necessitated further investigation. The Mann-Kendall (MK) trend test and Sen's slope methods were used to assess the trends and magnitude of change in observed annual rainfall and temperature time series, as well as bias-corrected RCM outputs. These methods have been widely used to assess the significance of trends in climatologic and hydrologic time-series studies (e.g., Tabari et al., 2015; Tekleab et al., 2013). The MK trend test is based on two hypotheses, in which the null hypothesis assumes that there is no trend and the alternative hypothesis assumes that there is a significant trend in the time series for a given significance level.

The MK test (S) Statistic is calculated using equation (4.5).

$S = \sum_{i=1}^{n-1}\sum_{j=i+1}^{n} sgn(xj - xi)$ ..... (4.5)

The test of significance is computed using equation (4.6)

$$\text{sgn}(x_j - x_i) = \begin{cases} +1 \; if((x_j - x_i) > 0 \\ 0 \; if(x_j - x_i) = 0 \\ -1 \; if \; ((x_j - x_i) < 0 \end{cases} \quad \ldots \ldots \ldots \ldots \ldots \ldots \ldots \ldots \ldots \ldots \ldots \ldots \ldots \ldots \ldots \ldots \ldots \ldots \ldots \ldots \ldots (4.6)$$

where $x_i \; and \; x_j$, are the annual values in years i and j, j > 1 respectively.

The standard MK statistic Z which is used to measure the significance of trends can be calculated using equation (4.7).

$$Z = \begin{cases} \frac{S-1}{\sqrt{Var\,(S)}} & if \; S > 0 \\ 0 & if \; S = 0 \\ \frac{S+1}{\sqrt{Var\,(S)}} & if \; S < 0 \end{cases} \quad \ldots\ldots\ldots\ldots\ldots\ldots\ldots\ldots\ldots\ldots\ldots\ldots\ldots\ldots\ldots\ldots\ldots\ldots\ldots\ldots.. (4.7)$$

The Z values are approximately normally distributed, and a positive Z value greater than 1.96 (based on normal probability tables) denotes a significant increasing trend at the significance level of 0.05, while a negative Z value less than −1.96 denotes a significant decreasing trend. The variance of S is calculated by

$$Var\,(S) = \frac{n(n-1)(2n+5) - \sum_{i=1}^{m} t_i\,(t_i - 1)(2t_i + 5)}{18} \quad \ldots\ldots\ldots\ldots\ldots\ldots\ldots\ldots\ldots\ldots\ldots\ldots\ldots\ldots\ldots\ldots\ldots\ldots (4.8)$$

Magnitude of slope

Whenever there is a linear trend in a time series, the true slope can be estimated by using a nonparametric method (Sen, 1968). Yue et al. (2002) reported that Sen's slope approach is robust at estimating the magnitude of a trend. The trend magnitude by this method is estimated as follows.

$$B = \text{Median} \frac{x_{j-x_i}}{t_{j-t_i}} \quad \ldots\ldots\ldots\ldots\ldots\ldots\ldots\ldots\ldots\ldots\ldots\ldots\ldots\ldots\ldots\ldots\ldots\ldots\ldots\ldots\ldots.................. (4.9)$$

Where x_j and x_i are data values at times t_j and t_i (j>1), respectively.

However, the MK trend test is highly influenced by serially correlated data. Therefore, to eliminate the effect of serial correlations on the MK trend test, several methods have been developed in the literature. These methods include pre-whitening (von Storch, 1999), variance correction (Hamed and Rao, 1998), and TFPW (Yue et al., 2002). Trend Free Pre-Whitening (TFPW) methods were used in this study, which accounts for all serial correlations that are significant at the 95% confidence level (Yue et al., 2002). The methods provide a better assessment of the significance of the trends for serially correlated data (e.g., Kumar et al., 2009; Zhang & Lu, 2009). Tekleab et

al. (2013) and Yue et al. (2002) described the procedure of trend-free pre-whitening (TFPW) methods for removing time series data for serial correlation.

4.3 Results and discussion

4.3.1 Performance of RCMs outputs in reproducing monthly mean rainfall

Figure 4.1a shows the magnitude and distribution of the mean monthly observed and raw RCM outputs of rainfall. Most of the raw RCM rainfall data captured the distribution of the mean monthly observed rainfall in the majority of the studied stations, although the time series was shifted by 1 to 2 months. The shift occurred, particularly during the peak rainfall period. Moreover, the raw RCMs indicated either an overestimation or an underestimation of the observed value at most stations. In most of the months, especially during the wet season, CCLM4 (CNRM) and CCLM4 (ICHEC) showed an overestimation of the observed values at most stations, whereas CCLM4 (MPI), all RCA4, and REMO (MPI) were characterized by underestimation. However, RCA4 (CNRM) and RCA4 (ICHEC) showed an exceptional overestimation at stations Mizan–Teferi and Masha during most of the rainy season. In most stations, the ensemble showed an underestimation of the observed value in the majority of the months. In the raw RCM comparison, the CCLM4 model performed better in reproducing the observed rainfall than the RCA4 and the REMO at most of the studied stations. Haile & Rientjes (2015) indicated an underestimation of the observed mean monthly rainfall by most of the RCMs in the Upper Blue Nile.

The bias correction techniques of individual RCMs and their ensemble, DM (Figure 4.1b) and LS (Figure 4.1c), well captured the magnitude and the mean monthly rainfall distribution in all stations. In the case of rainfall, a 1 to 2-month shift at the onset of the peak rainfall season was also corrected after the implementation of bias correction. After bias correction, most RCMs' shortcomings, such as overestimation by the CCLM4 and underestimation by the RCA4, REMO, and ensemble mean, significantly improved. The LS method performed slightly better than the DM method in capturing the observed rainfall at most of the studied stations. However, at Chora station, the LS method showed an overestimation of the observed rainfall during the rainy season (May to September) when correcting the data from CCLM4 (MPI).

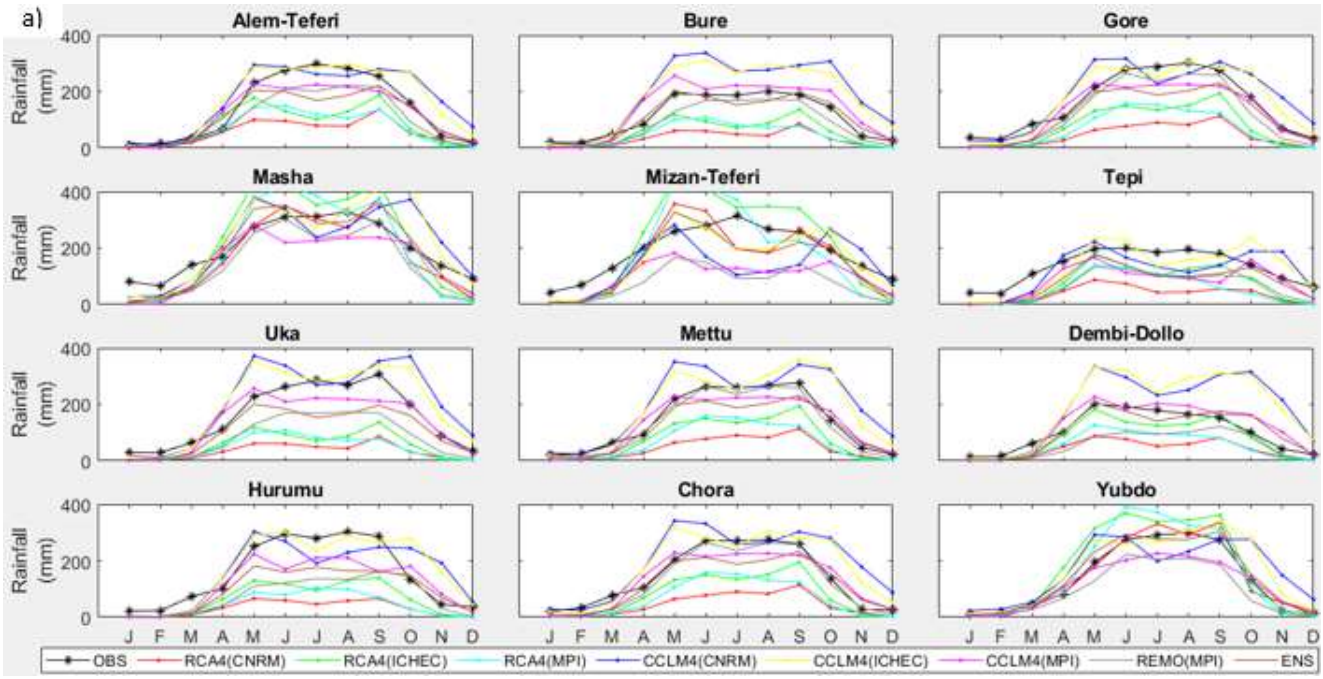
a)
Alem-Teferi
Bure
Gore
Masha
Mizan-Teferi
Tepi
Uka
Mettu
Dembi-Dollo
Hurumu
Chora
Yubdo
Rainfall (mm)
0
200
400
J F M A M J J A S O N D
OBS
RCA4(CNRM)
RCA4(ICHEC)
RCA4(MPI)
CCLM4(CNRM)
CCLM4(ICHEC)
CCLM4(MPI)
REMO(MPI)
ENS

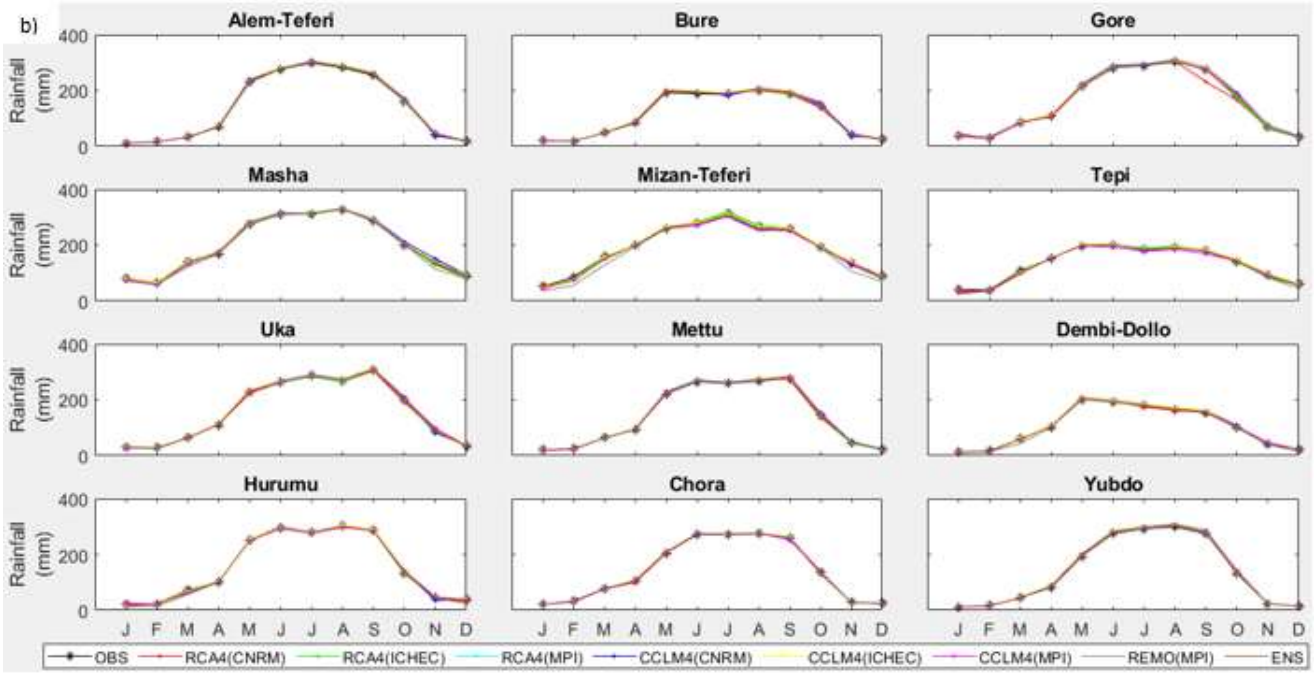
b)
Alem-Teferi
Bure
Gore
Masha
Mizan-Teferi
Tepi
Uka
Mettu
Dembi-Dollo
Hurumu
Chora
Yubdo
Rainfall (mm)
0
200
400
J F M A M J J A S O N D
OBS
RCA4(CNRM)
RCA4(ICHEC)
RCA4(MPI)
CCLM4(CNRM)
CCLM4(ICHEC)
CCLM4(MPI)
REMO(MPI)
ENS

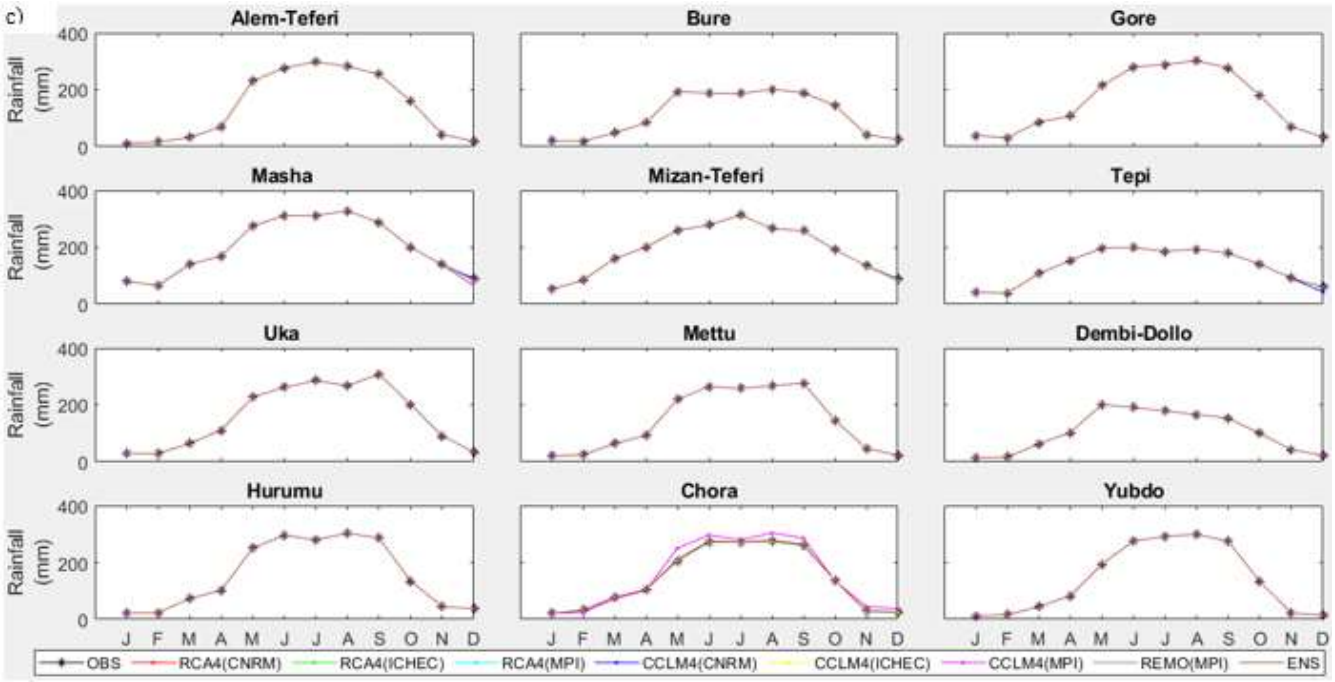

Figure 4.1 Mean monthly rainfall for; a) raw, b) distribution mapping (DM), and c) linear scaling (LS) RCMs outputs and observed data in 12 stations in the Baro−Akobo basin from 1975–2005.

4.3.2 Performance of RCMs outputs in reproducing mean monthly maximum and minimum temperatures

Figure 4.2a shows the magnitude and distribution of the mean monthly observed and raw RCM outputs of maximum temperatures. The majority of the individual raw RCMs and their ensemble mean accurately reproduced the distribution of mean monthly maximum temperatures in the majority of the stations. All raw RCMs except RCA4 (CNRM) and RCA4 (ICHEC) showed an underestimation of the observed mean monthly maximum temperature in most stations. Overestimation of the observed has prevailed at Gore and Dembi-Dollo. Comparing the raw RCM's skills, RCA4 (CNRM) performed better to reproduce the observed magnitude and distribution of the mean monthly maximum temperature in most of the stations.

All individual RCMs as well as their ensemble mean bias substantially improved the observed maximum temperature after applying bias correction (Figure 4.2b). The overestimation or underestimation of the observed mean monthly maximum temperature was adequately removed in all stations after applying the DM bias correction.

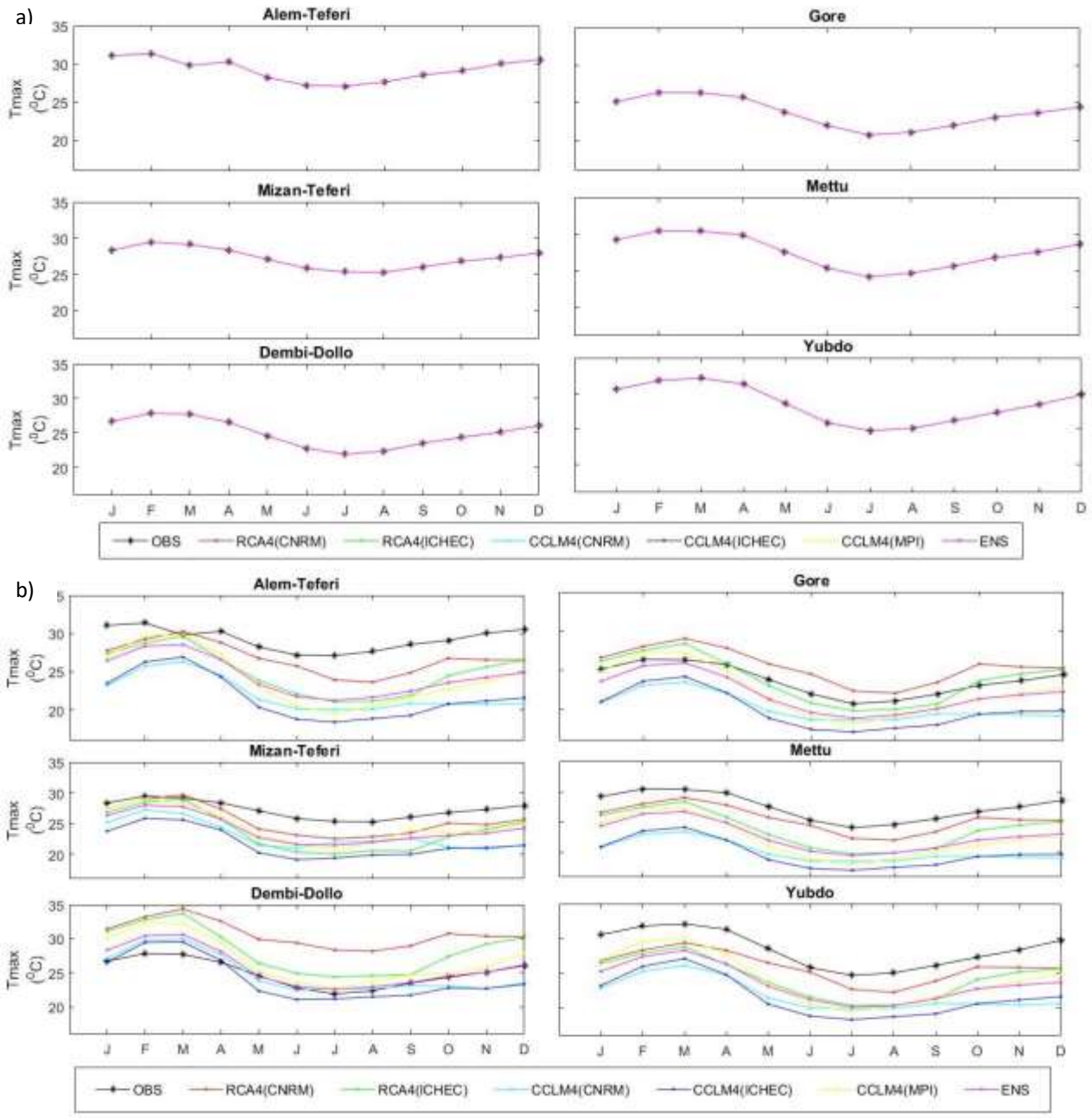

Figure 4.2 Mean monthly maximum temperature for a) raw, b) distribution mapping (DM) RCM outputs and observed data in the Baro−Akobo basin from 1975–2005.

Like the maximum temperatures, all the individual raw RCMs and their ensemble mean reproduce the distribution of the mean monthly minimum temperature in most of the stations (Figure 4.3a). However, the raw RCMs and their ensemble mean overestimated the observed over the majority of the stations, except RCA4 (ICHEC), which showed underestimation in some stations.

Comparing the raw RCMs' skills, RCA4 (ICHEC) performed better to reproduce the observed magnitude and shape of the minimum temperature in most of the stations.

The overestimation or underestimation of the observed mean monthly minimum temperature was adequately removed in most of the stations after applying DM bias correction (Figure 4.3b). However, CCLM4 (MPI) showed minor but consistent underestimation of the observed minimum temperature at Mizan-Teferi and overestimation at Mettu stations in most of the months.

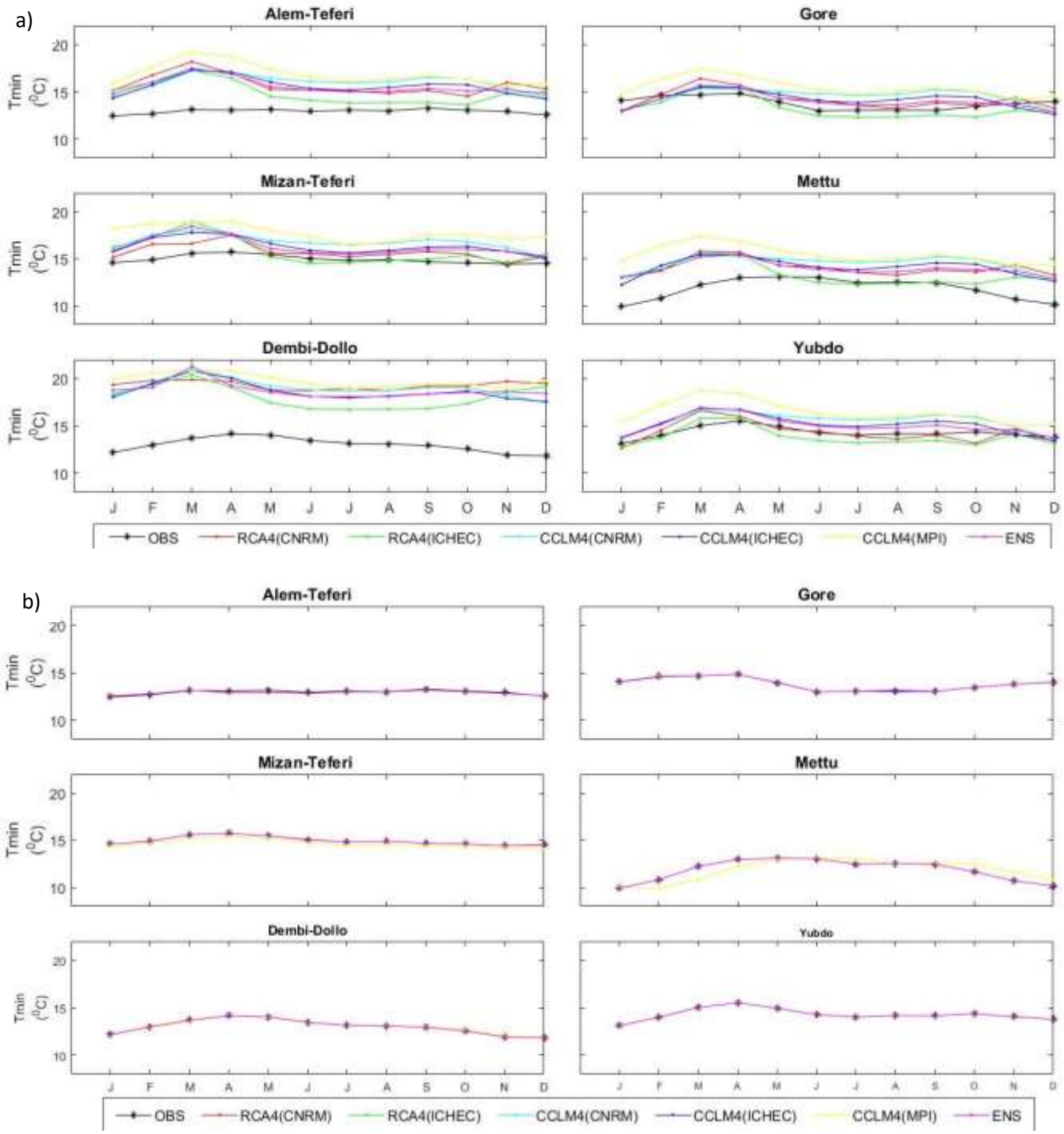

Figure 4.3 Mean monthly minimum temperature for a) raw, and b) distribution mapping (DM) RCM outputs and observed data in the Baro−Akobo basin from 1975–2005.

In general, the raw RCM simulations were characterized by overestimation and underestimation of rainfall and temperature in most of the stations. This could be due to rainfall and temperature varying spatially due to elevation differences among the considered meteorological stations. Other

studies (Teutschbein & Seibert, 2010; Worku et al., 2020b) have also reported the simulation of rainfall and temperature by climate models characterized by overestimation and underestimation in different locations.

Findings in this study indicated that distribution mapping and linear scaling adequately corrected the bias in RCMs simulated mean monthly rainfall, while distribution mapping also adequately corrected the bias in mean monthly maximum and minimum temperatures in the study region. The bias-corrected rainfall and temperatures could be used to study the effects of climate change on water resources in the future. However, it is essential to examine and compare their skill for a specific impact study. Other studies (Fang et al., 2015; Teutschbein & Seibert, 2012; Worku et al., 2020b) showed that these bias correction methods provided satisfactory performance in correcting mean monthly, annual rainfall, and temperature values.

4.3.3 Statistical performance evaluation of raw and bias corrected RCMs against observed climate data

4.3.3.1 Rainfall

The statistical metrics such as correlation coefficient, PBIAS, and RMSE showed a substantial difference between raw and bias-corrected RCM output as compared to the observed long-term monthly rainfall data (Figure 4.4). Individual raw RCMs, as well as ensemble simulations, are heavily biased from observed data. Raw RCA4 (CNRM), RCA4 (ICHEC), and RCA4 (MPI) output showed an underestimation of the values observed at most stations. The highest PBIAS −66.8% and RMSE (5.9 mm/day) were estimated at Hurumu and Mizan–Teferi stations when the observed rainfall was compared with the RCM outputs of RCA4 (CNRM) and RCA4 (ICHEC), respectively. On the other hand, CCLM4 (CNRM) and CCLM4 (ICHEC) showed an overestimation of the observed rainfall at most stations. The highest PBIAS (65.4%) was obtained at the Bure station by CCLM4 (ICHEC). The ensemble produced the lowest biases compared to the individual raw RCMs, with a higher R-value and lower PBIAS and RMSE in most stations.

The biases in the raw rainfall data were substantially reduced after the DM and LS bias corrections were applied. The LS was slightly better than the DM in correcting the bias from the individual raw RCMs and ensemble mean for most of the stations. In most cases, it provided 0 PBIAS, a lower RMSE, and a higher R-value. In both bias correction methods, the ensemble mean showed better performance in representing the observed rainfall in most of the stations with an R-value

above 0.8, a PBIAS of 0, and a low RMSE. Other studies (Endris et al., 2013; Nikulin et al., 2012; Worku et al., 2021) also reported that the ensemble outperformed the individual CORDEX Africa model outputs to represent observed rainfall and temperature data. It is worth mentioning that, future studies may use the ensemble mean of RCMs to understand the trends and impacts of climate change in the basin.

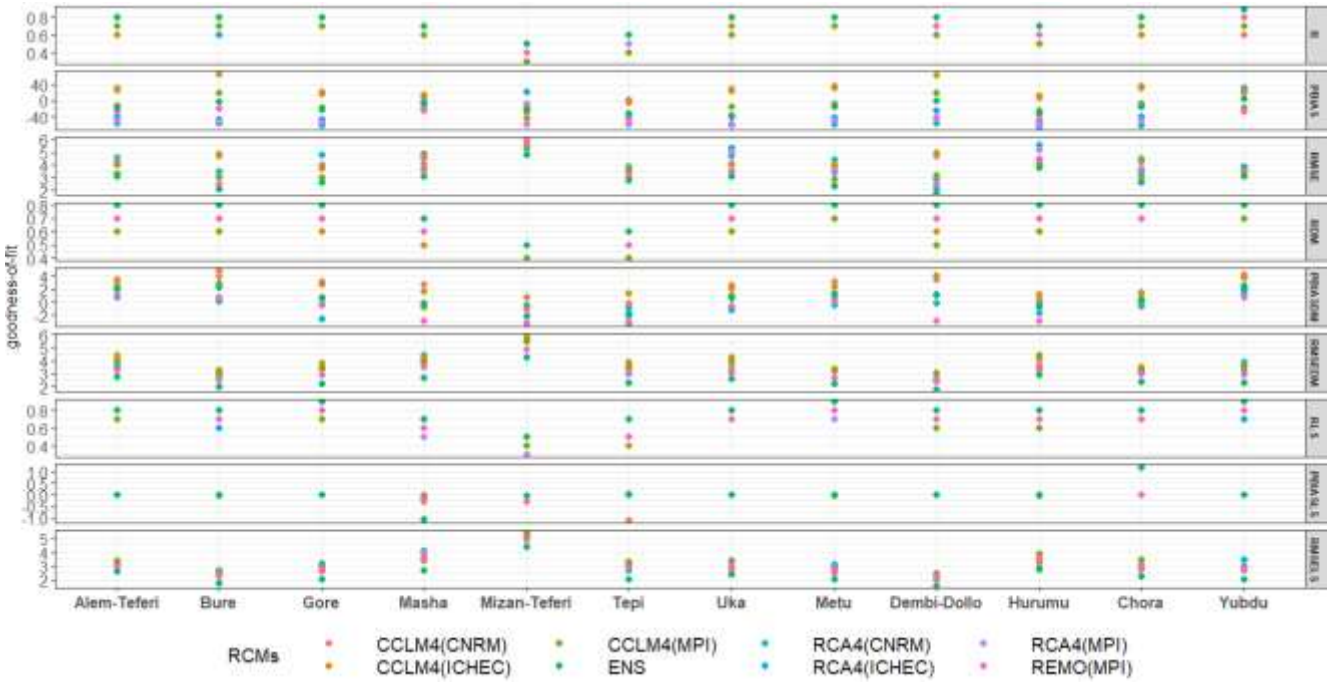

Figure 4.4 Statistical performance evaluation of the raw and bias-corrected RCMs outputs against the monthly observed rainfall at 12 stations in the Baro−Akobo basin from 1975–2005. The R, PBIAS, and RMSE represent the correlation coefficient, percent bias, and root mean square error, respectively of the comparison with raw data. RDM, PBIASDM, and RMSEDM represent the correlation coefficient, percent bias, and root mean square error, respectively of the comparison with bias corrected data using the distribution mapping (DM). RLS, PBIASLS, and RMSELS represent the correlation coefficient, percent bias, and root mean square error, respectively of the comparison with bias corrected data using linear scaling (LS).

4.3.3.2 Maximum temperature

Raw outputs of RCMs had substantial biases compared to the observed monthly maximum temperature in terms of R, PBIAS, and RMSE (Figure 4.5a). The raw CCLM4 (ICHEC) obtained a large source of bias during the raw RCMs comparison against the observed, such as PBIAS of

−27.7 at Yubdu and RMSE of 8.2 at Aleme-Teferi station. The bias correction using the DM reduced biases substantially at most of the stations. For example, a PBIAS of −27.7 at Yubdu and an RMSE of 8.2 at Aleme-Teferi station by CCLM44 (ICHEC) were removed after applying a robust bias correction. The DM is effective in providing an optimal value of goodness-of-fit, such as a PBIAS of close to 0, RMSE less than 2.85, and R-value > 0.8 in most RCMs and studied stations. Although bias correction for individual RCMs significantly reduces the bias on the observed maximum temperature, the ensemble performed better in all stations except Alem-Teferi, with a PBIAS of 0, RMSE 1.7, and R > 0.86.

4. 3.3.3 Minimum temperature

The goodness-of-fit evaluations based on R, PBIAS, and RMSE statistics show that the DM substantially improved the biases of the raw RCMs simulated monthly minimum temperature (Figure 4.5b). However, the performance of the bias correction for the minimum temperature is less than that of the maximum temperature. For example, the minimum temperature RCMs' bias corrections for all the RCMs at Alem-Teferi station and CCLM4 (MPI) at Mizan-Teferi station show lower PBIAS than the corresponding evaluation for the maximum temperature. Like the maximum temperature and rainfall, the RCMs ensemble mean for minimum temperature performed better than the individual RCMs in representing the observed minimum temperature at most stations. According to Kim et al. (2014), the skill for minimum temperature RCMs is lower than that for maximum temperature RCMs. The low performance of minimum temperature RCMs to reproduce the observed minimum temperature may be due to the effects of undulating topography and cloudiness most of the time (Themeßl et al., 2012).

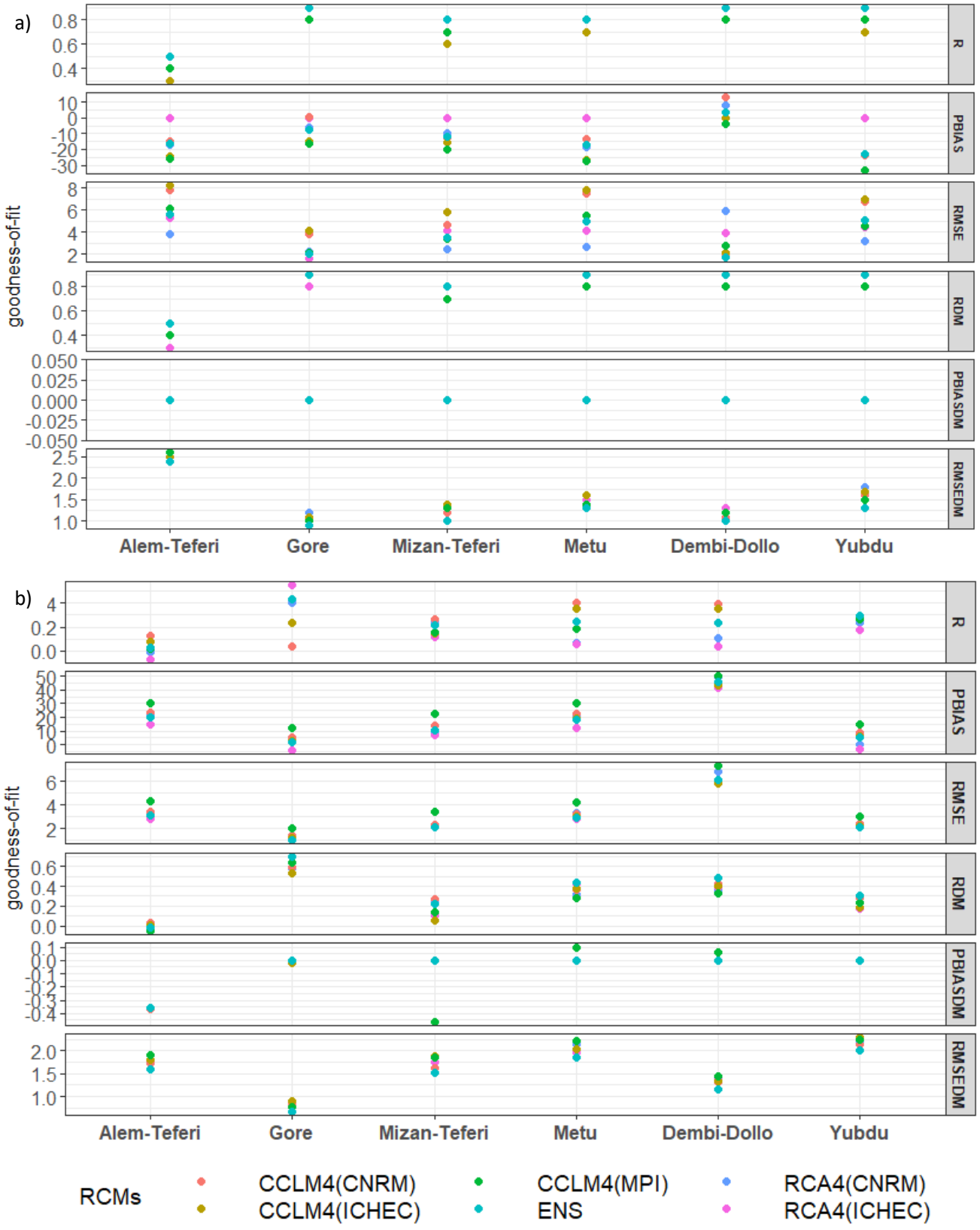
a)
b)
goodness-of-fit
R
PBIAS
RMSE
RDM
PBIASDM
RMSEDM
Alem-Teferi
Gore
Mizan-Teferi
Metu
Dembi-Dollo
Yubdu
RCMs
CCLM4(CNRM)
CCLM4(ICHEC)
CCLM4(MPI)
ENS
RCA4(CNRM)
RCA4(ICHEC)

Figure 4.5 Statistical performance evaluation of the raw and bias-corrected RCM outputs using distribution mapping (DM) against the observed; a) monthly maximum temperature b) monthly minimum temperature at six stations in the Baro–Akobo basin from 1975–2005. The R, PBIAS, and RMSE represent the correlation coefficient, percent bias, and root mean square error, respectively, of the comparison with raw data. RDM, PBIASDM, and RMSEDM represent the correlation coefficient, percent bias, and root mean square error, respectively, of the comparison with bias corrected data using the distribution mapping (DM).

Besides the goodness-of-fit evaluations, the CV and third quantile were used to compare the raw and bias-corrected RCMs outputs with the observed historical monthly rainfall. The raw RCMs show substantial bias, with an underestimation of the third quantile and an overestimation of the CV in most stations (Figure 4.6a). In terms of the third quantile, CCLM4 (CNRM) and CCLM4 (ICHEC) overestimate the observed third quantile, whereas CCLM4 (MPI), RCA4 group, REMO (MPI), and the ensemble were underestimated in most stations.

The third quantile and CV agreement were improved after applying DM (Figure 4.6b) and LS (Figure 4.6c) bias corrections to the raw RCM data. As it is presented in the figures, after applying bias correction, the difference between the third quantile and CV of the observed rainfall and all RCMs as well as their ensemble mean was minor. The LS was slightly better than the DM in reproducing the annual cycle, while the DM was better in representing the third quantile and CV in most of the stations. Teutschbein & Seibert (2012) also reported that DM was better in estimating frequency-based statistics such as the third quantile. However, in time-series-based metrics such as PBIAS and RMSE, the performance of mean-based methods (e.g., linear scaling) was slightly better than quantile-based methods (Fang et al., 2015). In general, in both bias correction methods, there is no substantial difference between these results, which indicates the corrected monthly rainfall time series are in good agreement with the observations.

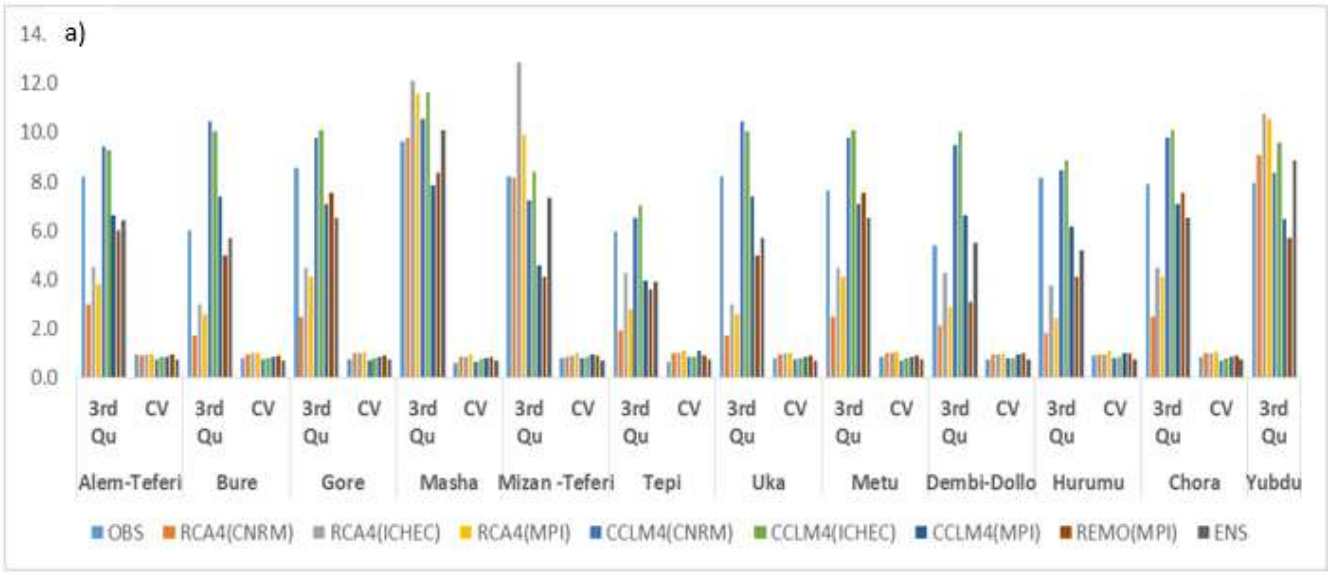
14. a)
12.0
10.0
8.0
6.0
4.0
2.0
0.0
3rd Qu
CV
Alem-Teferi
Bure
Gore
Masha
Mizan -Teferi
Tepi
Uka
Metu
Dembi-Dollo
Hurumu
Chora
Yubdu
OBS
RCA4(CNRM)
RCA4(ICHEC)
RCA4(MPI)
CCLM4(CNRM)
CCLM4(ICHEC)
CCLM4(MPI)
REMO(MPI)
ENS

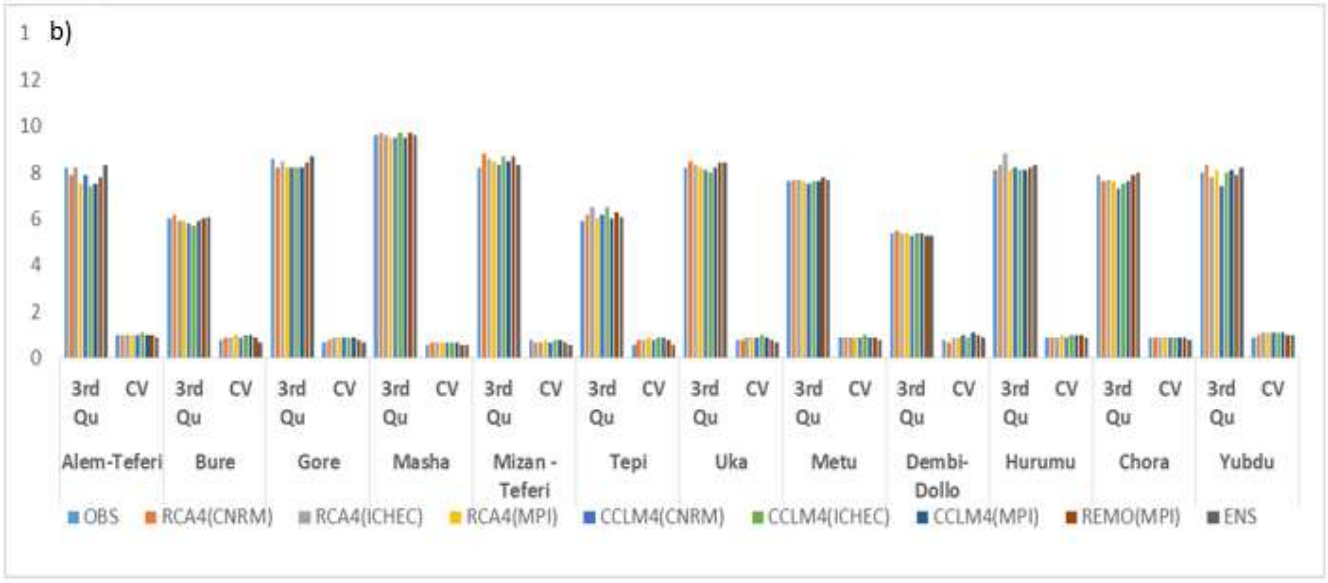
1 b)
12
10
8
6
4
2
0
3rd Qu
CV
Alem-Teferi
Bure
Gore
Masha
Mizan - Teferi
Tepi
Uka
Metu
Dembi-Dollo
Hurumu
Chora
Yubdu
OBS
RCA4(CNRM)
RCA4(ICHEC)
RCA4(MPI)
CCLM4(CNRM)
CCLM4(ICHEC)
CCLM4(MPI)
REMO(MPI)
ENS

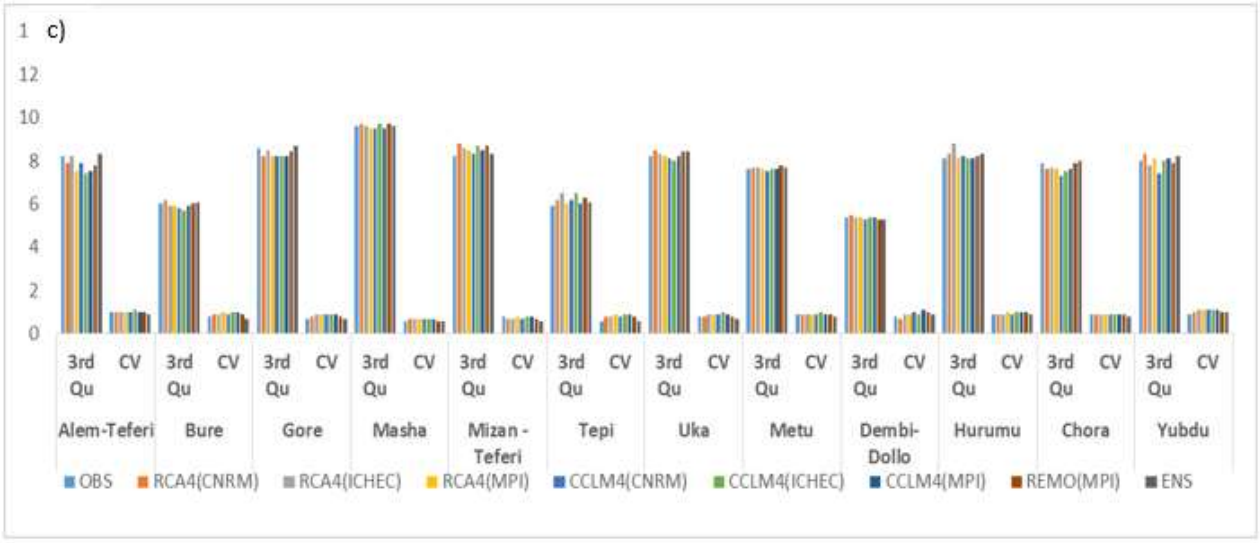

Figure 4.6 The coefficient of variation (CV) and third quantile values between the observed monthly rainfall and a) raw RCMs, b) distribution mapping, c) for linear scaling for the period of 1975–2005 for 12 studied stations.

4.3.5 Mann-Kendall (MK) trend test and Sen's slope estimate for annual rainfall, maximum and minimum temperature

The trend analysis of the observed annual rainfall series indicated decreasing trends at eight stations and increases at four stations (Table 4.2). The decreasing trends are statistically significant at Gore, Masha, Uka, and Mettu, whereas the increasing trends are not significant at all stations. The magnitudes of the significant decreasing trends at Gore, Masha, Uka, and Mettu stations were −6.89 and −8.9 mm/year, −12 and −17 mm/year, respectively (Table 4.3). A statistical assessment of rainfall trends in the upper Blue Nile River basin by Tabari et al. (2015) reported a decreasing annual rainfall trend at Gore station. Cheung et al. (2008) also reported a significant decreasing trend in the June to September rainfall in the southwestern and central parts of Ethiopia. Both DM and LS bias-corrected RCM and their ensemble rainfall data showed a similar trend to the observed rainfall data in most stations.

Table 4.2 Mann-Kendall trend tests result for observed and bias-corrected RCMs annual rainfall time series. Values in bold indicate statistically significant trends at the 5% level of significant level.

	Alem-Teferi	Bure	Gore	Masha	Mizan-Teferi	Tepi	Uka	Mettu	Dembi-Dollo	Hurumu	Chora	Yubdu
OBS	−0.03	0.67	**−2.49**	**−2.50**	−1.56	−1.26	**−5.60**	**−3.60**	0.47	0.24	−0.21	−0.96
RCA4(CNRM)_DM	−0.84	−1.36	−0.36	−0.82	−1.28	−1.91	**−2.21**	−0.08	−1.38	−0.34	0.52	0.31

RCA4(ICHEC)_DM	1.09	1.23	0.58	0.24	−0.99	0.07	0.74	0.61	−0.41	0.71	0.95	1.29
RCA4(ESM)_DM	0.91	−0.03	−0.11	−0.75	−1.01	−1.36	−0.31	0.24	−1.07	0.22	1.33	0.8
CCLM44(CNRM)_DM	−1.36	−1.66	−1.02	−0.92	−1.46	−1.63	−1.32	−1.02	−1.33	−1.26	−1.27	−1.73
CCLM44(ICHEC)_DM	−1.95	−1.68	**−2.11**	−3.40	−1.12	−1.28	−1.57	**−2.25**	−1.50	−1.18	−1.61	−1.27
CCLM44(ESM)_DM	−0.54	−0.82	−0.92	−1.12	−1.46	−1.19	−0.93	−1.19	−1.19	−1.22	−1.24	−0.95
REMO(MPI)_DM	**−2.01**	−1.24	**−2.48**	**−3.37**	−1.55	−1.90	**−2.07**	**−3.68**	−1.70	−1.52	**−2.00**	−1.03
ENS_DM	−1.87	**−3.80**	**−2.31**	**−2.72**	**−2.26**	−1.13	**−3.95**	−1.97	−1.44	−1.14	−1.54	−1.06
RCA4(CNRM)_LS	−0.96	−1.02	−0.06	0.2	−1.09	−1.97	**−2.21**	−0.03	−1.37	−0.34	0.52	0.31
RCA4(ICHEC)_LS	1.16	1.22	0.41	−0.02	−1.16	0.07	0.94	0.54	−0.91	0.71	0.95	1.29
RCA4(ESM)_LS	−0.49	0.17	−0.69	−1.33	0.31	−1.36	−0.21	−0.27	−1.77	0.12	1.63	0.8
CCLM44(CNRM)_LS	−1.46	−1.71	−1.60	−1.86	**−2.10**	−1.73	−1.32	−1.43	**−2.63**	−1.26	−1.87	−1.83
CCLM44(ICHEC)_LS	1.02	−1.95	−1.95	−1.46	**−3.51**	**−2.28**	−1.17	−1.82	**−3.50**	−1.18	−1.61	−1.75
CCLM44(ESM)_LS	−1.16	−1.16	**−1.37**	**−3.37**	−1.73	−1.39	−0.93	−1.70	−1.19	−1.22	−1.24	−0.95
REMO(MPI)_LS	−1.90	**−3.01**	−1.90	**−2.86**	−1.41	−1.94	**−2.27**	**−2.11**	−1.70	**−2.52**	**−3.00**	**−2.03**
ENS_LS	**−3.01**	**−3.01**	**−2.82**	−1.06	**−3.74**	**−3.13**	**−3.55**	**−2.11**	**−2.44**	−1.84	−1.94	−1.16

Table 4.3 Sen's slope result for observed and bias-corrected RCMs annual rainfall time series.

	Alem-Teferi	Bure	Gore	Masha	Mizan-Teferi	Tepi	Uka	Mettu	Dembi-Dollo	Hurumu	Chora	Yubdu
OBS	−0.2	1.3	−6.9	−8.9	1.9	−2.5	−12	−17	0.7	0.6	−0.3	−2.4
RCA4(CNRM)_DM	−2.06	−3.20	−3.23	−8.33	−17.1	−11.11	−6.84	−0.9	−2.11	−1.55	1.4	1.35
RCA4(ICHEC)_DM	6.22	5.24	5.01	2.15	−8.7	0.1	3.54	4.8	−1.95	5.87	6	11.3
RCA4(ESM)_DM	1.47	−0.36	−0.44	−2.18	−13.0	−7.70	−1.22	1.25	−2.11	1.35	4.2	5.03
CCLM44(CNRM)_DM	−10.84	−7.94	−9.75	−11.2	−10.8	−11.1	−8.89	−8.57	−5.44	−9.54	−10.8	−15.1
CCLM44(ICHEC)_DM	−10.51	−12.35	−10.6	−19.3	−25.39	−10.4	−12.4	−11.6	−11.5	−12.4	−11.5	−8.23
CCLM44(ESM)_DM	−4.65	−5.66	−7.22	−10.30	−14.81	−7.7	−8.42	−7.88	−10.77	−9.59	−11.3	−5.06
REMO(MPI)_DM	−14.07	−12.72	−11.2	−15.67	−12.9	−11.5	−16.2	−10.1	−8.14	−11.8	−8.8	−6.1
ENS_DM	−5.99	−6.66	−8.03	−10.40	−14.5	−5.45	−9.34	−6.47	−8.54	−7.75	−5.4	−3.7
RCA4(CNRM)_LS	−3.20	−3.31	−0.65	1.26	−8.50	−13.1	−5.84	−0.7	−4.11	−1.75	1.5	2.35
RCA4(ICHEC)_LS	4.99	4.2	3.26	−0.07	−9.01	0.6	3.54	4.02	−2.95	5.97	6.9	10.3
RCA4(ESM)_LS	−1.67	0.48	−1.24	−11.19	2.92	−7.70	−1.12	−0.92	−3.11	1.85	2.2	5.03
CCLM44(CNRM)_LS	−7.45	−5.69	−9.84	−15.73	−11.89	−11.1	−8.8	−6.85	−10.4	−8.54	−9.8	−15.1
CCLM44(ICHEC)_LS	−4.21	−6.36	−7.86	−14.94	−26.63	−14.3	−11.4	−8.61	−13.8	−11.5	−10.4	−9.2
CCLM44(ESM)_LS	−4.21	−12.00	−10.26	−16.62	−18.48	−7.7	−4.42	−6.92	−10.7	−8.59	−14.3	−5.5
REMO(MPI)_LS	−5.16	−12.00	−6.53	−9.49	−15.23	−11.5	−10.2	−9.27	−12.2	−10.8	−9.8	−5.22
ENS_LS	−5.16	−5.16	4.26	−10.73	−12.62	−9.45	−7.34	−6.75	−8.5	−7.25	−6.4	−2.7

There was an increasing but not significant trend in the observed annual maximum temperature at three stations and a significant increasing trend at three stations (Table 4.4). The significant

increasing trends were observed at Alem-Teferi, Mizan-Teferi, and Mettu stations, and the slope of the trends was 0.005, 0.003, and 0.008 °C/year, respectively (Table 4.5). All of the bias-corrected individual RCMs and their ensemble mean showed similar increasing trends to the observed stations. The maximum temperature shows an increasing trend in the study region, and these results are in good agreement (Christy et al., 2009). They showed an increasing trend in the eastern part of Africa. Likewise, the Intergovernmental Panel on Climate Change reported an increasing trend in observed temperatures across the African continent (IPCC, 2014).

When it comes to the minimum temperature, insignificant decreasing trends at two stations and an increasing trend at four stations were observed (Table 4.4). A significant increasing trend was observed only at Yubdu station, with the slope of the trend at 0.07 °C per year. Like the maximum temperature, all of the bias-corrected RCMs and their ensemble mean showed similar increasing trends observed in all stations (Table 4.4). The majority of the increasing minimum temperature trends are in good agreement (Tekleab et al., 2013). They showed an increasing trend in minimum temperatures for the majority of the stations in the Upper Blue Nile basin, Ethiopia.

Table 4.4 Mann-Kendall test result for observed and bias-corrected RCMs for annual maximum and minimum temperature time series. Values in bold indicate statistically significant trends at the 5% level of significant level.

Variable		Alem-Teferi	Gore	Mizan-Teferi	Mettu	Dembi-Dollo	Yubdu
Tmax	OBS	**2.15**	1.86	**2.18**	**3.26**	0.78	1.36
	RCA4(CNRM)_DM	1.53	0.65	1.33	0.73	0.75	0.8
	RCA4(ICHEC)_DM	**2.33**	1.03	1.57	1.12	0.97	1.13
	CCLM44(CNRM)_DM	**2.93**	1.19	1.92	1.31	1.24	1.43
	CCLM44(ICHEC)_DM	1.18	0.47	1.68	0.52	0.88	0.63
	CCLM44(ESM)_DM	**2.84**	1.35	1.39	1.5	1.3	1.6
	ENS_DM	**2.46**	1.01	1.67	1.09	1.12	1.23
Tmin	OBS	-0.2	1.53	0.3	-0.87	0.36	**3.74**
	RCA4(CNRM)_DM	**3.13**	**2.62**	**2.52**	**2.89**	**2.72**	**3.01**
	RCA4(ICHEC)_DM	**4.01**	**4.17**	**3.86**	**4.05**	**3.71**	**2.75**
	CCLM44(CNRM)_DM	**4.34**	**4.3**	**4.34**	**4.51**	**4.22**	**2.79**
	CCLM44(ICHEC)_DM	**2.48**	**3.09**	**3.86**	**2.43**	**2.99**	**3.96**
	CCLM44(ESM)_DM	**2.73**	**2.78**	**2.37**	**2.61**	**2.81**	**4.73**
	ENS_DM	**3.56**	**3.46**	**3.4**	**3.4**	**3.54**	**3.55**

Table 4.5 Sen's slope result for observed and bias-corrected RCMs for annual maximum and minimum temperature time series.

Variable		Alem-Teferi	Gore	Mizan-Teferi	Mettu	Dembi-Dollo	Yubdu
Tmax	OBS	0.005	0.01	0.003	0.008	0.002	0.004
	RCA4(CNRM)_DM	0.003	0.001	0.002	0.002	0.002	0.002
	RCA4(ICHEC)_DM	0.004	0.002	0.002	0.002	0.002	0.003
	CCLM44(CNRM)_DM	0.005	0.002	0.003	0.003	0.002	0.004
	CCLM44(ICHEC)_DM	0.002	0.001	0.003	0.001	0.002	0.002
	CCLM44(ESM)_DM	0.005	0.003	0.002	0.003	0.003	0.004
	ENS_DM	0.004	0.01	0.002	0.002	0.002	0.003
Tmin	OBS	-0.003	0.021	0.006	-0.035	0.003	0.07
	RCA4(CNRM)_DM	0.023	0.013	0.025	0.029	0.028	0.044
	RCA4(ICHEC)_DM	0.04	0.026	0.04	0.046	0.04	0.066
	CCLM44(CNRM)_DM	0.056	0.034	0.063	0.061	0.05	0.028
	CCLM44(ICHEC)_DM	0.045	0.026	0.056	0.044	0.043	0.041
	CCLM44(ESM)_DM	0.059	0.034	0.047	0.059	0.048	0.062
	ENS_DM	0.045	0.026	0.048	0.049	0.04	0.048

In general, the findings show that after applying the distribution mapping, the individual, as well as ensemble RCMs adequately simulate the trends in annual rainfall and maximum and minimum temperatures. Such robust RCM output could be used in future climate change impact studies on the basin. Dile et al. (2013) reported that statistically downscaled outputs of the HadCM3 model output can provide useful information to devise appropriate climate change adaptation and mitigation strategies. For instance, sustainable watershed management practices that help to cope with the challenges of climate change are examples of climate change adaptation and mitigation strategies.

Changes in rainfall and temperature due to climate change may exacerbate the socio-ecological risks in the study area by impacting the basic natural resources that rural households rely on. The majority of people in the Baro-Akobo basin are smallholder farmers who rely on agriculture and pastoralism for a living. A decreasing trend of rainfall and an increasing trend of temperature may affect the available surface and groundwater resources and thereby affect agricultural and ecological productivity, which are a source of livelihood for smallholder farmers. Therefore, to cope with the impacts of climate change in the study region, appropriate adaptation and mitigation strategies should be devised to reduce the severe impacts on the social-ecological systems in the basin.

4.4 Conclusion

This study evaluated the different RCMs driven by GCMs, which are part of the Coupled Model Intercomparison Project Phase 5 (CMIP5). The Baro–Akobo River basin, which has many ongoing and proposed water resource projects that may be impacted by climate change and variability, has been selected for evaluation. Statistical metrics, such as the coefficient of correlation, PBIAS, and root mean square error, were used to compare the raw and bias corrected RCM's outputs with the observed climate.

The findings of this study show that the raw RCM simulations were characterized by overestimation and underestimation of rainfall and temperature in most of the stations. This is likely due to rainfall and temperature varying spatially due to elevation differences among the considered meteorological stations. In most stations, no substantial difference is found after bias correction between the observed and the RCM simulations, and a relatively small variability range is identified in mean monthly distribution simulations and statistical performance evaluations for rainfall and temperatures during the period 1975–2005. The finding indicated that the DM bias correction methods for temperature and the LS and DM methods for rainfall provide a higher level of certainty in the reproduction of monthly rainfall and temperatures.

It is noted that in most stations, bias-corrected climate data resulted in a better representation of temperature than rainfall, indicating greater uncertainty still exists in model-simulated rainfall than temperature. In most stations, the ensemble has shown improved performance as compared to most individual RCM models. However, the findings show that the performance of the RCMs varies subject to the performance measures used for evaluation.

The MK trend test for observed data and most of the bias corrected RCMs and the ensemble showed a decreasing rainfall trend, while both the maximum and minimum temperature showed an increasing trend in most of the stations. Improving the understanding of rainfall and temperatures is of high importance for the basin, as the economy is primarily based on rainfed agriculture and therefore vulnerable to climate variability and climate change. Therefore, this study shows that the ensemble mean after bias correction has led to better performance when compared to most individual models when evaluated by several statistical metrics such as the RMSE, PBIAS, and correlation coefficient.

5. Evaluation of observed and satellite-based climate products for hydrological simulation in data-scarce Baro−Akobo River Basin, Ethiopia[2]

Abstract

Hydrological modeling in data-scarce areas is difficult. Recent advances in remote sensing make producing climate data easier and provide alternatives to conventional climate data sources, particularly for hydro-climatological studies in data-scarce regions. However, rigorous evaluations are warranted to evaluate the reliability and effectiveness of gridded climate products. This study evaluated the CFSR and CHIRPS products against the observed climate for hydrologic prediction at two streamflow gauging stations. The SWAT is used to simulate hydrological processes in watersheds. Model sensitivity analysis and calibration were conducted using the Sequential Uncertainty Fitting-2 (SUFI-2) algorithm in the SWAT-Calibration Uncertainty and Prediction (SWAT-CUP). Input data such as DEM, soil, land use, and hydro-climate data were used for the model. Streamflow simulation performance was evaluated using several statistical, hydrological, and prediction uncertainty measures of p-factor and r-factor within the SUFI-2 framework. Simulation of the model using the observed and gridded climate products provided satisfactory model performance in terms of the goodness of fit criteria and uncertainty prediction. Results show that CHIRPS rainfall combined with CFSR and observed temperatures demonstrates slightly better statistics and hydrological performance than observed, but shows a substantial difference from CFSR. The simulations with CHIRPS and observed yielded minor differences in the water balance component estimates, whereas the CFSR simulation gave lower average annual rainfall, resulting in lower water balance components. Quantifying the various components of the water balance in the watershed helps to tackle water and soil management issues. Overall, the combination of CHIRPS rainfall and CFSR temperature can serve as a better alternative climate input for hydrological applications in the study region.[2]

[2] This chapter is based on Mengistu, A.G., Woldesenbet, T.A, Dile, Y.T. Evaluation of observed and satellite-based climate products for hydrological simulation in data-scarce Baro–Akob River basin, Ethiopia. Ecohydrology & Hydrobiology, https://doi.org/10.1016/j.ecohyd.2021.11.006

5.1 Introduction

Hydrological modeling in data-poor regions across the globe has always been a challenge. This situation is exacerbated when dealing with large-scale and transboundary river basins (Cho et al., 2009). The lack of adequate hydroclimatic data makes sustainable water resource research and development daunting in times of global environmental challenges. For example, although the Nile River is the main water resource for several of the Nile Basin countries, it is under immense pressure from multiple compounding environmental, social, geopolitical, and legislative issues. One of the key challenges to the Nile Basin is climate variability and change, which are undermining smallholders' ability to continue rainfed agriculture and pastoral ways of life, for example in the Baro basin (Beyene et al., 2010; Kim et al., 2008; Pacini & Harper, 2016). Several previous studies provide evidence that streamflow alteration has many ecological consequences (e.g., Poff & Zimmerman, 2010). Hydrologic models have been used to assess changes in water resources in various catchments across scales (Srinivasan et al., 2010). However, hydrological modeling in large river basins with diverse terrain and sparse gauge networks often leads to poor simulation results (Cho et al., 2009).

The Baro–Akobo River basin is an important transboundary river basin with high geopolitical and hydrologic importance for its riparian countries. However, the basin lacks adequate ground measurements of meteorological and hydrological data. Moreover, the existing data has significant drawbacks, such as lots of missing records, a low density of stations, and short periods of times of record (Alemayehu et al., 2016; Mengistu et al., 2021). This calls for the need to look for alternative data products that can be used for hydrological modeling and application.

Several gridded rainfall products at different spatial and temporal resolutions are increasingly available for various applications (e.g., Tapiador et al., 2012). These rainfall products include TRMM (Tropical Rainfall Measuring Mission) multi-satellite precipitation analysis (TMPA) (Huffman et al., 2007), Climate Hazards Group InfraRed Precipitation with Station data (CHIRPS, Funk et al., 2015), Integrated Multi-satellitE Retrievals for Global Precipitation Measurement (IMERG, Huffman et al., 2019), Tropical Applications of Meteorology using Satellite Data and Ground-Based Observations (TAMSAT, Maidment et al., 2015), European Centre for Medium-Range Weather Forecasts (ECMWF, Balsamo et al., 2015), Precipitation Estimation from Remotely Sensed Information using Artificial Neural Networks (PERSIANN, Hsu et al., 1997),

and CPC Morphing Technique (CMORPH, Joyce et al., 2004). These gridded satellite rainfall products are subjected to systematic bias and random errors (Kidd, 2001), even though they provide long-term time series data in near-real-time with high spatial and temporal resolution. Hence, it is indispensable to evaluate the performance of these products before they are used for hydrologic modeling.

The performance evaluation of gridded rainfall products in different climatic and geographic regions has been undertaken in several studies. According to the findings, the product's performance is highly dependent on evaluation approaches (Worqlul et al., 2014), spatial resolution (Baez-Villanueva et al., 2018), and topography difference (Fenta et al., 2018).This demonstrates that the bias of gridded products in capturing rainfall values differs across climatic and geographic regions, which can be translated into streamflow simulations and water balance estimates. Thus, before using the gridded climate products for hydrological applications, validation and calibration are necessary for a specific region.

Several studies have been undertaken to evaluate gridded satellite rainfall products with ground observations across many watersheds (e.g., Bui et al., 2021; Dhanesh et al., 2020; Fuka et al., 2013; Hirpa et al., 2010; Mekonnen et al., 2021; Radcliffe & Mukundan, 2017; Rahman et al., 2020; Tuo et al., 2016; Yang et al., 2014). Most of the applications of hydrological modeling in Ethiopia have been concentrated in the Upper Blue Nile Basin. Bitew et al. (2012) evaluated multiple satellite remote sensing products such as CMORPH, TMPA 3B42RT, TMPA 3B42, and PERSIANN to simulate streamflow for the Koga watershed using the SWAT model. The study reported that CMORPH and 3B42RT were able to reproduce the streamflow but underestimated the peak flow, while simulations with the 3B42 and PERSIANN provided poor performance. Worqlul et al. (2014) applied a semi-distributed Hydrologiska Byråns Vattenbalansavdelning (HBV) hydrologic model and Parameter Efficient Distributed (PED) to evaluate TRMM 3B42, CFSR, and ground-based rainfall estimates for streamflow simulations in the Gilgel Abay and Main Beles watersheds. The results indicated that the simulated streamflows using the observed data performed better for both watersheds (except for the peak events) than the CFSR and TRMM satellite rainfall estimates. Dile & Srinivasan (2014) applied the SWAT model to evaluate CFSR in the Lake Tana basin of the Upper Blue Nile basin. They reported that both observed and CFSR climate simulations reproduced the observed streamflow well, although the rainfall data of the CFSR climate showed overestimations and underestimations of the observed rainfall in certain

parts of the basin. Fuka et al. (2013) used SWAT to compare the CFSR climate to the observed climate to simulate streamflow in the Gumera watershed in the Lake Tana basin, and found that both the observed and CFSR climates reproduced the observed streamflow at the watershed outlet. Likewise, Duan et al. (2016) evaluated the CFSR climate with the observed climate in the Upper Blue Nile basin, in which the performance of streamflow simulations with the CFSR climate was lower than the simulations with the observed climate. Dhanesh et al. (2020) compared the performance of CFSR and CHIRPS data to simulate streamflow using the SWAT model over ten watersheds distributed across different climatic regions, including Ethiopia. They reported that CHIRPS rainfall outperformed CFSR climate to predict streamflow in most of the studied watersheds.

Although climate data scarcity has limited progress in research in the study area, to the best of the authors' knowledge, no research has been conducted to evaluate the applicability of satellite-based climate data for hydrological studies in the basin. This study, therefore, aims to evaluate the applicability of the gridded climate products to predict observed streamflow in the Baro and Sore watersheds within the Baro–Akobo basin. The simulations with the CFSR and CHIRPS data were compared with the simulations that use observed climate since they have not been previously evaluated and tested over the study area. The CFSR climate was selected as it has complete climate variables, including rainfall, maximum and minimum temperature, wind speed, solar radiation, and relative humidity. Although the CHIRPS has only rainfall data, it was selected as it provided reasonable performance to reproduce observed flow in several watersheds (e.g., Dhanesh et al., 2020; Xian et al., 2019), and the CHIRPS comprises data from a higher number of rain gauges and is found to be better than other datasets, which makes it preferable for our study region (Dinku et al., 2018). Furthermore, the CFSR and CHIRPS datasets have long-term recorded data and relatively higher spatial and temporal resolutions. The performance of the climate datasets for hydrological predictions was evaluated using the SWAT model. SWAT is a physically-based model that was developed to understand the impacts of changes in land management and climate on water, sediment, and nutrients in varying-sized watersheds with different land uses, soils, and topography (Arnold et al., 1998). The model has been applied for various hydrological applications in multiple watersheds in Ethiopia and provided satisfactory performance (Dile et al., 2020; Mengistu & Sorteberg, 2012; Setegn et al., 2008; Teklay et al., 2021; White et al., 2011; Woldesenbet et al., 2018; Worku et al., 2021).

5.2 Materials and Methods

5.2.1 Data source

The SWAT model requires hydroclimate to set up, calibrate, and validate different biophysical processes in watersheds (Figure 5.1). Ground-based observed daily rainfall and maximum and minimum temperature records were provided by the Ethiopian National Meteorological Services Agency (NMA). Daily discharge data for Baro (near Gambella) and Sore (near Metu) gauge stations were provided by the Ethiopian Ministry of Water and Energy (MOWE).

The study also used reanalysis and satellite-based climate data, including CFSR and CHIRPS. The CFSR is a reanalysis dataset that is a widely used source of weather data and is obtained from http://globalweather.tamu.edu/. The CFSR product is a reanalysis dataset that combines the weather forecasts generated by the National Weather Service Global Forecast System and satellite data. The horizontal spatial resolution of CFSR is about 38 km, and it has been available since 1979 (Saha et al., 2010). The CFSR data consists of rainfall, maximum and minimum temperatures, wind speed, relative humidity, and solar radiation (Saha et al., 2010). The CHIRPS dataset consists of three products, including global climatology, satellite estimates, and gauge observations at different temporal resolutions (Funk et al., 2015). The datasets were produced using a relatively large collection of rain gauge data in East Africa and showed satisfactory prediction accuracy for Ethiopia when compared with observed meteorological data (Dinku et al., 2018). The CHIRPS rainfall products at 0.25° × 0.25° resolution covering the period 1981 to the present are available at (http://chg.geog.ucsb.edu/data/chirps/). Both the CFSR and CHIRPS data were obtained for a bounding box of 7° 3' to 9° 10' N latitudes and 34° 37' to 36° 17' E longitudes. Additionally, the SWAT model requires spatial data, including DEM, land use, and soil data, to generate topographic and other spatial input data to simulate processes at different spatial units (i.e., hydrological response units (HRUs), reaches, and subbasins). Arnold et al. (2012) define HRUs as the smallest units in the model where many of the biophysical processes are estimated.
The DEM data is required to delineate watersheds and create other topographic information such as slope, stream network, and channel length. A 30-meter (1 arc-second) resolution Shuttle Radar Topography Mission (SRTM) DEM dataset was obtained from the USGS website (https://earthexplorer.usgs.gov) (Figure 5.1). Land use data is employed to feed land use (agriculture, forest, etc.) and management information into the SWAT model, which is used to

simulate various biophysical processes. The land use maps of the year 2000 were obtained from the Ethiopian Mapping Agency (EMA). The dominant land-use types in the basin include forest, agriculture, and grassland. The SWAT model requires soil physicochemical properties such as soil texture, available water content, hydraulic conductivity, bulk density, and organic carbon content for multiple soil layers to simulate different biophysical processes. The soils' physical and chemical parameters were collected from the Harmonized World Soil Database (FAO/IIASA/ISRIC/ISS-CAS/JRC, 2008). The dominant part of the soil has clay (78.15%), followed by clay-loam (18.71%) and silt-clay (3.1%) soil textures.

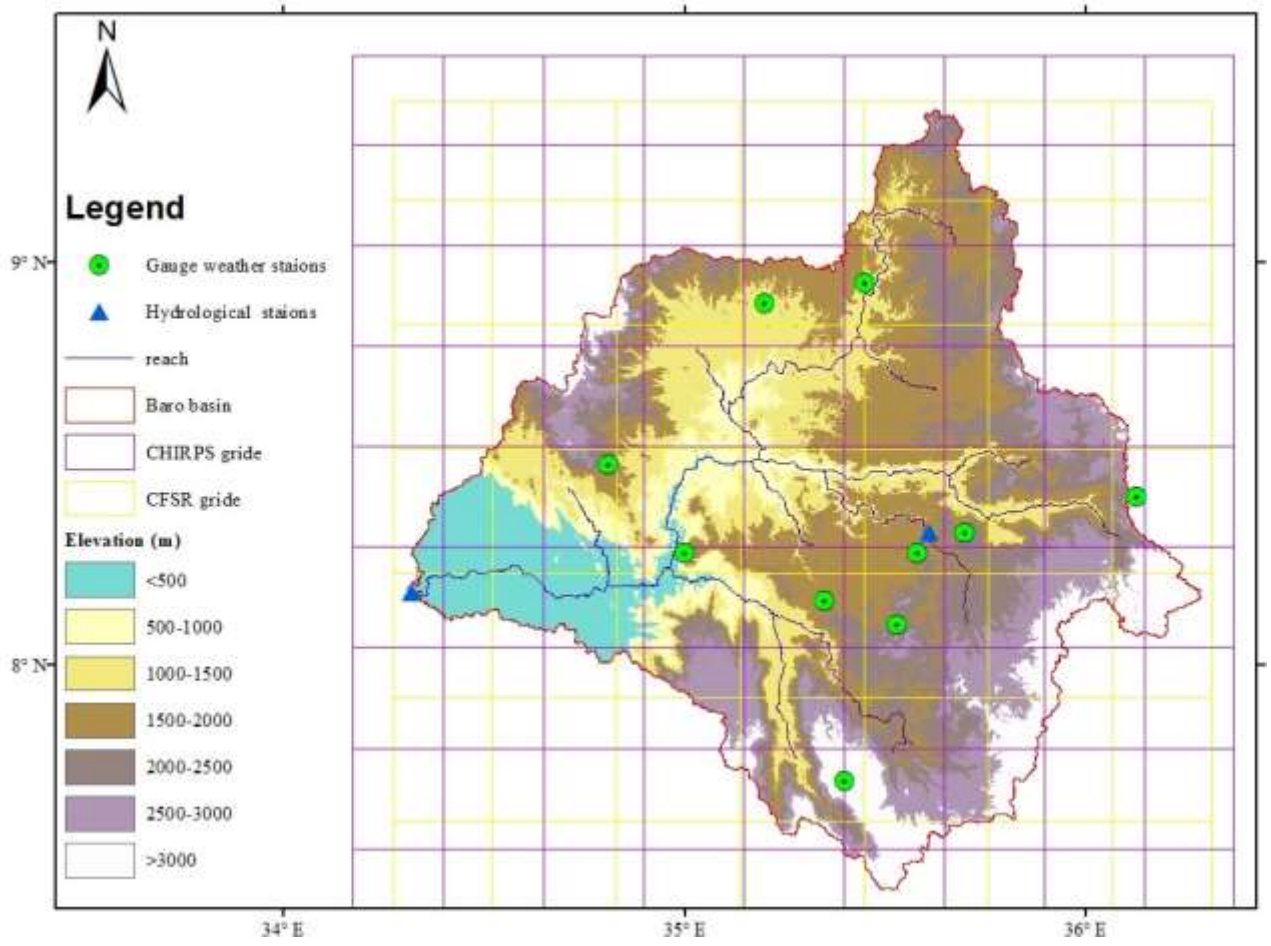

Figure 5.1 Location map of the Baro basin along with the spatial distribution of elevation and the hydro-meteorological stations at corresponding gridded climate products.

5.2.2 Model setup

To evaluate the performance of observed and gridded climate datasets for hydrological simulation, the SWAT model was used. The model can simulate major hydrologic processes that include

evapotranspiration, surface runoff, infiltration, and percolation (Arnold et al., 1998). Four SWAT models were created and run using four different climate dataset combinations: 1) observed climate, 2) CFSR, 3) CHIRPS+CFSR, and 4) CHIRPS+ observed. Since CHIRPS data has only rainfall, the remaining minimum, and maximum temperature data were based on observed and CFSR data, which helps to know under which combination of climate datasets CHIRPS performed best. The streamflow simulation of the performance of four climate datasets for the period 1981-201 was compared to identify a climate dataset that better simulates the biophysical processes in the watersheds.

5.3 Result and discussion

5.3.1. Parameter sensitivity

The parameter sensitivities were estimated based on p-values and t-statistics from the SUFI-2 sensitivity analysis of the eighteen studied parameters. The higher the t-statistic value and the smaller the p-value, the more sensitive the parameter is (Abbaspour et al., 2015). For the Baro watershed that uses observed climate data (Table 5.1), the most sensitive parameters based on their p-values and t-statistics were the curve number (CN2), base flow alpha factor (Alpha_BF), soil evaporation compensation factor (ESCO), available soil water capacity of the soil layer (SOL_AWC), and threshold water depth in the shallow aquifer required for return flow to occur (mm) (GWQMN). Likewise, for the Sore watershed, base flow alpha factor (Alpha_BF), curve number (CN2), and groundwater delay (GW_DELAY) were the most sensitive parameters (Table 5.1). These parameters were found to be sensitive, with the relative sensitivity values (p-values) ranging from 0.00 to 0.49. Most of the sensitive parameters were related to surface runoff, soil properties, channel flow, and groundwater processes. The sensitive parameters suggest that more emphasis should be placed on having representative land use and soil data to have a reasonable model simulation in the basins.

Table 5.1 The most sensitive parameters, including their range, fitted values of the calibrated model using observed climate datasets in descending order for Baro and Sore river staions.

Sensitivity		Range		Fitted value	
Baro	Sore	Baro	Sore	Baro	Sore
r_CN2.mgt	v_ALPHA_BF.gw	±25%	0-1	-0.01	0.46
v_ALPHA_BF.gw	r_CN2.mgt	0-1	±25%	0.29	-0.05

v_ESCO.hru	v_GW_DELAY.gw	0-1	0-500	0.75	25.2
r_SOL_AWC.sol	r_SOL_AWC.sol	±25	±25	0.09	0.05
v_GWQMN.gw	r_OV_N.hru	0-5000	0.02-0.4	286	0.15
r_SLSUBBSN.hru	v_ESCO.hru	0-0.2	0-1	0.18	0.91
v_GW_DELAY.gw	r_Soil_ Z.sol	0-500	±25%	209	-0.06
v_CH_K2.rte	v_ALPHA_BNK.rte	5-130	0-1	89.69	0.56
r_SOL_K.sol	v_GW_REVAP.gw	±25%	0.02-0.2	-0.21	0.01
r_Soil_ Z.sol	v_CH_N2.rte	±25%	0.01-0.3	0.01	0.26

The qualifier r refers to a relative change in the parameter where the value from the default simulation is multiplied by 1 plus the fitted value and v) refers to the existing parameter value from the default simulation to by the fitted value. The extensions (e.g., .mgt, hru, .sol, .gw. rte) indicate the SWAT parameter family.

Model sensitivity analysis and calibration using the CFSR climate provided CN2, ALPHA_BF, and ESCO as the most sensitive parameters for the Baro watershed and ALPHA_BF, ALPHA_BNK, and GWQMN as the most sensitive parameters for the Sore watershed. Likewise, model sensitivity analysis and calibration using the CHIRPS combined with CFSR datasets provided CN2, CH_N2, and ALPHA_BF for the Baro watershed and ALPHA _BF, CN2, and GW_DELAY as the most sensitive parameters for the Sore watershed. The 10 most sensitive parameters for the sensitivity analysis and calibration for the Baro and Sore watersheds, using CFSR and CHIRPS combined with CFSR, are presented in Annexes (5.1) and (5.2), respectively. It's noted that a slight difference was observed in the fitted value of the parameters between the CHIRPS combined with CFSR and the CHIRPS combined with observed, and so the table value of the latter one was not presented.

5.3.2. Model calibration and validation

The simulation performance of calibrated models between the observed and satellite estimate datasets was compared using several statistical indices at a monthly time scale (Table 5.2). The goodness-of-fit evaluation shows an acceptable agreement between the observed and satellite estimates. For the Baro watershed, the calibration of the model using monthly streamflow indicated very good model simulation performance according to recommendations by Moriasi et al. (2007). Comparatively, in terms of the different goodness-of-fit evaluations, the CHIRPS combined with the CFSR provided the best agreement with the observed, whereas the CFSR performed less in all

evaluations (Table 5.2). For example, the CHIRPS combined with the CFSR has the highest value of R^2 (0.93) and NSE (0.92), while the CFSR has the smallest value of R^2 (0.77) and NSE (0.75). In terms of the PBIAS simulations, the observed climate and CHIRPS combined with the CFSR climate showed minor streamflow overestimation with a value of -0.9 and -0.5, respectively. On the other hand, the calibrated model simulation with the CFSR climate underestimated the observed streamflow with a PBIAS value of 11.2%.

Considering the validation period, the NSE and R^2 values of the observed simulation were 0.87 and 0.85, which are compared with the CHIRPS combined with CFSR values of 0.92 and 0.9, respectively. Unlike the calibration period, the CFSR climate during the validation overestimated the observed streamflow, which had the highest PBIAS among the models (-8.8%). During the validation period, the simulations with observed and CHIRPS combined with CFSR and observed climate performed very well, while the simulations with CFSR climate performed satisfactorily in terms of R^2 and NSE values (Moriasi et al., 2007). Simulated streamflows of the observed climate for the Baro watershed were compared with the findings of Mengistu and Sorteberg (2012), and the results showed comparative agreement during the calibration and validation periods. However, their findings overestimated the streamflow during the validation period.

In the Sore watershed, simulations with both combinations of the CHIRPS climate provided the best performance, followed by the observed climate in terms of all the studied goodness-of-fit measures. Although not significant, simulations with all the climate data showed overestimations, as signified by a negative PBIAS. Similarly, the CHIRPS combined with the CFSR and observed provided better agreement with the observed during the validation period, whereas the CFSR performed less well in all goodness-of-fit evaluations. For example, in terms of the R^2, a relatively high value of 0.88 was obtained for CHIRPS combined with CFSR climate estimates, while the lowest value (R^2 = 0.63) was observed in the CFSR climate estimate (Table 5.2). Using the performance classification of Moriasi et al. (2007), the observed and both CHIRPS climates achieved very good performance in all statistical metrics, but CFSR did not exceed satisfactory performance in any of the statistical metrics except PBIAS.

Overall, simulations with all four climate data sets showed reasonable performance on a monthly time scale. However, simulations with the observed and both combinations of the CHIRPS climate performed almost equally and outperformed the simulation with the CFSR climate. In addition,

the model performance was better in the larger watershed (Baro) than in the smaller watershed (Sore).

Table 5.2 Estimated model performance values of calibrations and validation for the observed, CFSR, and CHIRPS datasets for monthly time scale.

		Baro station					Sore station				
Period	Climate data sets	R^2	NSE	PBIAS	P-factor	R-factor	R^2	NSE	BIAS	P-factor	R-factor
Calibration	Observed	0.93	0.88	-0.9	0.68	1.14	0.8	0.82	-5.9	0.68	0.81
	CFSR	0.77	0.75	11.2	0.79	1.11	0.7	0.71	-9.1	0.71	0.74
	CHIRIPS+CFSR	0.93	0.92	0.5	0.88	1.32	0.9	0.9	-5.8	0.81	0.94
	CHIRPS+Observed	0.91	0.9	1.1	0.87	1.23	0.9	0.87	-6.2	0.77	0.91
Validation	Observed	0.87	0.85	-2.4	0.75	1.20	0.86	0.84	-4.5	0.77	0.81
	CFSR	0.69	0.67	-8.8	0.70	1.11	0.63	0.62	-3.2	0.67	0.69
	CHIRPS+CFSR	0.92	0.9	1.1	0.83	1.23	0.88	0.9	-2.1	0.75	0.86
	CHIRPS+Observed	0.9	0.9	-3.2	0.81	1.2	0.87	0.88	-1.9	0.74	0.84

All four climate dataset simulations captured the seasonal patterns of the streamflow hydrograph reasonably well at the Baro and Sore River gauging stations, as shown in Figures 5.2 and 5.3, respectively. All the climate data simulations captured the rising and falling limbs of the hydrograph well during the calibration and validation periods in both watersheds. However, the observed and both the CHIRPS combination climate products comparatively well capture the seasonal patterns of the streamflow hydrograph, but the CFSR product was still the less performing product to capture the streamflow hydrograph. The relatively poor performance of CFSR can be attributed to the disparity between observed and CHIRPS rainfall, wherein CFSR in the Baro watershed was highly underestimated during the calibration period but highly overestimated during the validation period. The overestimation or underestimation of CFSR seems to be highest in both watersheds during the calibration and validation periods, with reportedly high negative or positive PBIAS in statistical metrics. Further, the Sore watershed, a relatively smaller watershed, shows less performance in capturing streamflow hydrographs than the Baro watershed. It was noted that, in both watersheds, the model's performance in streamflow simulation was weak in extreme simulation. It was more pronounced at the Sore watershed when using the CFSR dataset.

Similarly, several other studies have also reported the weak performance of the SWAT model in the simulation of peak flow (e.g., Demirel et al., 2009; Spellman et al., 2018).

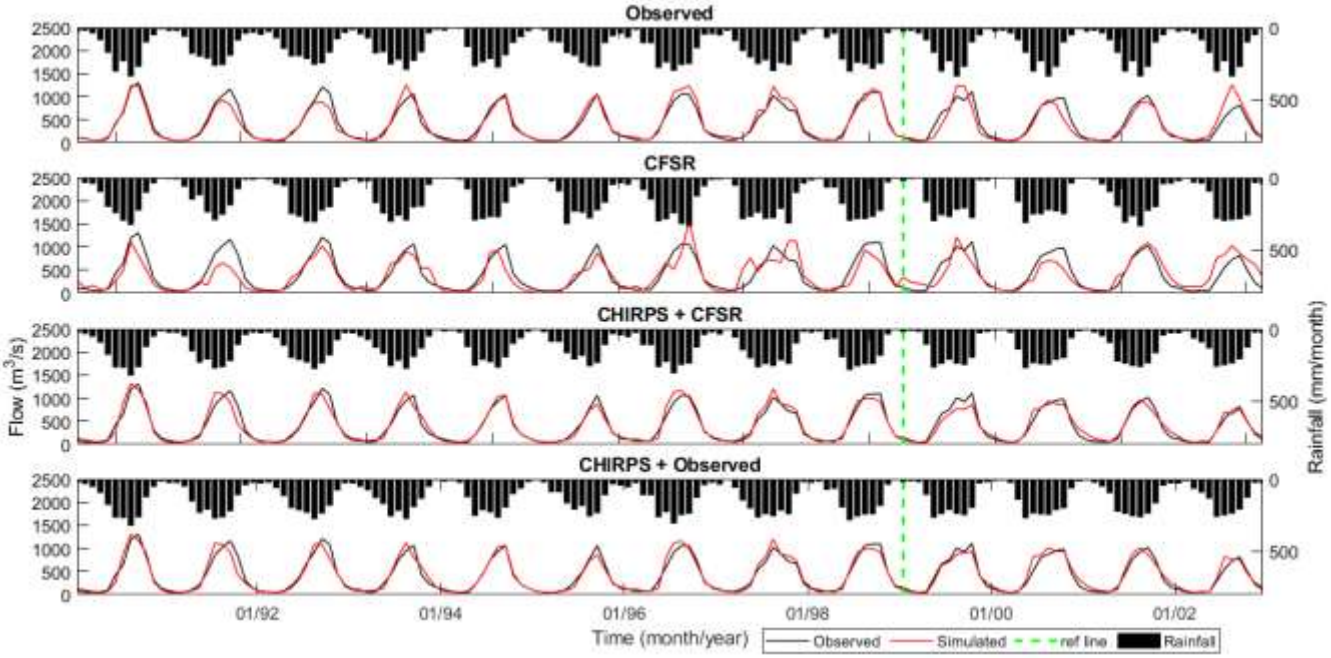

Figure 5.2 Monthly observed and simulated streamflow using observed, Climate Forecast System Reanalysis (CFSR) and Climate Hazards Group InfraRed Precipitation with Station (CHIRPS) climate at the Baro River gauging station. The green dashed vertical line is used to separate the calibration and validation periods. Model calibration and validation were done using the respective climate data.

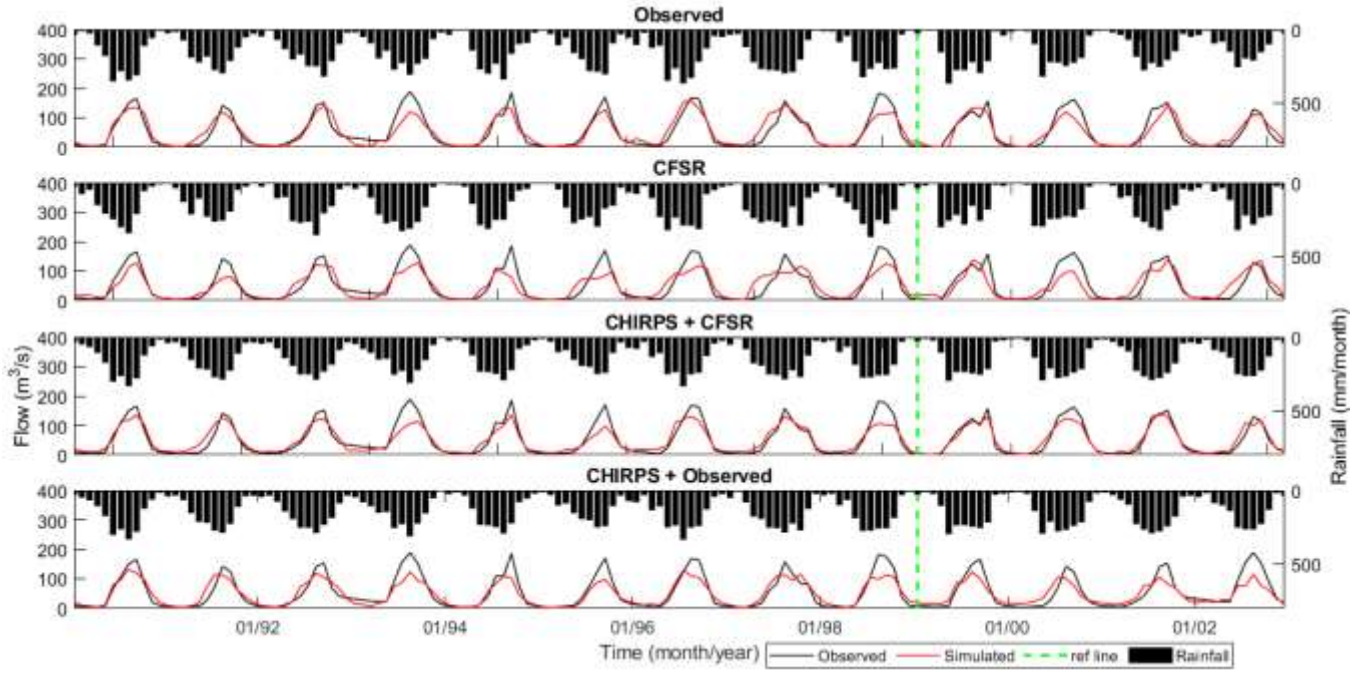

Figure 5.3 Monthly observed and simulated streamflow using observed, Climate Forecast System Reanalysis (CFSR) and Climate Hazards Group InfraRed Precipitation with Station (CHIRPS) climate at the Sore River gauging station. The green dashed vertical line is used to separate the calibration and validation periods. Model calibration and validation were done using the respective climate data.

5.3.3. Model prediction uncertainty

In the Baro watershed, all the climate datasets provided acceptable streamflow prediction uncertainty estimates during the calibration and validation periods. However, the observed during the calibration period resulted in a slightly lower p-factor of 0.68 (Table 5.2). The simulation with the CHIRPS combined with the CFSR climate provided the lowest prediction uncertainty, bracketing 88% of the observed streamflow within the 95PPU band. In terms of the r-factor, however, the simulations with the CFSR climate provided the lowest prediction uncertainty, which means they resulted in a smaller 95PPU uncertainty band. Likewise, during the validation period, the CHIRPS combined with the observed flow had the lowest prediction uncertainty, bracketing 83% of the observed streamflow within the 95PPU band, but it had the largest uncertainty band with the measure of the r-factor. In general, in all four climate datasets, the uncertainty analysis of the calibrated model provided acceptable p-factors and r-factors except the observed in the Baro

watersheds during the calibration period, which resulted in a slightly lower p-factor value (Abbaspour et al., 2015).

Similarly, the performance of streamflow prediction uncertainty during calibration and validation in Sore watersheds is encouraging for all climate datasets (Table 5.2). Streamflow simulation with the CHIRPS combined with CFSR climate provided the lowest prediction uncertainty with a p-factor of 0.81 during the calibration period. While streamflow prediction uncertainty was estimated with the r-factor, simulations with the CFSR climate had the lowest uncertainty. All the climate datasets perform consistently well in reaching desirable uncertainty predictions with acceptable values of p-factor and r-factor, but the observations at the Baro watershed during calibration and the CFSR at the Sore watershed during validation resulted in an unsatisfactory p-value of 0.67 and 0.68, respectively, which is slightly below the acceptable range (Abbaspour et al., 2015).

Different climate datasets generate distinct prediction uncertainties in modeling streamflow (Table 5.2). Overall, the simulation with CHIRPS combined with CFSR climate data had the best simulation uncertainty (i.e., higher p-factor) most of the time, and the simulation with the CFSR data set had the best r-factor value (lower r-factor) most of the time. The simulations at the Baro watershed produced higher p-factors but lower r-factors than those at the Sore watershed. This may be due to the assumption of a higher p-factor value, resulting in a lower r-factor value. Thus, according to Abbaspour et al. (2015), trade-offs must be made between achieving an acceptable p-factor and r-factor since achieving a larger p-factor will also result in a larger r-factor.

5.3.4 Analysis of water balance components

Besides flow hydrographs and several evaluation statistics, water balance components were also analyzed to further examine the effects of climate dataset inputs on hydrological simulation. Such analysis is especially helpful to assess if the satellite-based climate data can equally simulate the water balance components with the observed climate or provide drastically different estimates. Appropriate analysis and quantification of the various water balance components in the watershed help to tackle the water management issues. Thus, the evaluation of variation in these hydrologic components is helpful in the formulation of strategies by water planners and other stakeholders involved.

The CFSR and CHIRPS mean annual rainfall amounts for the entire watershed are lower than those observed. The estimate shows that CHIRPS is comparable with observed datasets, whereas

CFSR shows variability at the higher magnitude of mean annual rainfall (Table 5.3). Although we found that the estimates of the water balance components from the two CHIRPS climate datasets were quite close, we chose to estimate the water balance components using a combination of rainfall data from CHIRPS and temperature data from CFSR. According to an estimate of the observed mean annual water balance for the basin, water yield accounts for the largest portion of the water balance, accounting for about 57 percent (966 mm) of the total amount of rainfall (1692 mm), with actual evapotranspiration coming in second (713 mm) and percolation below the root zone (groundwater recharge) coming in third (493 mm). The results showed that the CFSR climate simulation produced substantially lower yearly rainfall while the CHIRPS simulation produced only modest variations in all of the estimated water balance components. This demonstrated that the CHIRPS dataset's water balance estimate is more closely matched to the observed water balance estimate than the CFSR estimate. Other research has also noted the CFSR's underestimation of the water balance estimate (e.g., Dile & Srinivasan, 2014). In contrast to the weather that was experienced in the Blue Nile River Basin's Gumera and Rib basins, their investigation revealed that CFSR had overestimated long-term average annual rainfall, which was reflected in the reduced water balance component. The CFSR produced an overestimation in the Gilgel Abay and Megch watersheds; hence, their estimate was inconsistent. In general, it can be seen that the CHIRPS estimate of the water balance is comparable to the observations, whereas the CFSR estimate of the mean annual water balance exhibits fluctuation at higher magnitudes. The difference in spatial resolution between datasets, for example, CHIRPS and CFSR, as well as the spatial variation in rainfall is the most likely explanations for the differences in performance in simulating streamflow and water balance among the climatic datasets. According to other studies (Baez-Villanueva et al., 2018), the performance of gridded climate datasets is greatly dependent on spatial resolution and topographic differences (Fenta et al., 2018).

The CHIRPS rainfall model's superior simulation was also noted in other studies (Bayissa et al., 2017; Dhanesh et al., 2020; Dinku et al., 2018). Compared to CFSR, the CHIRPS rainfall's better performance can be attributed to its increased spatial resolution. Funk et al. (2015) indicated that the CHIRPS rainfall is better at capturing the temporal and spatial variation of observed rainfall because of its superior algorithm for integrating satellite, observed, and reanalyzed rainfall products. Rainfall is also the primary input for hydrological modeling and the analysis of water resources because it is a key driver of hydrological processes (Cho et al., 2009). To overcome the

disadvantage of sparsely and unevenly distributed meteorological stations, a combination of rainfall from CHIRPS and temperature from CFSR products may be used. This alternative data source may be widely used in other Baro–Akobo River basins and the surrounding watersheds for hydrological simulation and water resources management. However, the investigation of a merging rainfall dataset from different sources with the observed or comparing with several products such as IMERGE and GPCC may be required to verify any substantial improvement in the hydrological simulations obtained from hydrological models.

Table 5.3 The mean annual estimated water balance components using observed, CFSR, and CHIRPS datasets.

Climate	Rainfall (mm)	ET (mm)	PERC (mm)	SURQ (mm)	GW_Q (mm)	LAT_Q (mm)	WYLD (mm)
Observed	1692	713	493	389	436	141	966
CFSR	1321	684	330	261	280	102	636
CHIRPS + CFSR	1680	685	611	292	552	154	999
CHIRPS + Observed	1680	683	609	289	550	153	995

ET = evapotranspiration, PERC = percolation below the root zone (groundwater recharge) SURQ = surface runoff, GW_Q = groundwater contribution to stream flow, LATQ = lateral flow into the stream, WYLD = water yield.

5.4 Conclusion

This study compared observed and satellite-based climate data to simulate hydrologic models for hydrologic applications in the Baro and Sore watersheds. The data evaluation was based on the SWAT model using the SUFI-2 algorithm in the SWAT-CUP for sensitivity, calibration, and uncertainty analysis.

The performance of modeling during calibration and validation is encouraging for CFSR and CHIRPS products in both watersheds. However, compared to the calibration period, in several statistical comparison models, performance with the four climate datasets decreased during the validation period for most of the statistical evolution. In addition, the model prediction uncertainty was more pronounced in the Sore watershed than in the Baro watershed.

The CHIRPS combined with the CFSR demonstrate slightly better statistical and hydrological performance than the CHIRPS combined with the observed temperature. The simulations with

CHIRPS and observed yielded minor differences in the water balance components, whereas the CFSR weather simulation gave much lower average annual rainfall, resulting in lower water balance components. The results showed that observed climate and rainfall from the Climate Hazards Group InfraRed Precipitation with Stations (CHIRPS) combined with the CFSR dataset yielded reasonable and comparable streamflow simulation performance. This suggests that the combination of precipitation from CHIRPS and temperature from CFSR can be used to simulate hydrologic models in areas where sufficient observed rainfall is scarce.

Though the direct use of rainfall and temperatures enables a more natural way to reduce the errors in the hydrological simulations induced particularly due to rainfall, the investigation of an integrated rainfall dataset from different sources or comparison with several products such as IMERGE and GPCC may be analyzed as a part of future work to verify any substantial improvement in the hydrological simulations obtained from hydrological models. In addition, the uncertainties associated with satellite data products will translate to unreliable estimates of the hydrological response due to the underestimation or overestimation of simulated hydrology. This can be addressed to an extent by applying bias correction of the satellite rainfall products with the observed data to obtain more realistic hydrological simulations.

6. Modeling the impacts of climate change on hydrological processes in the Baro–Akobo River basin, Ethiopia[3]

Abstract

Understanding the impacts of climate change on basin hydrology is critical for developing effective water management practices. This study was conducted to assess future climate change and its impact on the hydrology of the Baro–Akobo River basin in Ethiopia. Five bias-corrected regional climate models (RCMs) and their ensemble climate scenarios in the 2030s (2021–2050) and 2080s (2071–2100) periods under the two Representative Concentration Pathways (RCP4.5 and RCP8.5) scenarios were compared against the observed climate data for a baseline period (1981–2010). The daily and monthly simulated and observed streamflow during the calibration and validation period showed good agreement with the Nash-Sutcliffe efficiencies of 0.73 and 0.89 and coefficients of determination of 0.73 and 0.9, respectively. Though all RCMs agree concerning the increasing direction of the 2030s and 2080s maximum and minimum temperature changes, there is inconsistency in the magnitude and direction of the monthly projected rainfall changes. Under the ensemble, the annual maximum and minimum temperatures will increase by 2.6 and 3.6°C, respectively, and rainfall will decrease by 5% in the 2080s under the RCP8.5 scenario. The dry season and wet season rainfall are expected to decrease by 19 and 3.7%, respectively, under the RCP8.5 scenarios in the 2080s. Consequently, future climate change could cause a decrease in streamflow under the RCP4.5 and RCP8.5 scenarios. For most of the flow magnitude, the low range of variability approach (RVA) category shows an increasing trend, however, the middle and the high RVA categories show a decreasing trend. This study provides useful insights about potential climate change impacts on the hydrology of the basin, which could be useful to inform decision-makers in developing strategies such as water harvesting to mitigate the impact of climate change.

Keywords: climate projection, hydrological response, SWAT, Baro–Akobo basin.

[3] This chapter is based on Mengistu, A.G., Woldesenbet, T.A, Dile, Y.T, Bayabil, H.K. Modeling the impacts of future climate change on the hydrological processes in the Baro–Akobo River basin, Ethiopia. Under review in Acta Geophysica

6.1 Introduction

The Global Climate Model (GCM) climate predictions provide a general view of how the earth's climate system may be affected in the future (IPCC, 2007). Greenhouse gas emission has considerably increased since the industrial revolution and led to global warming (Vuuren et al., 2011). The finding of the IPCC showed that carbon dioxide (CO_2) concentration in the atmosphere increased from 280 ppm in 1750 to 367 ppm in 1999 (Houghton et al., 2001). The concentration is expected to reach 463–623 ppm in 2060, and it is anticipated to be between 470–1099 ppm by 2100 (IPCC, 2013). It is indicated that the increased greenhouse gas emissions will cause an increase in the average temperature of the earth by up to 1.4 – 5.8°C in the 2080s (Hoegh-Guldberg & Bruno, 2010). In general, rising global surface temperatures, variability of rainfall patterns both spatially and over time, and changes in the predictability of this variance are all expected in the future period (Bolch et al., 2012; Dile et al., 2013; Getachew et al., 2021; Liu, 2022; Worku et al., 2021).

The climate variability and change impacts will be substantial, particularly in developing countries where their economy is mainly dependent on rainfed agricultural production (Abdo et al., 2009; Getachew et al., 2021; Worqlul et al., 2018). For instance, research indicated that the Nile region and its sub-basins such as the Baro–Akobo River basin are one of the most vulnerable regions in the world concerning climate change because of its highly diverse climatic and topographical variations (Alemayehu et al., 2016; Beyene et al., 2010; Conway & Schipper, 2011; Kim et al., 2014). Climate change is expected to affect the livelihood of a great number of people living within the region (Conway & Schipper, 2011). In addition, poor agricultural land management practices coupled with increasing climate extremes are affecting the livelihoods of these communities (IPCC, 2007; NAPA, 2007). This advocates that climate change will be expected to significantly affect the livelihoods of the pastoralists and smallholder farmers, which warrants comprehensive climate impact studies to support climate change mitigation and adaptation policy. Thus, it is important to understand the impact of climate change on hydrology to implement suitable climate change adaptation and mitigation strategies. For instance, the development of small-scale irrigation where dry season streamflow is reliable (Worqlul et al., 2018), and water harvesting methods while the flow is abundant (Worku et al., 2020a) are among the possible mitigation strategies. Since the impacts might vary greatly between regions, it is crucial to carry out such research in key agroecological regions to develop and put into practice adaptation and mitigation methods.

Several studies were conducted in the Eastern Nile basin to simulate the impact of climate in the hydrology, particularly in the Upper Blue Nile basin (Abdo et al., 2009; Beyene et al., 2010; Dile et al., 2013; Elshamy et al., 2009; Fentaw et al., 2018; Mengistu & Sorteberg, 2012; Muleta, 2021; Setegn et al., 2011; Taye et al., 2018; Woldesenbet et al., 2018; Worku et al., 2021; Worqlul et al., 2018); but only limited studies were conducted in the Baro–Akobo River basin (Fentaw et al., 2018; Muleta, 2021). The majority of these studies were based on statistically downscaled single GCMs that relied on the third phase of the Coupled Model Intercomparison Project (CMIP3) (e.g., Abdo et al., 2009; Worqlul et al., 2018). Some of these studies used a single GCM/RCM with a single emission scenario (Muleta, 2021). Nevertheless, few studies use bias-corrected RCM outputs and their ensemble (Elshamy et al., 2009; Worku et al., 2021) as inputs to climate impact studies. As a result, these studies have revealed mixed findings on the influence of climate on hydrological modeling. For instance, an increase in streamflow was projected by (Dile et al., 2013; Fentaw et al., 2018) using GCM/RCM outputs in the Upper Blue Nile Basin. In contrast, Elshamy et al. (2009) and Worku et al. (2021) projected a decrease in the streamflow in the Ethiopian highlands using bias-corrected GCMs and RCMs, respectively. This implies that there is no conclusive finding regarding how climate change will affect streamflow. To the best of our knowledge, no study has examined the combined use of the soil and water assessment model and the indicators of hydrological alteration for hydrological evaluation under the RCP4.5 and RCP8.5 scenarios in the study basin. Therefore, it is important to identify and describe the climate change uncertainties in the basin using a multi-climate model combined with bias correction.

This research was carried out in the Baro–Akobo River basin, which is known as one of the most productive areas in the country and serves as the headstream of the Easter Nile River. Several projects related to irrigation and hydropower are ongoing under the government of Ethiopia (Sileet et al., 2013) that will pose environmental effects on the basin and downstream countries such as Sudan and Egypt. Moreover, the basin is highly vulnerable to changes in climate, and extreme occurrences such as drought and flooding are projected in the future (IPCC, 2014). Nonetheless, the basin has witnessed substantial climate change during the last four decades (NAPA, 2007), adding to the challenges of water resource management. The majority of the population relies on rain-fed agriculture for their living, which is constantly impacted by climate change. This shows that climate change would have a considerable influence on smallholder farmers' livelihoods, necessitating thorough climate impact assessments to support climate change adaptation strategies.

However, there is a limitation to integrating climate information and climate adaptation strategies to reduce climate change impacts in the basin (Conway and Schipper, 2011). The increasing demand for water in the basin due to socio-economic progress and high demand for irrigation and hydropower may cause conflict in the basin unless a comprehensive water resource management plan is developed. In addition, the impact of climate change on the different hydrological processes is poorly understood in this poorly gauged river basin. Therefore, assessing the availability of water resources in the basin in a changing climate is a prerequisite to implementing evidence-based water management options.

Thus, this study is important to provide plausible climate information generated from different bias-corrected RCMs and their ensemble rainfall and temperature outputs under different emission scenarios. It is useful to assess the impact of climate change on the hydrology of the basin in the future by considering various indicators of hydrological alteration that have been overlooked by previous studies. Such information plays a vital role in supporting the existing and planned water resources management practices in the basin. Therefore, the objectives of this study are to (1) evaluate the variations between multiple RCMs in simulating climate over the basin under the RCP4.5 and RCP8.5 scenarios and (2) evaluate the climate change impact on the basin hydrological processes implied by the ensemble results from the various RCMs of the RCP4.5 and RCP8.5 scenarios using the Soil and Water Assessment Tool (SWAT) model and the indicators of hydrological alteration.

6.2 Material and Methods

6.2.1 Data inputs

The SWAT model was used for this study. SWAT requires hydrologic, climate, and spatial data to simulate basin hydrological processes. Specific data inputs include streamflow, rainfall, maximum and minimum temperatures, relative humidity, solar radiation, and wind speed. In addition, spatial data inputs include DEM, soil, and land use maps.

Daily rainfall, maximum temperature (Tmax), and minimum temperature (Tmin) for the period 1981–2010 (the baseline period) were obtained from the Ethiopian National Meteorological Agency (ENMA). Further descriptions of the weather dataset are available (Mengistu et al., 2021a). For stations where there is no observation of solar radiation, sunshine, wind speed, and relative humidity, a gridded dataset from the Climate Forecast System Reanalysis (CFSR) was

used. CFSR is designed based on the coupled atmosphere–ocean–land surface–sea ice system to provide high resolution and the best estimate of climatic variables (Dile & Srinivasan, 2014; Fuka et al., 2013; Mengistu et al., 2021b; Saha et al., 2010; Woldesenbet & Elagib, 2021).

The USGS website provided a DEM with a resolution of 30 × 30 m. The DEM was used to define the basin boundary and provides impotent basin properties such as slope gradient, slope length, stream network, and stream characteristics (channel slope, width, and length). The soil physicochemical parameters were acquired from the African Soil Information System soil data (AfSIS), which provides soil information at 250 m spatial resolution and contains most of the soil parameters for six soil layers (Bayabil & Dile, 2020; Hengl et al., 2015). The pedo–transfer function was used to generate the parameters required by the SWAT model (Saxton & Rawls, 2006). The dominant soil textural class can be classified as clay, clay–loam, and silt–clay soils. ArcGIS 10.4 software was employed to prepare a raster spatial map of DEM and soil. Land use is another important spatial input data required for the SWAT model. Landsat 7ETM+ image was acquired from the (USGS) http://earthexplorer.usgs.gov/. Supervised classification methods with a MLC in ERDAS Imagine software were used for image classification. A total of 450 reference data points were acquired from Google Earth imagery. Of the total collected data, 2/3 were used for supervised image classification and the rest 1/3 were used for accuracy assessment. To determine the accuracy of land use classification, the users, producers, the overall classification, and the kappa coefficient were estimated using ERDAS Imagine software. The accuracy of classification had an overall classification accuracy of 84.6% and a kappa coefficient of 0.81. The dominant land-use types in the basin include forest, agriculture, and grassland. All the spatial datasets were projected to the same projection called the Universal Transverse Mercator (UTM) projection system of Zone 37N.

6.2.2 Regional climate model outputs

The GCM-driven RCM climate projections are provided by the Earth System Grid Federation and downloaded from the Africa-CORDEX data portal (https://esgf-data.dkrz.de/search/cordex-dkrz/) with a resolution of 50 x 50 km. The RCMs namely RCA4 (CNRM), RCA4 (ICHEC), CCLM4 (CNRM), CCLM4 (MPI), REMO (MPI), and their ensemble mean are used because of their good performance in climate simulation in most parts of Africa, including Ethiopia (Dibaba et al., 2019; Fentaw et al., 2018; Nikulin et al., 2012; Mengistu et al., 2021a; Worku et al., 2021). In each RCM,

two representative concentration pathways, RCP4.5 (moderate future emission) and RCP8.5 (extreme future emission), the current trend (Moss et al., 2010) were used for future scenarios. Three-time horizons under two representative concentration pathways (RCP4.5 and RCP8.5) were considered to represent the possible changes in rainfall and temperature. These time horizons include baseline (1981–2010), 2030s (2021–2050), and 2080s (2071–2100).

6.2.3 Bias-correction of regional climate models

The climate model data for the hydrological modeling (CMhyd) tool obtained from swat.tamu.edu/software was designed to work with the CORDEX data archive. CMhyd was designed to provide simulated climate data that can be considered representative of the location of the gauges used in a basin model setup. CMhyd is a tool that can be used to extract GCM and RCM data. Therefore, in this study, the historical and future climate model data are extracted for each of the gauge locations using the station's latitude, longitude, and elevation. Then the average value was used to estimate both the baseline and RCM climate in the basin. Detailed descriptions and information on the theory of linking climate and hydrologic models have been available (Christensen et al., 2008; Teutschbein & Seibert, 2012; Rathjens et al., 2016).

Climate models often provide biased representations of observed time series, making correction procedures necessary (Christensen et al., 2008; Teutschbein & Seibert, 2010; Varis et al., 2004). Different bias correction methods, such as linear scaling and distribution mapping methods, show comparable skill in adjusting the mean, standard deviation, and variance of rainfall and temperature events of RCM outputs. Compared to other bias correction methods the distribution mapping method shows better skill in adjusting the extreme values and wet day probability of RCM outputs with their baseline counterparts (Block et al., 2009; Teutschbein & Seibert, 2012; Worku et al., 2020). This study used the CMhyd tool to process the rainfall and temperature bias correction for each station using the distribution mapping methods.

For modifying RCM output, bias correction processes use a transformation algorithm (Piani et al., 2010). Identification of potential biases among the simulated and observed climate variables is the key concept, and it serves as the foundation for modifying control and scenario RCM runs. Bias correction methods are supposed to be stationary, i.e., the correction algorithm and its parameterization for current climate conditions are also valid for future conditions. To change the distribution functions of the modeled variables into the observed ones, the statistical

transformations use a mathematical function. Statistical transformations try to find a function h that fits a modeled variable such that its new distribution equals the distribution of the observed variable (Gudmundsson et al., 2012; Piani et al., 2010). These transformations are expressed mathematically as (equation 6.1):

$P_o = h\ (P_m)$……(6.1)

The distribution mapping approach fits the distribution of rainfall and temperature of RCMs with observational data using the Gamma distribution (Gudmundsson et al., 2012) and the Gaussian distributions (Cramér, 1999). The idea of distribution mapping is to correct the distribution function of RCM-simulated rainfall and temperature values to agree with the observed distribution function. This can be performed by creating a transfer function to shift the occurrence distributions of rainfall and temperature (Gudmundsson et al., 2012; Teutschbein and Seibert, 2012). For instance, the distribution mapping approach provides the following transformation between observed and modeled rainfall (equation 6.2):

$P_0 = F_O^{-1}\ (F_m(P_m))$ ……... (6.2)

P_0 is an observed rainfall

P_m is the model rainfall

F_m is the CDF related to P_m and

$F_O - 1$ is the inverse CDF of P_0.

6.2.4 Assessment of extreme rainfall indices

The difference between the baseline and future climate change scenarios was estimated using six extreme rainfall indices (Table 6.1). The indices selected include R10mm, R20mm, CDD, R95P, RX1 day, and RX5 day, as obtained from the Expert Team on Climate Change Detection and Indices (ETCCDI) (WMO, 2009). All of these indices were estimated using RClimDex (Zhang and Yang, 2004). Several studies used rainfall indices to assess the difference between the baseline and future climate change scenarios (IPPC, 2014; Shrestha & Roachanakanan, 2021).

Table 6.1 Description of the ETCCDI of extreme rainfall indices selected in the analysis.

Indices	Indices name	Description	Unit
R10	Number of heavy rainfall days	Annual count of days when rainfall > = 10mm	day

R20	Number of very heavy rainfall days	Annual count of days when rainfall > = 20mm	day
CDD	Consecutive dry days	Maximum number of consecutive days with rainfall <1mm	day
R95p	Very wet days	Annual total rainfall when rainfall >95th percentile	mm
RX1	Max one-day rainfall amount	Monthly maximum consecutive one-day rainfall	mm
RX5	Max five-day rainfall amount	Monthly maximum consecutive five-day rainfall	mm

6.2.6 Model calibration and validation

Successful application of a hydrologic model depends on parameter sensitivity analysis and model calibration and validation processes. The SUFI2 algorithm in the SWAT-CUP was used to conduct model parameter sensitivity analysis, calibration, and validation (Abbaspour et al., 2015). Eighteen relevant hydrological parameters (Koch et al., 2012; Mengistu et al., 2021b; Mengistu & Sorteberg, 2012) were selected for sensitivity analysis, and ten parameters with smaller p-values and greater t-stats were selected for the calibration and validation process. For the sensitivity analysis, parameters related to soil water, runoff, groundwater, and evapotranspiration were taken into account. The model's performance during the calibration and validation periods was assessed using suitable statistical measures (Moriasi et al., 2007). These statistical measures including the NSE, $R^{2,}$ and PBIAS were used for model performance evaluation.

To estimate the future climate change impact on streamflow, a total of five simulation periods were established from the best-performing RCMs (ensemble). Then the calibrated SWAT model is run for a baseline (1981–2010) and the 2030s (2021–2050) and the 2080s (2071–2100) periods under the RCP4.5 and RCP8.5 scenarios. The future climate change impact was examined by comparing the monthly, seasonal, and annual value of the baseline period with the value of the corresponding future period and climate impact scenarios.

6.2.7 Indicators of hydrologic alteration

In addition to SWAT, in this study, the hydrological parameters were estimated using the IHA 7.1 software (The Nature Conservancy, 2009). The software and method required at least 20 years of daily hydrological data, which includes streamflow, river stages, and groundwater levels (Richter et al., 1996). However, in this study, we have used the daily streamflow data to compare the pre-

impact (baseline) against post-impact (future periods and scenarios). For IHA setup, daily streamflow data for the baseline period (1981–2010) was regarded as natural flow and the future period and RCPs climate scenarios as altered flow. A comparable approach has been applied in other studies (Kiesel et al., 2019; López-Ballesteros et al. 2020; Woldesenbet, 2022). The IHA enables the user to examine a comparison analysis called the Range of Variability Approach (RVA) that practically assess the hydrologic alteration at a particular river site before and after an impact or amongst different long periods. RVA distributes the full range of pre-impact data for each parameter into 3 categories of equal range (low, middle, and high). The low category defines values below or equal to the 33rd percentile of the median, the middle defines values found between the 34th to 67th percentile, and the high defines values that are greater than the 67th percentile. The expected frequency with which the "post-impact" values would fall within each class was calculated using (equation 6.7).

$$\mathrm{HA} = \frac{\text{Observed frequency} - \text{Expected frequency}}{\text{Expected frequency}} \quad \ldots\ldots\ldots\ldots\ldots\ldots\ldots\ldots\ldots\ldots \; (6.7)$$

A positive hydrological alteration (HA) value indicates that the frequency of values in the category has increased from the pre-impact (baseline) to the post-impact (future periods and scenarios) (with a maximum value of infinity), whereas a negative value indicates that the frequency of values has decreased (with a minimum value of –1) (Richter et al., 1996).

6.3 Results

6.3.1 Performance of the regional climate model

The performance of the bias-corrected RCMs and their ensemble mean to simulate the basin climate using Taylor's diagram method is presented in Figure 6.1. A comparison of the various bias-corrected RCM simulations with the baseline data using Taylor's diagram shows that the ensemble has relatively better performance, while the CCLM4 (MPI) performance is low. The high correlation values and the lower RMSE and standard deviation (SD) values show a better performance of the ensemble in the basin climate simulation. For rainfall and Tmax, the points of the ensemble mean are closer to the baseline compared with the individual models, with R close to 1. On the other hand, the RMSE of the ensemble is also close to zero compared with the RMSE of the other individual models.

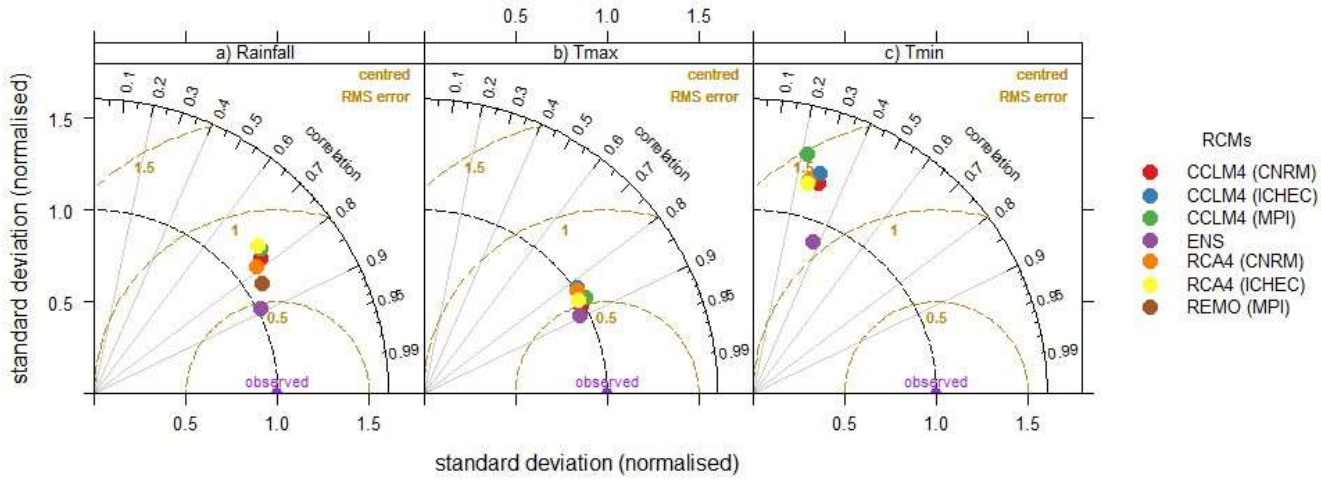

Figure 6.1 Comparison of the skill of bias-corrected climate models and their ensembles with observed monthly rainfall and maximum and minimum temperatures using Taylor's diagram.

In addition to the Taylor diagram, Figure 6.2 shows that the bias-corrected cumulative distribution function (CDF) of the baseline daily rainfall is best captured when using the ensemble mean instead of individual models. For example, in simulating the 75% percentile, approximately 7.7 mm/day was estimated from the baseline, a slightly lower amount of 7.2 mm/day from the ensemble, and the CCLM4 (CNRM) was estimated as low as 5.6 mm/day. While estimating the 95% percentile, all models, including the ensemble, overestimated the baseline; the baseline was estimated at 13.3 mm/day, the ensemble estimated 14 mm/day, and CCLM4 (CNRM) estimated as much as 20.5 mm/day.

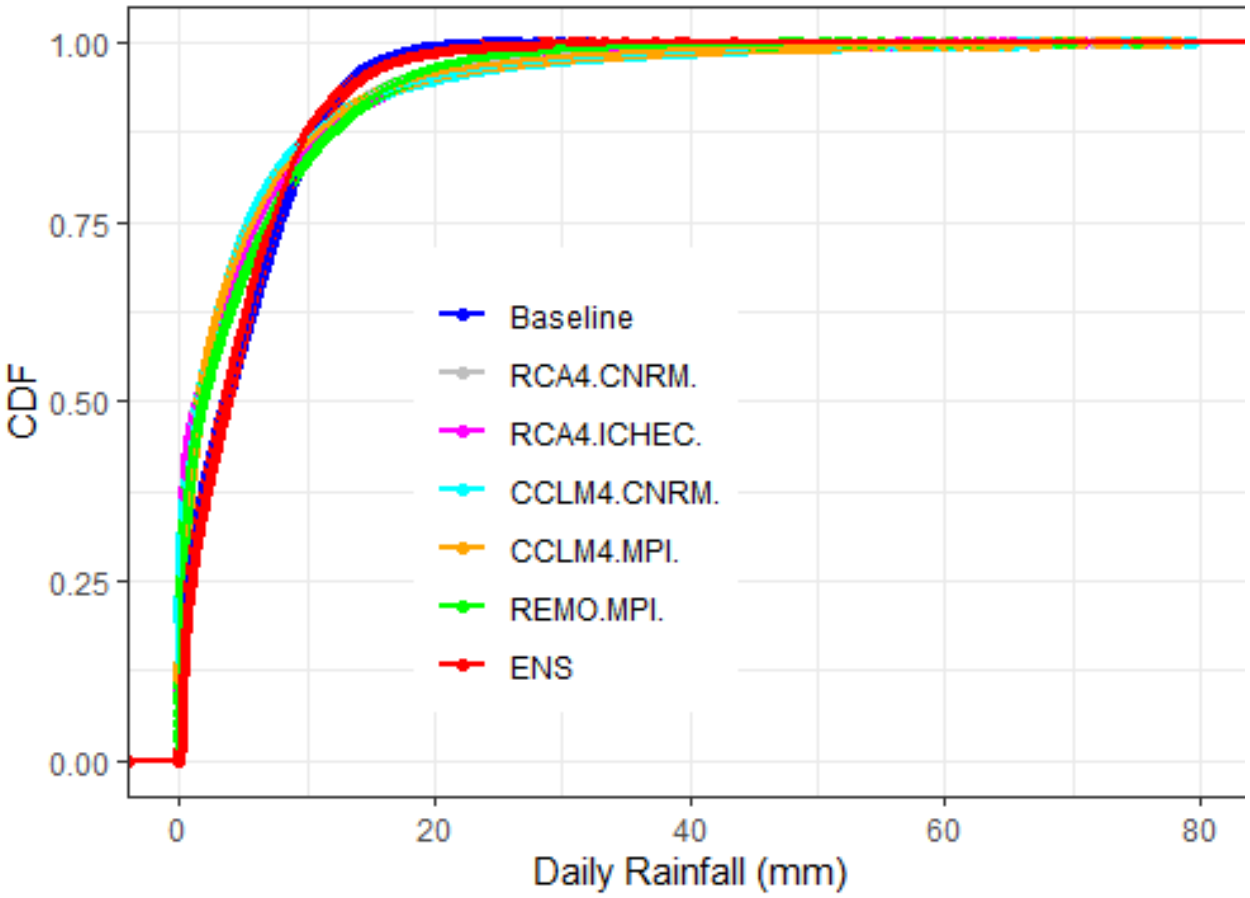

Figure 6.2 Comparison of the Cumulative Distribution Function (CDF) of the different RCMs simulations of rainfall estimates with baseline climate.

These statistical comparisons suggest climate change impact studies in the basin may benefit from using an ensemble of simulated rainfall and temperatures obtained from multiple regional climate models instead of simulated rainfall from individual models. Other studies comparing the historical performance of RCMs also show that multimodal ensembles often perform better than individual RCMs, with higher correlation and lower biases, SD, and RMSE (Kundzewicz et al., 2018; Mengistu et al., 2021a; Teutschbein & Seibert, 2010; Worku et al., 2021). IPCC findings also encourage the use of multi-modal ensembles with caution (Wilby, 2010).

6.3.2 Climate projection under future periods and climate scenarios

The future period projection of the mean monthly rainfall and Tmax and Tmin simulated by bias-corrected RCMs and their ensemble is presented in Figure. 6.3 and Figure 6.4, respectively. The projected mean monthly rainfall for the 2030s and 2080s under both climate change scenarios did

not show a consistent magnitude and direction compared with the baseline climate. The projected rainfall for most of the RCMs shows a decreasing trend in the majority of the months of the year under future periods and scenarios. For the RCP4.5 scenarios, monthly rainfall changes range from −61 to 52 % and −63 to 41% for the 2030s and 2080s, respectively. Both the largest decrease of 63% and an increase of 52% are estimated by RCA4 (CNRM). Similarly, for RCP8.5 scenarios, monthly rainfall changes range from −54 to 69% and −65 to 50% for the 2030s and 2080s, respectively. The largest decrease of 65% and an increase of 69% are estimated by the RCA4 (ICHEC) and RCA4 (CNRM) models, respectively. The typical dry months (January and February) show a consistent decreasing trend for all RCMs under future periods and scenarios, while from October to December, the majority of the RCMs show an increasing trend. For the RCP8.5 scenario, dry season rainfall changes from −25 to 4% and −33 to −4% for the 2030s and 2080s, respectively. Wet season rainfall for the RCP8.5 scenario ranges from −3.7 to 7.8% and −15% to 2.4 for the 2030s and 2080s, respectively, demonstrating a relatively narrower range of projection for the wet season than the dry season.

In general, there is much better consistency between climate model projections of temperature than rainfall. All bias corrected RCMs show a consistent increase in Tmax and Tmin as projected by RCP4.5 and RCP8.5 throughout the future period. For example, CCLM4 (ICHEC) under RCP8.5 shows the largest increase of 3.9 °C in Tmax in February by the 2080s, whereas CCLM4 (MPI) under RCP4.5 for the 2030s indicates the lowest increase in Tmax at 0.52 °C in July. Similarly, RCA4 (ICHEC) shows the highest increase of Tmin 5.34°C in May under RCP8.5 for the 2080s, whereas the CCLM4 (CNRM) model indicates the lowest increase of 1.39 °C in January under RCP4.5 for the 2030s. These results show that the change in both Tmax and Tmin for the 2080s is larger when driven by RCP8.5 compared to RCP4.5, and the increase in Tmin is larger than Tmax. The bias-corrected individual RCMs as well as the ensemble temperature projection show good consistency with the projected global climate change scenarios compared to the rainfall. However, in general, the climate projections show uncertainty in both rainfall and temperature projections for future periods and scenarios. The greater difference in the directions and magnitudes in the RCM's projections, particularly for rainfall, demonstrates a wide range of uncertainties associated with future rainfall projections. This result is consistent with other studies (Hawkins & Sutton, 2011), in which future period climate projections are inconsistent under different RCMs and RCPs, suggesting large uncertainty in the projection of climate, particularly in rainfall projection.

Kundzewicz et al. (2018) indicated that uncertainty in the future amount of greenhouse gas emissions and uncertainty related to the inadequate model representation of climate processes are the main sources of uncertainty in future climate projections. Beyene et al. (2010) predicted a wide range of individual GCM rainfall projections. Their finding under the A2 emission scenario shows that the Nile River Basin will experience a substantial decrease in December to February rainfall changes ranging from −24 to 37% and −40 to 18% for periods 2010–2039 and 2070–2099, respectively, which is somewhat comparable to our −25 to 4% and −33 to −4% for the periods 2030s and 2080s for the RCP8.5 scenario projection, respectively. Similarly, their findings show that the June to August rainfall for the entire Nile basin under the A2 emissions scenario varies from −21 to 34 and −42 to 15% for the periods 2010–2039 and 2070–2099, respectively. Their finding of a relatively narrower range of projections for June to August than December to February is comparable to our seasonal rainfall projection. According to the IPCC (2001), based on nine GCMs, the Nile basin will experience rainfall changes between 0 and 40 mm by the end of the twenty-first century. In contrast, Worqlul et al. (2018) have projected an increase in the dry season rainfall in the upper Blue Nile basin using the downscaled outputs of the HadCM3 climate model. Eastern and tropical Africa could show a 7% rise in rainfall (IPCC, 2007). In general, findings in the IPCC Third Assessment (McCarthy et al., 2001) showed that the predicted future changes in mean monthly and seasonal rainfall in Africa are not well defined. Predictions of future climate change at subregional and local scales are challenging due to the diversity of African climates, high rainfall variability, and a very poor monitoring network. As a result, such climate model comparison is critical prior to future climate impact studies, and selecting the best-performing model may reduce uncertainty.

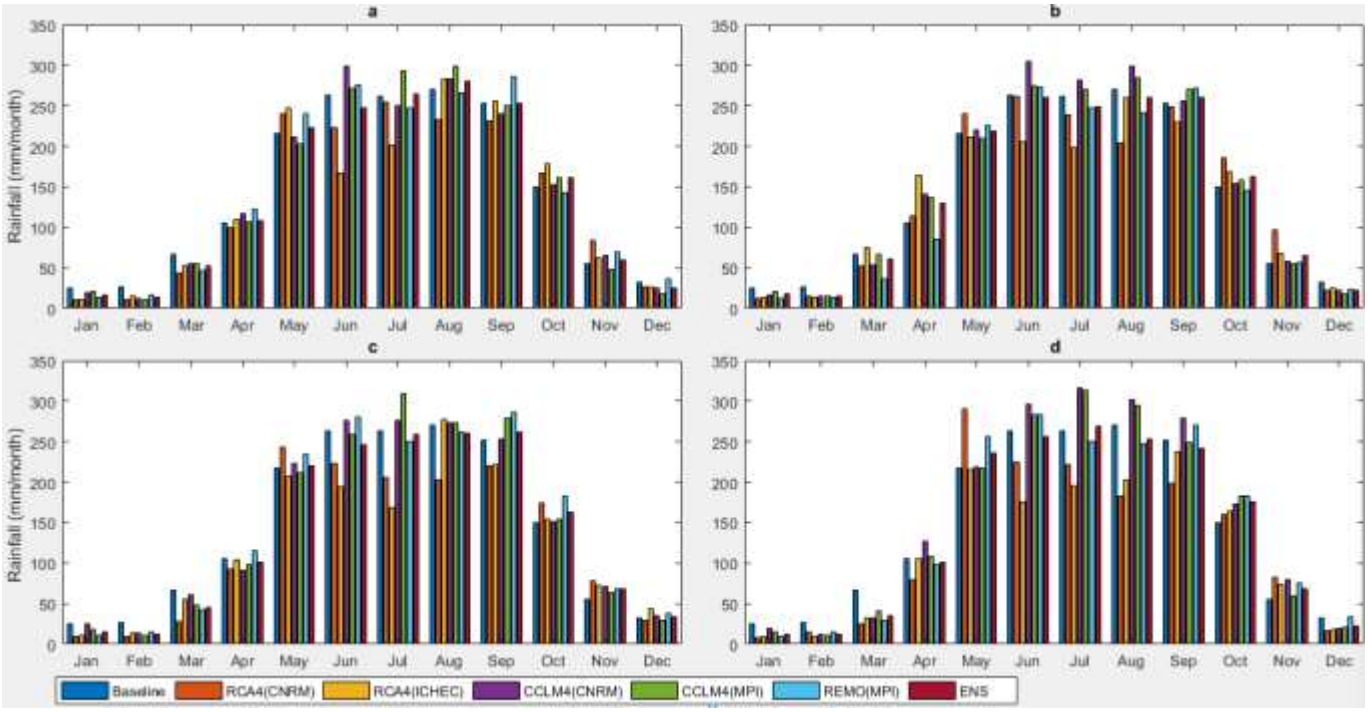

Figure 6.3 Long-term mean monthly rainfall for the baseline and future period and scenarios; a) RCP4.5 2030s, b) RCP8.5 2030s, c) RCP4.5 2080s, and d) RCP8.5 2080s.

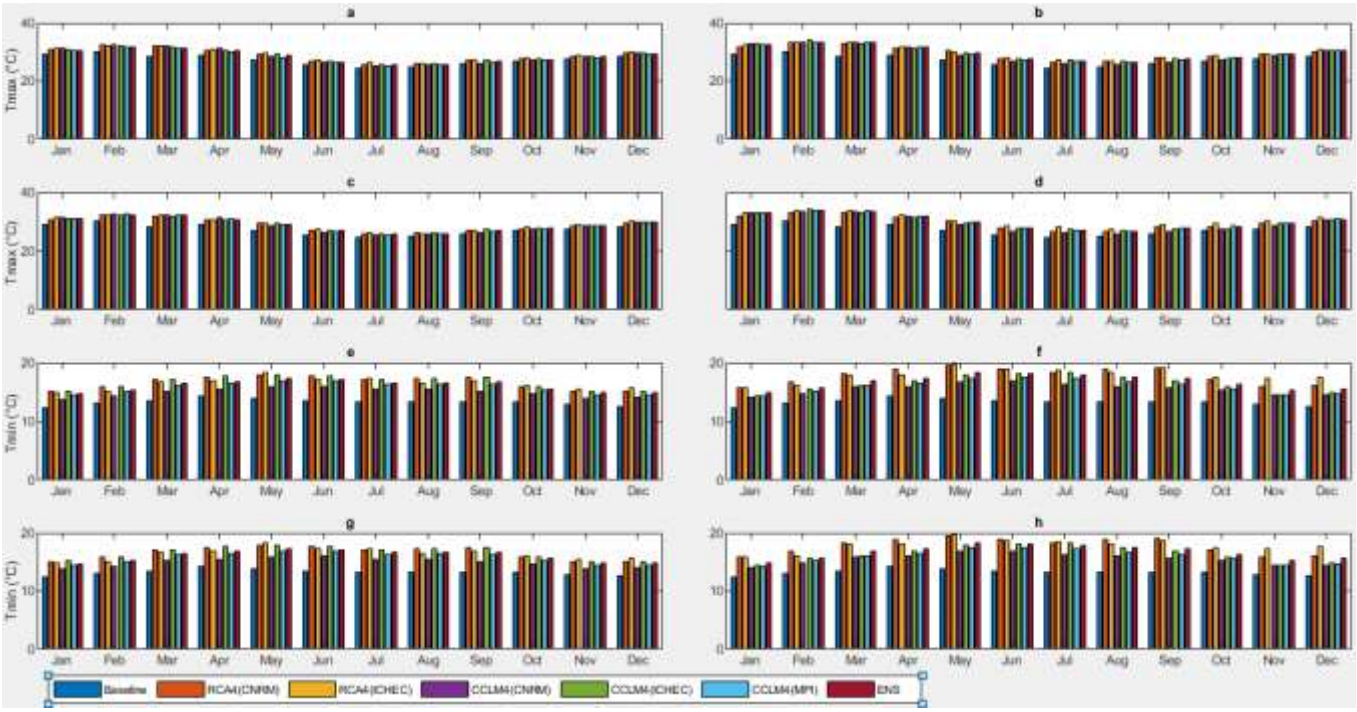

Figure 6.4 Long-term mean monthly temperature for the baseline and future period and scenarios. The first four-panel a), b), c), and d), and the next four– panels e), f), g), and h) represent RCP4.5

2030s, RCP8.5 2030s, RCP4.5 2080s, and RCP8.5 2080s for maximum temperature (°C), and minimum temperature (°C), respectively.

Because of the uncertainty amongst RCMs, the ensemble mean is used to obtain a generalized picture of the future climate and its hydrological impacts. Figure 6.5 depicts the change in projected ensemble monthly rainfall and minimum and maximum temperatures under RCP4.5 and RCP8.5 scenarios. The extent of changes and directions in the ensemble mean monthly rainfall vary, with the largest decrease of 41% in February under RCP8.5 for the 2080s and the largest increase of 22% in November under RCP4.5 for the 2080s. Further, the dry and wet seasons' mean rainfall is expected to decrease by up to 19% and 4%, respectively, under RCP8.5 by the 2080s. This indicates a relatively narrower range of projections for the wet season than the dry season. The decrease will be up to 5.1 percent for annual rainfall compared to the baseline period, which is expected under RCP8.5 in the 2080s scenarios. The projected Tmax and Tmin under the RCP4.5 and RCP8.5 scenarios showed an increasing mean value for both future periods. The mean annual Tmax is expected to increase by 1.2 to 1.6 ℃ under RCP4.5 and 2.4 to 2.6 ℃ under RCP8.5. Similarly, the mean annual Tmin would increase by 2.2 to 2.6 ℃ for RCP4.5 and 3.26 to 3.29 ℃ for RCP8.5.

The ensemble mean result is consistent with (Dibaba et al., 2020; Worku et al., 2021), who found a decreasing annual rainfall projection in the Ethiopian highlands under bias-corrected RCP4.5 and RCP8.5 scenarios. In addition, the temperature projection shows a higher increase in Tmin than Tmax under future periods and scenarios. The temperature projections are consistent with other Ethiopian studies and global temperature predictions. Several studies in Ethiopia (Elshamy et al., 2009; Muleta, 2021; Setegn et al., 2011; Woldesenbet et al., 2018; Worqlul et al., 2018) indicated an increase in temperatures as compared to historical observations. Furthermore, according to the endorsement of the IPCC (2013), a higher increase in temperature is predicted in the 2080s than in the 2030s. In other studies in Africa, Hulme et al. (2001) indicated that during the 20th century, mean annual temperatures increased by 2 °C, whereas mean annual rainfall decreased by 20%. The risks associated with extreme climate events are found to be high with an extra 1°C increase in warming. All these results demonstrate there will be a high rise in temperature unless considerable and sustainable actions are taken to limit greenhouse gas emissions particularly by the developed countries.

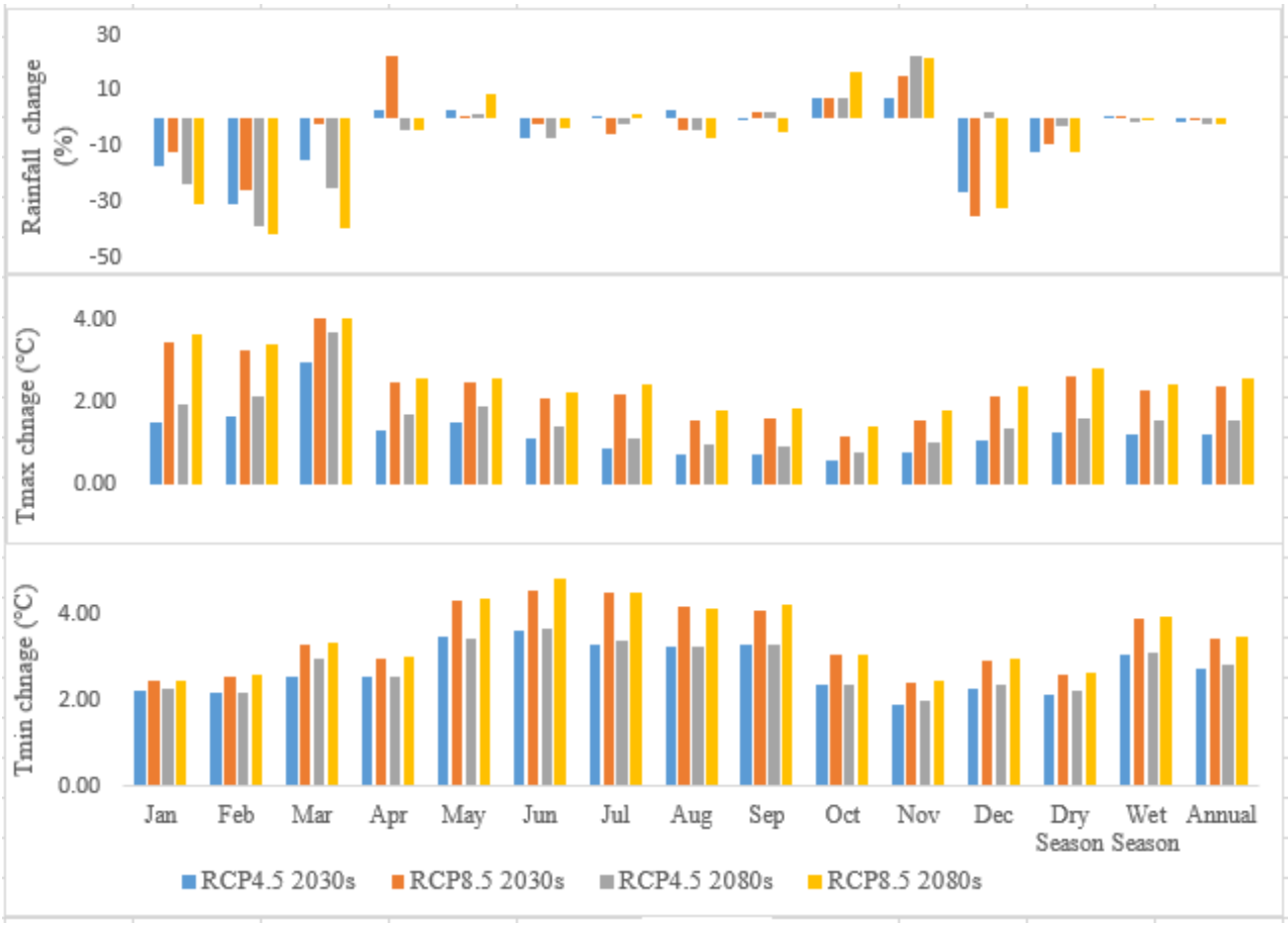

Figure 6.5 Projected changes in mean monthly, seasonal, and annual ensemble future climate change scenarios compared to the baseline condition.

To enhance our understanding of the future condition of extreme rainfall in the basin, the boxplot of selected extreme indices (R10, R20, CDD, R95p, RX5, and RX1) of daily rainfall amount is also shown in Figure. 6.6. The future projection under both RCPs indicated an increase in the R20, CDD, R95p, RX1, and RX5 indices, but the R10 indices show a decreasing value. For instance, the median values of the R95P, RX1, and RX5 indices estimated from the baseline were 196.8 mm, 25.9 mm, and 72 mm, respectively; when comparing these values with the counterpart of RCPs, there is a difference showing an increase as large as 230.4 mm, 28.1 mm under the RCP8.5 in the 2080s, and 83.6 mm under the RCP4.5 in the 2080s, respectively. Similarly, the mean number of days with rainfall greater than 20 mm (R20) in the baseline period is 3.9 days per year. In the 2030s, this is projected to increase to 4.2 and 5.4 days per year under the RCP4.5 and RCP8.5 scenarios, respectively. In the 2080s, this is projected to increase to 5.6 and 4.2 days per year under the RCP4.5 and RCP8.5 scenarios, respectively. The likely increase in rainfall extremes under

RCPs is consistent with the findings of upper Blue Nile basin studies (e.g., Worku et al., 2021; IPCC, 2014).

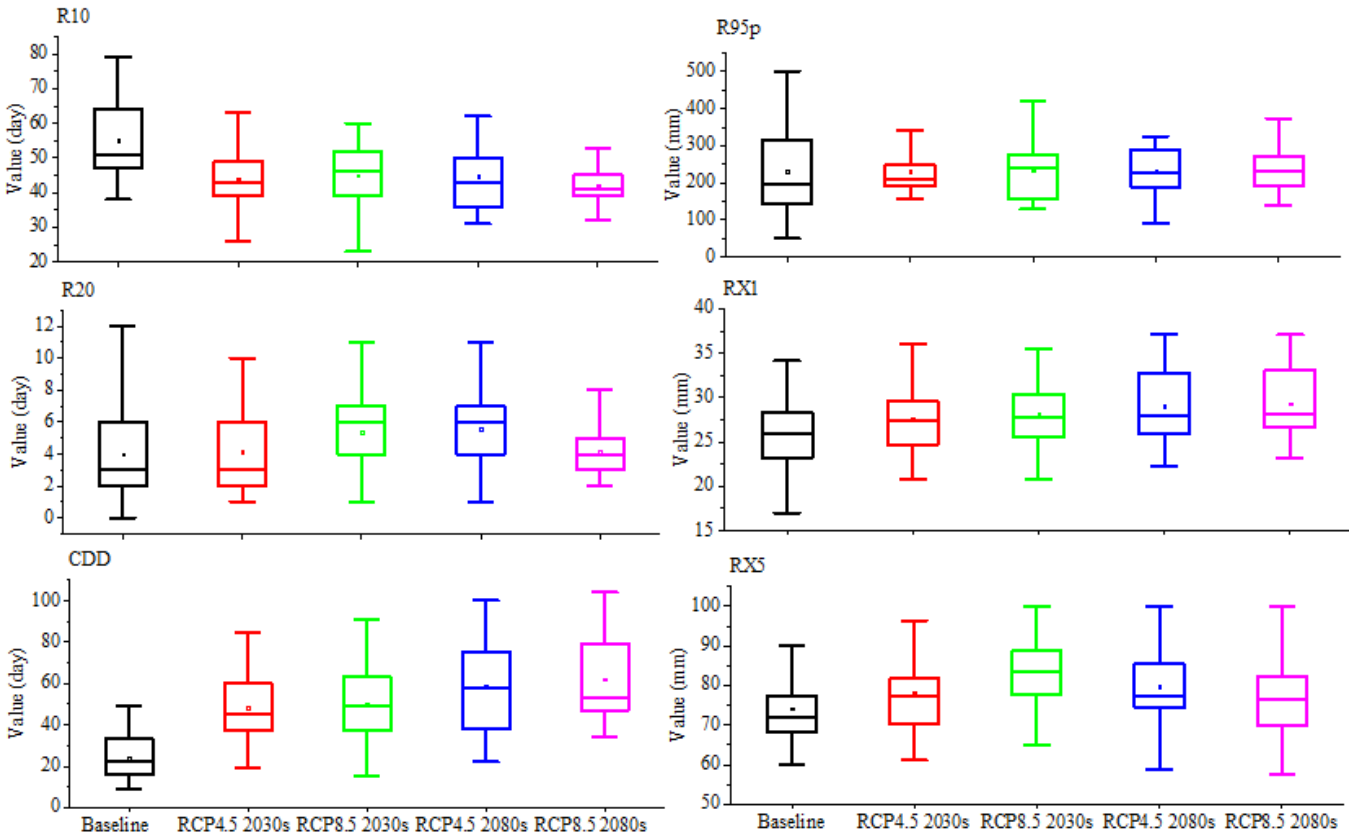

Figure 6.6 The difference in average daily rainfall indices between the baseline and climate change scenarios. For each baseline and emissions scenario, the horizontal line shows the median values, the box shows the 25th and 75th percentiles of the projections, and the vertical lines show the minimum and maximum values of the projected estimate.

An increase in rainfall extreme projections (e.g., R20, R95p, RX1, and RX5) in RCP scenarios could lead to a greater climatic risk to human livelihood and other environmental resources. On the other hand, a decline in rainfall projection (e.g., R10 and the mean value) could impact crop production and the amount of water available in rivers and streams. In general, the greater range of potential changes between the models and the different extreme indices suggests that we should be prepared for many probable impacts from changing rainfall and temperature.

6.3.4 Hydrological model sensitivity, calibration, and validation

Different hydrologic parameters (Table 6.2) of the basin were evaluated for their sensitivity during the calibration processes. Based on the global sensitivity analysis, CN2 (the curve number), the soil evaporation compensation factor (ESCO), and soil depth (SOL_Z) were recognized as the most sensitive parameters. As a result, a slight change in these parameters causes a rapid response in runoff generation. These parameters depend on several factors, such as soil type, soil permeability, and land use type. Groundwater "revap" coefficient (GW_REVAP), maximum canopy storage (CANMX), and base-flow alpha-factor (ALPHA_BF), were all identified to have a substantial impact on the calibration processes of the hydrological components. In general, the higher the t-statistic and the lower the p-value (Figure 6.7) indicate that the parameter is more sensitive in simulation (Abbaspour et al., 2015).

Table 6.2 The most sensitive parameters identified during the calibration period based on daily streamflow observations.

List of parameters	Description	Range	Final value
r_CN2.mgt	Curve number	±25%	0.07
v_ALPHA_BF.gw	Base-flow alpha-factor (Days)	0-1	0.3
v_ESCO.hru	Soil evaporation compensation factor	0-1	0.41
r_SOL_AWC.sol	Soil available water capacity (mm/mm)	±25%	-0.03
v_ GW_REVAP.gw	Groundwater "revap" coefficient	0.02-0.2	0.11
v_EPCO.hru	Plant uptake compensation factor	0-1	0.67
r_SOL_Z.sol	Soil depth (mm)	±25%	0.05
v_CANMX.hru	Maximum canopy storage (mm)	0-10	4.55
r_SOL_K.sol	Soil-saturated hydraulic conductivity (mm/hr)	±25%	0.04
r_SOL_BD.sol	Moist bulk density	±25%	0.09

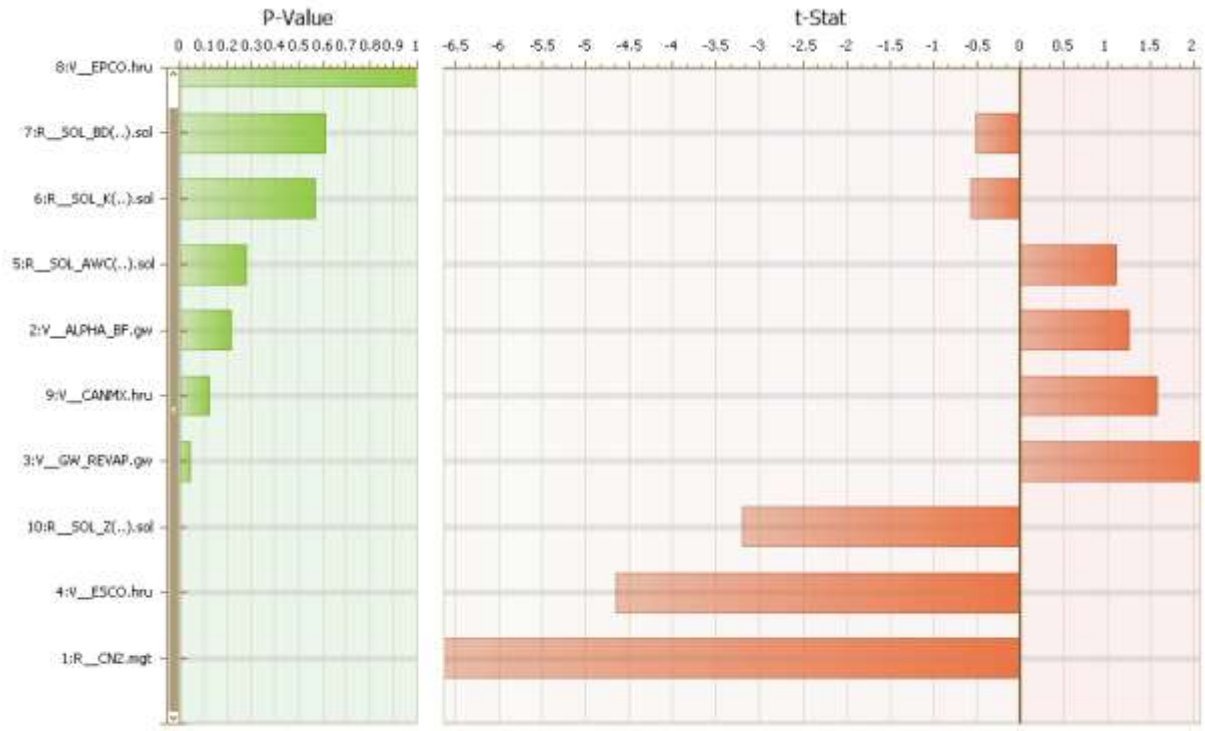

Figure 6.7 Global sensitivity analysis for daily streamflow simulation for the Baro River station.

The model calibration and validation show a reasonable agreement in terms of NSE, R^2, and PBIAS as well as the uncertainty analysis of p- and r-factors (Table 6.3). However, the statistical evaluation for the daily period was weaker than that for the monthly period. For example, considering the objective function for optimization, the daily NSE values were 0.73 and 0.8, while the monthly values were 0.89 and 0.85 for the calibration and validation periods, respectively. In general, results show that the SWAT model can reasonably simulate the hydrological characteristics of the basin (Moriasi et al., 2007). Similarly, the uncertainty analysis for the monthly simulation was better than the daily simulation. The streamflow simulation provided acceptable prediction uncertainty (p-factor and r-factor) estimates for both daily and monthly periods (Abbaspour et al., 2015).

Table 6.3 Performance analysis of the SWAT model to simulate streamflow during the calibration and validation period.

	Daily					Monthly				
Period	R^2	NSE	PBIAS	p-factor	r-factor	R^2	NSE	BIAS	p-factor	r-factor
Calibration	0.73	0.7	-4	0.71	0.49	0.9	0.89	-0.9	0.75	0.5

Validation	0.8	0.8	1.7	0.7	0.53	0.9	0.85	-2.4	0.72	0.4

In addition, the daily and monthly streamflow simulations during the calibration and validation period (Figure 6.8) show the model reasonably captured the streamflow hydrograph in terms of timing and magnitudes of flow, although some peak or low flow was either overestimated or underestimated. This finding is consistent with Mengistu & Sorteberg (2012), who show that the major pattern of the hydrograph is well captured by the model. Hence, the SWAT model can reasonably capture the future hydrological condition of the basin.

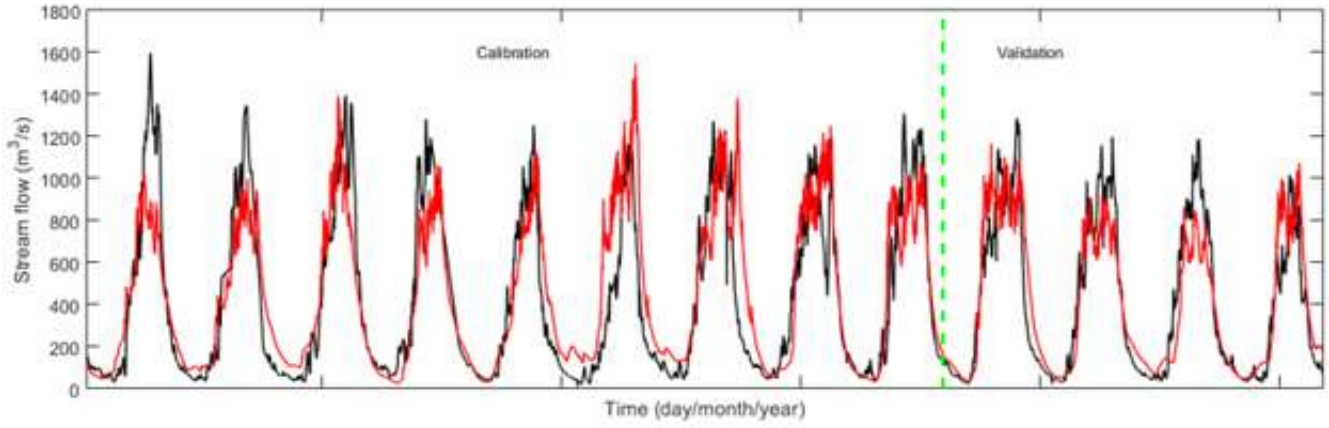

Figure 6.8 Observed and simulated streamflow for daily time scale calibration and validation period for Baro River station

6.3.5 Response of streamflow to future periods and climate scenarios

After calibrating the SWAT model, future climate impacts are projected using the ensemble of rainfall, Tmax, and Tmin. The influence of future climate on the streamflow was assessed at monthly, annual, and seasonal time scales. Table 6.4 presents the response of streamflow under the RCP4.5 and RCP8.5 scenarios. The estimate shows that the projected average monthly, seasonal, and annual streamflow is expected to decrease compared to 1981–2010, the baseline period. The mean of the results indicates decreases in streamflow in the ranges of −11 to −68% for monthly flows, −26 to −39% for dry season flow, −28 to −41% for wet-season flows, and −28 to – 40% for annual flows. The highest decreasing change was observed during April under the RCP8.5 2080s, the lowest was during September under the RCP4.5 2030s.

The decrease in rainfall combined with an increase in temperature will result in a decrease in seasonal and annual streamflow. Though the predicted climate change for both RCPs will lead to a decrease in streamflow in the river, the decrease will be greater for RCP8.5 in the 2080s than in the 2030s. The decrease in streamflow under the RCP8.5 scenario is in agreement with other previous studies in other parts of Ethiopia (Dibaba et al., 2020; Worku et al., 2021). The finding is also consistent with Beyene et al. (2010), who showed the Nile River is expected to decline in 2040–2069 and 2070–2099 due to the decline in rainfall and increased evaporation demand. As a result, greater streamflow reductions by the 2080s, particularly under the RCP8.5 scenario, indicate a future water availability challenge if climate change mitigation is not implemented. The projected decrease in streamflow rates will harm many sectors, including aquatic ecosystems, domestic, irrigation, and hydropower water use. The results of the current study indicated the necessity of employing sustainable water management strategies, which are timely needed ahead of future expected changes in the climate.

Table 6.4 The projected mean monthly, seasonal, and annual ensemble change in streamflow (%) in relation to the baseline climate.

Period	Jan	Feb	Mar	Apr	May	Jun	Jul	Aug	Sep	Oct	Nov	Dec	Dry season	Wet season	Annual
RCP4.52030s	−37	−54	−64	−62	−60	−41	−31	−18	−11	−21	−20	−33	−30	−28	−28
RCP8.52030s	−33	−54	−58	−58	−53	−38	−34	−20	−19	−19	−12	−35	−26	−29	−28
RCP4.52080s	−44	−58	−63	−64	−60	−47	−37	−26	−29	−22	−28	−41	−37	−35	−35
RCP8.52080s	−47	−62	−64	−68	−62	−57	−41	−38	−31	−27	−27	−49	−39	−41	−40

In addition to the mean streamflow simulation, the flow duration curves (FDC) were generated to examine the impact of high and low streamflow periods (Figure 6.9). Based on the FDC, future period simulation showed a general decreasing tendency in projected flow under the RCP4.5 and RCP8.5 scenarios. Except the extreme flow segment (i.e., 0–3% exceedance probability), the projection for simulation under both scenarios show a decreasing in flow. The decrees is greater for the low flow segment (i.e., 70–95% exceedance probability), particularly for RCP8.5 scenarios for 2080s. The extreme low-flow segment (i.e., 95–100% exceedance probability) showed a sharp fall in slope of the FDCs for both RCPs scenarios. Therefore, the climate change scenarios would cause temporary higher flood peaks; however, climate change in the future will be responsible for lower flows, particularly in the low flow, which may lead to droughts.

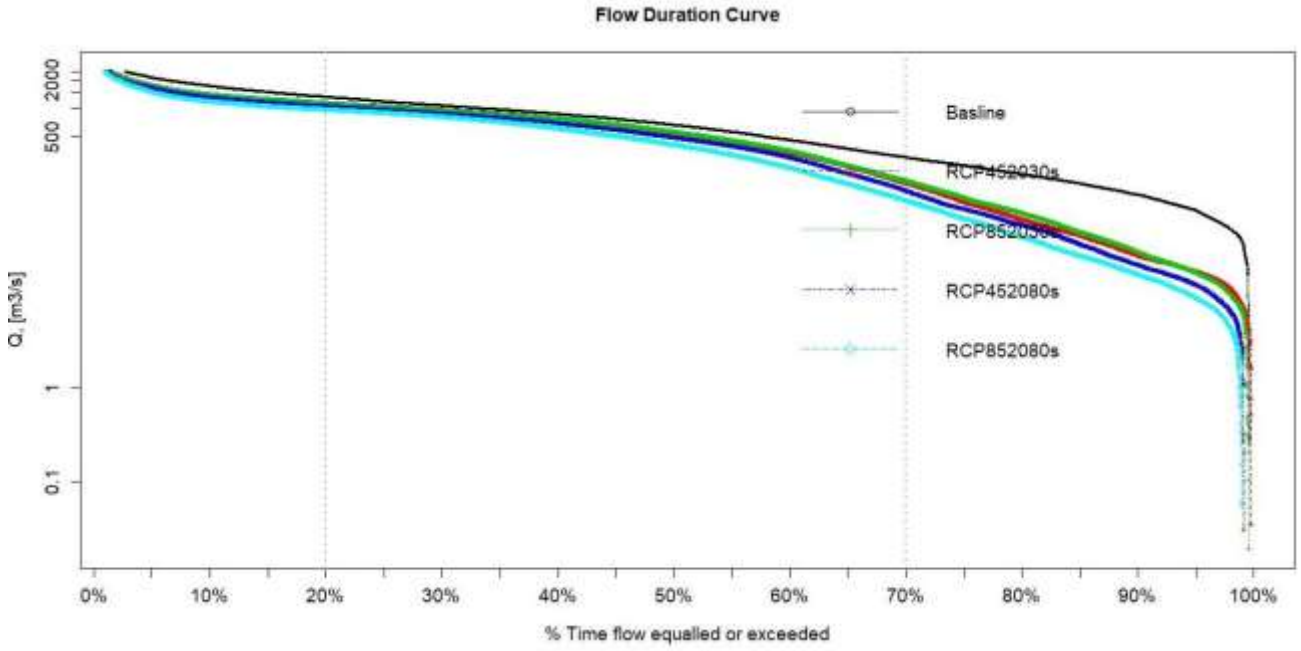

Figure 6.9 Flow duration curve for the comparison of the baseline period with the climate change scenarios.

6.3.6 Indicators of hydrological alteration under future period and climate scenarios

The IHA was also used to assess the key streamflow regime characteristics, such as magnitude, frequency, and duration. The median monthly flow simulation from the indicators of hydrological alteration shows a decreasing trend for all months of the year (Figure 6.10). When compared to the RCP4.5 scenarios, the RCP8.5 scenario for the 2080s has the most altered median value. The reduction in stream flow can be attributed to the increase in temperatures and the decrease in rainfall. This result is in agreement with other studies on climate change in Greece (Lopez-Ballesteros et al., 2020). They projected a decrease in the monthly and seasonal flow under the future climate change scenarios of RCP4.5 and RCP8.5.

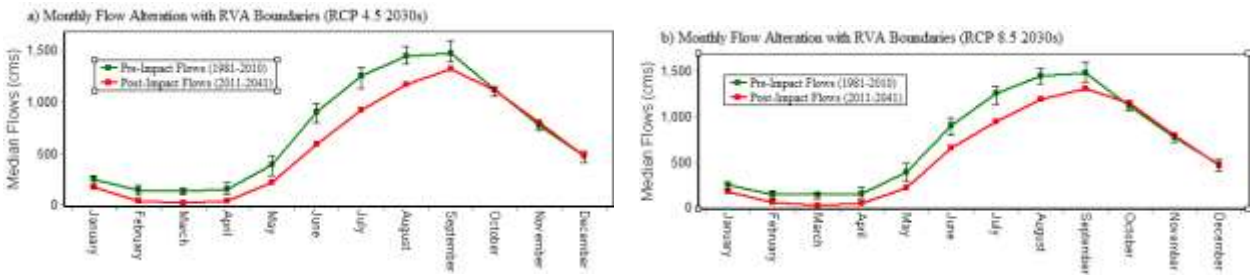

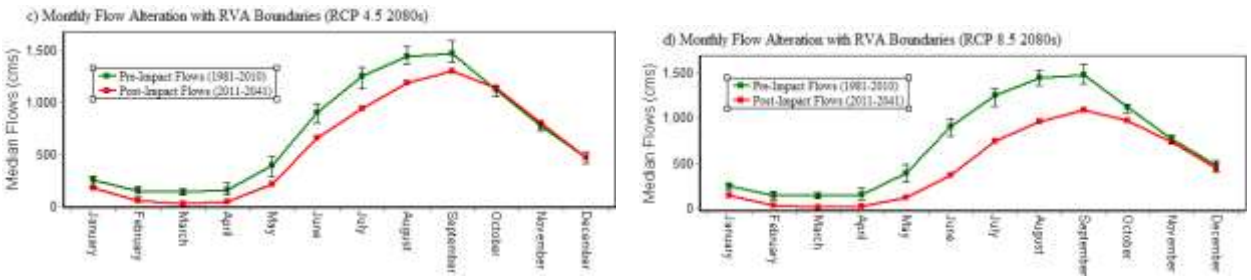

Figure 6.10 Monthly median streamflow for baseline conditions and future periods and scenarios for Baro river station.

The hydrological alteration value for different parameters are presented in Figure (6.11). In most months of the year, the monthly flows presented a decrease in the high and middle RVA categories, which means a decrease in the frequency of observed values compared to the lower RVA limit. Unlike the high and middle categories, the majority of the indicators related to monthly flows showed an increase in the low RVA category, which means an increase in the frequency of observed values above the upper RVA limit. In addition, the annual 1, 7, 30, and 90-day maximum flows indicated a decrease in the high and middle categories and an increase in the low RVA category for most of the scenarios. Likewise, in most scenarios the annual 1, 7, 30, and 90-day minimum flows showed a decrease in the high and middle RVA categories while increasing in the low RVA category. Besides, results also indicated a decrease in the high and middle RVA categories for the duration of the low and high pulse counts, but an increase in the low RVA category was projected. The 3 day max flow, and the date of maximum flow for high RVA category show an increasing trend for most of the scenarios.

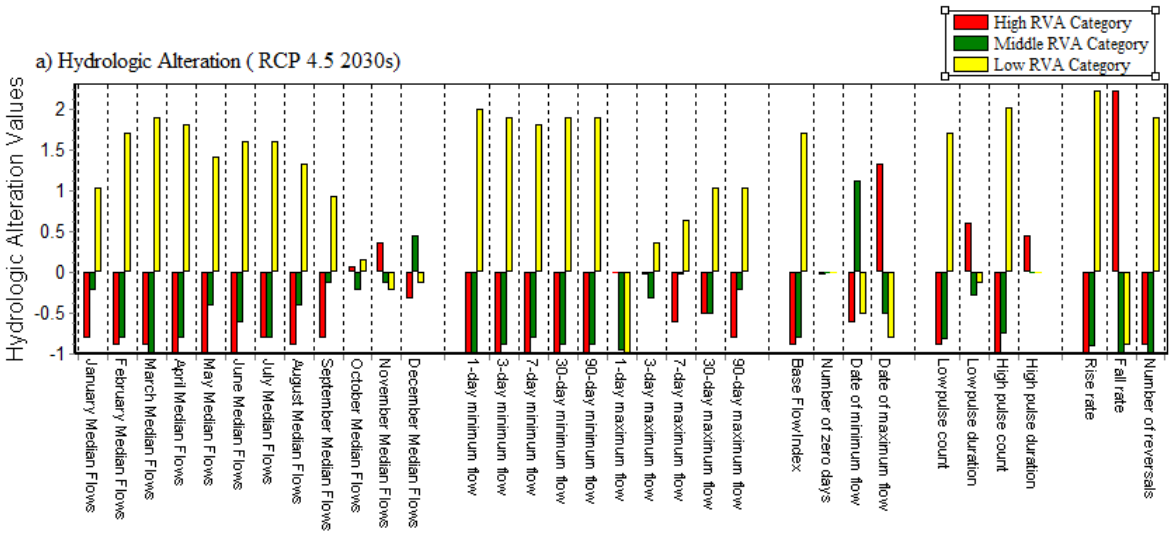

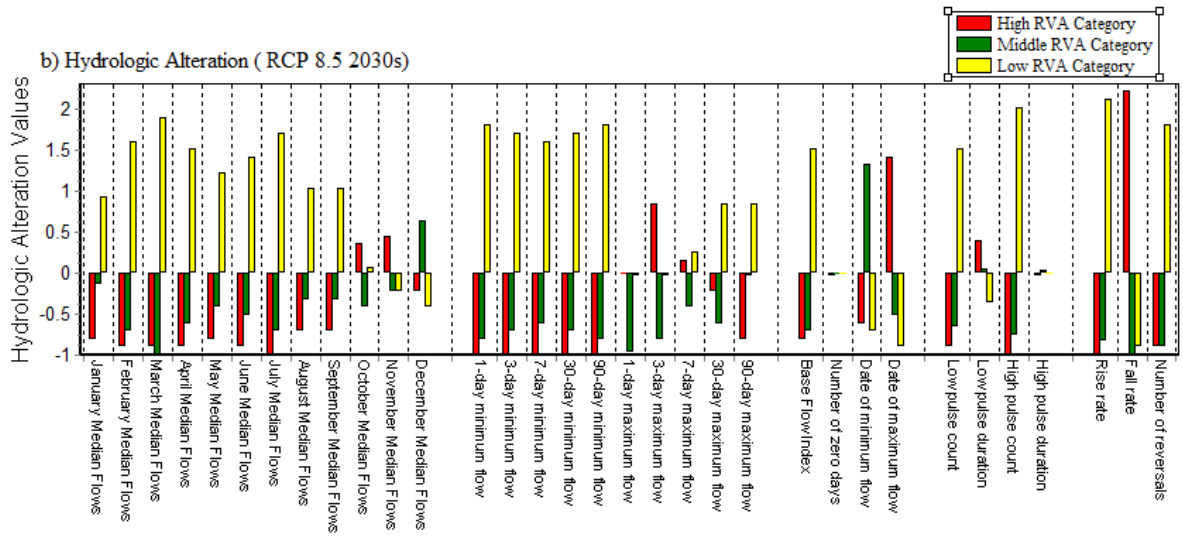
b) Hydrologic Alteration (RCP 8.5 2030s)
High RVA Category
Middle RVA Category
Low RVA Category
Hydrologic Alteration Values
2
1.5
1
0.5
0
-0.5
-1
January Median Flows
Febrtuary Median Flows
March Median Flows
April Median Flows
May Median Flows
June Median Flows
July Median Flows
August Median Flows
September Median Flows
October Median Flows
November Median Flows
December Median Flows
1-day minimum flow
3-day minimum flow
7-day minimum flow
30-day minimum flow
90-day minimum flow
1-day maximum flow
3-day maximum flow
7-day maximum flow
30-day maximum flow
90-day maximum flow
Base Flow Index
Number of zero days
Date of minimum flow
Date of maximum flow
Low pulse count
Low pulse duration
High pulse count
High pulse duration
Rise rate
Fall rate
Number of reversals

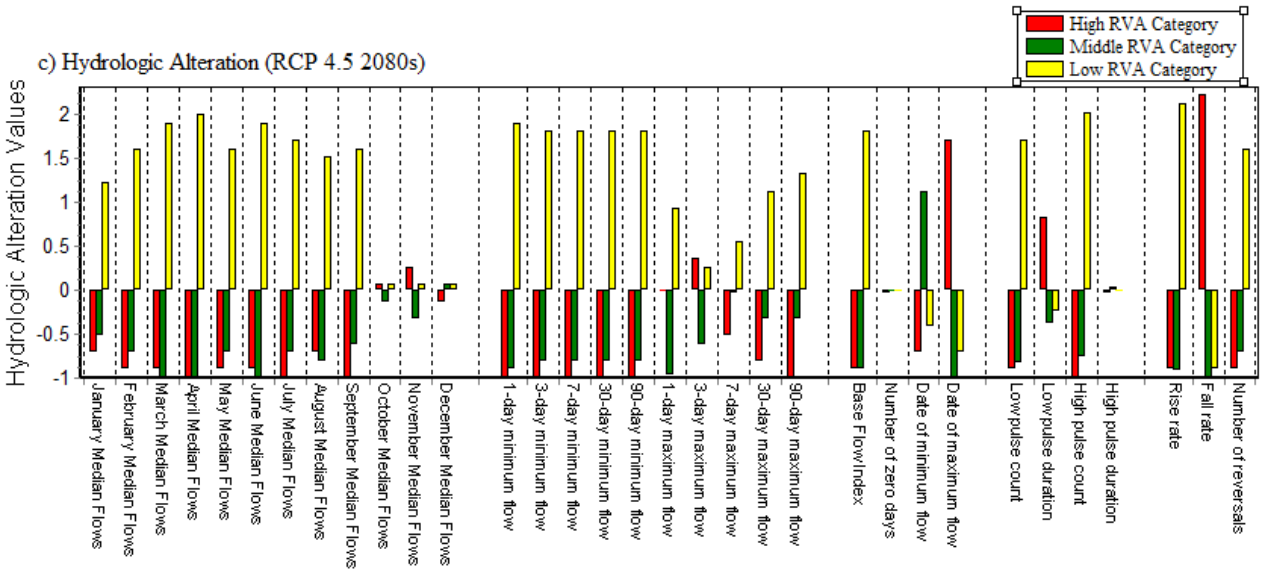
c) Hydrologic Alteration (RCP 4.5 2080s)
High RVA Category
Middle RVA Category
Low RVA Category
Hydrologic Alteration Values
2
1.5
1
0.5
0
-0.5
-1
January Median Flows
Febrtuary Median Flows
March Median Flows
April Median Flows
May Median Flows
June Median Flows
July Median Flows
August Median Flows
September Median Flows
October Median Flows
November Median Flows
December Median Flows
1-day minimum flow
3-day minimum flow
7-day minimum flow
30-day minimum flow
90-day minimum flow
1-day maximum flow
3-day maximum flow
7-day maximum flow
30-day maximum flow
90-day maximum flow
Base Flow Index
Number of zero days
Date of minimum flow
Date of maximum flow
Low pulse count
Low pulse duration
High pulse count
High pulse duration
Rise rate
Fall rate
Number of reversals

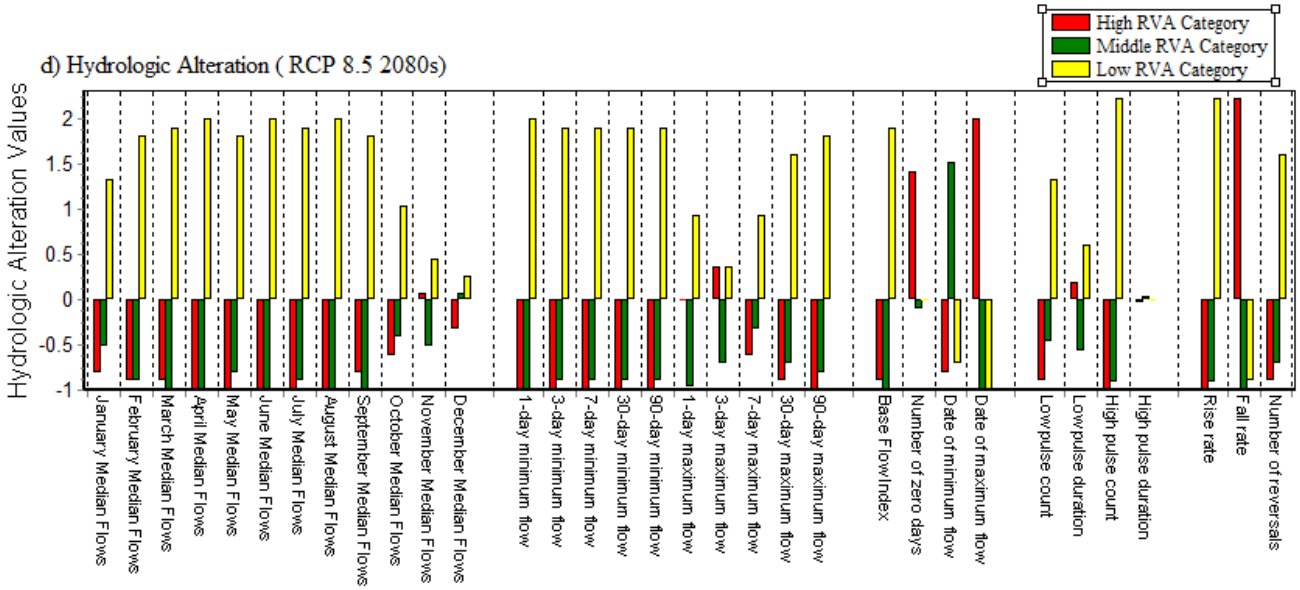

Figure 6.11 Values of hydrologic alteration within each RVA category for the baseline conditions and climate change scenarios.

The largest streamflow change is produced for RCP8.5 in the 2080s simulation. The study outputs of IHA on the streamflow projection in the basin show good consistency with previous studies on climate change impact in Greece (Lopez–Ballesteros et al., 2020). Their result shows that the decrease in the monthly and seasonal flow under future climate change scenarios for RCP8.5 is stronger than the RCP4.5 scenarios. Thus, climate change is expected to affect the amount and ecological quality of the streamflow, the resilience of riverine species, and the future availability of water resources.

In general, the effects of climate change on the hydrological cycle are substantial since water is essential to both the natural world and the socio-economic system. Water resource availability patterns and hydrological extreme events such as floods and droughts can vary as a consequence of climate change, which can have several indirect implications on agriculture, food, energy production, and general water infrastructure (IPCC, 2007; Kang et al., 2009). The impact will be greater in transboundary rivers like the Baro–Akobo River, where water is in high demand due to competing economic, political, and social interests of riparian nations, particularly when upstream nations can have a significant impact on downstream nations (Conway & Hulme, 1993; Hulme et al., 2005).

The outcomes of the climate projection study illustrate the implications of decreased water availability and their effects on agricultural output. As a result, this study suggests water harvesting structure strategies that could maintain water availability for agriculture and other ecosystem services to counteract future climate change impacts. The productivity of the large hydropower systems planned for the region as well as the rising demand for agricultural and transportation expansion could potentially be impacted from a water management perspective by the overall reduction of river flows and their increased variability. Therefore, the implementation of water resources development work such as hydraulic structures, which are related to irrigation and hydropower, should take the anticipated change in the climate into account. Additionally, it is necessary to implement Ethiopian Green Economy Climate-Resilience Strategies to halt trends in deforestation and land degradation to mitigate any potential shortage of stream flow, which has been a challenge for the water supply, irrigation, and hydropower development in the basin.

6.3 Model uncertainties

The impact of the climate change study on hydrology by applying hydrological models involves various uncertainties (Abdo et al., 2009; Fowler et al., 2007). In climate change studies, the choice of GCM and RCM is the greatest source of uncertainty (Kundzewicz et al., 2018). The discrepancy among the GCM models over regional climate change studies is manifested as a large source of uncertainty. Moreover, the climate models disagree on the magnitude and even the direction of change of climate variables in different parts of the world, particularly when it comes to rainfall (Zhang et al., 2014). In addition, the source of hydrological model uncertainty can be associated with model structure, parameter uncertainty, and data scarcity for calibration and validation processes as well as data inputs (e.g., lack of relevant spatial and temporal variability of data on climate, soils, and land uses) (Kundzewicz et al., 2018).

In this study, to reduce the uncertainties, an ensemble of multi-GCM-driven RCM simulations was used based on future impact assessments. The most plausible emission scenarios with robust bias correction techniques are used for the assessments of the RCMs to reduce uncertainty. The SWAT model was calibrated and validated for streamflow data before applying it to climate change impact assessments. In addition, before running the SWAT model, this study looked for the best available data, such as a high-resolution soil map (250 m), land use map (30 m), DEM (30 m), and weather data quality cheek, and all missing data were filled in to reduce uncertainties in the model

projection and try to understand the impact of climate change on the hydrological process in the basin. The performance of model showed good performance when evaluated in terms of the p-factor and the r-factor model uncertainty metrics.

6.4 Conclusions

This study assessed the future changes in rainfall and temperature for the basin under the RCP4.5 (the middle situation) and RCP8.5 (business-as-usual development pathways) scenarios using different bias-corrected regional climate models from the CORDEX-Africa project. The calibrated SWAT model and the IHA software were used for a future prediction of the hydrological processes in the basin. There is less agreement between the RCMs on the magnitude, direction, and monthly changes in rainfall, but there is a comparatively better agreement on temperature. In the ensemble, both maximum and minimum temperatures are projected to increase throughout the year. In contrast, annual rainfall is projected to decrease throughout the year, but the decrease is greater in the 2080s under the RCP8.5 scenarios.

The impact of climate change scenarios on hydrology shows that the monthly and seasonal variations of streamflow will be greater when compared to the annual variation. The hydrological flow indicators related to monthly flows indicate a decrease in the high and middle categories of variability, while the low category shows an increasing trend. As a result, the decrease in rainfall and the increase in maximum and minimum temperatures because of climate change may impact the soil water balance by increasing both plant transpiration and soil evaporation, which will have a negative impact on crop growth and agricultural productivity. Therefore, consideration should be given to irrigation infrastructure design. Furthermore, a water storage structure is required to offset the decrease in rainfall.

In general, this study indicated the likely impacts of the predicted warmer conditions and a decrease in seasonal water availability in the study region. This could jeopardize the water supply for irrigation, agriculture, and hydropower in the lower reaches of the catchment unless proper water management and water-saving structures are implemented. Therefore, the finding will be important for water resource policymakers to develop appropriate water management strategies such as watershed management and adaptation options to offset the adverse impacts of future climate change.

7. Modeling the impacts of projected climate and land use changes on the water balance in the Baro basin, Ethiopia. [4]

Abstract

In terms of land use and climate, the world is changing at an unprecedented rate and these changes have a significant influence on our water resources. This study was conducted to examine the individual and combined potential impacts of land use and climate change on the water balance of the Baro basin in Ethiopia for the baseline period (1985–2002) and near-future period (2023–2040) using the Soil and Water Assessment Tool (SWAT). The plausible land use scenarios considering current (CUR), business as usual (BAU), and further expansion of altitudinal forest and watershed management practices (CON), as well as climate change scenarios from regional climate model outputs (RCMs) under two representative concentration pathways (RCP4.5 and RCP8.5) for the 2023–2040 time frame, were used as inputs to the models. The monthly calibrated and validated SWAT model produced an acceptable result, which was then used for water balance simulations. Findings show that forest decreased from 54.5% to 48.9% and 41.2% while agricultural land increased from 21.8% to 29.7% and 39.8% under the CUR and BAU land use change scenarios, respectively. The results from the ensemble mean showed an increase in maximum and minimum temperatures and a decrease in rainfall under the RCP4.5 and RCP8.5 climate change scenarios, which in turn resulted in an increase in evapotranspiration (ET) and a decrease in water availability. Climate change outweighed the impact of land-use change, thus indicating an increase in annual ET by up to 12% and a decrease of 42% in surface runoff (SURQ) under the RCP8.5 scenario. The BAU land use scenario projection triggers a respective increase of 18% in annual SURQ and reduction of ET by 2%. However, under the CON land use scenario, SURQ decreased by 24%. The study concluded that future land use and climate change will further challenge the basin's water supply capacity to meet the increased water demand. Understanding the changes in the basin's water balance is critical for mitigation and adaptation options. As a result, this study

[4] This chapter is based on Mengistu, A.G., Woldesenbet, T.A, Dile, Y.T, Bayabil, H.K, Worku, G. 2022. Modeling the impacts of future climate change on the hydrological processes in the Baro-Akobo River basin, Ethiopia (Under Review).

proposes restoration efforts and climate-resilient water management strategies that can increase the resilience of the river basin.

Keywords: CA-ANN climate model evapotranspiration, surface runoff, Baro basin.

7.1 Introduction

Climate and land use change are the two most documented global changes, causing numerous effects on natural and socioeconomic ecosystems (UNEP, 2012; Zheng et al., 2016). Climate change is unequivocal, and there is evidence that shows global and regional climate change. According to the IPCC (2021), the mean temperature of the Earth's surface between 2011 and 2020 was 1.1ºC warmer than the pre-industrial period (1880–1900). Global temperatures are projected to rise by 2–4 °C by 2100 if greenhouse gas emissions can't be mitigated in the future. An increase in near-surface-specific humidity, water vapor, and precipitation has been observed on a global scale since 1950 (faster since the 1980s). However, these changes are not uniform among different regions of the world. For instance, an increase and a decrease in rainfall of 0.5–1% and 0.2–3% per decade were observed over the mid-high latitudes and the tropical areas of the world, respectively (IPCC, 2013). Thus, it is commendable to advance climate research using robust climate information for climate impact assessment and climate adaptation decision-making. A modeling approach is a common and valuable way to predict the dynamics of water under global change (Gomes et al., 2021). The outputs of GCMs or RCMs can be used to generate climate change scenarios. GCMs are poor at assessing site-specific climate effects reliably due to their low spatial resolution (Kay et al., 2009). RCMs offer a better representation of orographic effects and land-sea surface characteristics due to their larger resolution (10–50 km) (Teutschbein & Seibert, 2010).

Additional pressure on ecosystems and societies is caused by land use changes (UNEP, 2012). Land use change has happened on 32% of the worldwide land area from 1960 to 2019, which is fourfold greater than long-term land change assessments (Winkler et al., 2021). The unprecedented increase of cultivated land and urban areas at the expense of natural ecosystems such as forests and grazing land are the dominant land use changes (Lambin & Meyfroidt, 2011; Seto & Kaufmann, 2003). For instance, forest cover decreased from 0.05–0.06 billion km^2 in 1700 to 0.043–0.053 billion km^2 in 1990 (Lambin et al., 2003). Between 1990 and 2010, there was a land use change in Africa that included the conversion of 0.75 million km^2 of forest to agriculture and

grazing, the second-highest rate after South America. Over the same 20-year period, over 0.13 million km^2 of original East African forest were lost, and the surviving forest is fragmented and constantly in danger (FAO, 2010). These changes in land use have caused the rapid transformation of natural ecosystems such as water bodies and forests into human-dominated ecosystems such as cropland and urban areas (Kim et al., 2013; Lambin & Meyfroidt, 2011). The change from natural vegetation to cultivated land harms water resources (Zheng et al., 2016). Thus, understanding the impacts of land use change on water dynamics is crucial, particularly in countries like Ethiopia, whose societies are extremely dependent on rain-fed agriculture (UNEP, 2012; WWAP, 2015). Land use scenarios are generally based on a variety of techniques that have been used for land use change detection using remote sensing products, and cellular and agent-based models (Liping et al., 2018).

Effective water resource management necessitates an understanding of the basin's hydrologic response to climatic (rainfall and air temperature) and land use change (Kim et al., 2013). Coupled models are frequently used to give a clear insight into how land use and climate change affect hydrological systems (El-Khoury et al., 2015; Mehdi et al., 2015; Tong et al., 2012; Zheng et al., 2016). Climate change simulations combined with land use scenarios demonstrated nonlinear dynamics and uncertainty, whereby the direction and magnitude of impacts were not predictable from the separate changes alone (Jung et al., 2011; Mehdi et al., 2015). As a result, several studies found that simulated hydrological processes were more sensitive to climate change than land use change (Aboelnour & Gitau, 2019; Kim et al., 2013; Mekonnen et al., 2017). Other findings, however, show that the impact of land use change was greater than the impact of climate change (Mwangi et al., 2016; Yin et al., 2017). Further research is needed because complex interactions between land use and climate change may not only accelerate changes in hydrological processes (Legesse et al., 2003; Khoi & Suetsugi, 2014), but they may also cancel each other out (Zheng et al., 2016).

Though several studies have separately examined the impact of climate change (Abdo et al., 2009; Beyene et al., 2010; Dile et al., 2013; Elshamy et al., 2009; Gebremedhin et al., 2017; Mengistu & Sorteberg, 2012; Worku et al., 2021; Worqlul et al., 2018), or land use change (Engida et al., 2021; Koch et al., 2012; Teferi et al., 2013; Zeleke & Hurni, 2001), few studies have examined the combined climate and land use change impacts on the water balance of Ethiopia (Getachew et al., 2021; Teklay et al., 2021). However, the combined impact of climate and land-use change

scenarios on the water balance of the basin is not well understood. Moreover, the aforementioned climate change studies in the basin most often used a coarse spatial resolution of GCMs (Beyene et al., 2010; Mengistu & Sorteberg, 2012) to examine the impacts of climate change on the hydrology of the basin. However, the GCM model may not well represent the climate variables of the study basin, and it has implications on hydrology because of its coarse resolution (Abdo et al., 2009; Fowler et al., 2007; Kay et al., 2009; Sharma et al., 2007). Therefore, applying finer-resolution climate models, such as RCMs, for climatology and hydrology studies is crucial. RCM addresses the limitations of GCM models, particularly in representing the effect of topography on the different climatic parameters. In addition, most of the research studies investigating the impact of climate change on basin hydrology in Ethiopia in general and the Baro basin, in particular, have considered land use to remain static (e.g., Beyene et al., 2010; Mengistu & Sorteberg, 2012). In contrast, research that investigated the impact of land-use change considered climate as static (e.g., Alemayehu et al., 2016; Engida et al., 2021). Nevertheless, the climate and land use in the future will change continuously due to accelerated population growth, economic development, and global warming (McCartney & Girma, 2012).

Therefore, this study is conducted in the Baro River basin, which has been highly impacted by different environmental changes. The basin is characterized by various intense agricultural activities, is home to biodiversity, has a resettlement program, and several projects related to irrigation and hydropower development that are in the planning and implementation stages (e.g., Tams, Birbir A and Birbir R, Baro-1 and Baro-2, Geba-A and Geba-R), which may lead to further deforestation (Alemayehu et al., 2016; Awulachew et al., 2007; Sileet et al., 2013). On the other hand, the basin has been severely characterized by the loss of water bodies, drying streams, and significant land-use change as a result of several factors, including investment, population growth, and global climate change over the last four decades. This study is designed to examine the separate and combined impacts of climate and land use change on the water balance of the basin. Such information plays a vital role in supporting the existing and planned water resource management practices in the basin. The research tools used in this study include a bias corrected RCM for generating future climate change scenarios under different RCPs, a BAU and CON future land use scenario, and an eco-hydrological SWAT model (Arnold et al., 1998).

7.2 Materials and Methods

7.2.2. Data inputs

The SWAT requires hydroclimate and spatial data for model setup. Model calibration and validation were done using streamflow data from the Baro River. Daily observed rainfall, maximum temperature (T max), and minimum temperature (T min) for the period 1985–2002 from 10 weather stations were obtained from the Ethiopian National Meteorological Agency (ENMA). Further information, including the geographic locations of the weather stations and the dataset used in this study, can be found in Mengistu et al., 2021a. Missing records were estimated using the MICE approach available in R software (Zhang & Yang, 2004). The Ethiopian Ministry of Water, Irrigation, and Electricity provided daily observed streamflow data for the period 1990–2002, which was used for model calibration and validation. In this study, spatial data inputs such as the Digital Elevation Model (DEM), soil, and land use were used. A 30m × 30 m resolution DEM was obtained from the United States Geological Survey (USGS) Earth Explorer website (https://earthexplorer.usgs.gov). Soil physicochemical parameters were acquired from the African Soil Information System soil data (AfSIS) (Hengl et al., 2015), which provides soil information at 250 m spatial resolution for six soil depth layers (Bayabil & Dile, 2020; Dile et al., 2020). A pedotransfer function was used to generate the physico-chemical properties required by the SWAT model (Saxton & Rawls, 2006). The dominant soil textural classes in the basin include clay and clay loam soils, and their hydrologic soil groups fall under C and D. The land use map for the year 2002 was developed from the Landsat 7 ETM+ images using supervised classification with a maximum likelihood algorithm. The Landsat 7 ETM+ images were acquired from the USGS at http://earthexplorer.usgs.gov/.

7.3 Land use change analysis

7.3.1 Landsat Image classification

Land use change analysis focused on interpreting temporal changes in land use based on satellite imagery. The data collected to assess the temporal changes and develop a thematic land use map of the study basin includes both ancillary and satellite data. Data collected from fieldwork (Annexes 7.1 and 7.2) and Google Earth data were used for satellite image classification.

Landsat 4–5 Thematic Mapping (TM), Landsat 7 Enhanced Thematic Mapping (ETM+), and Landsat 8 Operational Land Inventory (OLI) for the years 1985, 2002, and 2019 were acquired from the USGS at http://earthexplorer.usgs.gov/; each imagery has a spatial resolution of 30 m (Annex 7.3). The images from December to February were chosen because fewer cloud cover and surface feature changes are expected in the study area. Google Earth imagery was also used to collect ground points for the images. A total of 450 reference data points for the 2019 land use maps were obtained, of which 200 points were obtained from the global positioning system (GPS) and the remaining 250 points were from Google Earth imagery. About two-thirds of the data collected were used for supervised image classification (training), and the remaining one-third was used for accuracy assessment (validation). The satellite data were projected using the same Zone 37N Universal Transverse Mercator (UTM) projection system as the World Geodetic System 1984 data. The image preprocessing techniques, including layer stacking, histogram equalization, and atmospheric and radiometric correction, were undertaken in ERDAS imagine 2014. The MLC algorithm was used for image classification based on data from training locations and visual interpretation of the images. To minimize the salt and pepper effect in the classified image, recoding followed by a majority filter with a 3×3 size kernel was applied (Kantakumar et al., 2016). For detailed information about the acquired satellite images and the classified land use type, please see Annexes 7.4 and 7.5, respectively.

7.3.2 Land use map accuracy assessment

Accuracy assessment, which is an indispensable part of image processing, was also undertaken in this study. To determine the accuracy of land use classification, the users, producers, the overall classification, and the kappa coefficient were estimated using ERDAS software. The accuracy of the classification for the year 2002, hereafter referred to as the reference (REF) land use map, had an overall classification accuracy of 84.6% and a kappa coefficient of 0.81, whereas the year 2019, hereafter referred to as the current (CUR) land use map, has an overall accuracy and kappa statistics of 87 and 0.83%, respectively. Finally, the land use maps obtained after the classification are then used for land use change studies and as inputs in the SWAT model to study future land use impacts.

7.3.3 Land use map transition potential modeling and validation

To determine the spatiotemporal changes during a specified period and determine the land use change transition to produce the land use change map, the MOLUSCE plugin for QGIS was used.

The model integrates some well-known algorithms for transition potential modeling, such as the ANN (multilayer perceptron), weights of evidence, multi-criteria evaluation, logistic regression, and CA algorithm, for future simulation (Abbas., 2021). The spatial factors used as input parameters were slope, aspect, and elevation. The spatial variables for model validation were chosen based on their relatively good association with the land use map, as measured by Cramer's coefficient. Pearson's correlation coefficient was used to measure the strength of a linear association between two satellite images. The relationship coefficient between 1985-2002 was 0.89 and between 2002-2019 was 0.91, which indicates a good registration efficiency between the two data sets.

In this study, the CA-ANN approach for transition potential modeling and projection was used. Land use data from 2002–2019 along with spatial variables were employed to project a land use map for 2019 and obtained a validation kappa value of 0.85 (Annex 7.8). After obtaining the projected land use map, the actual land use map of 2019 was compared with the projected data and obtained an overall acceptable kappa value of 0.71 (Annex 7.8). The Kappa values range from 1 to −1. Roy et al. (2014) classified Kappa values as poor if they were less than 0.40, fair to good if they were between 0.40 and 0.75, and excellent if they were greater than 0.75.

7.3.4 Projection of land use scenarios

Projecting land use change for more than 20 years may involve uncertainties due to changes in government policy and/or human behavior. It is challenging to set plausible land use and world market scenarios for a period greater than 20 years (Roosmalen et al., 2009). A scenario-based land use change impact study could help to assess the potential impacts of land use change on watershed hydrology (Cao et al., 2019). Therefore, following the achievement of acceptable results from model validation, the land use map for 2040 was predicted. For this purpose, the temporal land use data from 2002 and 2019, the spatial variables, and the transition probability matrix were employed to predict the land use map for 2040, hereafter in the text referred to as "business as usual" (BAU) land use scenarios. The BAU scenario is developed based on the historical land use map. The MOLUSCE module, which is available in QGIS, has been used in various studies to predict future land use changes (Abbas et al., 2021; Kamaraj & Rangarajan, 2022; Landry et al., 2019; Teklay et al., 2021). In contrast to BAU land use scenarios, the conservation scenario (CON) was developed with an emphasis on watershed management and ecological restoration to

counteract accelerated growth and promote sustainable socioeconomic development. The CON scenarios emphasize good policies for the better management of natural resources and sustainable agriculture. For developing a CON scenario best watershed management practices including terracing, contour farming, and filter strip were considered to be implemented during 2023–2040 in the Baro basin (Table 7.1). In addition to this, HRUs under cultivation on a slope above 15% were modified to be changed to forest land. The baseline land use of HRUs was modified by using ArcGIS spatial analyst tools. In general, the BAU scenario represents a future condition where no measures are taken to control land use change in the basin, while the CON scenario considers idealized land use conditions that follow spatial management and regulation.

Table 7.1 Best management practices and parameter values considered in conservation scenario.

Watershed management practices	Parameters	Calibrated value	Modified value	Reference
Stone bund and terrace (agriculture)	CN2 (.mgt)	83.2	74.2	(Berihun et al., 2020)
	USLE_P (.mgt)	0.37	0.32	(Betrie et al., 2010)
Area closure (grassland)	CN2 (.mgt)	82.4	79.96	(Berihun et al., 2020)
Filter strips	FILTERW(.hru)	0	1(m)	(Betrie et al., 2010)

7.3.5 Climate change scenarios

In addition to land use scenarios, CORDEX Africa (http://cordexesg.dmi.dk/esgfwebfe/) provided simulated climate data with a resolution of 0.44° (Nikulin et al., 2012). Detailed information on RCMs and their forcing GCMs used in this study can be found in (Mengistu et al., 2021a. For the near future (2023–2040), five bias-corrected RCM outputs and their ensembles were used under the midrange mitigation emission scenario (RCP4.5) and the extreme emission scenario (RCP8.5). The distribution mapping methods were employed (Mengistu et al., 2021a; Teutschbein & Seibert, 2012; Worku et al., 2020) to correct bias in future climate model outputs. Moreover, in this study, the best-performing climate models based on Taylor's diagram and the cumulative distribution of rainfall comparison were selected for further hydrological impact studies.

7.3.6 Combined climate and land use change Scenarios

To compare the individual and combined impacts with the baseline condition, eleven scenarios (two only climate change, three only land use, and five combining climate change and land use)

were developed. The combination of the observed climate data from 1985 to 2002 and the 2002 reference (REF) land use map was used as a baseline (BAS), which was used to compare the individual and combined land use and climate change impacts on the basin water balance (Table 7. 2). Then the calibrated model is used to simulate the different hydrological components, including evapotranspiration (ET), surface runoff (SURQ), groundwater flow (GWQ), and water yield (WYLD), for each HRU unit using the water balance equation, and their results are aggregated at the basin level. HRUs are the smallest units in the model, where many of the biophysical processes such as ET and SURQ are estimated using the water balance equation (Neitsch et al., 2011). The future land use and climate change impacts were examined by comparing the monthly, seasonal, and annual results of the baseline period with the results of the corresponding individual and combined land use and climate change scenarios. Furthermore, the inverse distance weighting (IDW) approach was applied to estimate the spatial distribution of the ET and SURQ, in the basin.

In addition, a two-sample t-test and the Mann Whitney (MW) U test (Stedinger et al., 1993) was employed to test the homogeneity of the mean of the two datasets. The statistical tests were performed to identify the impacts of land use, climate, and combined scenarios. The Levene test, which is based on the median value, was also employed to check the homogeneity of the standard deviation of the two datasets (Nordstokke et al., 2011). All the statistical tests were undertaken at a 95% confidence level to assess the significance of the difference between the baseline and each future scenario on the annual time scale.

Table 7.2 The combination of land use change and climate change scenarios with the baseline (BAS) condition represented in the SWAT model. Baseline simulation represents the combination of the reference land use (2002) and the observed climate (1985−2002).

No	Scenario setting	Land use	Climate	Climate and land use
1	BAS	REF	1985–2002	BAS
2	Land use change	CUR	1985–2002	CUR
3		BAU	1985–2002	BAU
4		CON	1985–2002	CON
5	Climate change	REF	RCP4.5	RCP4.5
6		REF	RCP8.5	RCP8.5

7	Land use and climate change	CUR	RCP4.5	CURRCP4.5
8		CUR	RCP8.5	CURRCP8.5
9		BAU	RCP4.5	BAURCP4.5
10		BAU	RCP8.5	BAURCP8.5
11		CON	RCP4.5	CONRCP4.5
12		CON	RCP8.5	CONRCP8.5

7.3.7 Calibration and validation of the model

The SUFI2 algorithm in the SWAT-CUP was used to conduct model parameter sensitivity analysis, calibration, and validation (Abbaspour et al., 2015). Based on the SWAT model default value and literature (Dile et al., 2013; Mengistu & Sorteberg, 2012; Mengistu et al., 2021b; Neitsch et al., 2011), eighteen model parameters were considered during the model parameter sensitivity analysis. The SWAT model was calibrated from 1990 to 1998 and validated from 1999 to 2002. Data from 1988 to 1989 was used for model warmup. To assess the model's skill, statistical metrics such as NSE, R^2, and PBIAS were used. In addition, the p-factor and the r-factor were used to measure and quantify the strength of calibration or uncertainty. The p-factor represents the percentage of observations covered by the 95PPU, and its value varies from 0 to 1, with the perfect value of 1, while the r-factor represents the thickness of the 95PPU, and its optimal value is 0. For streamflow simulation, the value of the r-factor is suggested to be less than a threshold of 1.5 to indicate an acceptable simulation result (Abbaspour et al., 2015).

7.4 Results and Discussion

7.4.1 Evaluation of land use classification accuracy and validation

From the confusion matrix report, the classification accuracy for the 2002 land use map had an overall accuracy of 84.6 % and a kappa coefficient of 0.81 (Annex 7.6), whereas the overall accuracy and kappa coefficient of the 2019 land use map was 87% and 0.83%, respectively (Annex 7.7). In general, the accuracy assessment report indicated a high level of agreement between the ground truth and classified land use types (Vivekananda et al., 2021). Considering the QGIS model's performance, the current classified map was used to validate the simulated land use map of 2019 and assess the performance of the model. Accordingly, the calculated Kappa index is estimated at 0.87, showing an agreement between the classified land use map and the simulated

map. In other studies, a strong agreement was achieved during the validation of the simulated land use map with that of the observed map (Abbas et al., 2021; Guidigan et al., 2019; Teklay et al., 2021).

7.4.2 Land use change scenarios

The land use change class statistics for the REF, CUR, BAU, and CON scenarios are presented in Table 7.3 and Figure 7.1. By visual observation and comparison with the 2002 (REF) land use map, it can be seen that there is a substantial increase in agricultural and urban land, while there is a decrease in other land use types for the CUR and BAU scenarios. The minor difference between the REF and CON land use scenarios was due to the conversion of smaller agricultural lands with slopes of more than 15% into forest land. Compared to the 2002 land use type, agriculture land increased in 2019 by 1913 km^2 with a percentage of 7.8%, which is the largest increase. Forest land, on the other hand, declined by 1344 km^2 with a percentage of 5.6%, the largest decline that can contribute to environmental degradation. The greatest expansion of agriculture at the expense of forest land is due to the increase in population growth that causes an increase in demand for cultivation lands such as agricultural cereal crops, field crops, and industrial crops, as well as urbanization. Concurrently, the prevalence of deforestation activities for urban and agricultural land expansion is also investigated in other studies (Alemayehu et al., 2016; Engida et al., 2021). Similarly, under the BAU scenarios, the increasing or decreasing rate of various land use types follows historical trends. In the BAU land use scenario, agricultural land is projected to increase from 5327 km^2 to 9725 km^2, about an 18% difference compared to the REF land use. In contrast, other land use types, including forests, scrubland, grassland, and water bodies, will decrease compared to the REF. Among these, the greatest decrease will be projected for forest land. It is projected to decrease from 13283 km^2 to 10054 km^2, with a percentage of 13.3%, which can significantly contribute to environmental degradation. In general, the simulated results show that such change will continue in the future because of the results of the Baro basin economic hub, population growth and urbanization, and the development of the infrastructure. These changes have a negative impact on natural resources, such as the hydrology of the basin. As a result, with the help of future simulation results, better planning and environmental management can control the adverse impact of these changes. The reduction in the forest, grassland, and shrubland is due to the increase in the urban area and agricultural land under the BAU scenario, as predicted in other Ethiopian watersheds (Dibaba et al., 2020; Teklay et al., 2021).

Table 7. 3 Land use coverage in (km^2) under the REF, CUR, BAU, and CON land use scenarios in the Baro basin. Values in the bracket in italics represent land use change in percentage (%).

Period	Forest	Shrub	Grass	Agriculture	Urban	Wetland	Water
200 2 REF)	13283 (54.5)	3382 (13.8)	2282 (9.2)	5327 (21.8)	8 (0.03)	40 (0.17)	56 (0.23)
2019 (CUR)	11939 (48.9)	3148 (12.9)	1947 (8)	7240 (29.7)	22 (0.09)	36 (0.15)	46 (0.19)
BAU	10054 (41)	3097 (12.7)	1407 (5.7)	9725 (39.8)	35 (0.14)	26 (0.11)	34 (0.14)
CON	13490 (55.4)	3361 (13.8)	2180 (8.8)	5225 (21.3)	30 (0.14)	38 (0.17)	54 (0.23)
2019−2002	−1344 *(−5.6)*	−234 *(−0.9)*	−335 *(−1.3)*	1913 *(7.86)*	14 *(0.06)*	−4 *(−0.02)*	−10 *(−0.04)*
2040−2002	−3229 *(−13.3)*	−285 *(−1.2)*	−875 *(−3.4)*	4398 *(18)*	27 *(0.11)*	−14. 9 *(−0.06)*	−22 *(−0.1)*

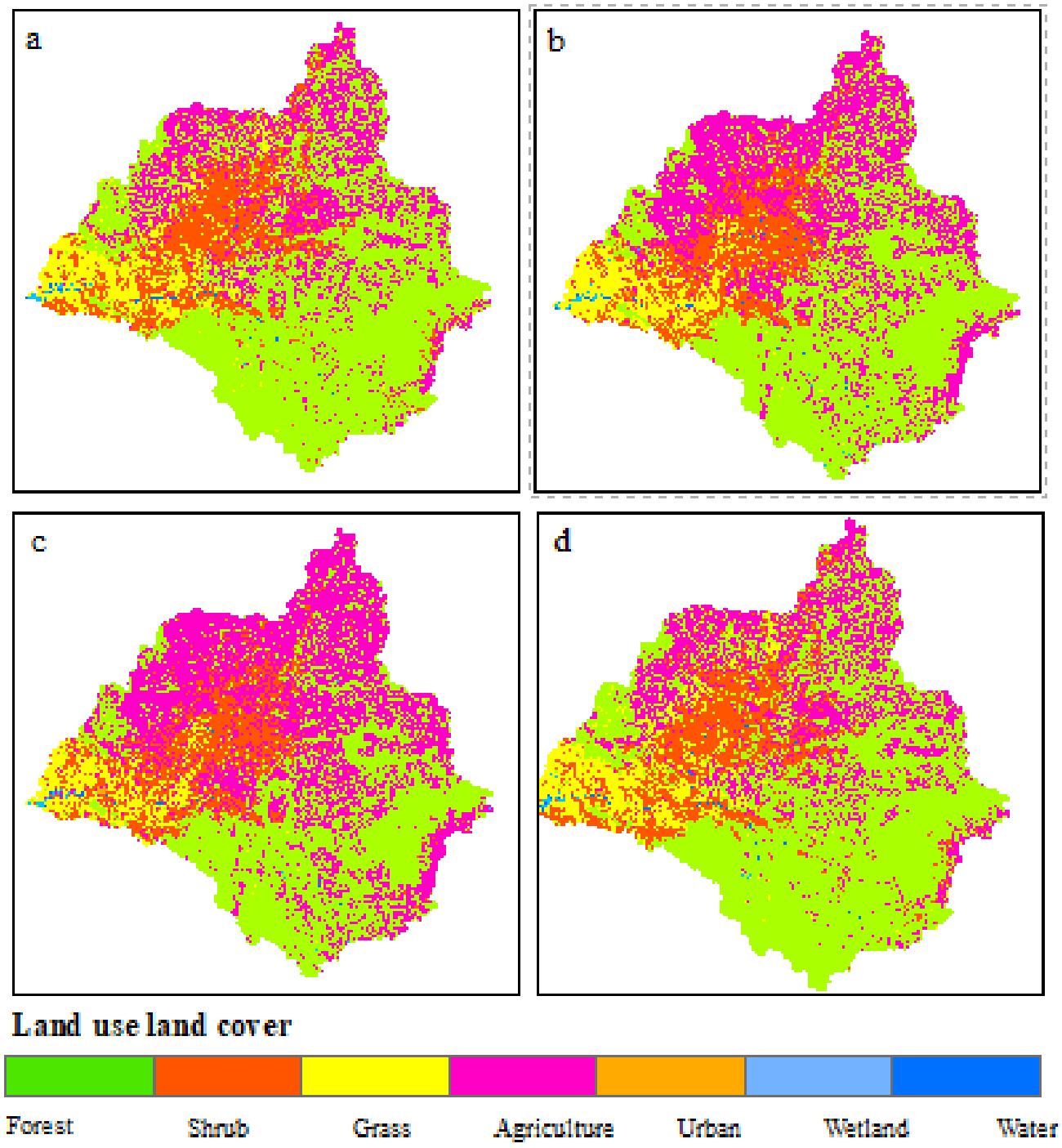

Figure 7.1 Land use maps in the Baro basin for the a) REF, b) CUR, c) BAU, and d) CON land use scenarios.

7.4.3 Climate change scenarios

The comparative performance in the future period projection of the mean monthly rainfall, Tmax, and Tmin simulated by RCMs and their ensemble mean are presented in Figure 7.2. The mean monthly rainfall projection under both climate change scenarios did not show a consistent magnitude and direction compared with the observed climate. Compared to what was observed, most of the models simulated a decrease in rainfall, particularly in the dry months, but some models simulated an increasing trend, mainly in the wet season. For instance, compared with the observed (1782 mm), the ensemble mean indicated a decrease in mean annual rainfall of 1705 mm (4%) and 1668 mm (6.4%) for RCP4.5 and RCP8.5, respectively. Compared with the observed (1782 mm), the RCA4 (CNRM) indicated a larger decrease in mean annual rainfall of 1627 mm (8.69%) under RCP4.5, but REMO (MPI) showed the largest increase of 1799 mm (0.9%) under RCP4.5. Considering the RCP 8.5 scenarios, REMO (MPI) shows the largest decrease (1602 mm), which is about 10%. In contrast, the future climate temperature projections for all RCMs and the ensemble show a consistent increase in Tmax and Tmin under both scenarios. For instance, the maximum temperature for the ensemble mean is expected to increase by 1.1 and 1.9 ℃ under the RCP4.5 and RCP8.5 scenarios, respectively. The RCA4 (ICHEC) indicated a larger increase in Tmax of 1.57℃ under RCP4.5, but the RCA4 (ICHEC) showed the largest increase of 2.2℃ under RCP8.5 scenarios. Similarly, the minimum temperature is expected to increase by 2.6 and 3.1 ℃ under the RCP4.5 and RCP8.5 scenarios, respectively. The CCLM4 (ICHEC) indicated a larger increase in Tmin at 3.18℃ under RCP4.5, but the RCA4 (ICHEC) showed the largest increase of 4.17℃ under RCP8.5 scenarios. The results show that the increase under the RCP8.5 scenario is greater than the RCP4.5 scenario for both Tmin and Tmax. In addition, the increase in Tmin is larger than the Tmax under both the RCP4.5 and RCP8.5 scenarios. The decrease in rainfall is consistent with other studies conducted in several Eastern Nile subbasins (Beyene et al., 2010; Dibaba et al., 2020; Worku et al., 2021). The Tmax and Tmin projections agree well with previous studies on the Eastern Nile and global temperature predictions (Beyene et al., 2010; Elshamy et al., 2009; Worqlul et al., 2018; Worku et al., 2021).

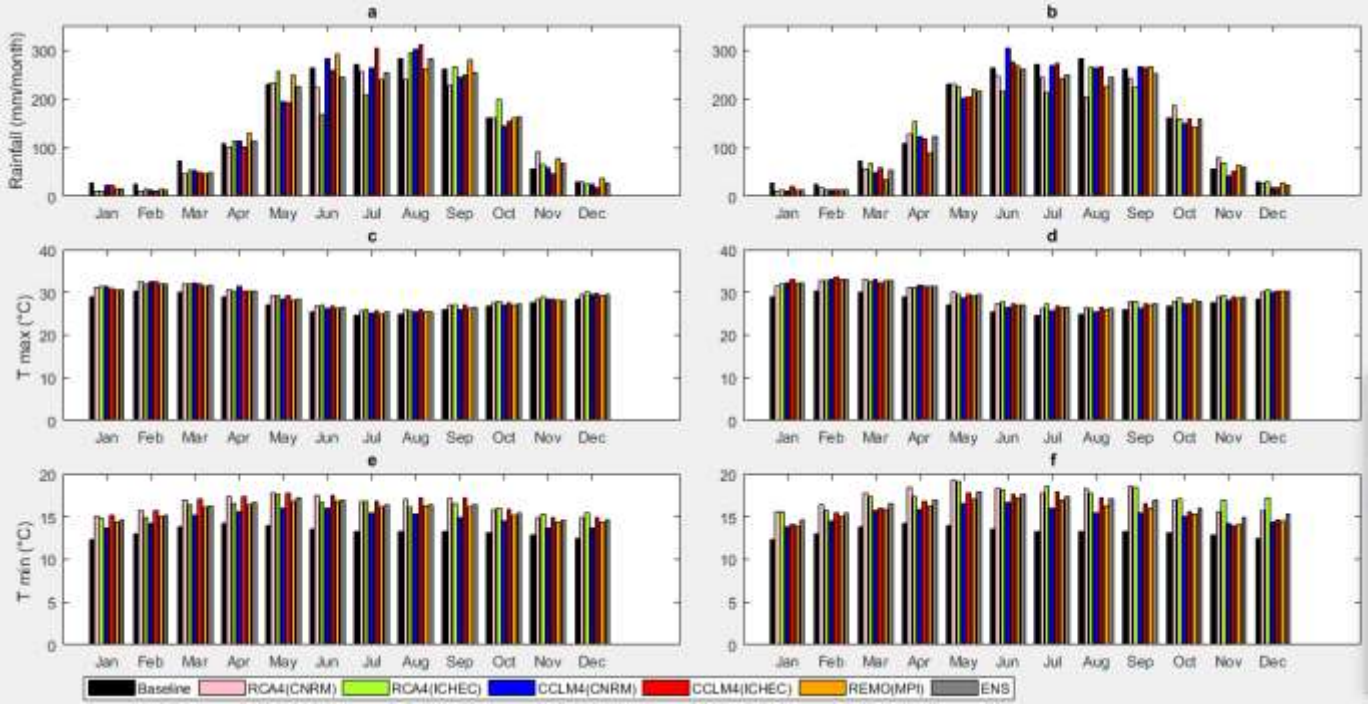

Figure 7.2 Mean monthly climate change scenarios of bias-corrected RCMs and their ensemble relative to the observed: a, b) rainfall for RCP4.5 and RCP8.5, c, d) maximum temperature for RCP4.5 and RCP8.5, and e, f) minimum temperature for RCP4.5 and RCP8.5, respectively.

The larger variation in the directions and magnitudes in bias-corrected RCMs projection particularly for rainfall demonstrates a wide range of uncertainties associated with future rainfall projections. Because of the uncertainty among the climate models, the ensemble which shows better performance in terms of Taylor diagram comparison is considered to obtain a generalized picture of the future climate change impact on the water balance. Moreover, several previous studies suggest the use of an ensemble for climate impact studies reduced uncertainty compared to the individual model (Fowler et al., 2007).

7.4.4 Hydrological model calibration, and validation

According to the results of the global sensitivity analysis using SUFI2 algorithms, the curve number (CN2) and base flow alpha factor (ALPHA_BF) were the most sensitive parameters during the model calibration process.

The SWAT model simulation shows very good agreement in terms of R^2, NSE, and PBIAS as well as the uncertainty analysis of the p-factor and r-factor during the calibration and validation period. Table 7.4. shows the optimal parameter values obtained using the SUFI-2 framework. For instance,

considering the objective function for optimization, the NSE values were 0.87 and 0.85 for the calibration and validation periods, respectively. Besides, the dotty plots in Annex 7.9 show the uncertainty of model parameters in streamflow prediction. The dotty plots are the plots that indicate parameter sensitivity and the distribution of sampling points by plotting parameter values or relative changes against an objective function (NSE).

The prediction uncertainty in SUFI2 is depicted by the 95PPU (95 percent prediction uncertainty), which is represented by the green-colored region in Figure 7.3 for the calibration and validation periods. The flow hydrograph was well modeled, but the peak flow and the low flows were either underestimated or overestimated in the model. The p-factor and r-factor indices are estimated to assess the model uncertainty. The results show that the p-factor estimated was 0.75 and 0.72 for calibration and validation, respectively. This means that 75% and 72% of the observed discharge was enveloped by the 95PPU during the calibration and validation periods, respectively. The r-factor, which is another index and is the thickness of the 95PPU envelope, was 0.5 for the calibration period and 0.4 for the validation period. A p-factor greater than 0.7 and an r-factor less than 1.5 display that the model is best at simulating streamflow (Abbaspour et al., 2015). In general, the SWAT model simulation results look acceptable for the prediction of streamflow. During the calibration and validation, most of the observed values were within the boundaries of 95PPU, which show that SWAT model uncertainties were falling within the permissible limits. Therefore, the SWAT model can be used for various applications, such as the hydrologic impact of land use and climate change in the Baro river basin, water resources planning, and management.

Table 7.4 Calibration and validation performance indicators of the SWAT model at the Baro River station.

Period	Statistical indicators				
	R^2	NSE	BIAS	p−factor	r−factor
Calibration (1990-1998)	0.88	0.87	−0.9	0.75	0.5
Validation (1999-2002)	0.86	0.85	−2.4	0.72	0.4

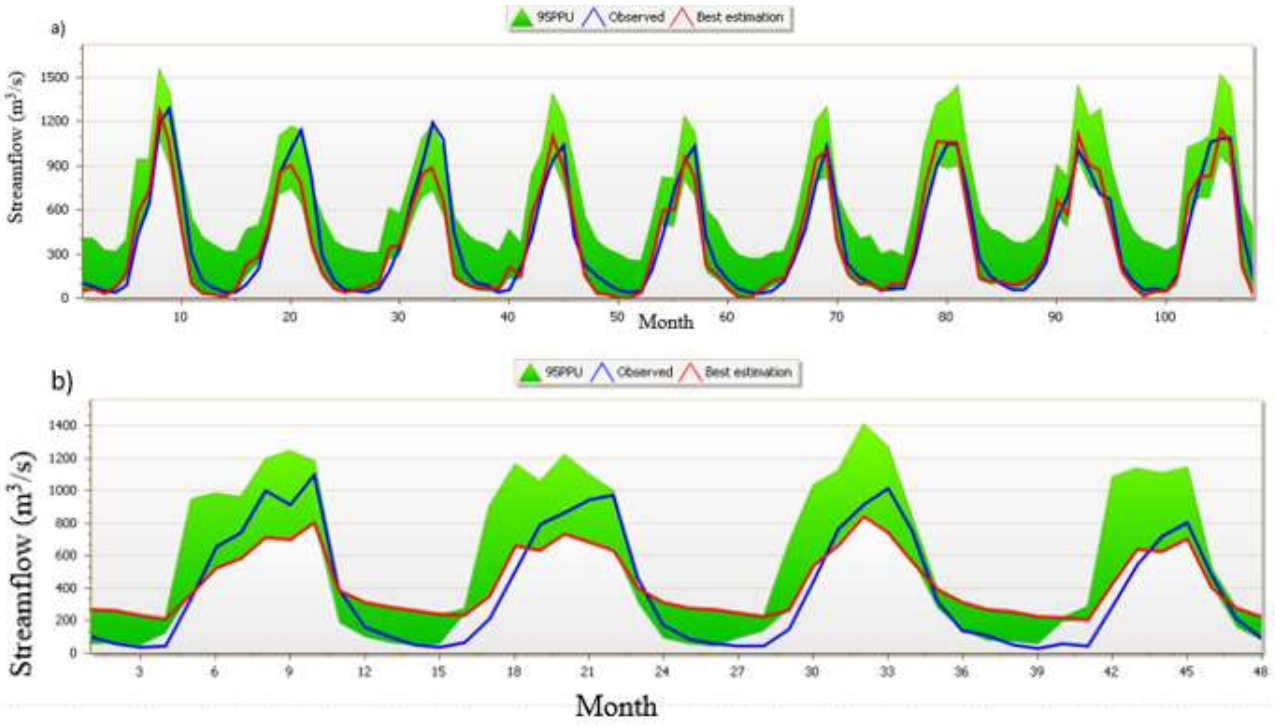

Figure 7.3 Comparison of monthly observed and simulated streamflow during a) calibration and b) validation period, and 95% prediction uncertainty band (95PPU).

7.4.5 The impact of land use change on water balance

The change in water balance for monthly simulations for different land use scenarios is shown in Figure 7.4. The main idea of water balance changes refers to the balance between the input and output of water, where precipitation can be defined as input and evapotranspiration, surface runoff, and groundwater recharge as output (Madani et al., 2018). The mean monthly simulation shows that the ET under the CUR and BAU scenarios is slightly lower than the BAS simulation in most months of the year, with the largest decreases of 4.96 mm and 9.38 mm in March under the CUR and BAU scenarios, respectively. ET projection under CON scenarios shows a slightly increasing trend during most months of the year, with the highest increase in June (1.9 mm). This may be due to the supposed reforestation program under the CON scenarios. Simulation for SURQ under the CUR and the BAU scenario shows an increasing trend in most months, with the largest increases of 8.4 mm and 12.11 mm in August and September, respectively. In contrast, the monthly simulation for SURQ under the CON scenarios indicates a substantially decreasing trend for all months of the year, with the largest decrease of 16 mm in August.

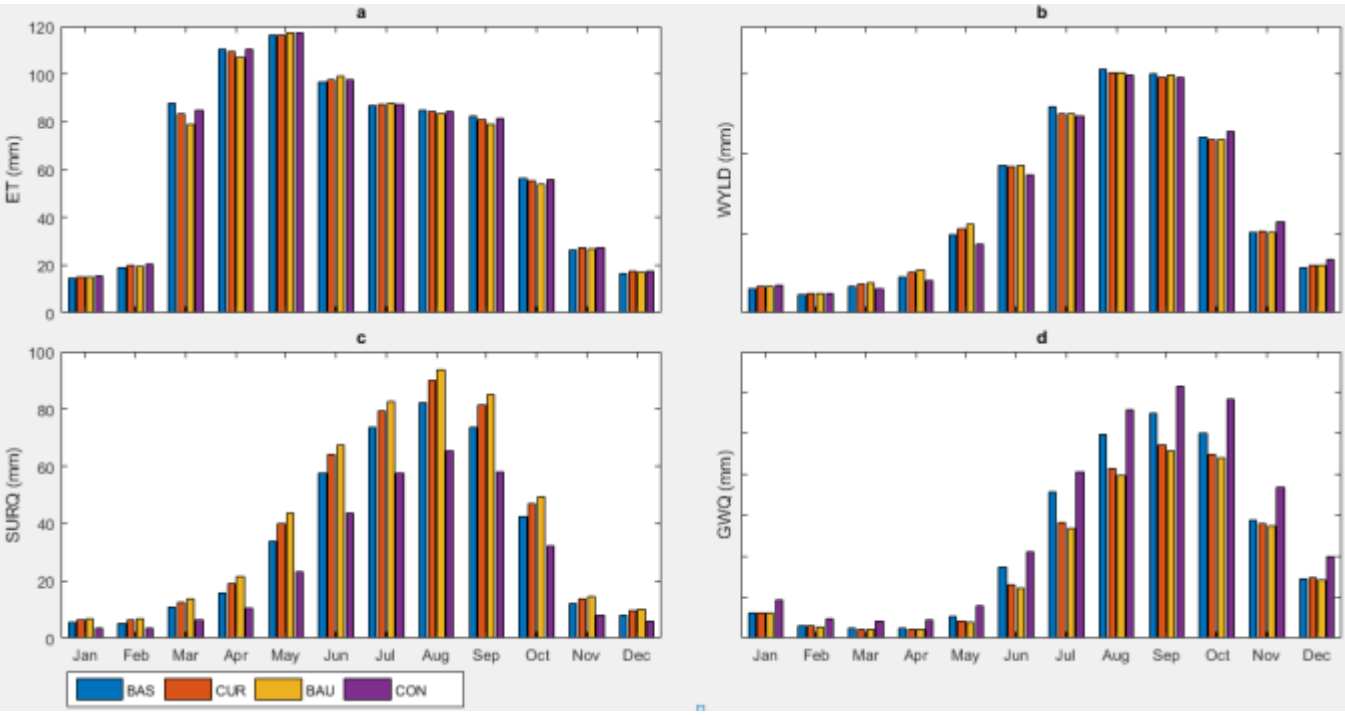

Figure 7.4 Mean monthly simulated water balance for land use change scenarios relative to the reference land use map.

In addition, the change in water balance for seasonal and annual scales under different land use scenarios is depicted in Table 7.5 and Figure 7.5. At seasonal and annual time scales, a minor decrease in ET under the CUR and BAU scenarios is projected. However, SURQ shows a substantial increase in the range of 10 to 18% under the CUR and BAU scenarios, respectively. In contrast, SURQ showed a substantial decrease (36%) under the CON scenario, particularly in the dry season. Furthermore, results show that changes in projected GWQ show a decreasing trend for the CUR and BAU land use scenarios but an increase under the CON scenarios.

The highest increase in SURQ and decline in ET and GWQ under the CUR and BAU land use scenarios compared to the BAS scenarios were associated with the expansion of agricultural and urban lands and the larger decrease in forest land. For example, in comparison to the BAS, the land use simulation for the BAU shows an increase of 18% in agricultural land and a decrease of 13% in forest land. The projected decrease in ET under the CUR and BAU scenarios can be attributed mainly to the decrease in forest cover and the increase in agricultural land. Agricultural land consumes less water than forest land, resulting in a decrease in ET. This may be because forest-dominated land use scenarios may contribute more heat and moisture to the atmosphere

compared to agricultural land-dominated scenarios. Evidence also shows that forests contribute more heat and moisture to the atmosphere compared to agricultural land (Madan et al., 2018; Robinson & Dupeyrat, 2005).

On the other hand, the simulated SURQ for the future has substantially increased under the BAU scenario. This is mainly attributed to agricultural land and has been positively correlated with surface runoff. Consequently, the massive conversion of land use to intensive agriculture and urban development will decrease the soil infiltration capacity, causing a substantial portion of rainfall to be directly converted to surface runoff. The reduction of soil water infiltration, in turn, causes groundwater flow to decline. A study by Woldesenbet et al. (2018) in the Upper Blue Nile basin shows a strong positive association between agricultural land and the mean annual SUR. The conversion of natural vegetation to cultivated or impervious land cover increases runoff generation is also supported by several other studies (e.g., Fan & Shibata, 2015; Tekleab et al., 2014; Woldesenbet, 2022; Yang et al., 2013). In contrast, under CON scenarios, the decrease in SURQ is attributed to the increase in forest land area due to reforestation and the construction of watershed management practices, which improves the soil's water holding capacity, infiltration, and recharge rate. Several studies show that the construction of soil and water conservation structures, such as bunds and terrace decreased the SURQ and increased the amount of soil water and the GWQ. The decrease in SURQ and increase in GWQ under the CON scenario are consistent with other studies conducted in the Ethiopian highlands (Mekonen & Tesfahunegn, 2011; Berihun et al., 2020). For example, Berihun et al. (2020) reported that watershed management practices reduced the SURQ by 65–78% in the Kecha watershed in northeastern Ethiopia.

.

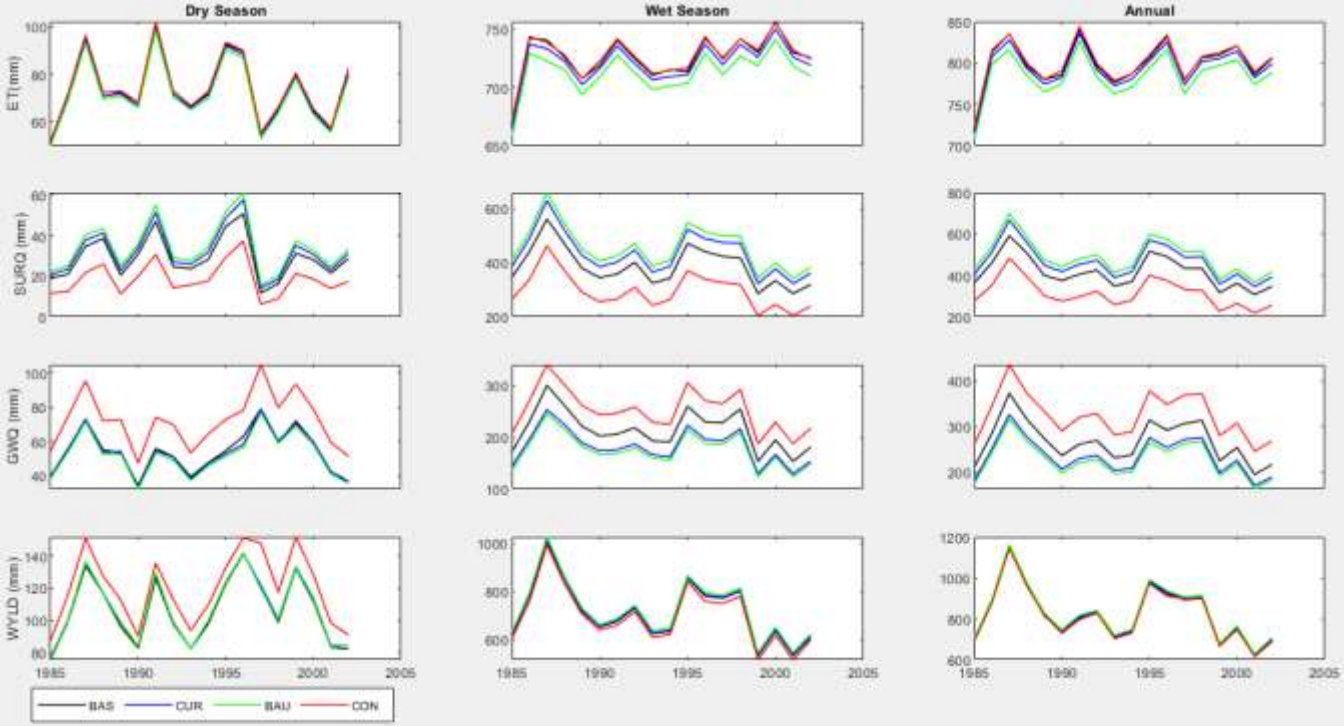

Figure 7.5 Simulated seasonal and annual patterns of water balance for land use change scenarios relative to the reference land use map.

A substantial expansion of agricultural land at the expense of forest, shrubs, and grassland was predicted in the BAU scenarios. In comparison to the baseline, the land use simulation for BAU shows an increase of 18% in agricultural land and a decrease of 13% in forest land. The projected decrease in ET under the CUR and BAU scenarios can be attributed mainly to the decrease in forest cover and the increase in agricultural land. Agricultural land consumes less water compared to forest land, which probably resulted in a decrease in ET. On the other hand, the simulated SURQ for the future has substantially increased under the BAU scenario. This is mainly attributed to agricultural land having a positive correlation with surface runoff. A study by Woldesenbet et al. (2018) in the Upper Blue Nile basin shows a strong positive association between agricultural land and the mean annual SURQ. In contrast, under CON scenarios, the decrease in SURQ is attributed to the increase in forest land area, which improves the water-holding capacity of the soil, infiltration, and recharge rate. Concurrent with this study, the change in evapotranspiration and surface runoff due to land use change is also examined by several other studies in the Ethiopian highlands and other regions of the world (Guzha et al., 2018; Teklay et al., 2021). For example, watershed management practices reduced surface runoff by 65–78% in the Kecha watershed, in

northeastern Ethiopia (Berihun et al., 2020). On the other hand, Hyandye et al. (2018) in the Ndembera watershed in Tanzania also explored that a 7% expansion of forest triggers an 8% increase in evapotranspiration.

7.4.6 The impact of climate change on water balance

The response of water balance to changes in climate change scenarios at a monthly time scale is presented in Figure 7.6. The simulated ET under both RCP4.5 and RCP8.5 emission scenarios is larger than the BAS condition except in January, February, and December. The largest increase in ET has been projected under RCP8.5 scenarios; this may be due to the increase in both the Tmax and Tmin being greater than in the RCP4.5 scenarios. Under RCP8.5, the largest increase in ET is projected to occur in October (24 mm), while the largest decrease may occur in December (10 mm). Similarly, under RCP4.5, a maximum increase and decrease are projected in the same month with a value of 20.5 mm and 11 mm, respectively. The ET simulation shows an increasing trend for both emission scenarios. This is due to the consistently increasing temperature and decrease in rainfall for most months of the year. On the other hand, the projected mean monthly SURQ and WYLD are expected to decrease compared to the BAS. The mean of the results indicates that the decreases are in the range of 9 mm to 45.6 mm for SURQ and 5.2 to 38.6 mm for WYLD. The largest decreasing value was estimated under RCP8.5 scenarios.

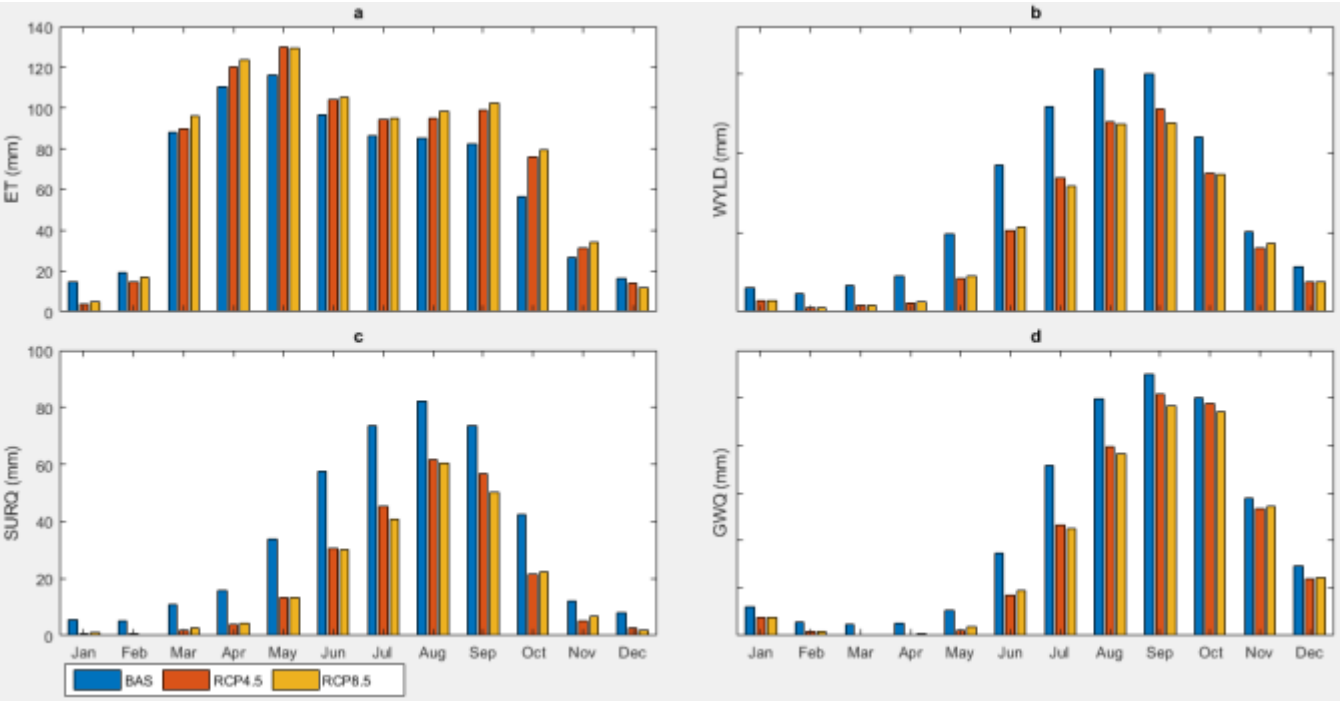

Figure 7.6 Mean monthly simulated water balance for climate change scenarios relative to the observed climate.

Further, the mean seasonal and annual pattern in the water balance for the climate change scenarios is depicted in Table 7.5 and Figure 7.7. Under both climate change scenarios, the water balance projections except for ET indicated a decreasing mean value in terms of dry, wet, and annual time scales. On most hydrological variables, the decrease is more pronounced during the dry season than during the wet and annual time scales. For example, in the dry season, SURQ will decrease by 72% under RCP4.5, but it decreases by 38.6% and 41% in the wet season and annual time scales, respectively. Several studies in Ethiopia (Dibaba et al., 2020; Elshamy et al., 2009; Worku et al., 2020a) also reported a decrease in SURQ under the climate change scenarios compared to the baseline period. The greater decrease in the dry season flow in the Baro River is consistent (Mengistu & Sorteberg, 2012).

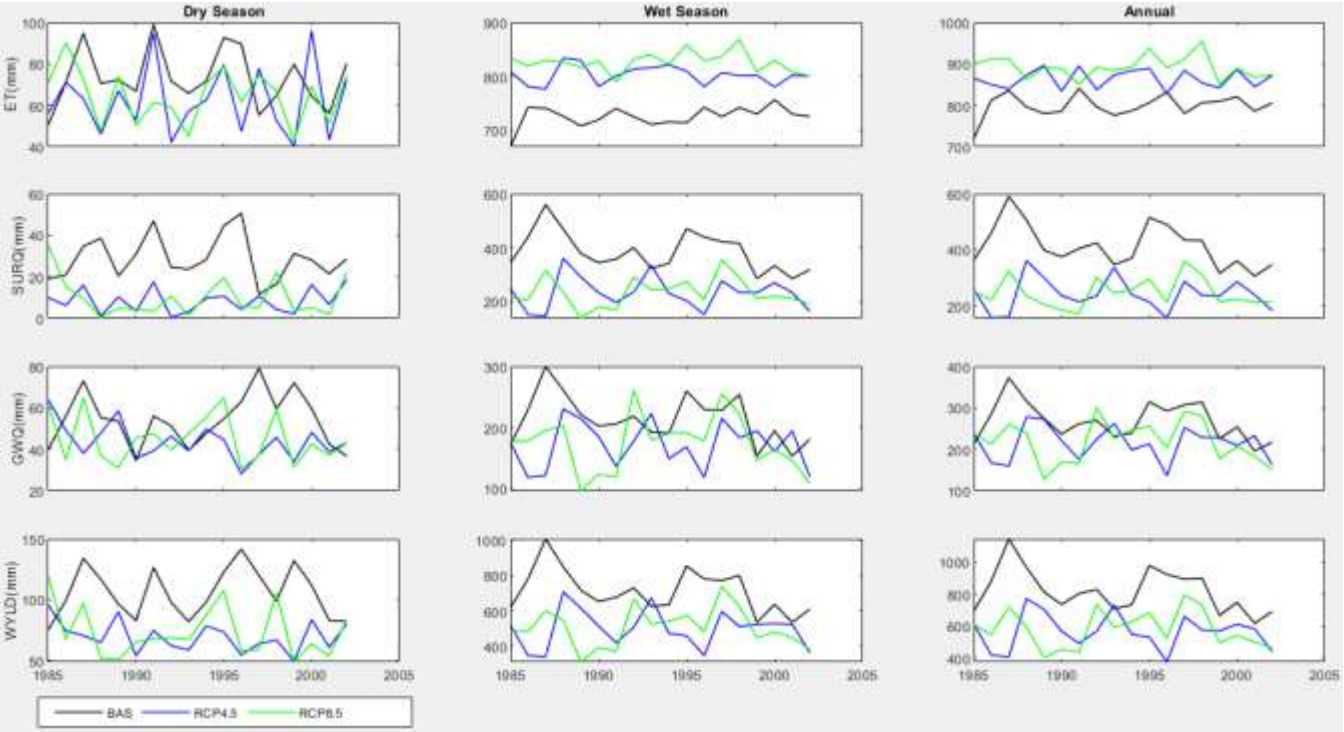

Figure 7.7 Simulated seasonal and annual patterns of water balance for climate change scenarios relative to the observed climate.

7.4.7 The impact of land use change and climate change on the water balance

On the monthly scale, the separate and combined impacts of land use and climate change scenarios on the water balance are presented in Figure 7.8. Results show a substantial change in hydrological processes is simulated in the combined land use and climate change scenarios. The combined scenarios trigger an increase in mean annual ET in most months of the year, with the largest increase of 20.5 mm under CURRCP8.5 occurring during October and the largest decrease occurring in January with a value of 11.3 mm under CONRCP4.5. SURQ indicated decreasing trends in most months of the year. The highest decrease (38.4 mm) was in July under the CONRCP8.5 scenario. The results for WYLD and GWQ also show a decreasing value under all scenarios.

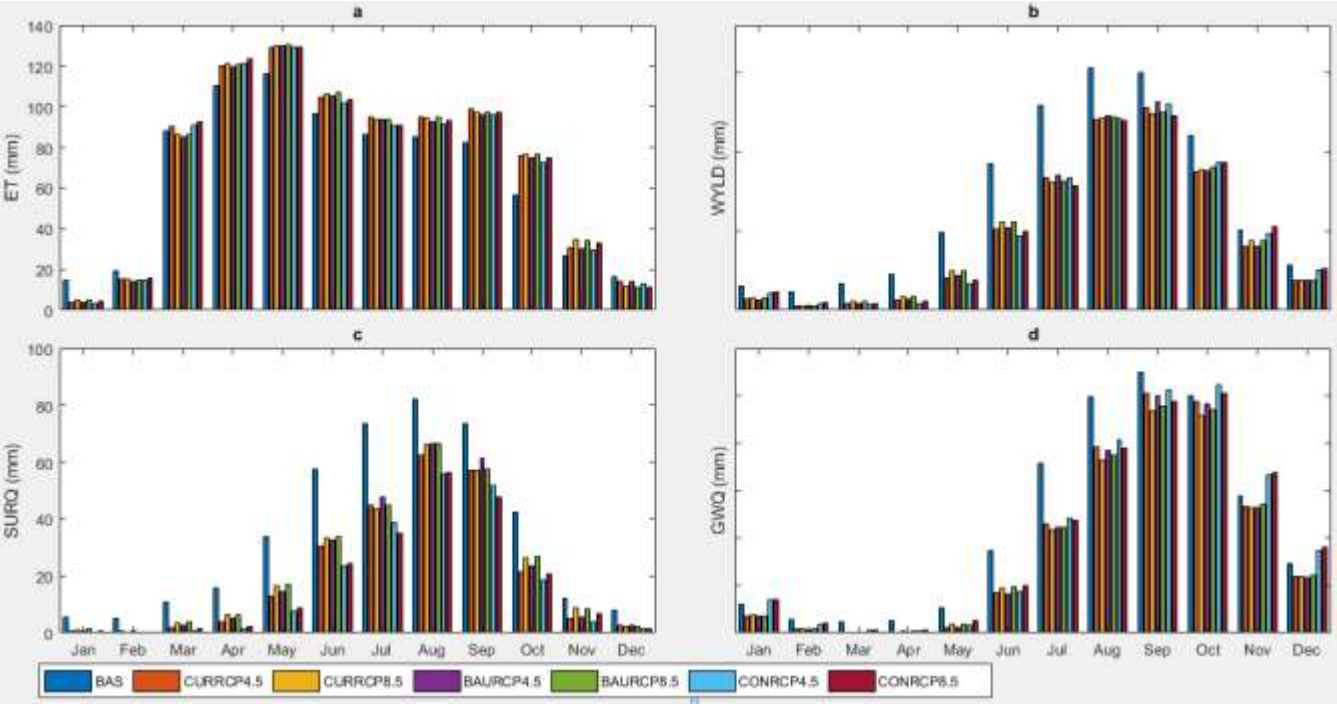

Figure 7.8 Mean monthly simulated water balance for the separate and combined land use and climate change scenarios relative to the baseline.

The mean seasonal and annual pattern in the water balance for the combined land use and climate change scenarios is depicted in Table 7.5 and Figure. 7.9. The combined effects of all land use and climate change scenarios on SURQ and GWQ are simulated to decrease most of the time at the seasonal and annual scales. For example, the combined impact of BAURCP8.5 leads to a 34% decrease in the mean annual SURQ and an increase in ET of up to 9%. Under the CUR and BAU

scenarios, land use change only resulted in a minor decrease in evapotranspiration but a significant increase in SURQ and WYLD. In contrast, the projected climate change only leads to a decrease in SURQ, WYLD, and GWQ and an increase in the ET under both the RCP4.5 and RCP8.5 scenarios. As a result, the combined climate and land use change scenarios (CURRCP4.5 and 8.5 and BAURCP4.5 and 8.5) lead to a decrease in SURQ, WYLD, and GWQ and an increase in ET. However, the combined impact under CONRCP4.5 and CONRCP4.5.8 shows an increase in GWQ during the dry season. Worku et al. (2020b) also show that watershed management practices such as terracing have significantly decreased SURQ and thus significantly increased soil water in the Jemma sub-basin of the Ethiopian highlands when the baseline condition is compared to future climate scenarios. In general, the findings show that the effects of the combined climate and land use change scenarios show some similarity with the effects of climate change scenarios. As a result, the study demonstrates that water balances such as ET and SURQ are more sensitive to climate change than land use change. Several studies conducted around the world (e.g., Aboelnour et al., 2019; Kim et al., 2013; Pan et al., 2017) and in other parts of Ethiopia (Dibaba et al., 2020) also found that climate change was generally more significant than land use change in determining the basin's hydrological response.

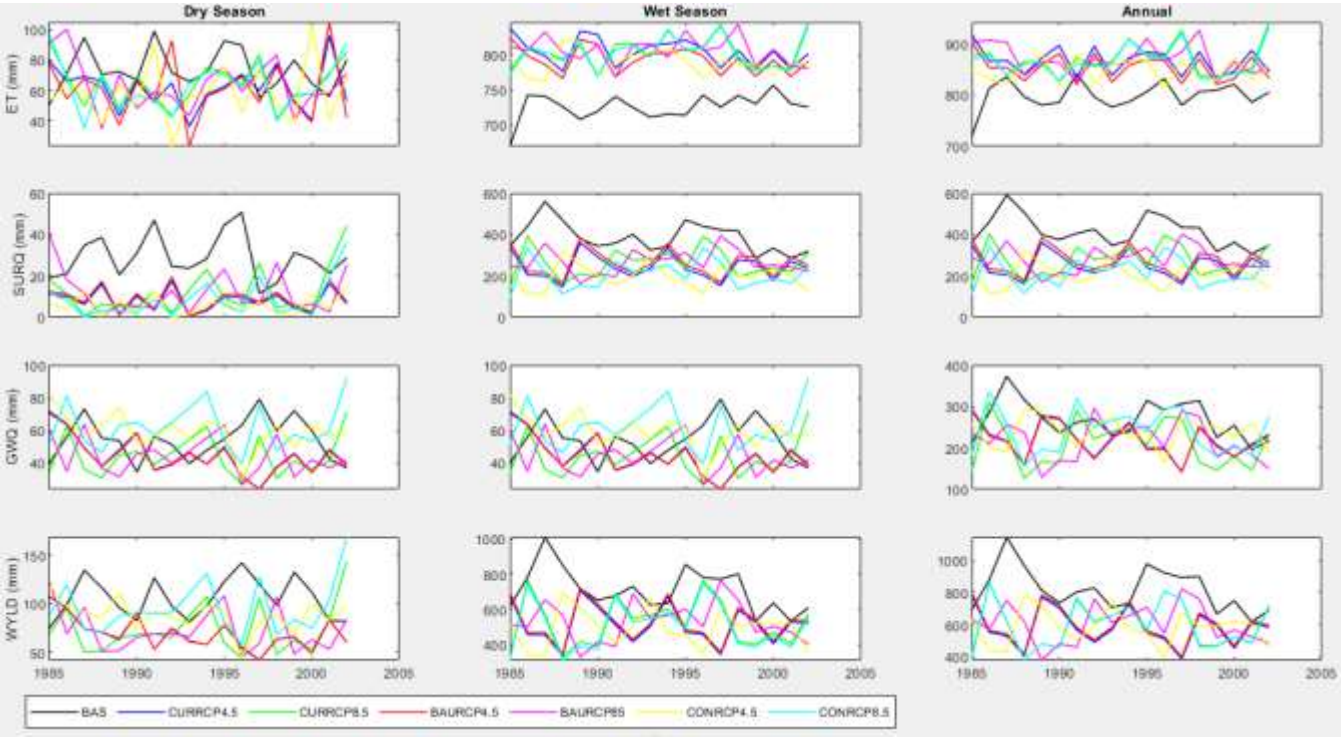

Figure 7.9 Simulated seasonal and annual pattern of water balance for separate and combined land use and climate change scenarios relative to the baseline.

Table 7.5 Seasonal and annual changes in water balance for the separate and combined land use and climate change scenarios compared with the baseline. Values in the bracket denote percentage change (%)

Scenario		time	ET (mm)	SURQ (mm)	GWQ (mm)	WYLD (mm)
Land use	BAS	DRY	78.06	31.35	51.69	105.21
		WET	718.59	380.28	211.66	705.46
		Annual	796.65	411.63	263.34	810.67
	CUR	DRY	77.72 (−0.43)	34.54 (10)	50.96 (−1.4)	106.63 (1)
		WET	713.92 (−0.65)	425.97 (12)	180.48 (−14.7)	708.67 (0.46)
		Annual	791.64 (−0.63)	460.51(11.8)	231.44 (−12)	815.29 (0.57)
	BAU	DRY	76.34 (−2.3)	36.98 (18)	49.51(−4)	106.50 (1.22)
		WET	705.79 (−1.78)	449.34 (18)	173.59 (−17.9)	717.81 (1.75)
		Annual	782.13 (−1.82)	486.31(18)	223.10 (−15)	824.30 (1.68)
Climate	CON	DRY	79.22 (1.48)	19.96 (−36)	69.37 (34.2)	118.03 (12.18)
		WET	719.36 (0.11)	290.46 (−23)	250.54 (18.3)	690.14 (−2.17)
		Annual	798.58 (0.24)	310.41(−24)	319.91 (21.4)	808.17 (−0.31)
	RCP4.5	DRY	63.45 (−18.7)	8.54 (−72.7)	42.96 (−16.8)	68.36 (−35.03)
		WET	808.47 (12.5)	233.20 (−38.6)	170.26 (−19.5)	497.22 (−29.57)
		Annual	871.92 (9)	241.73 (−41)	213.22 (−19)	565.58 (−30.23)
	RCP8.5	DRY	67.22 (−13.8	9.92 (−68)	43.75 (−15)	71.27 (−32.25)
		WET	828.35 (15.27)	225.49 (−40.7)	168.68 (−20)	491.77 (−30.29)
		Annual	895.57 (12)	235.41 (−42.5)	212.42 (−19)	563.04 (−30.54)
Combined	CURRCP4.5	DRY	63.71 (−18.38)	8.57 (−72.6)	42.45 (−17.8)	67.68 (−35.67)
		WET	809.70 (12.67)	237.32 (−37.5)	172.51 (−18)	504.31 (−28.51)
		Annual	873.41 (9.6)	245.89 (−40.)	214.96 (−18)	572.00 (−29.44)
	CURRCP8.5	DRY	65.51 (−16.07)	12.42 (−60)	42.74 (−17)	72.57 (−31.02)
		WET	805.62 (12.11)	252.90 (−33)	162.00 (−23)	509.80 (−27.73)
		Annual	871.13 (9.3)	265.32 (−35.5)	204.74 (−22)	582.38 (−28.16)
	BAURCP4.5	DRY	62.19 (−20.33)	9.62 (−69)	41.94 (−18.8)	67.71 (−35.64)
		WET	797.97 (11.04)	256.16 (−32.6)	170.43 (−19)	517.01(−26.7)
		Annual	860.15 (8)	265.78 (−34)	212.37 (−19)	584.72 (−27.87
	BAURCP8.5	DRY	64.42 (−17.47)	11.90 (−62)	43.20 (−16)	71.89 (−31.66)
		WET	805.55 (12)	257.94 (−32.6)	167.19 (−21)	515.58 (−26.9)
		Annual	869.97 (9.2)	269.84 (−34)	210.39 (−20)	587.47 (−27.53)
	CONRCP4.5	DRY	60.46 (−22.54)	7.96 (−74.6)	59.05 (14)	88.48 (−15.9)
		WET	794.88 (10.61)	197.75 (−48.5)	178.43 (−15.6)	493.99 (−29.97)

	Annual	855.34 (7.36)	202.6 (−51)	237.48 (−9.8)	582.47 (−28.14)
	DRY	63.91 (−18.12)	8.54 (−72.7)	60.58 (17)	93.70 (−10.94)
CONRCP8.5	WET	803.67 (11.8)	196.82 (−48)	175.95 (−16.8)	492.61 (−30.17)
	Annual	867.58 (8.9)	205.1 (−50)	236.53 (−10)	586.31 (−27.67)

ET =evapotranspiration, SURQ = surface runoff, GWQ = ground water, WYLD = water yield

7.4.8 Spatial distribution of water balance under the individual and combined climate and land use change scenarios

The spatial distribution under the baseline and the different separate and combined land use and climate change impacts on the evapotranspiration and surface runoff in the Baro basin are shown in Figures 7.10 and 11, respectively. The corresponding statistical mean difference between the baseline and different scenarios is shown in Table 7.6. As shown in the figures, the spatial variation of evapotranspiration ranges from 500 to 1100 mm, and that of surface runoff ranges from 50 to 900 mm. The highest ET was found in the basin around the forest dominated and high rainfall area in the southern parts of the basin particularly for land use change scenarios Fig 9 a-d. In contrast, the lowest ET was found in the western part of the basin, which has relatively low forest cover and rainfall. Similarly, the western part of the basin is expected to experience the greatest decline in SURQ under both climate change scenarios.

Spatial distributions of decline in forest and shrubland were also in accordance with areas with increases in SURQ and decreases in ET. The red color indicates an increase in SURQ relative to the BAS, while the gray color indicates a decrease in SURQ relative to the BAS. The increase in SURQ under the CUR and BAU scenarios compared to the BAS is associated with the highest expansion of agricultural lands, urban expansion, and the decline of forest and shrubland. This reveals that a conversion of land use to intensive agriculture and settlements will reduce the soil infiltration capacity, causing a large portion of rainfall to be directly converted to surface runoff. On the other hand, the highest decline of the SURQ is projected around the western part of the basin under both climate change scenarios and the combined land use and climate change scenarios. These show the large impacts of climate change and the minor impacts of land use change on SURQ variation relative to the BAS. The decline in SURQ over the basin could be due to the decrease in rainfall and increase in both Tmax and Tmin under both climate change scenarios. Reduced SURQ and the increased in ET in the basin could affect the availability of water resources in the basin and aggravate moisture stress downstream. Aside from climate change

pressure, increased water abstractions may also contribute to a decrease in water resources. Furthermore, the increasing demand for the growing population to use groundwater could additionally contribute to the decline of groundwater by increasing groundwater withdrawal. The study by Dibaba et al. (2020) in Ethiopian highland shows that, due to the high changes in land use, springs in the watershed are dried out and the level of water in hand-dug wells decreases.

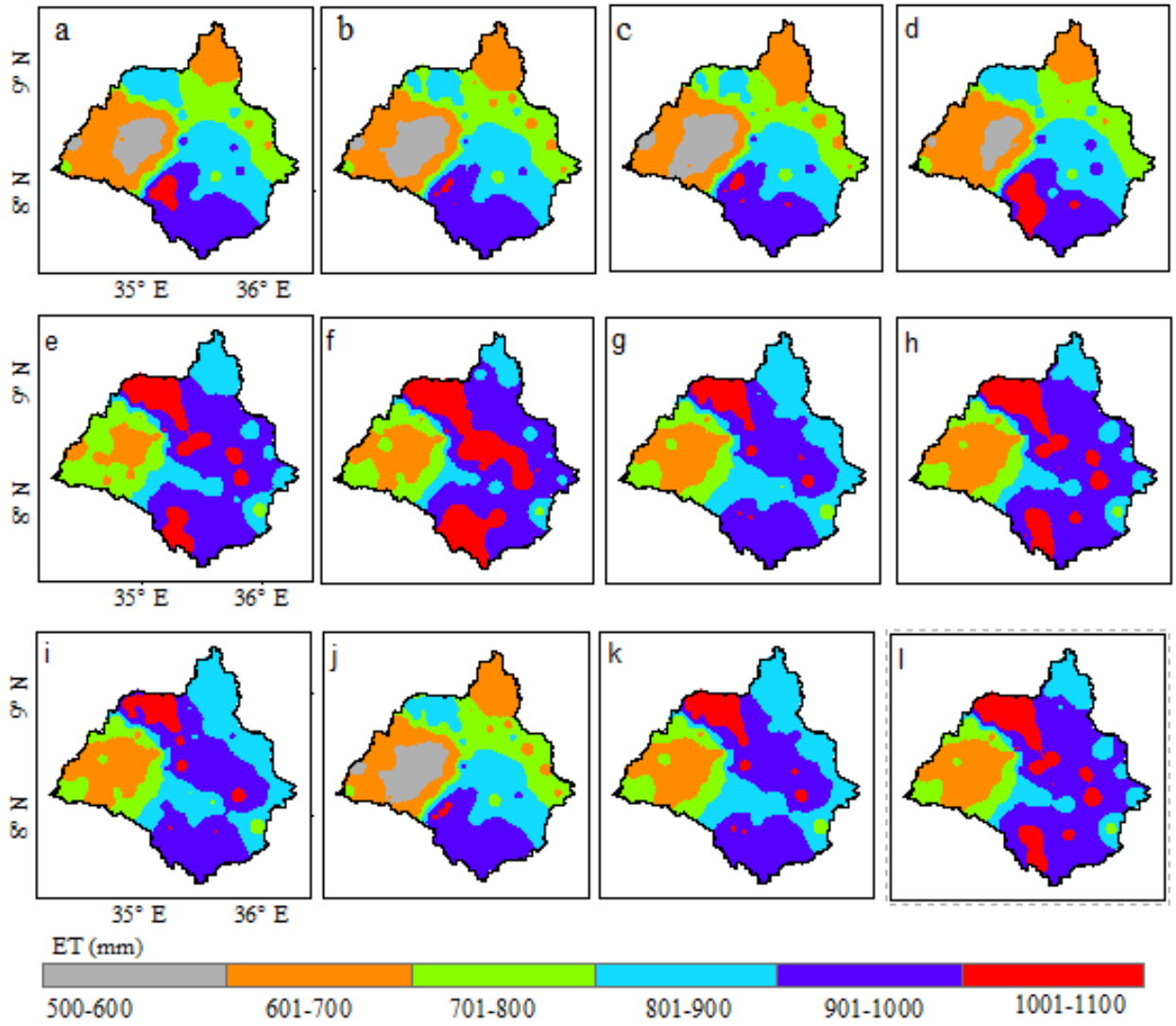

Figure 7.10 The spatial distribution of the ET under the individual and combined climate change and land use scenarios: (a) BAS scenario (1985–2002); (b-d) land use change for CUR, BAU and CON scenarios, respectively; (e) and (f) climate change for RCP4.5 and RCP8.5 scenarios, respectively; (g-l) combined land use and climate change for CURRCP4.5, CURRCP8.5, BAURCP4.5, BAURCP8.5, CONRCP4.5, CONRCP8.5 scenarios, respectively.

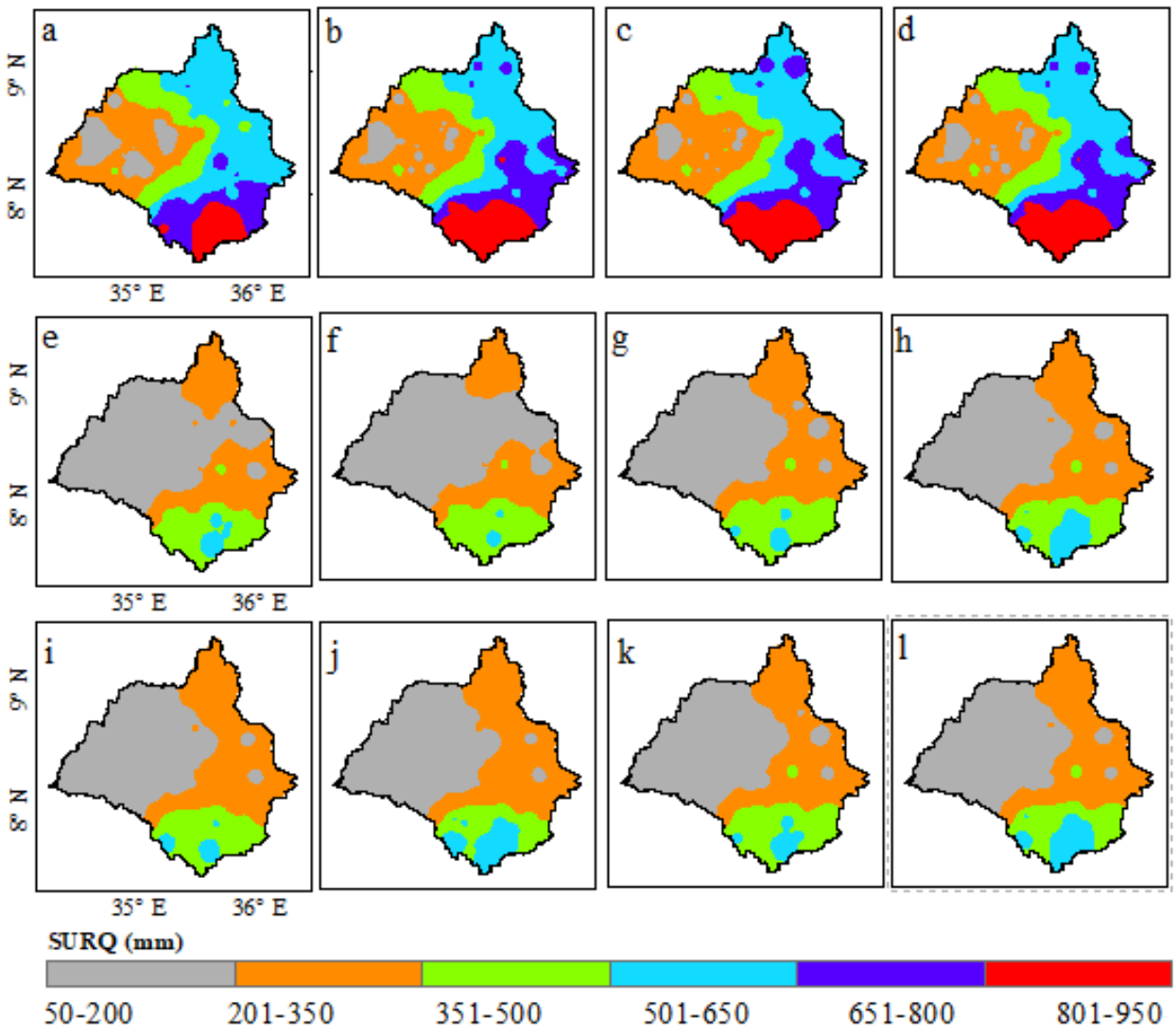

Figure 7.11 The spatial distribution of the SURQ under the individual and combined climate change and land use scenarios: (a) BAS scenario (1985–2002); (b-d) land use change for CUR, BAU, and CON scenarios, respectively; (e) and (f) climate change for RCP4.5 and RCP8.5 scenarios, respectively; (g-l) combined land use and climate change for CURRCP4.5, CURRCP8.5, BAURCP4.5, BAURCP8.5, CONRCP4.5, CONRCP8.5 scenarios, respectively.

7.4.8 Statistical analysis

Table 7.6 presents the mean and variance test between the baseline and each separate and combined land use and climate change scenario for the selected water balance. Results for the homogeneity of the mean test (t-test and MW) and the variance test (Levene test) using a significant level of 5 % showed that the mean difference of ET was not significant for any of the separate and combined scenarios. Whereas the statistical test employed for SURQ shows a significant difference for all

separate and combined impacts except for the CUR and BAU land use scenarios. The GW is significant only for RCP8.5 scenarios, while it is not significant for other separate and combined climate and land use scenarios. The WYLD did not show a significant difference for all land use scenarios, but it did show a significant difference for the climate and combined scenarios. Overall, the change in most of the hydrological processes between the baseline and future land use scenarios was insignificant. This is because the converted land use areas were smaller than the threshold level, which caused a significant change in hydrological processes. The estimate for ET and WYLD has been consistent with a study conducted in the West African basins (Li et al., 2007). They found that deforestation below 50% has no significant impact on water yield.

Table 7.6 Summarize the homogeneity of mean and variance test for annual water balance for the separate and combined scenarios compared with the baseline at a 5% significance level. A single asterisk (*) represents the difference between the mean and variance of the baseline and the scenarios are not statistically significant and the double (**) represents significant differences.

Variable	Metrics	land use			Climate		Combined					
		Cur	BAU	CON	RCP4.5	RCP8.5	Cur 4.5	Cur 8.5	BAU 4.5	BAU 8.5	CON 4.5	CON 8.5
ET	t−test	*	*	*	*	*	*	*	*	*	*	*
	MW−test	*	*	*	*	*	*	*	*	*	*	*
	Leven−test	*	*	*	*	*	*	*	*	*	*	*
SURQ	t−test	*	*	**	**	**	**	**	**	**	**	**
	MW−test	*	*	**	**	**	**	**	**	**	**	**
	Leven−test	*	*	**	**	**	**	**	*	**	**	**
GWQ	t−test	*	*	**	**	**	*	**	**	**	**	**
	MW−test	*	*	*	*	**	*	*	*	*	*	*
	Leven−test	*	*	*	*	**	*	*	*	*	*	*
WYLD	t−test	*	*	**	**	**	*	*	*	**	**	**
	MW−test	*	*	*	**	**	*	*	*	**	**	**
	Leven−test	*	*	*	**	**	**	**	**	**	**	**

Model uncertainties

The impact of land use and climate change studies on hydrology and the application of hydrological models involves various uncertainties (Fowler et al., 2007; Hayhoe et al., 2017; Karlsson et al., 2016; Teklay et al., 2021). This study used a land use change model, a climate change model, and a hydrological model, whereby each model can be a source of large uncertainty

affecting the outcomes. For the land use change model, the study used a combination of the MOLUSCE and MCE methods to project future land use. However, this method and assumption base land use in the future on the extrapolation of trends, whereas future trends are uncertain due to uncertainties in future population growth, economic policy, and government policy (Marhaento et al., 2018; Van Roosmalen et al., 2009). The best management practices can be modeled using the SWAT model based on literature, but they have not been validated by field data. For the climate model, the choice of GCM or RCM is the greatest source of uncertainty in climate change studies (Chen et al., 2011; Kundzewicz et al., 2018). The discrepancy among the GCM models over regional climate change studies is widely recognized as a large source of uncertainty. Moreover, the climate models disagree on the magnitude, and even the direction of change of climate variables in different parts of the world, particularly when it comes to rainfall (Beyene et al., 2010; Zhang et al., 2014). For the hydrological model, the source of uncertainty can be associated with model structure, parameter uncertainty, and data scarcity for calibration and validation processes as well as data inputs (e.g., lack of relevant spatial and temporal variability of data on climate, soils, and land uses) (Brigode et al., 2013).

Despite these potential sources of uncertainty, this study made efforts to reduce uncertainties stemming from land use, climate change, and hydrological modeling. One possibility of accounting for some of the uncertainties is using an ensemble of climate models (Kundzewicz et al., 2018). Consequently, an ensemble of multi-GCM-driven RCM simulations was used based on the different magnitudes and directions of change in the future climate. Besides, climate change scenarios were developed from RCM simulations that have high resolution (10–50 km). The most plausible emission scenarios with robust bias correction techniques are used for the assessments of the RCMs to reduce uncertainty. The SWAT model was calibrated and validated for streamflow data before applying it to climate change impact assessments. The performance of the model was evaluated in terms of appropriate statistical metrics. In addition, this study is looking for the best available data, such as a high-resolution soil map (250 m), a land use map (30 m), and a DEM (30 m), to reduce uncertainties in the model projection and try to understand the impact of land use and climate change on the hydrological process in the basin.

7.5. Conclusion

This study evaluated the separate and combined impacts of climatic and land use changes on hydrologic processes in the Baro basin. A calibrated SWAT model was run for three land use

scenarios, two future climate scenarios, and six combinations of land use and climate change that were used in this study. The distribution mapping methods were used to correct for both the daily rainfall and temperature datasets. Statistical tests were employed for evapotranspiration, water yield, runoff, and groundwater to test the mean annual difference between the baseline and simulated scenarios.

Under climate change scenarios, the consistent increases in Tmax and Tmin and the decreases in rainfall in most of the months are expected to increase the evapotranspiration and decrease the water availability in the Baro basin. The projected climate change alone leads to a decrease in surface runoff, water yield, and groundwater and increases the ET under both the RCP4.5 and RCP8.5 scenarios.

In comparison with the REF land use map, the BAU projected land use shows a substantial increase in agricultural land with a percentage of 18% that should be regulated to have sustainable development and maintain a green environment. On the other hand, a substantial decrease in forest land with a percentage of 13.4% should also be regulated to control environmental degradation. The business-as-usual scenario indicated the great expansion of agricultural land at the expense of forests, which led to an increase in mean annual surface runoff of 18% in 2040. In contrast, the conservation scenario decreases the surface runoff by 24%. The land use map of the CUR and BAU scenarios alone leads to an increase in surface runoff, water yield, and decreased groundwater and ET.

In most scenarios, there is a tendency for the combined land use and climate change scenarios' hydrologic responses to be similar to those of climate change alone. This demonstrates that climate change has a greater impact on mean monthly, seasonal, and annual hydrological processes than land use change. Generally, the estimated water balance will have negative impacts on future agricultural production and water availability. As a result, the implementation of integrated basin management strategies such as water harvesting, soil and water conservation, and afforestation could minimize the negative impacts.

8. Synthesis, conclusions, recommendations, and future research direction

8.1 Synthesis

The Baro–Akobo River basin is of high strategic significance for Ethiopian development, at both the regional and national levels. For this reason, advances in the general understanding and evaluation of the individual and combined impacts of future changes in the hydrology of the basin under the changing climate and land use conditions are urgently needed. This study was first intended to examine the past and potential future climates and their impacts on the hydrological processes of the basin. The observed station climate data from 1975–2005 was used to compare the raw and the bias corrected climate model data obtained from the CORDEX-Africa portal. Furthermore, climate model data under the representative concentration pathway (RCP) 4.5 and 8.5 scenarios for the periods 2030 (2021–2050) and 2080 (2071–2100) was used to examine the future climate and its impact on the hydrological processes using the SWAT model and IHA software. On the other hand, to examine land use change, this study used land use data from the USGS website, which provides Landsat satellite image data for the periods 1985, 2002, and 2019. The classified land use data from 1985 to 2002 was used to validate the land use data of 2019, and land use data from 2002 to 2019 was used to predict future land use changes using the CA-ANN approach. Three different climate data sets (observed, CFSR, and CHIRPS) and the 2002 land use map were adopted for the SWAT model's calibration and validation. Then the calibrated and validated SWAT model was applied to simulate the basin hydrology under various climate and land use change scenarios. Eleven different scenarios (two for the impact of climate change, three for land use change, and five for the combined impact of climate and land use) were developed to compare with the baseline.

8.1.1 Statistical regional climate model evaluation

Recently, the CORDEX initiative has made several RCM outputs available for end users throughout the African continent. Before climate simulations obtain applications for impact and adaptation studies, the skill of the simulation results has to be examined. In this study, the climate skills of seven individual RCMs and their ensemble mean in the basin were investigated. The observed data for performance assessment was collected from the weather stations of the National Meteorological Agency of Ethiopia (www.ethiomet.gov.et/). The models were examined using several statistical measures, such as root mean squared error, correlation coefficient, bias, and plots

of the observed vs. simulated annual cycle. The results show that the majority of the raw climate models capture the unimodal pattern of the annual rainfall cycle. However, the models showed either a shifting of the rainy season or a considerable overestimation or underestimation. For instance, CCLM4 (CNRM) overestimated the rainfall in the majority of the months in several stations but underestimated it in some stations, for instance, in Mizan-Tefri, and shifted the peak rainfall period. RCA4 (CNRM and MPI) underestimated the rainfall in the majority of the months at several stations but overestimated it at some stations, for instance in Masha and Yubdu and shifted the peak rainfall period. Although the ensemble better captured the unimodal rainfall pattern, it underestimated rainfall in most months, including the peak rainfall period. The results showed that using the raw RCM data resulted in greater uncertainty in the rainfall simulation in the basin. In all cases, it is noted that climate model data resulted in a better representation of temperature than rainfall, indicating that greater uncertainty still exists in model simulated rainfall than temperature. Moreover, RCA4 (CNRM) for maximum temperature and RCA4 (ICHEC) for minimum temperature best captured the monthly pattern and the corresponding peak period. In general, no single RCM performed best across all stations when comparing monthly and annual climate characteristics. This is likely because rainfall and temperatures vary spatially due to elevation differences among considered meteorological stations. Due to the difference in initial boundary conditions, local forcing, the parameters considered, and the parameterization of variables, climate models have different performances in simulating the climate of a specific geographic region. The biases in RCMs may also stem from the boundary conditions (GCMs). Moreover, different RCMs may perform differently when forced to perform under similar boundary conditions (GCMs). This implies that the best-performing RCMs vary within the study basin, and thus site-specific evaluation of RCMs and bias correction is indispensable before applying the data for impact assessment. It is also essential to identify GCMs and RCMs that can simulate the historical climate of the study basin.

Bias adjustment could help reduce uncertainties arising from systematic biases in the RCMs. Bias correction procedures assume that the bias correction algorithms and their parameterization for baseline climate conditions are also valid under future climate conditions. Therefore, it was worthwhile to adjust such biases through a robust statistical bias correction approach before using RCM simulations to generate climate scenarios and climate impact scenarios. The comparison of the distribution mapping methods and linear scaling methods under different metrics demonstrated

comparable performance in correcting the climate simulations of the RCM against the observed. No substantial difference is found after bias correction between the observed and the RCM simulations, and a relatively small variability range is identified in terms of the statistical metrics used for rainfall and temperature evaluation during the period 1975–2005. All of the models well captured the unimodal pattern of the annual rainfall cycle with less bias. Among the models, the ensemble mean best captures the annual cycle with less bias and high correlation at several stations. Several researchers who worked primarily with model evaluation in various parts of the world have acknowledged the use of ensembles in improving the quality of individual climate models. Therefore, to reduce the uncertainties that arise from RCM choice, many studies frequently use the ensemble method, where the projection results from more than one climate model are combined. The results of this study also supported the effectiveness of the ensemble approach in improving climate data quality. The better performance of bias corrected RCMs in reproducing the annual cycle could provide important information for farmers and water resource managers.

8.1.2 Future climate change scenarios

To account for the climate model uncertainties in future simulations, five RCMs and the ensemble mean based on two RCP scenarios (RCP4.5 and 8.5) were considered for the periods 2021–2050 (2030s) and 2071–2100 (2080s). These RCP scenarios are selected following the priority given by the CORDEX-Africa project. Furthermore, to develop climate change scenarios useful for assessing hydrological impacts, the raw data from each RCP's climate model was bias-corrected for systematic bias using distribution mapping techniques. In correspondence with the projected strong tropical ocean warming (IPCC, 2013), the majority of the climate scenarios and their ensembles reveal a decrease in rainfall in the 2030s and 2080s future periods over the basin, but the temperature shows a consistent increase throughout the future period. Under the ensemble mean of RCMs, a higher decrease in rainfall is projected under the RCP8.5 emission scenario than in the RCP4.5 emission scenario. The dry and wet season means of rainfall are expected to decrease by 19% and 4%, respectively, under the RCP8.5 scenario by the 2080s. This indicates a relatively narrower range of projections for the wet season than the dry season. Higher and lower increases of Tmin and Tmax are estimated from climate scenarios under RCP8.5 and RCP4.5, respectively, following the Fifth IPCC finding that attributed emission scenarios as major drivers of temperature change. Again, in agreement with the projected concentration of greenhouse gases, a higher increase in Tmax and Tmin is projected in the 2080s than in the 2030s. The Tmax and Tmin are

expected to increase up to 2.6 ℃ and 3.29 ℃ for RCP8.5 in the 2080s, respectively. In general, Tmax and Tmin under the considered climate scenarios have demonstrated strong consistency with the projected global temperature. To assist our understanding of the future condition of extreme rainfall in the basin, descriptions of selected indices of daily rainfall amount were undertaken. An increase in rainfall extreme projections (e.g., R20, R95p, Rx1, and RX5) in RCP scenarios could lead to a greater climatic risk to human livelihood and other environmental resources. This extreme rainfall event in the basin showed a similar trend to the global extreme rainfall prediction, which exhibited an increase since the 1950s (IPCC, 2019). This confirms that, due to changes in the pressure systems and sea surface temperatures of the equatorial eastern Pacific, Gulf of Guinea, Atlantic, and Indian Oceans in the future period, the mean rainfall and extreme rainfall in the basin may be further perturbed in the future period. On the other hand, a decline in rainfall projection (e.g., R10 and the mean value) could impact crop production and the amount of water available in rivers and streams. In general, the greater range of potential changes between the models and the different extreme indices suggests that we should be prepared for many probable impacts from changing rainfall and temperature.

8.1.3 SWAT hydrological model evaluations

The temporal and spatial data sets were used to set up the SWAT model. Three independent climate datasets, including observed, CHIRPS, and CFSR, were applied to calibrate and validate the model at Baro and Sore river stations. The model has been used to represent the main hydrological processes within small and large basins. In SWAT, sub-basins are firstly divided based on the DEM and are then further subdivided into a series of HRUs according to the elevation, land use, and soil types of the basin. The HRUs are the smaller estimation units, where the hydrological components such as ET, SURQ, and GWQ are estimated based on the water balance equation (Neisch et al., 2011). Parameter sensitivity analysis, calibration, and validation are undertaken by SWAT-CUP, which is an automatic sensitivity analysis tool in the SWAT model (Abbaspour et al., 2015). To assess the skill of the SWAT model in streamflow simulations, different metrics such as NSE and PBIAS between the observed and estimated values were provided (Moriasi et al., 2007). The curve number (CN2), soil evaporation and compensation coefficient (ESCO), and Baseflow alpha factor (ALPHA_BF) were found to be the most sensitive parameter. When considering simulation results, CHIRPS combined with CFSR was as good as the observed climate dataset for reproducing the monthly streamflow data. Moreover, when considering simulation

results at daily time steps, the performance of the model to reproduce daily streamflow was not as good as that at monthly time steps. Once the model was calibrated and validated, different climate and land use scenarios were applied to evaluate their impact on hydrological processes at the basin scale.

8.1.4 Climate change impacts

To understand more about the future availability of water resources, hydrological process analysis was performed on a monthly, seasonal, and annual basis using the SWAT model and the IHA method. The decrease in mean rainfall and the increase in temperature due to future climate change imply a general decrease in streamflow and, thus, an increase in evapotranspiration. The strongest climate change impact is produced for RCP8.5 for the 2080s, which indicates a larger decrease in rainfall and streamflow and an increase in temperature for all seasons. The FDC also shows a decreasing trend in most of the flow except for the extreme flow segment. Moreover, the hydrological flow indicators related to monthly flows show a decrease in the high and middle ranges of variability categories, while the low category shows an increasing trend. In general, decreases in surface water, water yield, and groundwater, as well as an increase in evapotranspiration, could affect the availability of water resources in the basin and aggravate moisture stress downstream. The largest decrease in streamflow under the RCP8.5 scenario is in agreement with other previous climate change impact studies in other parts of Ethiopia (Dibaba et al., 2020; Worku et al., 2021). The finding is also consistent with Beyene et al. (2010), who showed that the Nile River is expected to decline in 2040–2069 and 2070–2099 due to the decline in rainfall and increased evaporation demand.

8.1.5 Land use change impacts

The historical trend of land use change over the last four decades was performed using Landsat satellite image data. The satellite image was used for predicting future land use. The current land-use distribution in the watershed is mainly the result of various anthropogenic processes that have occurred during the last four decades, including the diminishing and abandonment of vegetation such as forests, shrubs, and grazing. This has led to an expansion of agricultural land, which nowadays occupies nearly 18% of the basin's area, and urbanization. In addition to the current land use scenario, two other plausible scenarios were generated on the basis of realistic assumptions. The land use map uses a set of spatial interaction rules and machine learning

(artificial neural networks) algorithms to generate a future land use scenario, namely "business as usual." The third scenario considers a further increase in altitudinal forest expansion. The conservation scenario (CON) includes the substitution of mountainous agriculture and grassland for forests and applying watershed management practices in agricultural areas. When hypothetical (but plausible) land-use scenarios are considered, surface runoff (and ET) are affected as well; i.e., a decrease in surface runoff and an increase in ET are observed in the case of a conservation scenario, and the opposite effect is observed when a BAU scenario is considered.

8.1.6 Climate and land use change impacts

Eleven different scenarios (two for the impact of climate change, three for land use change, and five for the combined impact of climate and land use) were developed to compare with the baseline. For which the SWAT model was used to simulate several water balance components. The components of water balance, including surface runoff, ET, and groundwater and water yield content, were simulated for a basin to assess its sensitivity to changes in climate and land use. Under climate change conditions (increasing both Tmax and Tmin and decreasing rainfall) surface runoff, GWQ, and WYLD will suffer reductions (up to 42%) and an increase in ET (12%), where the RCP8.5 climate scenario is considered. In contrast, the BAU land use scenario projection triggers a respective increase in the mean annual SURQ of 18% and decreases ET by up to 2%. According to the SWAT model, this indicates climate change will have bigger impacts on the availability of water resources than land use changes. As a result, the water balance is more sensitive to climate change than to land use changes; the change in the estimated water balance under both climate and land use change scenarios is consistent with that under the only climate change scenario.

Finally, while formulating adaptation and mitigation plans for a potential future climate and land use change threat, decision-makers who use climate and land use models output, such as managers of water and land resources, designers of water infrastructure, and policymakers, must carefully examine the validity of the data. Particularly, the community of climate users must conduct a thorough assessment and choose the best climate model to depict the climate in the area of interest while the modelers continue to work on improving their models.

8.2 Conclusions

By considering the historical and projected climate variables and land use changes, the possible impacts of these changes on the water resources of the basin have been examined. Before quantifying the separate and combined impact of climate and land use change on hydrology, a couple more activities were carried out, including (1) the two major climatic inputs, rainfall, and temperature, were bias-corrected; (2) a comparison of the performance of regional climate models in simulating the historical climate; (3) hydrological model calibration, validation, and sensitivity analysis; (4) developing baseline and future climate data using a bias-corrected multi-RCM and land use scenarios; and (5) quantifying the individual and combined impacts of climate and land use change on hydrology.

The RCM outputs from CCLM4, RCA4, and REMO capture the historical rainfall and temperature characteristics of the basin. However, all RCMs after bias correction showed better performance in reproducing the magnitude and distribution of the mean monthly rainfall and temperature and improved all the statistical metrics. The Mann-Kendall trend test (TFPW methods) for observed and most individual bias corrected RCMs, as well as the ensemble mean, revealed a decreasing trend in rainfall, while maximum and minimum temperatures showed an increasing trend in the majority of the stations. The ensemble mean of RCMs coupled with the distribution mapping methods is superior in several statistical metrics.

The study shows the reliability of gridded climate data as an alternative to observed station data in limited or missing data cases for hydrological studies. CHIRPS combined with CFSR, in particular, performs comparably with the observed data set.

In future climates, there will be much better consistency between climate model projections of temperature and rainfall. The rainfall under different regional climate models shows unpredictable rainfall predictions under RCP4.5 and RCP8.5 climate scenarios. This shows that local and regional factors (internal variability) are also important drivers of rainfall in the basin. As projected in all bias-corrected RCMs, RCP8.5 is generally warmer than RCP4.5, and the 2080s are warmer than the 2030s. An increase in rainfall extremes and temperatures projected in RCP scenarios could lead to a greater climatic risk to human livelihood and other environmental resources. On the other hand, a decline in rainfall projection (e.g., R10 and the mean value) could impact crop production and the amount of water available in rivers and streams. In general, the greater range of potential

changes between the models and the different extreme indices suggests that we should be prepared for many probable impacts from changing rainfall and temperature. If sustained and significant reductions in greenhouse gas emissions are not achieved, such temperature and rainfall changes could occur in the 21st century and beyond.

The good agreement between observed and simulated daily and monthly values for streamflow over the period of 1990–2002 proves that the SWAT model can provide good estimates of streamflow and other hydrological processes in the basin. Based on the bias-corrected ensemble climate model simulation, the basin may experience a decrease in rainfall and an increase in temperature under the RCP4.5 and RCP8.5 scenarios compared to the baseline condition (1985–2002). This can be attributed to the decrease in surface runoff, groundwater, and water yield and an increase in evapotranspiration. Except for the extreme flow segment (i.e., 0–3% exceedance probability), the projection for simulation under both scenarios shows a decreasing flow. The projection of land-use change in the business-as-usual (BAU) scenario demonstrated the expansion of agriculture in the Baro basin. As a result of this change, surface runoff is projected to increase while evapotranspiration is projected to decrease in the future. On the contrary, under a conservation land use scenario, a surface runoff will decrease while evapotranspiration increases. The increase in SURQ caused by land-use change factors is less than the offsetting decrease resulting from climate change. In addition, the minimal decrease in evapotranspiration under the BAU scenario is outweighed by increases in climate change scenarios. The assessment indicated that climate change is the main driver of the water balance in the basin. The outcomes of the climate projection study illustrate the implications of decreased water availability and its effect on agricultural output. Thus, climate change is expected to affect much more the amount and ecological quality of streamflow, the resilience of riverine species, and the future availability of water resources more than land use change.

Uncertainties in climate-change impact assessments in hydrology and water resources are almost unavoidable, but the results are probably valid under the currently used climate and land-use scenarios in the study area. However, the results and methodology of this study still have implications for water-resource management and land-use planning in the future for the study area and other regions facing similar stresses from climate and land use change.

The climatic scenarios that were projected here were hypothetical and therefore cannot be considered assessments of the absolute future climatic conditions of the basin. However, these SWAT predictions provide insight into the potential magnitude of hydrologic changes that could occur as a result of future climatic changes.

8.3 Recommendations

Based on the findings of the study, it is recommended that a reliable climate service system be established to increase stakeholder access to climate information. For instance, an increase in rainfall extremes and a typical decrease in dry season flow were predicted by future climate scenarios, and the stakeholders' decision-making on adaptation will be greatly influenced by this information. The climate services system can provide data on seasonal changes in temperature and rainfall, which further enables farmers to adjust their cultivation calendar. Climate research and climate modeling are getting better, and this could increase the accuracy and minimize the uncertainty of the models.

Water losses from seepage and evaporation must be minimized, along with attempts to improve water availability through water harvesting. It is also necessary to investigate other water management strategies to boost water productivity. Reduced water losses and increased water productivity from water harvesting structures will be achieved through extension efforts, training, communications, and networking activities.

As a result, this study suggests water harvesting strategies that could maintain water availability for agriculture and other ecosystem services to counteract future climate change impacts.

The productivity of the large hydropower systems planned for the region as well as the rising demand for agricultural and transportation expansion could potentially be impacted from a water management perspective by the overall reduction of river flows and their increased variability. Therefore, the implementation of water resources development work such as hydraulic structures, which are related to irrigation and hydropower, should take into account the anticipated change in climate and land use. Otherwise, the hydraulic structures may not be functional in the wake of climate change.

Afforestation/re-afforestation programs, including the implementation of suitable soil and water conservation measures based on the biophysical, land use, slope, and elevation of the watersheds, are all highly important to address the challenge of deforestation and surface runoff in the basin.

8.4 Future research direction

Climate change scenarios can be generated using more RCMs and CMIP6 simulations than in this research. Additionally, it is vital to assess RCM outputs that are forced by reanalysis datasets, for example, ERA-Interim reanalysis. That would make it easier to determine whether biases are due to RCMs or driving model schemes.

Studies to look into the impact of water harvesting structures on goals of sustainable development, such as agricultural productivity, livelihood security, poverty reduction, and access to clean water, can be planned. This can aid in effectively integrating development policies and plans with climate adaptation methods.

A pixel-to-point method is used to compare the two datasets (the observed and the RCMs) at different spatial scales, which may lead to uncertainties in the skill of the RCMs. Thus, this study recommends that future studies should put a lot of effort into matching the spatial scale of RCMs and observations, either by installing a dense rain gauge within the pixel or by downscaling the spatial resolution of RCMs.

HIRPS combined with either CFSR or observed temperatures, and the observed alone, outperformed the CFSR rainfall and temperature products in driving SWAT for hydrological simulations. Though the direct use of rainfall and temperatures enables a more natural way to reduce the errors in the hydrological simulations induced particularly by rainfall, the investigation of an integrated rainfall dataset from different sources or comparison with several products such as IMERGE and GPCC may be analyzed as a part of future work to verify any significant improvement in the hydrological simulations obtained from hydrological models. In addition, the uncertainties associated with satellite data products will translate to an unreliable estimate of the hydrological response due to the underestimation or overestimation of simulated hydrology. This can be addressed to an extent by applying several bias corrections to the satellite rainfall products with the observed data to obtain more realistic hydrological simulations. Therefore, future studies on the hydrologic evaluation of a multiple bias correction approach considering several satellite rainfall products for the Baro–Akobo River basin are required.

In addition to SWAT and IHA, another tool, such as the Regional-Hydro-Ecologic Simulation System (RHESSys), should be used to study basin hydrology and nutrient and erosion dynamics under changing climate and land use.

This study attempts to evaluate individual and combined climate and land use changes using a hydrological model. However, future studies involving the hydrologic impact levels of different soil and water conservation practices, different climatic zones, and different elevation zones should be conducted.

This study demonstrates the efficacy and effectiveness of watershed management practices (BMPs) for sustainable water resource development in the Baro basin. However, the streamflow and the sediment yield at the outlet of a specific catchment or watershed should be initiated using measured data. In addition, the effectiveness of different watershed management practices such as stone-bund, and buffer strips should be investigated through field experiments to determine which one is best.

Reference

Abbas, Z., Yang, G., Zhong, Y., & Zhao, Y. (2021). Spatiotemporal change analysis and future scenario of lulc using the CA-ANN approach: A case study of the greater bay area, China. *Land*, *10*(6). https://doi.org/10.3390/land10060584

Abbaspour, K. C., Rouholahnejad, E., Vaghefi, S., Srinivasan, R., Yang, H., & Kløve, B. (2015). A continental-scale hydrology and water quality model for Europe : Calibration and uncertainty of a high-resolution large-scale SWAT model. *JOURNAL OF HYDROLOGY*, *524*, 733–752. https://doi.org/10.1016/j.jhydrol.2015.03.027

Abbaspour, K. C., Yang, J., Maximov, I., Siber, R., Bogner, K., Mieleitner, J., Zobrist, J., & Srinivasan, R. (2007). Modelling hydrology and water quality in the pre-alpine/alpine Thur watershed using SWAT. *Journal of Hydrology*, *333*(2–4), 413–430. https://doi.org/10.1016/j.jhydrol.2006.09.014

Abbott, M (1196). Distributed Hydrological Modelling; Kluwer Academic: Dordrecht, The Netherlands; Boston, MA, USA, ISBN 0792340426.

Abdo, K. S., Fiseha, B. M., Rientjes, T. H. M., Gieske, A. S. M., & Haile, A. T. (2009). *Assessment of climate change impacts on the hydrology of Gilgel Abay catchment in Lake Tana basin , Ethiopia*. *Hydrological Processes*, 3661–3669. https://doi.org/10.1002/hyp

Aboelnour, M., & Gitau, M. W. (2019). *Hydrologic Response in an Urban Watershed as A ff ected by Climate and Land-Use Change*. Water. 1–23. DOI:10.3390/w11081603

Alemayehu, T., Kebede, S., Liu, L., Nedaw, D. (2016) Groundwater Recharge under Changing Landuses and Climate Variability : The Case of Baro–Akobo River Basin, Ethiopia. Journal of Environment and Earth Science. ISSN 2224-3216 (Paper) 2225-0948 Vol.5, No.8, 2015.

Alley, RB and Coauthors. (2007) Summary for policymakers. Climate Change 2007: The Physical Science Basis, S. Solomon et al., Eds., Cambridge University Press, 1–18.

Almeida, C. M., Gleriani, J. M., Castejon, E. F., & Soares-Filho, B. S. (2008). Using neural networks and cellular automata for modelling intra-urban land-use dynamics. International Journal of Geographical Information Science, 22(9), 943–963 https://doi.org/10.1080/13658810701731168.

Anh, H., Nguyen, T., Sophea, T., Gheewala, S. H., & Rattanakom, R. (2021). Integrating remote sensing and machine learning into environmental monitoring and assessment of land use change Intergovernmental Panel on Climate Change. Sustainable Production and Consumption, 27, 1239–1254. https://doi.org/10.1016/j.spc.2021.02.025

Arnell, N. W. (2004). Climate change and global water resources : SRES emissions and socio-economic scenarios. 14, 31–52. https://doi.org/10.1016/j.gloenvcha.2003.10.006.

Arnold, J. G., Srinivasan, R., Muttiah, R. S., & Williams, J. R. (1998). Large area hydrologic modeling and assessment Part I: Model development. Journal of American Water Resources Assoisation, 34(1), 73– 89. https://doi.org/10.1111/j.1752-1688.1998.tb05961.x

Arnold, J. G., Kiniry, J. R., Srinivasan, R., Williams, J. R., Haney, E. B., & Neitsch, S. L. (2012). *Soil & Water Assessment Tool. Version 2012*. 654. http://swat.tamu.edu/media/69296/SWAT-IO-Documentation-2012.pdf

Arsenault, R., & Brissette, F. (2016). Multi-model averaging for continuous streamflow prediction in ungauged basins. *Hydrological Sciences Journal*, *61*(13), 2443–2454. https://doi.org/10.1080/02626667.2015.1117088

Asner, G. P., Loarie, S. R., & Heyder, U. (2010). Combined effects of climate and land-use

change on the future of humid tropical forests. Conservation Letters. 3, 395–403. https://doi.org/10.1111/j.1755- 263X.2010.00133.x

Aspinall, R. (2004). Modelling land use change with generalized linear models — a multi-model analysis of change between 1860 and 2000 in Gallatin Valley, Montana. Journal of Environmental Management.72, 91–103. https://doi.org/10.1016/j.jenvman.2004.02.009

Awulachew, S. B., Yilma, A. D., Loulseged, M., Loiskandl, W., Ayana, M., & Alamirew, T. (2007). Water Resources and Irrigation develop- ment in Ethiopia. International Water Management Institute

Ayele, T., Ahmed, N., Ribbe, L., & Heinrich, J. (2016). Science of the Total Environment Hydrological responses to land use/cover changes in the source region of the Upper Blue Nile Basin, Ethiopia. *Science of the Total Environment*. https://doi.org/10.1016/j.scitotenv.2016.09.124

Ayele, T., Ahmed, N., Ribbe, L., & Heinrich, J. (2018). Science of the Total Environment Catchment response to climate and land use changes in the Upper Blue. *Science of the Total Environment*, *644*, 193–206. https://doi.org/10.1016/j.scitotenv.2018.06.198

Bae, D. H., Jung, I. W., & Lettenmaier, D. P. (2011). Hydrologic uncertainties in climate change from IPCC AR4 GCM simulations of the Chungju Basin, Korea. *Journal of Hydrology*, *401*(1–2), 90–105. https://doi.org/10.1016/j.jhydrol.2011.02.012

Baez-Villanueva, O. M., Zambrano-Bigiarini, M., Ribbe, L., Nauditt, A., Giraldo-Osorio, J. D., & Thinh, N. X. (2018). Temporal and spatial evaluation of satellite rainfall estimates over different regions in Latin America. *Atmospheric Research*, *213*(2017), 34–50. https://doi.org/10.1016/j.atmosres.2018.05.011

Bal, M., Kumar, A., & Naik, B. (2021). Remote Sensing Applications : Society and Environment Hydrological modeling with respect to impact of land-use and land-cover change on the runoff dynamics in Budhabalanga river basing using ArcGIS and SWAT model. *Remote Sensing Applications: Society and Environment*, *23*(September 2020), 100527. https://doi.org/10.1016/j.rsase.2021.100527

Baldauf, M., Seifert, A., Förstner, J., Majewski, D., Raschendorfer, M., & Reinhardt, T. (2011). Operational convective-scale numerical weather prediction with the COSMO model: Description and sensitivities. *Monthly Weather Review*, *139*(12), 3887–3905. https://doi.org/10.1175/MWR-D-10-05013.1

Balsamo, G., Albergel, C., Beljaars, A., Boussetta, S., Brun, E., Cloke, H., Dee, D., Dutra, E., Munõz-Sabater, J., Pappenberger, F., De Rosnay, P., Stockdale, T., & Vitart, F. (2015). ERA-Interim/Land: A global land surface reanalysis data set. *Hydrology and Earth System Sciences*, *19*(1), 389–407. https://doi.org/10.5194/hess-19-389-2015

Ban, Y., Gong, P., & Giri, C. (2015). Global land cover mapping using Earth observation satellite data: Recent progress and challenges. ISPRS Journal of Photogrammetry and Remote Sensing, 103, 1–6. https://doi.org/10.1016/j.isprsjprs.2015.01.001

Basheer, A. K., Lu, H., Omer, A., Ali, A. B., & Abdelgader, A. M. S. (2016). Impacts of climate change under CMIP5 RCP scenarios on the streamflow in the Dinder River and ecosystem habitats in Dinder National Park, Sudan. *Hydrology and Earth System Sciences*, *20*(4), 1331–1353. https://doi.org/10.5194/hess-20-1331-2016

Bates, B. C., Kundzewicz, Z. W., Wu, S., & Palutikof, J. P. (2008). Climate Change and water – IPCC Technical Paper VI. Climate change and water. IPCC Secretariat, Geneva

Bayabil, H. K., & Dile, Y. T. (2020). Improving hydrologic simulations of a small watershed through soil data integration. *Water (Switzerland)*, *12*(10).

https://doi.org/10.3390/w12102763
Bayissa, Y., Tadesse, T., Demisse, G., & Shiferaw, A. (2017). Evaluation of satellite-based rainfall estimates and application to monitor meteorological drought for the Upper Blue Nile Basin, Ethiopia. *Remote Sensing*, *9*(7), 1–17. https://doi.org/10.3390/rs9070669
Tegene. B (2002). Land-Cover/Land-Use Changes in the Derekolli Catchment of the South Welo Zone of Amhara Region, Ethiopia. Eastern Africa Social Science Research Review, 18(1), 1–20. https://doi.org/10.1353/eas.2002.0005
Bekele, D., Alamirew, T., Kebede, A., Zeleke, G., & Melesse, A. M. (2021). Modeling the impacts of land use and land cover dynamics on hydrological processes of the Keleta watershed, Ethiopia. *Sustainable Environment*, *7*(1), 1947632. https://doi.org/10.1080/27658511.2021.1947632
Berihun, M. L., Tsunekawa, A., Haregeweyn, N., Dile, Y. T., Tsubo, M., Fenta, A. A., Meshesha, D. T., Ebabu, K., Sultan, D., & Srinivasan, R. (2020). Evaluating runoff and sediment responses to soil and water conservation practices by employing alternative modeling approaches. *Science of the Total Environment*, *747*, 141118. https://doi.org/10.1016/j.scitotenv.2020.141118
Betel, H., and P. Flocchini. (2011). "On the relationship between fuzzy and Boolean cellular automata". Theoretical Computer Science 412 (8–10): 703–713.
Betrie, G. D., Mohamed, Y. A., Griensven, A. Van, & Srinivasan, R. (2010). *Sediment management modelling in Blue Nile Basin using SWAT model*. 5497–5524. https://doi.org/10.5194/hessd-7-5497-2010
Bewket, W., & Sterk, G. (2005). Dynamics in land cover and its effect on stream flow in the Chemoga watershed, Blue Nile basin, Ethiopia. *Hydrological Processes*, *19*(2), 445–458. https://doi.org/10.1002/hyp.5542
Beyene, T., Lettenmaier, D. P., & Kabat, P. (2010). *Hydrologic impacts of climate change on the Nile River Basin : implications of the 2007 IPCC scenarios*. Climatic Change 433–461. https://doi.org/10.1007/s10584-009-9693-0
Bhattacharya, T., Khare, D., & Arora, M. (2020). Evaluation of reanalysis and global meteorological products in Beas river basin of North-Western Himalaya. *Environmental Systems Research*, *9*(1), 1–29. https://doi.org/10.1186/s40068-020-00186-1
Bhowmik, A. K., & Costa, A. C. (2015). Representativeness impacts on accuracy and precision of climate spatial interpolation in data-scarce regions. *Meteorological Applications*, *22*(3), 368–377. https://doi.org/10.1002/met.1463
Bishop, C. M. (1995). Neural networks for patterns recognition. Oxford: Oxford University, 482pp.
Bitew, M. M., Gebremichael, M., Ghebremichael, L. T., & Bayissa, Y. A. (2012). Evaluation of high-resolution satellite rainfall products through streamflow simulation in a hydrological modeling of a small mountainous watershed in Ethiopia. *Journal of Hydrometeorology*, *13*(1), 338–350. https://doi.org/10.1175/2011JHM1292.1
Block, P. J., Souza Filho, F. A., Sun, L., & Kwon, H. H. (2009). A streamflow forecasting framework using multiple climate and hydrological models. *Journal of the American Water Resources Association*, *45*(4), 828–843. https://doi.org/10.1111/j.1752-1688.2009.00327.x
Bolch, T., Kulkarni, A., Kääb, A., Huggel, C., Paul, F., Cogley, J. G., Frey, H., Kargel, J. S., Fujita, K., Scheel, M., Bajracharya, S., & Stoffel, M. (2012). The state and fate of himalayan glaciers. *Science*, *336*(6079), 310–314. https://doi.org/10.1126/science.1215828
Boyer, C., Chaumont, D., Chartier, I., & Roy, A. G. (2010). Impact of climate change on the

hydrology of St. Lawrence tributaries. *Journal of Hydrology*, *384*(1–2), 65–83. https://doi.org/10.1016/j.jhydrol.2010.01.011

Bradshaw, C.J.A., Sodhi, N.S., Peh, K.S.H., Brook, B.W. (2007). Global evidence that deforestation amplifies flood risk and severity in the developing world. Glob. Change Biol. 13, 1–17

Brigode, P., Oudin, L., & Perrin, C. (2013). Hydrological model parameter instability: A source of additional uncertainty in estimating the hydrological impacts of climate change? *Journal of Hydrology*, *476*, 410–425. https://doi.org/10.1016/j.jhydrol.2012.11.012

Brown, A.E., Zhang, L., McMahon, T.A., Western, A.W., and Vertesse, R.A. (2005). A review of paired catchment studies for determining changes in water yield resulting from alterations in vegetation. Journal of Hydrology 310: 28-61.

Bui, M. T., Lu, J., & Nie, L. (2021). Evaluation of the Climate Forecast System Reanalysis data for hydrological model in the Arctic watershed Målselv. *Journal of Water and Climate Change*, 1–24. https://doi.org/10.2166/wcc.2021.346

Camici, S., Ciabatta, L., Massari, C., & Brocca, L. (2018). How reliable are satellite precipitation estimates for driving hydrological models: A verification study over the Mediterranean area. *Journal of Hydrology*, *563*, 950–961. https://doi.org/10.1016/j.jhydrol.2018.06.067

Candela, L., Tamoh, K., Olivares, G., & Gomez, M. (2012). Modelling impacts of climate change on water resources in ungauged and data-scarce watersheds. Application to the Siurana catchment (NE Spain). *Science of the Total Environment*, *440*, 253–260. https://doi.org/10.1016/j.scitotenv.2012.06.062

Cao, M., Zhu, Y., Quan, J., Zhou, S., Lü, G., Chen, M., & Huang, M. (2019). Spatial Sequential Modeling and Predication of Global Land Use and Land Cover Changes by Integrating a Global Change Assessment Model and Cellular Automata. *Earth's Future*, *7*(9), 1102–1116. https://doi.org/10.1029/2019EF001228

Chaturvedi, R. K., Joshi, J., Jayaraman, M., Bala, G., & Ravindranath, N. H. (2012). Multi-model climate change projections for India under representative concentration pathways. *Current Science*, *103*(7), 791–802.

Chen, H., Fleskens, L., Baartman, J., Wang, F., Moolenaar, S., & Ritsema, C. (2020). Impacts of land use change and climatic effects on streamflow in the Chinese Loess Plateau: A meta-analysis. *Science of the Total Environment*, *703*, 134989. https://doi.org/10.1016/j.scitotenv.2019.134989

Chen, J., Brissette, F. P., Poulin, A., & Leconte, R. (2011). Overall uncertainty study of the hydrological impacts of climate change for a Canadian watershed. *Water Resources Research*, *47*(12), 1–16. https://doi.org/10.1029/2011WR010602

Cheung, W. H., Senay, B., & Singh, A. (2008). *Trends and spatial distribution of annual and seasonal rainfall in Ethiopia*. *1734*(March), 1723–1734. https://doi.org/10.1002/joc

Cho, J., Bosch, D., Lowrance, R., Strickland, T., & Vellidis, G. (2009). Effect of Spatial Distribution of Rainfall on Temporal and Spatial Uncertainty of SWAT Output. *American Society of Agricultural and Biological Engineers*, *52*(1998), 1545–1555.

Christensen, J. H., Boberg, F., Christensen, O. B., & Lucas-Picher, P. (2008). On the need for bias correction of regional climate change projections of temperature and precipitation. *Geophysical Research Letters*, *35*(20). https://doi.org/10.1029/2008GL035694

Christensen, J. H., Carter, T. R., Rummukainen, M., & Amanatidis, G. (2007). Evaluating the performance and utility of regional climate models: The PRUDENCE project. *Climatic Change*, *81*(SUPPL. 1), 1–6. https://doi.org/10.1007/s10584-006-9211-6

Christy, J. R., Norris, W. B., & McNider, R. T. (2009). Surface temperature variations in east

Africa and possible causes. *Journal of Climate*, *22*(12), 3342–3356. https://doi.org/10.1175/2008JCLI2726.1
Conway. (2005). From headwater tributaries to international river : Observing and adapting to climate variability and change in the Nile basin. Global Environmental Change.15, 99–114. https://doi.org/10.1016/j.gloenvcha.2005.01.003
Conway, D., & Hulme, M. (1993). Recent fluctuations in precipitation and runoff over the Nile sub-basins and their impact on main Nile discharge. *Climatic Change*, *25*(2), 127–151. https://doi.org/10.1007/BF01661202
Conway, D., & Schipper, E. L. F. (2011). Adaptation to climate change in Africa: Challenges and opportunities identified from Ethiopia. *Global Environmental Change*, *21*(1), 227–237. https://doi.org/10.1016/j.gloenvcha.2010.07.013
Couclelis, H. (1985). "Cellular worlds: a framework for modeling micro-macro dynamics". Environment and Planning A 17 (5): 585–596.
Cramér, H., 1999. Mathematical Methods of Statistics, ninth. ed. Princeton University Press
Crouzeilles, R., Curran, M., Ferreira, M.S., Lindenmayer, D.B., Grelle, C.E., Benayas, J. M., 2016. A global meta-analysis on the ecological drivers of forest restoration success. Nature Commun. 7, 11666. https://doi.org/10.1038/ncomms11666.
Cunderlik, J. (2003). Hydrological model selection for CFCAS project, Assessment of water resource risk and vulnerability to change in climate condition, University of Western Ontario.
Davies, R.A.G., Midgley, S.J.E., Chesterman, S. (2010) Climate risk and vul- nerability mapping for Southern Africa: status quo (2008) and future (2050). In: ONEWORLD (ed) Regional Climate Change Programme: Southern Africa. Cape Town, South Africa
Daye, D. D., & Healey, J. R. (2015). Impacts of land-use change on sacred forests at the landscape scale. Global Ecology and Conservation, 3, 349–358. https://doi.org/10.1016/j.gecco.2014.12.009
Demirel, M. C., Venancio, A., & Kahya, E. (2009). Flow forecast by SWAT model and ANN in Pracana basin, Portugal. *Advances in Engineering Software*, *40*(7), 467–473. https://doi.org/10.1016/j.advengsoft.2008.08.002
Desalegn, T., Cruz, F., Kindu, M., Turrión, M. B., & Gonzalo, J. (2014). Land-use/land-cover (LULC) change and socioeconomic conditions of local community in the central highlands of Ethiopia. International Journal of Sustainable Development and World Ecology, 21(5), 406–413. https://doi.org/10.1080/13504509.2014.961181
Dhanesh, Y., Bindhu, V. M., Senent-Aparicio, J., Brighenti, T. M., Ayana, E., Smitha, P. S., Fei, C., & Srinivasan, R. (2020). A comparative evaluation of the performance of CHIRPS and CFSR data for different climate zones using the SWAT model. *Remote Sensing*, *12*(18). https://doi.org/10.3390/RS12183088
Dibaba, W. T., Demissie, T. A., & Miegel, K. (2020). Watershed hydrological response to combined land use/land cover and climate change in highland ethiopia: Finchaa catchment. *Water (Switzerland)*, *12*(6). https://doi.org/10.3390/w12061801
Dile, Y. T., Ayana, E. K., Worqlul, A. W., Xie, H., Srinivasan, R., Lefore, N., You, L., & Clarke, N. (2020). Evaluating satellite-based evapotranspiration estimates for hydrological applications in data-scarce regions: A case in Ethiopia. *Science of the Total Environment*, *743*, 140702. https://doi.org/10.1016/j.scitotenv.2020.140702
Dile, Y. T., Berndtsson, R., & Setegn, S. G. (2013). *Hydrological Response to Climate Change for Gilgel Abay River , in the Lake Tana Basin - Upper Blue Nile Basin of Ethiopia*. PLoS

ONE. *8*(10), 12–17. https://doi.org/10.1371/journal.pone.0079296
Dile, Y. T., & Srinivasan, R. (2014). *Evaluation of CFSR Climate Data for Hydrologic Prediction in Data- Scarce Watersheds. Journal of the American Water Resources Association (JAWRA) 50(5): 1226-1241. DOI: 10.1111/jawr.12182*
Dinku, T., Funk, C., Peterson, P., Maidment, R., Tadesse, T., Gadain, H., & Ceccato, P. (2018). Validation of the CHIRPS satellite rainfall estimates over eastern Africa. *Quarterly Journal of the Royal Meteorological Society*, *144*(November 2017), 292–312. https://doi.org/10.1002/qj.3244
Diro, G.T., Grimes, D.I.., Black, E. (2011). Teleconnections between Ethiopian summer rainfall and sea surface temperature: part I — observation and modelling. Clim Dyn. 37, 103–119. https://doi.org/10.1007/s00382-010-0837-8
Duan, Z., Liu, J., Tuo, Y., Chiogna, G., & Disse, M. (2016). Evaluation of eight high spatial resolution gridded precipitation products in Adige Basin (Italy) at multiple temporal and spatial scales. *Science of the Total Environment*, *573*, 1536–1553. https://doi.org/10.1016/j.scitotenv.2016.08.213
El-Khoury, A., Seidou, O., Lapen, D. R. L., Que, Z., Mohammadian, M., Sunohara, M., & Bahram, D. (2015). Combined impacts of future climate and land use changes on discharge, nitrogen and phosphorus loads for a Canadian river basin. *Journal of Environmental Management*, *151*, 76–86. https://doi.org/10.1016/j.jenvman.2014.12.012
Elshamy, M.E., Seierstad, I.A., Sorteberg, A. (2009). Impacts of climate change on Blue Nile flows using bias-corrected GCM scenarios. Hydrol Earth Syst Sci 13:551–565. https://doi.org/10.5194/hess- 13-551-2009
Endris, H. S., Omondi, P., Jain, S., Lennard, C., Hewitson, B., Chang'a, L., Awange, J. L., Dosio, A., Ketiem, P., Nikulin, G., Panitz, H. J., Büchner, M., Stordal, F., & Tazalika, L. (2013). Assessment of the performance of CORDEX regional climate models in simulating East African rainfall. *Journal of Climate*, *26*(21), 8453–8475. https://doi.org/10.1175/JCLI-D-12-00708.1
Engida, T., Nigussie, T. A., Aneseyee, A. B., & Barnabas, J. (2021). Land Use/Land Cover Change Impact on Hydrological Process in the Upper Baro Basin, Ethiopia. *Applied and Environmental Soil Science*, *2021*(July). https://doi.org/10.1155/2021/6617541
Fallah Shamsi, S. (2010). Integrating Linear Programming and Analytical Hierarchical Processing in Raster-GIS to Optimize Land Use Pattern at Watershed Level. Journal of Applied Sciences and Environmental Management, 14(2). https://doi.org/10.4314/jasem.v14i2.57868
FAO, 1984. Geomorphology and Soils. Assistance to Land Use Planning. Addis Ababa: 328
FAO, 2010: Global Forest Resources Assessment: Main report, Food and Agriculture Organization of the United Nations, Rome, Italy, 378, 2010.
Fan, M., & Shibata, H. (2015). Simulation of watershed hydrology and stream water quality under land use and climate change scenarios in Teshio River watershed , northern Japan. *Ecological Indicators*, *50*, 79–89. https://doi.org/10.1016/j.ecolind.2014.11.003
Fang, G. H., Yang, J., Chen, Y. N., & Zammit, C. (2015). Comparing bias correction methods in downscaling meteorological variables for a hydrologic impact study in an arid area in China. *Hydrology and Earth System Sciences*, *19*(6), 2547–2559. https://doi.org/10.5194/hess-19-2547-2015
Farinosi, F., Arias, M. E., Lee, E., Longo, M., Pereira, F. F., Livino, A., Moorcroft, P. R., & Briscoe, J. (2019). Future Climate and Land Use Change Impacts on River Flows in the

Tapajós Basin in the Brazilian Amazon. Earth's Future, 7(8), 993–1017. https://doi.org/10.1029/2019EF001198

Fenta, A. A., Yasuda, H., Shimizu, K., Ibaraki, Y., Haregeweyn, N., Kawai, T., Belay, A. S., Sultan, D., & Ebabu, K. (2018). Evaluation of satellite rainfall estimates over the Lake Tana basin at the source region of the Blue Nile River. *Atmospheric Research*, *212*(2017), 43–53. https://doi.org/10.1016/j.atmosres.2018.05.009

Mekonnen, F.D., Duan, Z., Rientjes, T., & Disse, M. (2018). Analysis of combined and isolated effects of land-use and land-cover changes and climate change on the upper Blue Nile River basin's streamflow. *Hydrology and Earth System Sciences*, *22*(12), 6187–6207. https://doi.org/10.5194/hess-22-6187-2018

Fentaw, F., Hailu, D., Nigussie, A., & Melesse, A. M. (2018). Climate Change Impact on the Hydrology of Tekeze Basin, Ethiopia: Projection of Rainfall-Runoff for Future Water Resources Planning. *Water Conservation Science and Engineering*, *3*(4), 267–278. https://doi.org/10.1007/s41101-018-0057-3

Fiseha, B. M., Setegn, S. G., Melesse, A. M., Volpi, E., & Fiori, A. (2014). Impact of Climate Change on the Hydrology of Upper Tiber River Basin Using Bias Corrected Regional Climate Model. *Water Resources Management*, *28*(5), 1327–1343. https://doi.org/10.1007/s11269-014-0546-x

Fowler, H. J., Ekström, M., Blenkinsop, S., & Smith, A. P. (2007). Estimating change in extreme European precipitation using a multimodel ensemble. *Journal of Geophysical Research Atmospheres*, *112*(18). https://doi.org/10.1029/2007JD008619

Fowler, H. J., & Kilsby, C. G. (2007). Using regional climate model data to simulate historical and future river flows in northwest England. *Climatic Change*, *80*(3–4), 337–367. https://doi.org/10.1007/s10584-006-9117-3

Fuka, D. R., Walter, M. T., Macalister, C., Degaetano, A. T., Steenhuis, T. S., & Easton, Z. M. (2013). *Using the Climate Forecast System Reanalysis as weather input data for watershed models*. https://doi.org/10.1002/hyp.10073

Funk, C., Peterson, P., Landsfeld, M., Pedreros, D., Verdin, J., Shukla, S., Husak, G., Rowland, J., Harrison, L., Hoell, A., & Michaelsen, J. (2015). The climate hazards infrared precipitation with stations - A new environmental record for monitoring extremes. *Scientific Data*, *2*, 1–21. https://doi.org/10.1038/sdata.2015.66

Gao, Y. C., & Liu, M. F. (2013) Evaluation of high-resolution satellite precipitation products using rain gauge observations over the Tibetan Plateau. Hydrol. Earth Syst. Sci., 17, 837–849, https://doi.org/10.5194/hess-17-837-2013

Gassman, P. W., M. R. Reyes, C. H., Green, and J. G. Arnold (2007). The Soil and Water Assessment Tool: Historical development, applications, and future research directions, Trans. ASABE, 50(4), 1211–1250.

Gautam, N. P., & Arora, M. (2015). Study of Climate Change using GCM Downscaling: Special Reference to Indian Subcontinent. *Hydro Nepal: Journal of Water, Energy and Environment*, *16*(16), 36–39. https://doi.org/10.3126/hn.v16i0.12222

Gebrehiwot, S. G., Seibert, J., Annemieke, I. G., & Bishop, K. (2013). Hydrological change detection using modeling : Half a century of runoff from four rivers in the Blue Nile Basin. *WATER RESOURCES RESEARCH*, *49*, 3842–3851. https://doi.org/10.1002/wrcr.20319

Gebremedhin, M. A., Abraha, A. Z., & Fenta, A. A. (2017). *Changes in future climate indices using Statistical Downscaling Model in the upper Baro basin of Ethiopia*. Theor Appl Climato. https://doi.org/10.1007/s00704-017-2151-4

Getachew, B., Manjunatha, B. R., & Bhat, H. G. (2021). Modeling projected impacts of climate and land use/land cover changes on hydrological responses in the Lake Tana Basin, upper Blue Nile River Basin, Ethiopia. *Journal of Hydrology*, *595*(January), 125974. https://doi.org/10.1016/j.jhydrol.2021.125974

Getachew, F., Bayabil, H. K., Hoogenboom, G., Teshome, F. T., & Zewdu, E. (2021). Irrigation and shifting planting date as climate change adaptation strategies for sorghum. *Agricultural Water Management*, *255*(June), 106988. https://doi.org/10.1016/j.agwat.2021.106988

Getirana, A. C. V., Espinoza, J. C. V., Ronchail, J., & Filho, O. C. R. (2011). Assessment of different precipitation datasets and their impacts on the water balance of the Negro River basin. *Journal of Hydrology*, *404*(3–4), 304–322. https://doi.org/10.1016/j.jhydrol.2011.04.037

Giorgi, F. (2006). Regional climate modeling: Status and perspectives. *Journal De Physique. IV : JP*, *139*, 101–118. https://doi.org/10.1051/jp4:2006139008

Giorgi, F., Jones, C., & Asrar, G. (2009). Addressing climate information needs at the regional level: the CORDEX framework. *... Organization (WMO) Bulletin*, *November 2008*. http://www.euro-cordex.net/uploads/media/Download_01.pdf

Gomes, L. C., Bianchi, F. J. J. A., Cardoso, I. M., Schulte, R. P. O., Fernandes, R. B. A., & Fernandes-Filho, E. I. (2021). Disentangling the historic and future impacts of land use changes and climate variability on the hydrology of a mountain region in Brazil. *Journal of Hydrology*, *594*, 125650. https://doi.org/10.1016/j.jhydrol.2020.125650

Göncü, S., & Albek, E. (2010). Modeling climate change effects on streams and reservoirs with HSPF. *Water Resources Management*, *24*(4), 707–726. https://doi.org/10.1007/s11269-009-9466-6

Gudmundsson, L., Bremnes, J. B., Haugen, J. E., & Engen-Skaugen, T. (2012). Technical Note: Downscaling RCM precipitation to the station scale using statistical transformations – A comparison of methods. *Hydrology and Earth System Sciences*, *16*(9), 3383–3390. https://doi.org/10.5194/hess-16-3383-2012

Guidigan, M. L. G., Sanou, C. L., Ragatoa, D. S., Fafa, C. O., & Mishra, V. N. (2019). Assessing Land Use/Land Cover Dynamic and Its Impact in Benin Republic Using Land Change Model and CCI-LC Products. *Earth Systems and Environment*, *3*(1), 127–137. https://doi.org/10.1007/s41748-018-0083-5

Guo, H., Hu, Q., & Jiang, T. (2008). Annual and seasonal streamflow responses to climate and land-cover changes in the Poyang Lake basin, China. *Journal of Hydrology*, *355*(1–4), 106–122. https://doi.org/10.1016/j.jhydrol.2008.03.020

Guo, Y., Fang, G., Xu, Y., Tian, X., & Xie, J. (2019). Identifying how future climate and land use / cover changes impact streamflow in Xinanjiang Basin , East China. Science of the Total Environment. https://doi.org/10.1016/j.scitotenv.2019.136275

Gupta, H. V., Kling, H., Yilmaz, K. K., & Martinez, G. F. (2009). Decomposition of the mean squared error and NSE performance criteria: Implications for improving hydrological modelling. *Journal of Hydrology*, *377*(1–2), 80–91. https://doi.org/10.1016/j.jhydrol.2009.08.003

Guzha, A. C., Rufino, M. C., Okoth, S., Jacobs, S., & Nóbrega, R. L. B. (2018). Impacts of land use and land cover change on surface runoff, discharge and low flows: Evidence from East Africa. *Journal of Hydrology: Regional Studies*, *15*(November 2017), 49–67. https://doi.org/10.1016/j.ejrh.2017.11.005

Haile, A.T., & Rientjes, T. (2015). Evaluation of regional climate model simulations of rainfall over the Upper Blue Nile basin. Atmospheric Research 161–162, 57–64. https://doi.org/10.1016/j.atmosres.2015.03.013

Haile, E. G., & Assefa, M. M. (2012) The Impact of Land Use Change on the Hydrology of the Angereb Watershed, Ethiopia. International Journal of Water Science 14 (2012), 1-7. DOI: 10.5772/56266

Hamed, K.H., Rao, A.R. (1998) A modified Mann-Kendall trend test for autocorrelated data. J Hydrol 204:182–196

Han, H., Yang, C., & Song, J. (2015). Scenario Simulation and the Prediction of Land Use and Land Cover Change in Beijing, China. Sustainability. 4260–4279. https://doi.org/10.3390/su7044260

Hawkins, E., & Sutton, R. (2011). The potential to narrow uncertainty in projections of regional precipitation change. *Climate Dynamics*, *37*(1), 407–418. https://doi.org/10.1007/s00382-010-0810-6

Hayhoe, K., Edmonds, J., Kopp, R. E., LeGrande, A. N., Sanderson, B. M., Wehner, M. F., & Wuebbles, .J. (2017). Climate models, scenarios, and projections. *Climate Science Special Report: Fourth National Climate Assessment*, *I*, 133–160. https://doi.org/10.7930/J0WH2N54.U.S.

He, M., & Hogue, T. S. (2011). Integrating hydrologic modeling and land use projections for evaluation of hydrologic response and regional water supply impacts in semi-arid environments. Environ Earth Sci. https://doi.org/10.1007/s12665-011-1144-3

Hengl, T., Heuvelink, G. B. M., Kempen, B., Leenaars, J. G. B., Walsh, M. G., Shepherd, K. D., Sila, A., MacMillan, R. A., De Jesus, J. M., Tamene, L., & Tondoh, J. E. (2015). Mapping soil properties of Africa at 250 m resolution: Random forests significantly improve current predictions. *PLoS ONE*, *10*(6), 1–26. https://doi.org/10.1371/journal.pone.0125814

Hoegh-Guldberg, O., & Bruno, J. F. (2010). The impact of climate change on the world's marine ecosystems. In *Science* (Vol. 328, Issue 5985, pp. 1523–1528). https://doi.org/10.1126/science.1189930

Houghton, J.T. (2001). Climate change 2001. The Scientific Basis: Contribution of Working Group I to the Third Assessment Report of the Intergovernmental Panel on Climate Change, Houghton JT (ed.). Cambridge University Press: Cambridge, UK and New York, USA

Hsu, K. L., Gao, X., Sorooshian, S., & Gupta, H. V. (1997). Precipitation estimation from remotely sensed information using artificial neural networks. *Journal of Applied Meteorology*, *36*(9), 1176–1190. https://doi.org/10.1175/1520-0450(1997)036<1176:PEFRSI>2.0.CO;2

Hu, J., Lü, Y., Fu, B., Comber, A. J., & Harris, P. (2017). Quantifying the effect of ecological restoration on runoff and sediment yields: A meta-analysis for the Loess Plateau of China. *Progress in Physical Geography*, *41*(6), 753–774. https://doi.org/10.1177/0309133317738710

Huffman, G. J., Adler, R. F., Bolvin, D. T., Gu, G., Nelkin, E. J., Bowman, K. P., Hong, Y., Stocker, E. F., & Wolff, D. B. (2007). The TRMM Multisatellite Precipitation Analysis (TMPA): Quasi-global, multiyear, combined-sensor precipitation estimates at fine scales. *Journal of Hydrometeorology*, *8*(1), 38–55. https://doi.org/10.1175/JHM560.1

Huffman, G. J., Bolvin, D. T., Nelkin, E. J., & Tan, J. (2019). *Integrated Multi-satellitE Retrievals for GPM (IMERG) Technical Documentation*. *01*(01). https://gpm.nasa.gov/sites/default/files/document_files/IMERG_doc_190909.pdf

Hulme, M., Doherty, R., Ngara, T., New, M. G., & Low, P. S. (Ed.) (2005). Global warming and African climate change: a reassessment. In Climate Change and Africa (pp. 29- 40) https://doi.org/10.1017/CBO9780511535864

Hulme M., Doherty R., Ngara, T., New, M., Lister ,D. 2001. African climate change: 1900–2100. Climate Res., 17, 145–168. http://dx.doi.org/10.3354/cr017145

Hyandye, C. (2015). GIS and Logit Regression Model Applications in Land Use/Land Cover Change and Distribution in Usangu Catchment. American Journal of Remote Sensing, 3(1), 6. https://doi.org/10.11648/j.ajrs.20150301.12

Hyandye, C. B., Worqul, A., Martz, L. W., & Muzuka, A. N. N. (2018). The impact of future climate and land use/cover change on water resources in the Ndembera watershed and their mitigation and adaptation strategies. *Environmental Systems Research*, *7*(1). https://doi.org/10.1186/s40068-018-0110-4

IGBP, 2001. Global change and earth system: a planet under pressure. Global Environmental Change Programmes

IPCC, 2001. Climate Change 2001: The Scientific Basis. The Third Assessment Report of the Intergovernmental Panel on Climate Change, Cambridge University Press, New York.

IPCC, 2007: Climate Change 2007: The Physical Science Basis. Contribution of Working Group I to the Fourth Assessment Report of the Intergovernmental Panel on Climate Change. Cambridge, UK, New York, US, Cambridge University Press

IPCC, 2014. Climate Change 2014: Impacts, Adaptation, and Vulnerability. Part A: Global and Sectoral Aspects. Contribution of Working Group II to the Fifth Assessment Report of the Intergovernmental Panel on Climate Change [Field, C.B., V.R. Barros, D.J. Dokken, K.J.

IPCC, 2013. Climate Change 2013: The Physical Science Basis. Working Group I Contribution to the Fifth Assessment Report of the Intergovernmental Panel on Climate Change.

IPCC, 2019: Climate Change and Land: an IPCC special report on climate change, desertification, land degradation, sustainable land management, food security, and greenhouse gas fluxes in terrestrial ecosystems (P.R. Shukla, J. Skea, E. Calvo Buendia et al. 2019). In press

IPCC, 2021. Climate Change 2021: Intergovernmental Panel on Climate Change, Working Group I Technical Support Unit

Islam, K., Rahman, F., & Jashimuddin, M. (2018). Modeling land use change using Cellular Automata and Arti fi cial Neural Network : The case of Chunati Wildlife Sanctuary , Bangladesh. *Ecological Indicators*, *88*(December 2017), 439–453. https://doi.org/10.1016/j.ecolind.2018.01.047

Jacob, D., Elizalde, A., Haensler, A., Hagemann, S., Kumar, P., Podzun, R., Rechid, D., Remedio, A. R., Saeed, F., Sieck, K., Teichmann, C., & Wilhelm, C. (2012). Assessing the transferability of the regional climate model REMO to different coordinated regional climate downscaling experiment (CORDEX) regions. *Atmosphere*, *3*(1), 181–199. https://doi.org/10.3390/atmos3010181

Jafarpour, K., Shamsoddini, A., Najaf, M., Binti, F., Ros, C., & Khedmatzadeh, A. (2022). Predicting spatial and decadal of land use and land cover change using integrated cellular automata Markov chain model based scenarios (2019 – 2049) Zarriné-R ū d River Basin in Iran ☆. Environmental Challenges, 6(July 2021), 100399. https://doi.org/10.1016/j.envc.2021.100399

Joyce, R. J., Janowiak, J. E., Arkin, P. A., & Xie, P. (2004). CMORPH: A method that produces global precipitation estimates from passive microwave and infrared data at high spatial and temporal resolution. *Journal of Hydrometeorology*, *5*(3), 487–503. https://doi.org/10.1175/1525-7541(2004)005<0487:CAMTPG>2.0.CO;2

Jung, I., Chang, H., & Moradkhani, H. (2011). *Quantifying uncertainty in urban flooding analysis considering hydro-climatic projection and urban development effects*. 617–633. https://doi.org/10.5194/hess-15-617-2011

Jury, M. R., & Funk, C. (2013). Climatic trends over Ethiopia: Regional signals and drivers. *International Journal of Climatology*, *33*(8), 1924–1935. https://doi.org/10.1002/joc.3560

Kamaraj, M., & Rangarajan, S. (2022). Predicting the future land use and land cover changes for Bhavani basin, Tamil Nadu, India, using QGIS MOLUSCE plugin. *Environmental Science and Pollution Research*. https://doi.org/10.1007/s11356-021-17904-6

Kang, Y., Khan, S., & Ma, X. (2009). Climate change impacts on crop yield, crop water productivity and food security - A review. *Progress in Natural Science*, *19*(12), 1665–1674. https://doi.org/10.1016/j.pnsc.2009.08.001

Kantakumar, L. N., Kumar, S., & Schneider, K. (2016). Spatiotemporal urban expansion in Pune metropolis, India using remote sensing. *Habitat International*, *51*, 11–22. https://doi.org/10.1016/j.habitatint.2015.10.007

Karlsson, I. B., Sonnenborg, T. O., Refsgaard, J. C., Børgesen, C. D., Olesen, J. E., Jeppesen, E., & Karsten, H. (2016). Combined effects of climate models, hydrological model structures and land use scenarios on hydrological impacts of climate change. *JOURNAL OF HYDROLOGY*. https://doi.org/10.1016/j.jhydrol.2016.01.069

Kay, A. L., Davies, H. N., Bell, V. A., & Jones, R. G. (2009). Comparison of uncertainty sources for climate change impacts: Flood frequency in England. *Climatic Change*, *92*(1–2), 41–63. https://doi.org/10.1007/s10584-008-9471-4

Khawaldah, H. A., Farhan, I., & Alzboun, N. M. (2020). *Simulation and prediction of land use and land cover change using GIS, remote sensing and CA-Markov model*. *6*(2), 215–232. https://doi.org/10.22034/gjesm.2020.02.07

Kidd, C. (2001). Satellite rainfall climatology: A review. *International Journal of Climatology*, *21*(9), 1041–1066. https://doi.org/10.1002/joc.635

Kiesel, J., Gericke, A., Rathjens, H., Wetzig, A., Kakouei, K., Jähnig, S. C., & Fohrer, N. (2019). Climate change impacts on ecologically relevant hydrological indicators in three catchments in three European ecoregions. *Ecological Engineering*, *127*(July 2018), 404–416. https://doi.org/10.1016/j.ecoleng.2018.12.019

Kim, J., Choi, J., Choi, C., & Park, S. (2013). Impacts of changes in climate and land use/land cover under IPCC RCP scenarios on streamflow in the Hoeya River Basin, Korea. *Science of the Total Environment*, *452–453*, 181–195. https://doi.org/10.1016/j.scitotenv.2013.02.005

Kim, J., Waliser, D. E., Mattmann, C. A., Goodale, C. E., Hart, A. F., Zimdars, P. A., Crichton, D. J., Jones, C., Nikulin, G., Hewitson, B., Jack, C., Lennard, C., & Favre, A. (2014). Evaluation of the CORDEX-Africa multi-RCM hindcast: Systematic model errors. *Climate Dynamics*, *42*(5–6), 1189–1202. https://doi.org/10.1007/s00382-013-1751-7

Kim, U., & Kaluarachchi, J. J. (2009). Climate change impacts on water resources in the upper Blue Nile River Basin, Ethiopia. In *Journal of the American Water Resources Association* (Vol. 45, Issue 6). https://doi.org/10.1111/j.1752-1688.2009.00369.x

Kim, U., Kaluarachchi, J. J., & Smakhtin, V. U. (2008). Generation of monthly precipitation under climate change for the upper Blue Nile River Basin, Ethiopia. *Journal of the American Water Resources Association*, *44*(5), 1231–1247. https://doi.org/10.1111/j.1752-1688.2008.00220.x

Kiprotich, P., Wei, X., Zhang, Z., Ngigi, T., Qiu, F., & Wang, L. (2021). Assessing the impact of land use and climate change on surface runoff response using gridded observations and swat+. *Hydrology*, *8*(1). https://doi.org/10.3390/hydrology8010048

Koch, F. J., Van Griensven, A., Uhlenbrook, S., Tekleab, S., & Teferi, E. (2012). The effects of

land use change on hydrological responses in the Choke Mountain Range (Ethiopia) - A new approach addressing land use dynamics in the model SWAT. *IEMSs 2012 - Managing Resources of a Limited Planet: Proceedings of the 6th Biennial Meeting of the International Environmental Modelling and Software Society*, 3022–3029.

Krause, P., Boyle, D. P., & Bäse, F. (2005). Comparison of different efficiency criteria for hydrological model assessment. *Advances in Geosciences*, *5*, 89–97. https://doi.org/10.5194/adgeo-5-89-2005

Kumar, S., Merwade, V., Kam, J., & Thurner, K. (2009). Streamflow trends in Indiana: Effects of long term persistence, precipitation and subsurface drains. *Journal of Hydrology*, *374*(1–2), 171–183. https://doi.org/10.1016/j.jhydrol.2009.06.012

Kumar, S., Radhakrishnan, N., & Mathew, S. (2014). Land use change modelling using a Markov model and remote sensing. *Geomatics, Natural Hazards and Risk*, *5*(2), 145–156. https://doi.org/10.1080/19475705.2013.795502

Kundzewicz, Z. W., Krysanova, V., Benestad, R. E., Hov, Piniewski, M., & Otto, I. M. (2018). Uncertainty in climate change impacts on water resources. *Environmental Science and Policy*, *79*(October 2017), 1–8. https://doi.org/10.1016/j.envsci.2017.10.008

Lahmer, W., Pfützner, B., & Becker, A. (2001). Assessment of land use and climate change impacts on the mesoscale. Physics and Chemistry of the Earth, Part B: Hydrology, Oceans and Atmosphere, 26(7–8), 565–575. https://doi.org/10.1016/S1464-1909(01)00051-X

Lambin, E. F., Geist, H. J., & Lepers, E. (2003). Dynamics of land-use and land-cover change in tropical regions. *Annual Review of Environment and Resources*, *28*(January 2003), 205–241. https://doi.org/10.1146/annurev.energy.28.050302.105459

Lambin, E. F., & Meyfroidt, P. (2011). Global land use change, economic globalization, and the looming land scarcity. *Proceedings of the National Academy of Sciences of the United States of America*, *108*(9), 3465–3472. https://doi.org/10.1073/pnas.1100480108

Landry, M., Guidigan, G., Sanou, C. L., Saberma, D., & Cham, R. (2019). Assessing Land Use / Land Cover Dynamic and Its Impact in Benin Republic Using Land Change Model and CCI - LC Products. *Earth Systems and Environment*, *3*(1), 127–137. https://doi.org/10.1007/s41748-018-0083-5

Laprise, R., Hernández-Díaz, L., Tete, K., Sushama, L., Šeparović, L., Martynov, A., Winger, K., & Valin, M. (2013). Climate projections over CORDEX Africa domain using the fifth-generation Canadian Regional Climate Model (CRCM5). *Climate Dynamics*, *41*(11–12), 3219–3246. https://doi.org/10.1007/s00382-012-1651-2

Lau, K., and B. Kam. 2005. "A cellular automata model for urban land-use simulation". Environment and Planning B: Planning and Design 32 (2): 247–263

Legesse, D., Vallet-Coulomb, C., & Gasse, F. (2003). Hydrological response of a catchment to climate and land use changes in Tropical Africa: Case study south central Ethiopia. *Journal of Hydrology*, *275*(1–2), 67–85. https://doi.org/10.1016/S0022-1694(03)00019-2

Li, K. Y., Coe, M. T., Ramankutty, N., & Jong, R. De. (2007). Modeling the hydrological impact of land-use change in West Africa. *Journal of Hydrology*, *337*(3–4), 258–268. https://doi.org/10.1016/j.jhydrol.2007.01.038

Li, T., & Li, W. (2015). Multiple land use change simulation with Monte Carlo approach and CA-ANN model, a case study in Shenzhen, China. *Environmental Systems Research*, *4*(1), 1–10. https://doi.org/10.1186/s40068-014-0026-6

Li, X., & Yeh, A. G. O. (2002). Neural-network-based cellular automata for simulating multiple land use changes using GIS. *International Journal of Geographical Information Science*,

16(4), 323–343. https://doi.org/10.1080/13658810210137004
Li, Z., Liu, W. zhao, Zhang, X. chang, & Zheng, F. li. (2009). Impacts of land use change and climate variability on hydrology in an agricultural catchment on the Loess Plateau of China. Journal of Hydrology, 377(1–2), 35–42. https://doi.org/10.1016/j.jhydrol.2009.08.007
Liping, C., Yujun, S., & Saeed, S. (2018). Monitoring and predicting land use and land cover changes using remote sensing and GIS techniques—A case study of a hilly area, Jiangle, China. *PLoS ONE*, *13*(7), 1–23. https://doi.org/10.1371/journal.pone.0200493
Liu, X. (2022). *Global Agricultural Water Scarcity Assessment Incorporating Blue and Green Water Availability Under Future Climate Change Earth ' s Future*. https://doi.org/10.1029/2021EF002567
López-Ballesteros, A., Senent-Aparicio, J., Martínez, C., & Pérez-Sánchez, J. (2020). Assessment of future hydrologic alteration due to climate change in the Aracthos River basin (NW Greece). *Science of the Total Environment*, *733*, 139299. https://doi.org/10.1016/j.scitotenv.2020.139299
Lørup, J. K., Refsgaard, J. C., and Mazvimavi, D. (1998). Assessing the effect of land use change on catchment runoff by combined use of statistical tests and hydrological modelling: case studies from Zimbabwe, J. Hydrol., 205, 147–163, doi:10.1016/S0168-1176(97)00311-9.
Luo, X., Wu, W., He, D., Li, Y., & Ji, X. (2019). Hydrological Simulation Using TRMM and CHIRPS Precipitation Estimates in the Lower Lancang-Mekong River Basin. *Chinese Geographical Science*, *29*(1), 13–25. https://doi.org/10.1007/s11769-019-1014-6
Madani, E.M, Jansson, P.E, Babelon, I. (2018). Differences in water balance between grassland and forest watersheds using long-term data , derived using the CoupModel. 72–89. https://doi.org/10.2166/nh.2017.154
Maidment, R. I., Allan, R. P., & Black, E. (2015). in precipitation over Africa. *Geophysical Research Letters*, *42*(19), 1–10. https://doi.org/10.1002/2015GL065765.
Mango, L. M., Melesse, A. M., McClain, M. E., Gann, D., & Setegn, S. G. (2011). Land use and climate change impacts on the hydrology of the upper Mara River Basin, Kenya: Results of a modeling study to support better resource management. *Hydrology and Earth System Sciences*, *15*(7), 2245–2258. https://doi.org/10.5194/hess-15-2245-2011
Mannan, A., Liu, J., Zhongke, F., Ullah, T., Saeed, S., Mukete, B., Chaoyong, S., Yongxiang, F., Ahmad, A., Amir, M., Ahmad, S., & Shah, S. (2019). Application of land-use / land cover changes in monitoring and projecting forest biomass carbon loss in Pakistan. Global Ecology and Conservation, 17(35), e00535. https://doi.org/10.1016/j.gecco.2019.e00535
Marhaento, H., Booij, M. J., & Hoekstra, A. Y. (2018). Hydrological response to future land-use change and climate change in a tropical catchment. *Hydrological Sciences Journal*, *63*(9), 1368–1385. https://doi.org/10.1080/02626667.2018.1511054
McCartney, M. P., Alemayehu, T., Awulachew, S. B., & Seleshi, Y. (2009). Evaluation of current and future water resource development in the Blue Nile. In *IWMI RR, forthcoming*.
Mccartney, M. P., & Girma, M. M. (2012). *Evaluating the downstream implications of planned water resource development in the Ethiopian portion of the Blue Nile River*. *April 2015*, 37–41. https://doi.org/10.1080/02508060.2012.706384
Mehdi, B., Ludwig, R., & Lehner, B. (2015). Evaluating the impacts of climate change and crop land use change on streamflow, nitrates and phosphorus: A modeling study in Bavaria. *Journal of Hydrology: Regional Studies*, *4*(PB), 60–90. https://doi.org/10.1016/j.ejrh.2015.04.009

Meiyappan, P., & Jain, A. K. (2012). Three distinct global estimates of historical land-cover change and land-use conversions for over 200 years. Frontiers of Earth Science, 6(2), 122–139. https://doi.org/10.1007/s11707-012-0314-2

Mekonnen, D.F, Duan, Z., Rientjes, T., & Disse, M. (2017). Analysis of the combined and single effects of LULC and climate change on the streamflow of the Upper Blue Nile River Basin (UBNRB): Using statistical trend tests, remote sensing landcover maps and the SWAT model. *Hydrology and Earth System Sciences Discussions*, 1–26. https://doi.org/10.5194/hess-2017-685

Mekonnen, K., Melesse, A. M., & Woldesenbet, T. A. (2021). Spatial evaluation of satellite-retrieved extreme rainfall rates in the Upper Awash River Basin, Ethiopia. *Atmospheric Research*, *249*, 105297. https://doi.org/10.1016/j.atmosres.2020.105297

Mekuria, A., Vlek, P. L. G., & Denich, M. (2011). *Application of The Caesium-137 Technique to Soil Degradation Studies in The Southwestern Highlands of Ethiopia*.

Mengistu, A. G., Woldesenbet, T. A., & Dile, Y. T. (2021). Evaluation of the performance of bias-corrected CORDEX regional climate models in reproducing Baro–Akobo basin climate. *Theoretical and Applied Climatology*, *144*(1–2), 751–767. https://doi.org/10.1007/s00704-021-03552-w

Mengistu, A. G., Woldesenbet, T. A., & Dile, Y. T. (2021). Evaluation of observed and satellite-based climate products for hydrological simulation in data-scarce Baro–Akobo River Basin, Ethiopia. *Ecohydrology & Hydrobiology*. https://doi.org/10.1016/j.ecohyd.2021.11.006

Mengistu, D. T., & Sorteberg, A. (2012). *Sensitivity of SWAT simulated streamflow to climatic changes within the Eastern Nile River basin*. 391–407. https://doi.org/10.5194/hess-16-391-2012

Midekisa, A., Holl, F., Savory, D. J., Andrade-Pacheco, R., Gething, P. W., Bennett, A., & Sturrock, H. J. W. (2017). Mapping land cover change over continental Africa using Landsat and Google Earth Engine cloud computing. PLoS ONE, 12(9), 1–15. https://doi.org/10.1371/journal.pone.0184926

Moriasi, D.N., Arnold, J., Van Liew, M., Bingner, R.L., Harmel, R.D., Veith, T.L. (2007). Model Evaluation Guidelines for Systematic Quantification of Accuracy in Watershed Simulations: American Society of Agricultural and Biological Engineers ISSN 0001−2351.

Moriasi, D. N., Gitau, M. W., Pai, N., & Daggupati, P. (2015). Hydrologic and water quality models: Performance measures and evaluation criteria. *American Society of Agricultural and Biological Engineers. DOI 10.13031/trans.58.10715*

Moss, R. H., Edmonds, J. A., Hibbard, K. A., Manning, M. R., Rose, S. K., Van Vuuren, D. P., Carter, T. R., Emori, S., Kainuma, M., Kram, T., Meehl, G. A., Mitchell, J. F. B., Nakicenovic, N., Riahi, K., Smith, S. J., Stouffer, R. J., Thomson, A. M., Weyant, J. P., & Wilbanks, T. J. (2010). The next generation of scenarios for climate change research and assessment. *Nature*, *463*(7282), 747–756. https://doi.org/10.1038/nature08823

Muleta, T. N. (2021). Climate change scenario analysis for Baro-Akobo river basin, Southwestern Ethiopia. *Environmental Systems Research*, *10*(1). https://doi.org/10.1186/s40068-021-00225-5

Murphy, J. (1999). An evaluation of statistical and dynamical techniques for downscaling local climate. *Journal of Climate*, *12*(8 PART 1), 2256–2284. https://doi.org/10.1175/1520-0442(1999)012<2256:aeosad>2.0.co;2

Mwangi, H. M., Julich, S., Patil, S. D., & Mcdonald, M. A. (2016). Relative contribution of land use change and climate variability on discharge of upper Mara River , Kenya. Journal of

Hydrology : Regional Studies. 244–260. https://doi.org/10.1016/j.ejrh.2015.12.059
NAPA, 2007 Preparation of National Adaptation Programme of Action (NAPA) of Ethiopia. Addis Abeba
Nash, J. E., & Sutcliffe, J. V. (1970). River Flow Forecasting Through Conceptual Models - Part I - A Discussion of Principles. *Journal of Hydrology*, *10*(1970), 282–290.
Neitsch, SL., Arnold, J.G., Kiniry, J.R., Williams, J.R. (2011). Soil and water assessment tool theoretical documentation version 2009. Texas Water Resources Institute. https:// hdl. handle. net/ 1969.1/ 128050
NMA, 1996. Climate and agro-climatic resources of Ethiopia. NMA (National Meteorological Agency) Meteorological Research Report Series, Vol. 1, No.1, Addis Ababa
Nikulin, G., Jones, C., Giorgi, F., Asrar, G., Büchner, M., Cerezo-Mota, R., Christensen, O. B., Déqué, M., Fernandez, J., Hänsler, A., van Meijgaard, E., Samuelsson, P., Sylla, M. B., & Sushama, L. (2012). Precipitation climatology in an ensemble of CORDEX-Africa regional climate simulations. *Journal of Climate*, *25*(18), 6057–6078. https://doi.org/10.1175/JCLI-D-11-00375.1
NOAA, 2022. National Oceanic and Atmospheric Administration. NOAA Climate.gov
Nordstokke, D.W., Zumbo, B.D., Cairns, S.L., Saklofske, D.H. (2011). The operating characteristics of the nonparametric Levene test for equal variances with assessment and evaluation data. Pract. Assessment, Res. Eval. 16, 1–8.
Osborn, T. J., & Hulme, M. (1997). Development of a relationship between station and grid-box rainday frequencies for climate model evaluation. *Journal of Climate*, *10*(8), 1885–1908. https://doi.org/10.1175/1520-0442(1997)010<1885:DOARBS>2.0.CO;2
Pacini, N., & Harper, D. M. (2016). Hydrological characteristics and water resources management in the Nile Basin. *Ecohydrology and Hydrobiology*, *16*(4), 242–254. https://doi.org/10.1016/j.ecohyd.2016.09.001
Pahlavani, P., Omran, H. A., & Bigdeli, B. (2017). A multiple land use change model based on artificial neural network, Markov chain, and multi objective land allocation. Earth Observation and Geomatics Engineering, 1(2), 82–99. https://doi.org/10.22059/eoge.2017.220342.1006
Pan, S., Liu, D., Wang, Z., Zhao, Q., Zou, H., Hou, Y., & Liu, P. (2017). Runoff Responses to Climate and Land Use / Cover. 1–23. https://doi.org/10.3390/w9070475
Pereira, L., Paula, A., Xavier, C., Marques, R., Augusto, C., & Santos, G. (2019). Modeling land cover change based on an artificial neural network for a semiarid river basin in northeastern Brazil. Global Ecology and Conservation, e00811. https://doi.org/10.1016/j.gecco.2019.e00811
Piani, C., Haerter, J. O., & Coppola, E. (2010). Statistical bias correction for daily precipitation in regional climate models over Europe. *Theoretical and Applied Climatology*, *99*(1–2), 187–192. https://doi.org/10.1007/s00704-009-0134-9
Poff, N. L., & Zimmerman, J. K. H. (2010). Ecological responses to altered flow regimes: A literature review to inform the science and management of environmental flows. *Freshwater Biology*, *55*(1), 194–205. https://doi.org/10.1111/j.1365-2427.2009.02272.x
Pradhanang, S. M., Mukundan, R., Schneiderman, E. M., Zion, M. S., Anandhi, A., Pierson, D. C., Frei, A., Easton, Z. M., Fuka, D., & Steenhuis, T. S. (2013). Streamflow Responses to Climate Change: Analysis of Hydrologic Indicators in a New York City Water Supply Watershed. *Journal of the American Water Resources Association*, *49*(6), 1308–1326. https://doi.org/10.1111/jawr.12086

Praskievicz, S., & Chang, H. (2009). A review of hydrological modelling of basin-scale climate change and urban development impacts. Progress in Physical Geography impacts https://doi.org/10.1177/0309133309348098

Quan, N. V, Don, N. C., & Kim, G. S. (2019). *Integrated impacts of climate change and land use change on surface hydrology in the future in Nakdong river basin in Korea*. *20*(8), 379–392.

Radcliffe, D. E., & Mukundan, R. (2017). PRISM vs. CFSR Precipitation Data Effects on Calibration and Validation of SWAT Models. *Journal of the American Water Resources Association*, *53*(1), 89–100. https://doi.org/10.1111/1752-1688.12484

Rahman, K., Shang, S., Shahid, M., & Wen, Y. (2020). Hydrological evaluation of merged satellite precipitation datasets for streamflow simulation using SWAT: A case study of Potohar Plateau, Pakistan. Journal of Hydrology, 587(May), 125040. https://doi.org/10.1016/j.jhydrol.2020.125040

Ramdani, F., Setiawan, B. D., Rusydi, A. N., & Tanzil, M. (2021). *An artificial neural network approach to predict the future land use land cover of Great Malang region , Indonesia*. *2050*(March), 1–21. https://doi.org/10.20944/preprints202103.0247.v1

Rathjens, H., Bieger, K., Srinivasan, R., & Arnold, J. G. (2016). *CMhyd User Manual Documentation for preparing simulated climate change data for hydrologic impact studies*. p.16p.

Richter, B. D., Baumgartner, J. V, Powell, J., David, P., Richter, B. D., Baumgartner, J. V, Powell, J., & Braunt, D. P. (1996). *A Method for Assessing Hydrologic Alteration within Ecosystems Published by : Wiley for Society for Conservation Biology All use subject to https://about.jstor.org/terms A Method for Assessing Hydrologic Alteration within Ecosystems*. *10*(4), 1163–1174.

Rockel, B., Will, A., & Hense, A. (2008). The regional climate model COSMO-CLM (CCLM). *Meteorologische Zeitschrift*, *17*(4), 347–348. https://doi.org/10.1127/0941-2948/2008/0309

Roy, H. G., Fox, D. M., & Emsellem, K. (2014). Predicting land cover change in a Mediterranean catchment at different time scales. *Lecture Notes in Computer Science (Including Subseries Lecture Notes in Artificial Intelligence and Lecture Notes in Bioinformatics)*, *8582 LNCS*(PART 4), 315–330. https://doi.org/10.1007/978-3-319-09147-1_23

Saha, S., Moorthi, S., Pan, H. L., Wu, X., Wang, J., Nadiga, S., Tripp, P., Kistler, R., Woollen, J., Behringer, D., Liu, H., Stokes, D., Grumbine, R., Gayno, G., Wang, J., Hou, Y. T., Chuang, H. Y., Juang, H. M. H., Sela, J., Goldberg, M. (2010). The NCEP climate forecast system reanalysis. *Bulletin of the American Meteorological Society*, *91*(8), 1015–1057. https://doi.org/10.1175/2010BAMS3001.1

Salathé, E. P. (2003). Comparison of various precipitation downscaling methods for the simulation of streamflow in a rainshadow river basin. *International Journal of Climatology*, *23*(8), 887–901. https://doi.org/10.1002/joc.922

Samuelsson, P., Gollvik, S., Kupiainen, M., Kourzeneva, E., & van de Berg, W. (2015). The Surface Processes of the Rossby Centre Regional Atmospheric Climate Model (RCA4). *SMHI: Norrköping, Sweden*, *1*, 2358–2381.

Saxton, K. E., & Rawls, W. J. (2006). Soil Water Characteristic Estimates by Texture and Organic Matter for Hydrologic Solutions. *Soil Science Society of America Journal*, *70*(5), 1569–1578. https://doi.org/10.2136/sssaj2005.0117

Schmidli, J., Goodess, C. M., Frei, C., Haylock, M. R., Hundecha, Y., Ribalaygua, J., & Schmith, T. (2007). Statistical and dynamical downscaling of precipitation: An evaluation

and comparison of scenarios for the European Alps. *Journal of Geophysical Research Atmospheres*, *112*(4), 1–20. https://doi.org/10.1029/2005JD007026
Searcy, J. K., & Hardison, C. H. (1960). Double-Mass Curves. WaterSupply Paper 1541B, 66. http://dspace.udel.edu:8080/dspace/handle/19716/1592
Seibert J, Vis MJP (2012) Teaching hydrological modeling with a user-friendly catchment-runoff-model software package. Hydrol Earth Syst Sci 16:3315–3325. https://doi.org/10.5194/hess-16-3315-2012.
Seiller, G., Anctil, F., & Perrin, C. (2012). Multimodel evaluation of twenty lumped hydrological models under contrasted climate conditions. *Hydrology and Earth System Sciences*, *16*(4), 1171–1189. https://doi.org/10.5194/hess-16-1171-2012
Sen, P (1968) Estimates of the regression coefficient based on Kendall's tau. J Am Stat Assoc 63:1379– 1389
Stedinger, J.R., Vogel, R.M., Foufoula-Georgiou, E., 1993. Frequency Analysis of Extreme Events. Handb. Hydrol. 18.1.
Setegn, S. G., Rayner, D., Melesse, A. M., Dargahi, B., & Srinivasan, R. (2011). Impact of climate change on the hydroclimatology of Lake Tana Basin, Ethiopia. *Water Resources Research*, *47*(4), 1–13. https://doi.org/10.1029/2010WR009248
Setegn, S. G., Srinivasan, R., & Dargahi, B. (2008). Hydrological Modelling in the Lake Tana Basin, Ethiopia Using SWAT Model. *The Open Hydrology Journal*, *2*(1), 49–62. https://doi.org/10.2174/1874378100802010049
Seto, K. C., & Kaufmann, R. K. (2003). Modeling the drivers of urban land use change in the Pearl River Delta, China: Integrating remote sensing with socioeconomic data. *Land Economics*, *79*(1), 106–121. https://doi.org/10.2307/3147108
Sharma, D., Gupta, A. Das, & Babel, M. S. (2007). *Spatial disaggregation of bias-corrected GCM precipitation for improved hydrologic simulation : Ping River Basin , Thailand*. 1373–1390.
Shrestha, S., & Roachanakanan, R. (2021). Heliyon Extreme climate projections under representative concentration pathways in the Lower Songkhram River Basin , Thailand. *Heliyon*, *7*(December 2019), e06146. https://doi.org/10.1016/j.heliyon.2021.e06146
Siddiqui, A., Siddiqui, A., Maithani, S., Jha, A. K., Kumar, P., & Srivastav, S. K. (2017). The Egyptian Journal of Remote Sensing and Space Sciences Urban growth dynamics of an Indian metropolitan using CA Markov and Logistic Regression. *The Egyptian Journal of Remote Sensing and Space Sciences*. https://doi.org/10.1016/j.ejrs.2017.11.006
Sileet, T. M., Shamy, M. E. S., Aty, M. A., & Sharaky, A. M. (2013). The Development of the Baro-Akobo-Sobat sub basin and its Impact on Downstream Nile Basin Countries. *Nile Water Science & Engineering Journal*, *6*(2), 38–53.
Sinha, S., Sharma, L. K., & Nathawat, M. S. (2015). Improved Land-use/Land-cover classification of semi-arid deciduous forest landscape using thermal remote sensing. *Egyptian Journal of Remote Sensing and Space Science*, *18*(2), 217–233. https://doi.org/10.1016/j.ejrs.2015.09.005
Srinivasan, R., Zhang, X., & Arnold, J. (2010). SWAT ungauged: Hydrological budget and crop yield predictions in the upper Mississippi River basin. *American Society of Agricultural and Biological Engineers*, *53*(5), 1533–1546. https://doi.org/10.13031/2013.34903
Subedi, P., Subedi, K., & Thapa, B. (2013). Application of a Hybrid Cellular Automaton – Markov (CA-Markov) Model in Land-Use Change Prediction : A Case Study of Saddle Creek Drainage Basin , Florida. 1(6), 126–132. https://doi.org/10.12691/aees-1-6-5

Sun, G., M. Riedel, R. Jackson, R. Kolka, D. Amatya, and J. Shepard. (2004). Influences of management of Southern forests on water quantity and quality. In Southern Forest Sciences: Past, Current, and Future, 394. Gen. Tech. Rep/ SRS-75. H. M. Rauscher and K. Johnsen, eds. Ashville, N.C.: U.S. Forest Service, Southern Research Station.

Surfleet, C. G., Tullos, D., Chang, H., & Jung, I. W. (2012). Selection of hydrologic modeling approaches for climate change assessment: A comparison of model scale and structures. *Journal of Hydrology*, *464–465*, 233–248. https://doi.org/10.1016/j.jhydrol.2012.07.012

Swank, W. T., J. M. Vose, and K. J. Elliott. (2001). Long-term hydrological and water quality responses following commercial clearcutting of mixed hardwoods on a southern Appalachian catchment. Forest Ecol. Mgmt. 143: 163-178.

Szuster, B., Chen, Q., & Borger, M. (2011). "A comparison of classification techniques to support land cover and land use analysis in tropical coastal zones". Applied Geography 31 (2): 525–532.

Tabari, H., Taye, M. T., & Willems, P. (2015). Statistical assessment of precipitation trends in the upper Blue Nile River basin. *Stochastic Environmental Research and Risk Assessment*, *29*(7), 1751–1761. https://doi.org/10.1007/s00477-015-1046-0

Tamm, O., Maasikamäe, S., Padari, A., & Tamm, T. (2018). Catena Modelling the e ff ects of land use and climate change on the water resources in the eastern Baltic Sea region using the SWAT model. *Catena*, *167*(April), 78–89. https://doi.org/10.1016/j.catena.2018.04.029

Tan, X., Liu, S., Tian, Y., Zhou, Z., Wang, Y., & Jiang, J. (2022). *Impacts of Climate Change and Land Use / Cover Change on Regional Hydrological Processes : Case of the Greater Bay Area*. *9*(January), 1–16. https://doi.org/10.3389/fenvs.2021.783324

Tapiador, F. J., Turk, F. J., Petersen, W., Hou, A. Y., García-ortega, E., Machado, L. A. T., Angelis, C. F., Salio, P., Kidd, C., Huffman, G. J., & Castro, M. De. (2012). Global precipitation measurement : Methods , datasets and applications. *Atmospheric Research*, *104–105*, 70–97. https://doi.org/10.1016/j.atmosres.2011.10.021

Taye, M. T., Dyer, E., Hirpa, F. A., & Charles, K. (2018). Climate change impact on water resources in the Awash basin, Ethiopia. *Water (Switzerland)*, *10*(11), 1–16. https://doi.org/10.3390/w10111560

Taye, M. T., Ntegeka, V., Ogiramoi, N. P., & Willems, P. (2011). Assessment of climate change impact on hydrological extremes in two source regions of the Nile River Basin. *Hydrology and Earth System Sciences*, *15*(1), 209–222. https://doi.org/10.5194/hess-15-209-2011

Teferi, E., Bewket, W., Uhlenbrook, S., & Wenninger, J. (2013). Understanding recent land use and land cover dynamics in the source region of the Upper Blue Nile, Ethiopia: Spatially explicit statistical modeling of systematic transitions. *Agriculture, Ecosystems and Environment*, *165*, 98–117. https://doi.org/10.1016/j.agee.2012.11.007

Teklay, A., Dile, Y. T., Asfaw, D. H., Bayabil, H. K., & Sisay, K. (2021). Impacts of Climate and Land Use Change on Hydrological Response in Gumara Watershed, Ethiopia. *Ecohydrology and Hydrobiology*, *21*(2), 315–332. https://doi.org/10.1016/j.ecohyd.2020.12.001

Tekleab, S., Mohamed, Y., & Uhlenbrook, S. (2013). Hydro-climatic trends in the Abay/Upper Blue Nile basin, Ethiopia. *Physics and Chemistry of the Earth*, *61–62*, 32–42. https://doi.org/10.1016/j.pce.2013.04.017

Tekleab, S., Mohamed, Y., Uhlenbrook, S., Wenninger, J. (2014). Hydrologic responses to land cover change: the case of Jedeb mesoscale catchment, Abay/Upper Blue Nile basin, Ethiopia. Hydrological Processes, 28(20): 5149-5161. DOI: 10.1002/hyp.9998

Teutschbein, C., & Seibert, J. (2010). Regional climate models for hydrological impact studies at the catchment scale: A review of recent modeling strategies. *Geography Compass*, *4*(7), 834–860. https://doi.org/10.1111/j.1749-8198.2010.00357.x

Teutschbein, C., & Seibert, J. (2012). Bias correction of regional climate model simulations for hydrological climate-change impact studies: Review and evaluation of different methods. *Journal of Hydrology*, *456–457*, 12–29. https://doi.org/10.1016/j.jhydrol.2012.05.052

Themeßl, M. J., Gobiet, A., & Heinrich, G. (2012). Empirical-statistical downscaling and error correction of regional climate models and its impact on the climate change signal. *Climatic Change*, *112*(2), 449–468. https://doi.org/10.1007/s10584-011-0224-4

Toma, M. B., Belete, M. D., & Ulsido, M. D. (2022). *Historical and future dynamics of land use land cover and its drivers in Ajora - Woybo watershed , Omo - Gibe basin , Ethiopia*. *April*, 1–27. https://doi.org/10.1111/nrm.12353

Tong, S. T. Y., Sun, Y., Ranatunga, T., He, J., & Yang, Y. J. (2012). Predicting plausible impacts of sets of climate and land use change scenarios on water resources. *Applied Geography*, *32*(2), 477–489. https://doi.org/10.1016/j.apgeog.2011.06.014

Tu, J. (2009). Combined impact of climate and land use changes on streamflow and water quality in eastern Massachusetts, USA. Journal of Hydrology, 379(3–4), 268–283. https://doi.org/10.1016/j.jhydrol.2009.10.009

Tuo, Y., Duan, Z., Disse, M., & Chiogna, G. (2016). Evaluation of precipitation input for SWAT modeling in Alpine catchment: A case study in the Adige river basin (Italy). *Science of the Total Environment*, *573*, 66–82. https://doi.org/10.1016/j.scitotenv.2016.08.034

Turner, I.i., B. L., Skole, D., Sanderson, S., Fischer, G., Fresco, L., & Leemans, R. (1995). Landuse and land-cover change. Science/Research plan. (IGBP Report; No. 35). IGBP. https://www.ihdp.unu.edu/file/get/8605

Turrado, C. C., López, M. del C. M., Lasheras, F. S., Gómez, B. A. R., Rollé, J. L. C., & Juez, F. J. de C. (2014). Missing data imputation of solar radiation data under different atmospheric conditions. Sensors (Switzerland), 14(11), 20382–20399. https://doi.org/10.3390/s141120382

Uhlenbrook, S., Mohamed, Y., and Gragne, A. S. (2010) Analyzing catchment behavior through catchment modeling in the Gilgel Abay, Upper Blue Nile River Basin, Ethiopia. Hydrol. Earth Syst. Sci., 14, 2153–2165, https://doi.org/10.5194/hess-14-2153-2010

UNEP, 2012. United Nations Environmental Programme. Global Environment Outlook 4 (No. 4). UNEP, Valletta, Malta.

UNESCO, 2012. "Ecological Sciences for Sustainable Development." from www.unesco.org.

van Buuren, S., & Groothuis-Oudshoorn, K. (2011). mice: Multivariate imputation by chained equations in R. *Journal of Statistical Software*, *45*(3), 1–67. https://doi.org/10.18637/jss.v045.i03

Van Roosmalen, L., Sonnenborg, T. O., & Jensen, K. H. (2009). Impact of climate and land use change on the hydrology of a large-scale agricultural catchment. *Water Resources Research*, *45*(7), 1–18. https://doi.org/10.1029/2007WR006760

van Ruijven, B. J., Levy, M. A., Agrawal, A., Biermann, F., Birkmann, J., Carter, T. R., Ebi, K. L., Garschagen, M., Jones, B., Jones, R., Kemp-Benedict, E., Kok, M., Kok, K., Lemos, M. C., Lucas, P. L., Orlove, B., Pachauri, S., Parris, T. M., Patwardhan, A., … Schweizer, V. J. (2014). Enhancing the relevance of shared socioeconomic pathways for climate change impacts, adaptation and vulnerability research. *Climatic Change*, *122*(3), 481–494. https://doi.org/10.1007/s10584-013-0931-0

Vivekananda, G. N., Swathi, R., & Sujith, A. (2021). Multi-temporal image analysis for LULC classification and change detection. *European Journal of Remote Sensing*, *54*(2), 189–199. https://doi.org/10.1080/22797254.2020.1771215

Vitousek, P. (1994). Beyond Global Warming: Ecology and Global Change. Ecology, 75(7), 1861–1876. https://doi.org/10.2307/1941591

von Storch H (1999) Analysis of climate variability—applications of statistical techniques. Springer-Verlag, New York

Vuuren, D. P., Van, Edmonds, J., Kainuma, M., Riahi, K., Nakicenovic, N., Smith, S. J., & Rose, S. K. (2011). *The representative concentration pathways : an overview*. 5–31. Climatic Change. https://doi.org/10.1007/s10584-011-0148-z

Wakjira, D. T., & Gole, T. W. (2016). *Customary Forest Tenure In SouthwesT*. *8028*(June). https://doi.org/10.1080/14728028.2007.9752607

Wang S, Zhang Z, Sun G, Strauss P, Guo J, Tang Y, Yao A. 2012. Multi- site calibration, validation, and sensitivity analysis of the MIKE SHE Model for a large watershed in northern China. Hydrology and Earth System Sciences 16: 4621–4632. DOI: 10.5194/hess-16-4621-2012

White, E. D., Easton, Z. M., Fuka, D. R., Collick, A. S., Adgo, E., Mccartney, M., Awulachew, S. B., Selassie, Y. G., & Steenhuis, T. S. (2011). *Development and application of a physically based landscape water balance in the SWAT model*. *925*(October 2010), 915–925. https://doi.org/10.1002/hyp.7876

White, M. D., & Greer, K. A. (2006). The effects of watershed urbanization on the stream hydrology and riparian vegetation of Los Peñasquitos Creek, California. *Landscape and Urban Planning*, *74*(2), 125–138. https://doi.org/10.1016/j.landurbplan.2004.11.015

Wilby, R. L. (2010). Evaluating climate model outputs for hydrological applications. *Hydrological Sciences Journal*, *55*(7), 1090–1093. https://doi.org/10.1080/02626667.2010.513212

Wilby, R. L., Hay, L. E., Gutowski, W. J., Arritt, R. W., Takle, E. S., Pan, Z., Leavesley, G. H., & Clark, M. P. (2000). Hydrological responses to dynamically and statistically downscaled climate model output. *Geophysical Research Letters*, *27*(8), 1199–1202. https://doi.org/10.1029/1999GL006078

Wilk, J., Kniveton, D., Andersson, L., Layberry, R., Todd, M. C., Hughes, D., Ringrose, S., & Vanderpost, C. (2006). Estimating rainfall and water balance over the Okavango River Basin for hydrological applications. *Journal of Hydrology*, 18–29. https://doi.org/10.1016/j.jhydrol.2006.04.049

Winkler, K., Fuchs, R., Rounsevell, M., & Herold, M. (2021). Global land use changes are four times greater than previously estimated. *Nature Communications*, *12*(1), 1–10. https://doi.org/10.1038/s41467-021-22702-2

Woldesenbet, T. A. (2022). Impact of land use and land cover dynamics on ecologically-relevant flows and blue-green water resources. *Ecohydrology and Hydrobiology*, *xxxx*. https://doi.org/10.1016/j.ecohyd.2022.03.002

Woldesenbet, T. A., & Elagib, N. A. (2021). Spatial-temporal evaluation of different reference evapotranspiration methods based on the climate forecast system reanalysis data. In *Hydrological Processes* (Vol. 35, Issue 6). https://doi.org/10.1002/hyp.14239

Woldesenbet, TA, Elagib, NA, Ribbe, L, Heinrich, J. (2018). Catchment response to climate and land use changes in the Upper Blue Nile sub- -basins, Ethiopia. Science of the Total Environment 644, 193– 206.

Woldesenbet, TA, Elagib, NA, Ribbe, L, Heinrich, J. (2017). Hydrological responses to land use/cover changes in the source region of the Upper Blue Nile Basin, Ethiopia. Science of The Total Environment 575, 724– 741. doi: 10.1016/j.scitotenv.2016.09.124.

Wood, A. W., Leung, L. R., Sridhar, V., & Lettenmaier, D. P. (2004). Hydrologic implications of dynamical and statistical approaches to downscaling climate model outputs. *Climatic Change*, *62*(1–3), 189–216. https://doi.org/10.1023/B:CLIM.0000013685.99609.9e

World Bank, 2006. Sustainable Land Management: Challenges, Opportunities and Trade-offs, Washington DC, USA

Worku, G., Teferi, E., Bantider, A., & Dile, Y. T. (2020a). Prioritization of watershed management scenarios under climate change in the Jemma sub-basin of the Upper Blue Nile Basin, Ethiopia. *Journal of Hydrology: Regional Studies*, *31*(January), 100714. https://doi.org/10.1016/j.ejrh.2020.100714

Worku, G., Teferi, E., Bantider, A., & Dile, Y. T. (2020b). Statistical bias correction of regional climate model simulations for climate change projection in the Jemma sub-basin, upper Blue Nile Basin of Ethiopia. *Theoretical and Applied Climatology*, *139*(3–4), 1569–1588. https://doi.org/10.1007/s00704-019-03053-x

Worku, G., Teferi, E., Bantider, A., & Dile, Y. T. (2021). Modelling hydrological processes under climate change scenarios in the Jemma sub-basin of upper Blue Nile Basin, Ethiopia. *Climate Risk Management*, *31*(July 2020), 100272. https://doi.org/10.1016/j.crm.2021.100272

Worqlul, A., Taddele, Y. D., Ayana, E. K., Jeong, J., Adem, A. A., & Gerik, T. (2018). Impact of climate change on streamflow hydrology in headwater catchments of the upper Blue Nile Basin, Ethiopia. *Water (Switzerland)*, *10*(2). https://doi.org/10.3390/w10020120

Worqlul, A. W., Maathuis, B., Adem, A. A., Demissie, S. S., & Langan, S. (2014). Comparison of TRMM, MPEG and CFSR rainfall estimation with the ground observed data for the Lake Tana Basin, Ethiopia. *Hydrology and Earth System Sciences Discussions*, *11*(7), 8013–8038. https://doi.org/10.5194/hessd-11-8013-2014

WWAP, 2015. WWAP (World Water Assessment Programme). (2015). The United Nations World Water Development Report 2015: Water for a Sustainable World. Paris, UNESCO.

Yan, T., Bai, J., Arsenio, T., Liu, J., & Shen, Z. (2019). Future climate change impacts on streamflow and nitrogen exports based on CMIP5 projection in the Miyun Reservoir Basin, China. *Ecohydrology and Hydrobiology*, *19*(2), 266–278. https://doi.org/10.1016/j.ecohyd.2018.09.001

Yang, H., Faramarzi, M., & Abbaspour, K. C. (2013). *Assessing Freshwater Availability in Africa under the Current and Future Climate with Focus on Drought and Water Scarcity*. *December*, 1–6.

Yang, L., Feng, Q., Yin, Z., Wen, X., Si, J., Li, C., & Deo, R. C. (2017). Identifying separate impacts of climate and land use/cover change on hydrological processes in upper stream of Heihe River, Northwest China. *Hydrological Processes*, *31*(5), 1100–1112. https://doi.org/10.1002/hyp.11098

Yang, Q., Li, X., & Shi, X. (2008). “Cellular automata for simulating land use changes based on support vector machines”. Computers & geosciences 34 (6): 592–602

Yang, Y., Wang, G., Wang, L., Yu, J., & Xu, Z. (2014). Evaluation of gridded precipitation data for driving SWAT model in area upstream of three gorges reservoir. *PLoS ONE*, *9*(11). https://doi.org/10.1371/journal.pone.0112725

Yin, J., He, F., Xiong, Y. J., & Qiu, G. Y. (2017). *Effects of land use / land cover and climate*

changes on surface runoff in a semi-humid and semi-arid transition zone in northwest China. 183–196. https://doi.org/10.5194/hess-21-183-2017

Yue S, Pilon P, Phinney R, Cavadias G (2002) The influence ofautocor- relation on the ability to detect trend in hydrological series. Hydrol Process 16:1807–1829

Zeleke, G., & Hurni, H. (2001). Implications of land use and land cover dynamics for mountain resource degradation in the Northwestern Ethiopian highlands. *Mountain Research and Development*, *21*(2), 184–191. https://doi.org/10.1659/0276-4741(2001)021[0184:IOLUAL]2.0.CO;2

Zhang, L., Nan, Z., Yu, W., Zhao, Y., & Xu, Y. (2018). Comparison of baseline period choices for separating climate and land use/land cover change impacts on watershed hydrology using distributed hydrological models. *Science of the Total Environment*, *622–623*, 1016–1028. https://doi.org/10.1016/j.scitotenv.2017.12.055

Zhang R, Corte-Real J, Moreira M, et al (2019) Downscaling climate change of mean climatology and extremes of precipitation and temperature: Application to a Mediterranean climate basin. Int J Climatol 39:4985–5005. https://doi.org/10.1002/joc.6122

Zhang, S., & Lu, X. X. (2009). Hydrological responses to precipitation variation and diverse human activities in a mountainous tributary of the lower Xijiang, China. *Catena*, *77*(2), 130–142. https://doi.org/10.1016/j.catena.2008.09.001

Zhang, X., Xu, Y. P., & Fu, G. (2014). Uncertainties in SWAT extreme flow simulation under climate change. *Journal of Hydrology*, *515*, 205–222. https://doi.org/10.1016/j.jhydrol.2014.04.064

Zhang, X., Zhang, L., Zhao, J., Rustomji, P., and Hairsine, P.(2008). Responses of streamflow to changes in climate and land use/cover in the Loess Plateau, China, Water Resour. Res., 44, W00A07, doi:10.1029/2007WR006711.

Zheng, J., Sun, G., Li, W., Yu, X., Zhang, C., Gong, Y., & Tu, L. (2016). Impacts of land use change and climate variations on annual inflow into the Miyun Reservoir, Beijing, China. *Hydrology and Earth System Sciences*, *20*(4), 1561–1572. https://doi.org/10.5194/hess-20-1561-2016.

Annexes

Annex 5.1 The ten most sensitive parameters including their range, fitted values of the calibrated model using CFSR climate datasets in descending order.

Sensitivity		Range		Fitted value	
Baro station	Sore station	Baro station	Sore station	Baro station	Sore station
r_CN2.mgt	v_ALPHA_BF.gw	±25%	0-1	0.16	0.46
v_ALPHA_BF.gw	v_ALPHA_BNK.rte	0-1	0-1	0.26	0.56
v_ESCO.hru	v_GWQMN.gw	0-1	0-5000	0.91	1632
r_SOL_K.sol	r_CN2.mgt	±80%	±25%	-0.17	0.01
r_Soil_ Z.sol	v_GW_DELAY.gw	±25%	0-500	0.27	25.2
r_SOL_AWC.sol	r_SOL_AWC.sol	±25%	±25	0.31	0.35
v_GWQMN.gw	r_OV_N.hru	0-5000	0.02-0.4	1854	0.15
v_GW_DELAY.gw	v_ESCO.hru	0-500	0-1	280	0.91
r_EPCO.hru	v_CH_N2.rte	0-1	0.01-0.3	0.65	0.26
v_CH_N2.rte	r_Soil_ Z	0.01-0.3	±25%	0.1	-0.06

The qualifier R refers to a relative change in the parameter where the value from the default simulation is multiplied by 1 plus the fitted value and V) refers to the existing parameter value from the default simulation is to by the fitted value. The extensions (e.g., .mgt, hru, .sol, .gw. rte) indicate the SWAT parameter family.

Annex 5.2. The ten most sensitive parameters including their range, fitted values of the calibrated model using CHIRPS climate datasets in descending order.

Sensitivity		Range		Fitted value	
Baro station	Sore station	Baro station	Sore station	Baro station	Sore station
r_CN2.mgt	v_ALPHA_BF.gw	±25%	0-1	0.1	0.46
v_CH_N2.rte	r_CN2.mgt	0.01-0.3	±25%	0.17	-0.01
v_ALPHA_BF.gw	v_GW_DELAY.gw	0-1	0-500	0.4	25.3
r_Soil_ Z.sol	r_SOL_AWC.sol	±25%	±25	-0.06	0.35
r_SOL_AWC.sol	r_OV_N.hru	±25%	0.02-0.4	-0.05	0.15
v_GWQMN.gw	v_GW_REVAP.gw	0-5000	0.02-0.2	1476	0.01
v_ESCO.hru	r_SOL_BD.sol	0-1	±20%	0.86	-0.23
r_SOL_K.sol	v_ESCO.hru	±80%	0-1	-0.55	0.91
v_ALPHA_BNK.rte	r_Soil_ Z	0-1	±25%	0.27	-0.06
v_GW_DELAY.gw	v_CH_N2.rte	0-500	0.01-0.3	160	0.26

The qualifier R refers to a relative change in the parameter where the value from the default simulation is multiplied by 1 plus the fitted value and V) refers to the existing parameter value

from the default simulation to the fitted value. The extensions (e.g., .mgt, hru, .sol, .gw. rte) indicate the SWAT parameter family.

Annex 6.1 Presents a summary of IHA Parameters and their Ecosystem Influences

IHA Parameter Group	Hydrologic Parameters	Ecosystem Influences
1. Magnitude of monthly water conditions	Mean or median value for each calendar month	Habitat availability for aquatic organisms ·Soil moisture availability for plants · Availability of water for terrestrial animals · Availability of food/cover for furbearing mammals · Reliability of water supplies for terrestrial animals · Access by predators to nesting sites · Influences water temperature, oxygen levels, photosynthesis in water column
2. Magnitude and duration of annual extreme water conditions	Annual minima, 1-day mean Annual minima, 3-day means Annual minima, 7-day means Annual minima, 30-day means Annual minima, 90-day means Annual maxima, 1-day mean Annual maxima, 3-day means Annual maxima, 7-day means Annual maxima, 30-day means Annual maxima, 90-day means Number of zero-flow days Base flow index: 7-day minimum flow/mean flow for year	· Balance of competitive, ruderal, and stress-tolerant organisms · Creation of sites for plant colonization · Structuring of aquatic ecosystems by abiotic vs . biotic factors · Structuring of river channel morphology and physical habitat conditions · Soil moisture stress in plants · Dehydration in animals · Anaerobic stress in plants · Volume of nutrient exchanges between rivers and floodplains · Duration of stressful conditions such as low oxygen and concentrated chemicals in aquatic environments · Distribution of plant communities in lakes, ponds, floodplains
3. Timing of annual extreme water conditions	Julian date of each annual 1-day maximum Julian date of each annual 1-day minimum	· Compatibility with life cycles of organisms · Predictability/avoidability of stress for organisms · Access to special habitats during reproduction or to avoid predation · Spawning cues for migratory fish · Evolution of life history strategies, behavioral mechanisms

4. Frequency and duration of high and low pulses	Number of low pulses within each water year Mean or median duration of low pulses (days) Number of high pulses within each water year Mean or median duration of high pulses (days)	Frequency and magnitude of soil moisture stress for plants · Frequency and duration of anaerobic stress for plants · Availability of floodplain habitats for aquatic organisms · Nutrient and organic matter exchanges between river and floodplain · Soil mineral availability · Influences bedload transport, channel sediment textures, and duration of substrate disturbance (high pulses)

Annex 7.1 Ground truth point collection using Garmin72 GPS from the forest and agricultural land

Annex 7.2 Poor land management practice (farming on a steep slope), dying stream during the dry season

Annex 7.3 Landsat imagery including path/ raw and acquisition dates

Path/raw	Acquisition date	Sensor	Resolution (m)
170/55,170/56,171/55 and 171/56	Dec−Feb, 1985/87	TM	30
170/55,170/56,171/55 and 171/56	DEC−FEB, 2002/03	ETM+	30
170/55,170/56,171/55 and 171/56	DEC−FEB, 2017/19	LC8	30

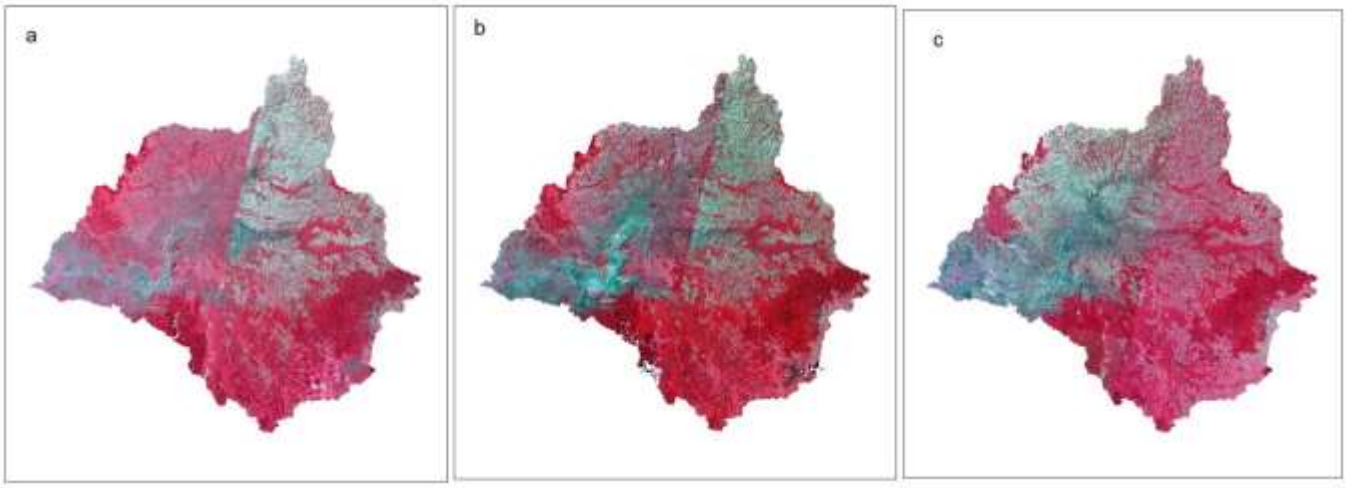

Annex 7.4 Land use land cover map for 1985 (a), 2002 (b), 2019(c)

Annex 7.5 Land use type with description

Land use	Description
Forest	Areas covered with dense trees include evergreen forest land, mixed forest, plantation forests, and riparian vegetation. Represents deep to dark red to bright red color in 4, 3,2 band combination of Landsat image.
Shru bland	Areas with shrubs, bushes, and small trees, with little wood, mixed with some grasses. Represents red−brown to bright red in the Landsat image (4, 3, 2 band combination).
Agriculture	Areas used for crop cultivation (irrigated and rain−fed agriculture), fallow land. Represents grey and brown color in 4,3,2 band combination of the Landsat image
Urban	Areas of human settlements, roads, artificial surfaces, etc. Represents cyane blue color in 4,3,2 band combination of land sat image
Water bodies	Areas permanently covered with standing or moving water such as inland waters, dugouts, and streams. Represents black color in 4, 3, 2 band combination of Landsat image
Wetland	Waterlogged areas, wetlands, and flood plain areas. Represents light red color in 4, 3, 2 band combination of Landsat image

Annex 7.6 Presents the confusion matrix of the 2002 classification map of the Baro basin

Class Name	Reference data

	Forest	Shrub	Grass	Agriculture	Wetland	Water	Row total	User's accuracy (%)
Forest	33	1	0	0	0	1	35	94.29
Shrub	0	21	1	3	0	0	25	84
Grass	0	5	16	3	1	0	25	64
Agriculture	0	2	3	30	0	0	35	85.71
Wetland	1	0	0	0	14	0	15	93.33
Water	0	2	1	0	0	12	15	80
Column total	34	31	21	36	15	13	150	
Producer's accuracy (%)	97.1	67.7	76.2	83.33	93.33	92.31		126
Overall accuracy (%)	84.6							
Overall kappa statistics	0.81							

Annex 7.7 Presents the confusion matrix of the 2019 classification map of the Baro basin

Class Name	Reference data							
	Forest	Shrub	Grass	Agriculture	Wetland	Water	Row total	User's accuracy (%)
Forest	32	1	0	0	0	2	35	91.43
Shrub	0	21	1	3	0	0	25	84
Grass	0	3	20	2	0	0	25	80
Agriculture	0	2	2	30	1	0	35	85.71
Wetland	1	0	0	0	14	0	15	93.33
Water	0	2	0	0	0	13	15	86.67
Column total	33	29	23	35	15	15	150	
Producer's accuracy (%)	97	72.4	86.9	85.7	93.3	86.6		130
Overall accuracy (%)	87							
Overall kappa statistics	0.83							

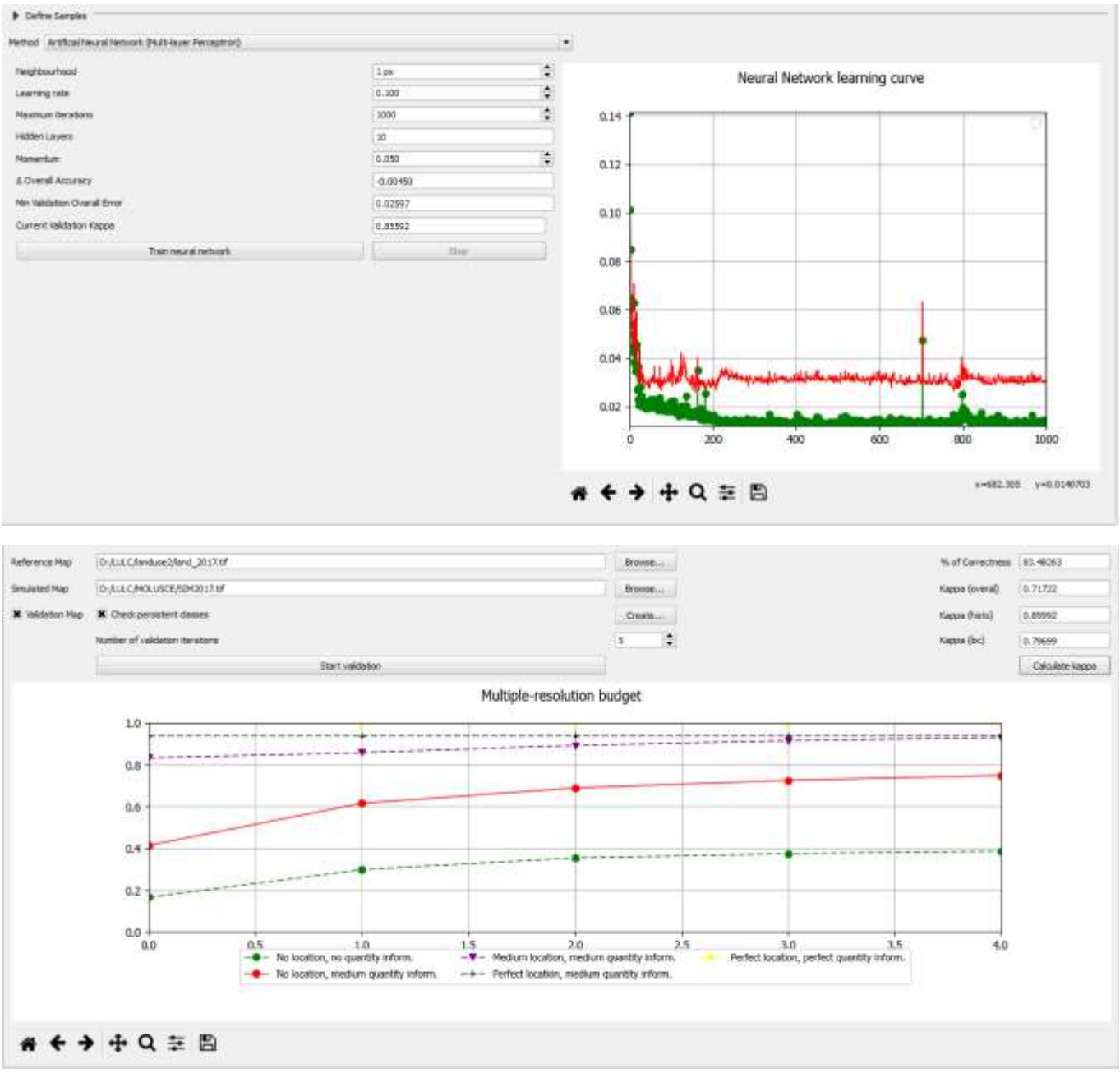

Annex 7.8 Artificial network learning curve and validation result of kappa statistics for simulation of land use map of 2019 based on the 1985 and 2002 land use map.

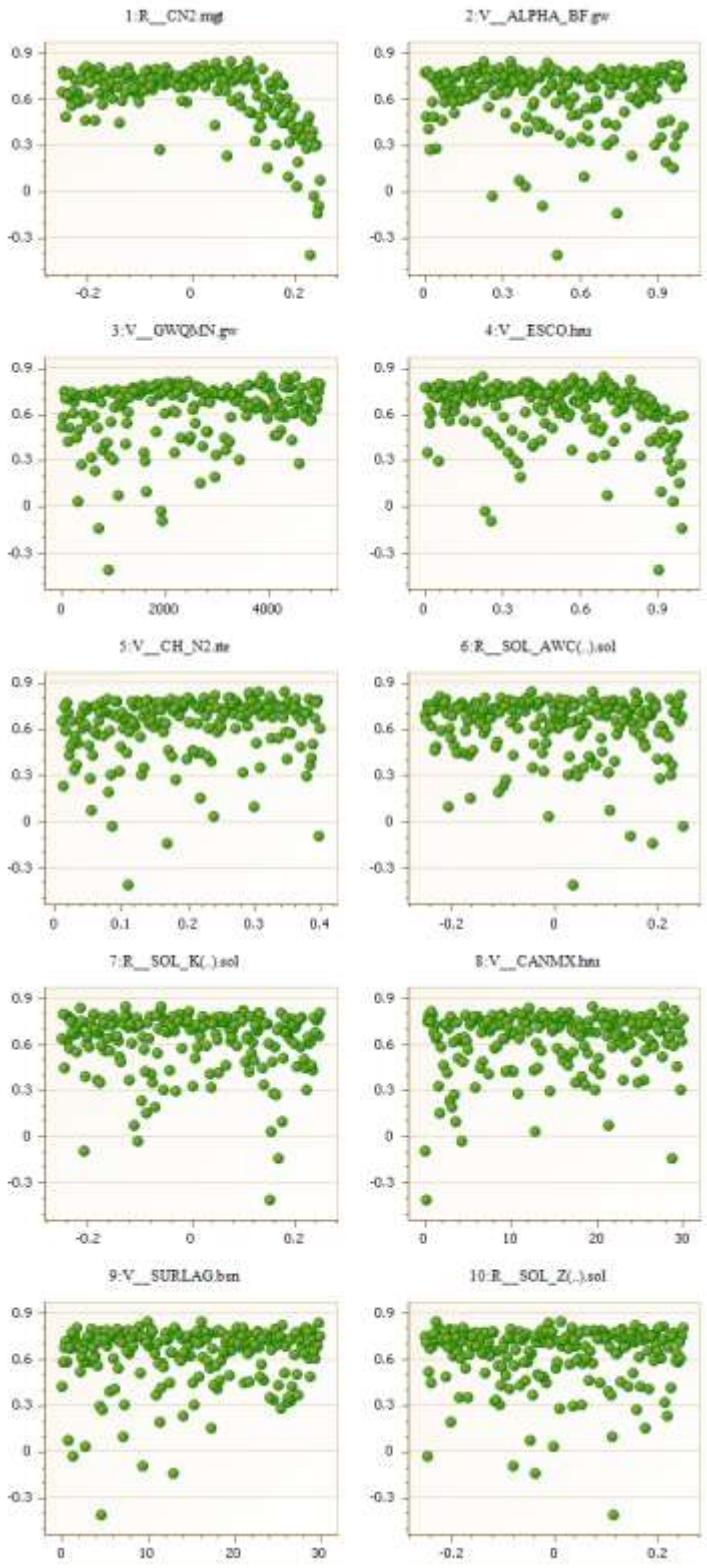

Annex 7.9 Dotty plots of the calibration parameters with objective function of NSE against SWAT parameter optimization for monthly time scale.

.List of original research articles

Theoretical and Applied Climatology (2021) 144:751–767
https://doi.org/10.1007/s00704-021-03552-w

ORIGINAL PAPER

Evaluation of the performance of bias-corrected CORDEX regional climate models in reproducing Baro–Akobo basin climate

Abiy Getachew Mengistu[1,2] · Tekalegn Ayele Woldesenbet[2] · Yihun Taddele Dile[3]

Received: 7 September 2020 / Accepted: 1 February 2021 / Published online: 26 February 2021

Abstract

The applicability of the regional climate model (RCMs) for catchment hydroclimate is obscured due to their systematic bias. As a result, bias correction has become an essential precondition for the study of climate change. This study aimed to evaluate the skill of seven rainfall and five maximum and minimum temperature RCM outputs against observed data in simulating the characteristics of climate at several locations over the Baro–Akobo basin in Ethiopia. The evaluation was performed based on raw and bias-corrected RCMs against observed for a long-term basis. Several statistical metrics were used to compare RCMs against observed using a pixel-to-point approach. In this finding, raw RCMs showed pronounced biases such as lower correlation and higher PBIAS in estimating rainfall and minimum temperature than maximum temperature. However, most RCMs after bias correction showed better performance in reproducing the magnitude and distribution of the mean monthly rainfall and temperature and improve all the statistical metrics. The Mann–Kendall trend test for observed and bias-corrected RCMs indicated a decreasing annual rainfall trend while the maximum and minimum temperature showed an increasing trend in most stations. In most statistical metrics, the ensemble mean resulted in better agreement with observation than individual models in most stations. In general, after bias correction, the ensemble adequately simulates the Baro–Akobo basin climate and can be used for evaluation of future climate projections in the region.

Contents lists available at ScienceDirect

Ecohydrology & Hydrobiology

journal homepage: www.elsevier.com/locate/ecohyd

Original Research Article

Evaluation of observed and satellite-based climate products for hydrological simulation in data-scarce Baro -Akob River Basin, Ethiopia

Abiy Getachew Mengistu[a,b,*], Tekalegn Ayele Woldesenbet[b], Yihun Dile Taddele[c]

[a] Department of Natural Resource Management, Mizan–Tepi University, Mizan, Teferi, Ethiopia
[b] Ethiopian Institute of Water Resource, Addis Ababa University, Addis Ababa, Ethiopia
[c] College of Agriculture and Life Sciences, Texas A&M University, College Station, TX, USA

ARTICLE INFO

Article history:
Received 10 August 2021
Revised 16 October 2021
Accepted 24 November 2021
Available online xxx

Keywords:
SWAT
Observed
CFSR
CHIRPS
Hydrological modeling
Baro-Akobo basin

ABSTRACT

Hydrological modeling in the data-scarce regions is challenging. Recent advances in remote sensing make producing climate data easier and provided alternatives to the conventional climate data sources, particularly for hydro-climatological studies in the data-scarce regions. However, rigorous evaluations are warranted to evaluate the reliability and effectiveness of gridded climate products. This study evaluated the CFSR and CHIRPS products against the observed climate for hydrologic prediction at two streamflow gauging stations. The Soil and Water Assessment Tool (SWAT) is used to simulate hydrological processes in the watersheds. Model sensitivity analysis and calibration were conducted using the Sequential Uncertainty Fitting-2 (SUFI-2) algorithm in the SWAT-Calibration Uncertainty and Prediction (SWAT-CUP). Streamflow simulation performance was evaluated using several statistical, hydrological performances and prediction uncertainty of p-factor and r-factor within the SUFI-2 framework. Simulation of the model using the observed and gridded climate products provided satisfactory model performance in terms of the goodness of fit criteria and uncertainty prediction. Results show that CHIRPS rainfall combined with CFSR and observed temperatures demonstrates slightly better statistics and hydrological performance than observed, but shows substantial difference than CFSR. The simulations with CHIRPS and observed yielded minor differences in the water balance component estimates where the CFSR simulation gave lower average annual rainfall, resulting in lower water balance components. Quantifying the various water balance component in the watershed helps to tackle the water management issues. Overall, the CHIRPS rainfall combined with CFSR temperature can serve as a better alternative climate input for hydrological applications in the study region

X

Acta Geophysica
https://doi.org/10.1007/s11600-022-00956-8

RESEARCH ARTICLE - HYDROLOGY

Modeling the impacts of climate change on hydrological processes in the Baro–Akobo River basin, Ethiopia

Abiy Getachew Mengistu[1,2] · Tekalegn Ayele Woldesenbet[2] · Yihun Taddele Dile[3] · Haimanote Kebede Bayabil[4]

Received: 13 April 2022 / Accepted: 13 October 2022

Abstract

Understanding the impacts of climate change on basin hydrology is critical for developing effective water management practices. This study was conducted to investigate climate change and its impact on the hydrological processes of the Baro–Akobo River basin in Ethiopia. Five bias-corrected regional climate models and their ensemble were developed to examine future climate changes in the 2030s (2021–2050) and 2080s (2071–2100) periods under the two Representative Concentration Pathways (RCP) 4.5 and RCP8.5 scenarios compared to a baseline (1981–2010) period. The calibrated model performed well with Nash–Sutcliffe efficiency and coefficient of determination of each 0.73 for daily and 0.89 and 0.9 for monthly simulation, respectively. Though all RCMs agree concerning the increasing direction of the 2030 and 2080s maximum and minimum temperature changes, there is inconsistency in the magnitude and direction of monthly projected rainfall changes. With the ensemble, the maximum and minimum temperatures will increase by 2.6 and 3.6 °C, respectively, and rainfall will decrease by 5% in the 2080s under RCP8.5 scenarios. The dry and wet season rainfall are expected to decrease by 19 and 3.7% under the RCP8.5 scenarios in the 2080s. Consequently, future climate change could cause a decrease in the annual surface runoff and water yield, while evapotranspiration could increase under the RCP4.5 and RCP8.5 scenarios. This study provides useful insights about potential climate change impacts on the hydrology of the basin, which could be useful to inform decision-makers in developing strategies such as water harvesting to mitigate the impact of climate change.

Contents lists available at ScienceDirect

Heliyon

journal homepage: www.cell.com/heliyon

Research article

Modeling impacts of projected land use and climate changes on the water balance in the Baro basin, Ethiopia

Abiy Getachew Mengistu [a,b,*], Tekalegn Ayele Woldesenbet [a], Yihun Taddele Dile [c], Haimanote Kebede Bayabil [d], Gebrekidan Worku Tefera [e]

[a] Ethiopian Institute of Water Resources, Addis Ababa University, Addis Ababa, Ethiopia
[b] Department of Natural Resource Management, Mizan-Tepi University, Mizan, Tefari, Ethiopia
[c] College of Agriculture and Life Sciences, Texas A&M University, College Station, TX, USA
[d] Agricultural and Biological Engineering, Tropical Research and Education Center, Institute of Food and Agricultural Sciences, University of Florida, Homestead, FL, 33031, USA
[e] College of Agriculture and Human Sciences, Prairie View A&M University, TX, 77446, USA

ARTICLE INFO

Keywords:
CA-ANN
climate model
evapotranspiration
surface runoff
Baro basin

ABSTRACT

In terms of land use and climate, the world is changing at an unprecedented rate and these changes have a significant influence on our water resources. This study was conducted to examine the individual and combined potential impacts of land use and climate change on the water balance of the Baro basin in Ethiopia for the baseline period (1985–2002) and near-future period (2023- 2040) using the Soil and Water Assessment Tool (SWAT). The plausible land use scenarios considering current (CUR), business as usual (BAU), and further expansion of altitudinal forest and watershed management practices (CON), as well as climate change scenarios from regional climate model outputs (RCMs) under two representative concentration pathways (RCP4.5 and RCP8.5) for the 2023-2040 time frame, were used as inputs to the models. The monthly calibrated and validated SWAT model produced an acceptable result, which was then used for water balance simulations. Findings show that forest decreased from 54.5% to 48.9% and 41.2% while agricultural land increased from 21.8% to 29.7% and 39.8% under the CUR and BAU land use change scenarios, respectively. The results from the ensemble mean showed an increase in maximum and minimum temperatures and a decrease in rainfall under the RCP4.5 and RCP8.5 climate change scenarios, which in turn resulted in an increase in evapotranspiration (ET) and a decrease in water availability. Climate change outweighed the impact of land-use change, thus indicating an increase in annual ET by up to 12% and a decrease of 42% in surface runoff (SURQ) under the RCP8.5 scenario. The BAU land use scenario projection triggers a respective increase of 18% in annual SURQ and reduction of ET by 2%. However, under the CON land use scenario, SURQ decreased by 24%. The study concluded that future land use and climate change will further challenge the basin's water supply capacity to meet the increased water demand. Understanding the changes in the basin's water balance is critical for mitigation and adaptation options. As a result, this study proposes restoration efforts and climate-resilient water management strategies that can increase the resilience of the river basin.

* Corresponding author. Ethiopian Institute of Water Resources, Addis Ababa University, Addis Ababa, Ethiopia.
E-mail addresses: abiygetachew@aau.edu.et (A.G. Mengistu), tekalegnay@yahoo.com (T.A. Woldesenbet), yihundile.taddele@ag.tamu.edu (Y.T. Dile), hbayabil@ufl.edu (H.K. Bayabil), kidanewl@gmail.com (G.W. Tefera).

https://doi.org/10.1016/j.heliyon.2023.e13965
Received 8 October 2022; Received in revised form 14 February 2023; Accepted 16 February 2023
Available online 24 February 2023